

International Conference on Urban Comfort and Environmental Quality

URBAN-CEQ

28-29 September 2017 - University of Genoa, Italy

Edited by

Massimiliano Burlando, Maria Canepa, Adriano Magliocco, Katia Perini, Maria Pia Repetto



CONFERENCE SCIENTIFIC COMMITTEE

Hashem Akbari (*Concordia University Montreal*)

Jonas Allegrini (*ETH Zürich*)

Thomas Auer (*TU München*)

Bert Blocken (*TU Eindhoven*)

Riccardo Buccolieri (*Università del Salento*)

Massimiliano Burlando (*Università di Genova*)

Luisa Cabeza (*University of Lleida*)

Jan Carmeliet (*ETH Zürich*)

Matteo Carpentieri (*University of Surrey*)

Julià Coma Arpon (*University of Lleida*)

Silvana Di Sabatino (*Università di Bologna*)

Mario Grosso (*Politecnico di Torino*)

Adriano Magliocco (*Università di Genova*)

Gabriel Perez (*University of Lleida*)

Katia Perini (*Università di Genova*)

Paolo Prati (*Università di Genova*)

Chao Ren (*Chinese University of Hong Kong*)

Maria Pia Repetto (*Università di Genova*)

Alan Robins (*University of Surrey*)

Ted Stathopoulos (*Concordia University*)

Timothy Van Renterghem (*Ghent University*)

CONFERENCE ORGANISING COMMITTEE

Massimiliano Burlando (*Università di Genova - DICCA*)

Maria Canepa (*Università di Genova - DAD*)

Patrizia De Gaetano (*Università di Genova - DICCA*)

Andrea Giachetta (*Università di Genova - DAD*)

Adriano Magliocco (*Università di Genova - DAD (Co-chairman)*)

Katia Perini (*Università di Genova - DAD*)

Chiara Piccardo (*Università di Genova - DAD*)

Marina Pizzo (*Università di Genova - DICCA*)

Maria Pia Repetto (*Università di Genova - DICCA (Co-chairman)*)

Alessio Ricci (*Università di Genova - DICCA*)



UNIVERSITÀ DEGLI STUDI
DI GENOVA

International Conference on Urban Comfort and Environmental Quality

URBAN-CEQ

28-29 September 2017 - University of Genoa, Italy

Edited by

Massimiliano Burlando, Maria Canepa, Adriano Magliocco, Katia Perini, Maria Pia Repetto





is the bookmark of the University of Genoa



**UNIVERSITÀ DEGLI STUDI
DI GENOVA**



URBAN-CEQ

International Conference on Urban Comfort and Environmental Quality

28-29 September 2017

University of Genoa, Italy

This volume contains the blind peer reviewed papers accepted for the International Conference on Urban Comfort and Environmental Quality held at University of Genoa, Italy, during 28-29 September 2017. The papers provide a current snapshot of leading research on urban comfort and environmental quality

Editor

GENOVA UNIVERSITY PRESS

Piazza della Nunziata, 6 16124 Genova

Tel. 010 20951558

Fax 010 20951552

e-mail: ce-press@liste.unige.it

<http://gup.unige.it/>

The authors are at disposal for any eventual rights about published images.
Copyrights are protected by law.

All rights reserved by copyright law

ISBN: 978-88-97752-91-2

Print on September 2017

CONTENTS

FOREWORD	008
MODELS AND TOOLS FOR URBAN CLIMATE STUDIES	010
<i>CFD simulations and field measurements of urban microclimate in a real compact heterogeneous urban area</i>	011
N. Antoniou, H. Montazeri, M. Neophytou, B. Blocken	
<i>The POR-FESR MEMORIA project: an integrated models-sensors approach for the air quality assessment</i>	016
P. Brotto, L. Caponi, L. Brugnatti, F. Tarchino, S. Frassetto	
<i>Key Performance Indicators to assess the local climate potential of three passive cooling heat sinks</i>	020
G. Chiesa	
<i>Early-design tool to optimize outdoor activities localization based on microclimate criteria</i>	025
G. Chiesa, M. Grosso	
<i>Mathematical Generative Approach on Performance Based Urban Form Design</i>	030
A. Chokhachian, K. Perini, S. Giulini, T. Auer	
<i>Flow adjustment and turbulence in staggered high-rise building arrays by wind tunnel measurements and numerical simulations</i>	036
J. Hang, R. Buccolieri, M. Sandberg	
<i>A study of the pressure coefficient at a tunnel portal</i>	044
T. Kubwimana, E. Bergamini, P. Salizzoni, P. Méjean	
<i>Modelling the effect of urban design on thermal comfort and air quality: the SMARTUrban Project</i>	049
L. Massetti, M. Petralli, G. Brandani, M. Napoli, F. Ferrini, A. Fini, F. Torrini, D. Pearlmutter, S. Orlandini, A. Giuntoli	
<i>Wind comfort analysis in urban complex area: the example of the new Erzelli Technologic District</i>	058
M.P. Repetto, G. Solari, M. Burlando, A. Freda	
<i>A numerical study of pressure coefficients distribution on high-rise buildings with balconies</i>	063
X. Zheng, M. Montazeri, B. Blocken	

URBAN COMFORT STUDIES	068
<i>Dynamic Response of Pedestrian Thermal Comfort under Outdoor Transient Conditions</i> K. Ka-Lun Lau, Y. Shi, E. Y.Y. Ng	069
<i>Air movement representation as a tool for quality design and assessment of the built environment</i> M. L. Germanà, S. Vattano, A. Tavolante	076
<i>Urban comfort evaluation in an Italian historical district: the impact of architectural details in wind tunnel and CFD analysis</i> A. Ricci, A. Freda, M.P. Repetto, M. Burlando, B. Blocken	086
<i>Mapping outdoor comfort for increasing environmental quality: a design proposal for Munich's Viktualienmarkt</i> D. Santucci, G. Volpicelli, A. Battisti, T. Auer	090
<i>Relationship between city size, coastal land use and summer daytime air temperature rise with distance from coast</i> H. Takebayashi, T. Tanaka, M. Moriyama, H. Watanabe, H. Miyazaki, K. Kittaka	098
GREEN AND BLUE STRATEGIES AND TECHNOLOGIES FOR URBAN ENVIRONMENT	103
<i>Improving Outdoor Thermal Comfort in Masdar City, Abu Dhabi, UAE.</i> L. Bande, M. Jha, M. Mirkovic, A. Afshari, K. Alawadi	104
<i>Assessment of Bioclimatic Comfort of Residential Areas to Improve the Quality of Environment by Using Urban Greening and Hard Landscaping</i> I.V. Dunichkin, O. I. Poddaeva, K.S Golokhvast	118
<i>Mitigation Technologies for urban open spaces: a study of vegetation and cool materials effects on pedestrian comfort in Rome</i> F. Laureti, A. Battisti	122
<i>Environmental and energetic assessment of a vertical greening system installed in Genoa, Italy</i> F. Magrassi, K. Perini	132
<i>Smart filters of particulate matter: plants in urban areas</i> E. Roccotiello, S. Romeo, L. Cannatà, M. G. Mariotti	137
<i>A general overview on urban adaptation strategies to climate change and sea level rise.</i> G.E. Rossi, C. Lepratti, R. Morbiducci	142
<i>Nature-based stormwater strategies and urban environmental quality</i> P. Sabbion, M. Canepa	150

HEAT ENERGY DEMAND AND INDOOR COMFORT	157
<i>An integrated methodology for the simulation and the management of climate adaptive solution for buildings and open spaces: the case study of the Duchesca district in Naples, Italy</i> E. Bassolino, F. Scarpati	158
<i>Designing and Evaluating District heating Networks with Simulation Based Urban Planning</i> C. Bonnet, I. Bratov, G. Schubert, A. Chokhachian, F. Petzold, T. Auer	167
<i>Urban climate influence on building energy use</i> K. R. Gunawardena, T. Kershaw	175
<i>Influence of exterior convective heat transfer coefficient models on the energy demand of buildings with varying geometry</i> S. Iousef, H. Montazer, B. Blocken, P.J.V. van Wesemae	185
<i>On the effect of passive building technologies and orientation on the energy demand of an isolated lightweight house</i> R. Vasaturo, I. Kalkman, T. van Hooff, B. Blocken, P. van Wesemael	190
<i>The Gavoglio area: a military area in the earth of Genoa to be rediscovered and regenerated</i> C. Vite, C. Lepratti, R. Morbiducci	195

FOREWORD

More than two thirds of European citizens live in cities, where many environmental problems are concentrated, such as lack of thermal comfort and poor air quality, which seems to be also responsible for life-threatening conditions. It is more and more necessary to link urban regeneration strategies to objectives of environmental quality improvement. That is why many researchers, working in Universities and Research Centres, are focusing their activity on the evaluation of environmental quality of urban areas, considering a wide range of environmental problems and air quality and their effects on citizen life conditions and health.

The Architecture and Design Department (DAD) and the Department of Civil Engineering, Chemistry and Environmental Engineering (DICCA) – two departments of the Polytechnic School, University of Genova – decided to organize the International Conference on Urban Comfort and Environmental Quality (URBAN-CEQ) to gather architects and engineers committed to environmental quality research. These are specialists of fluid dynamics, of urban design and urban planning using tools and models to analyse the urban environmental quality, aiming to organize strategies and technologies to improve life conditions.

The Organizing Committee includes, from one side (DAD), professors and researchers belonging to the Italian Society of Architectural Technology (Società Italiana della Tecnologia dell'Architettura –SITdA), from the other side (DICCA), the wind engineering expertise from the school of Genova, which is worldwide recognized for its longstanding tradition. The organization of the conference rises from a cultural context of scientific disciplines integration and relies on the cooperation of a wide international Scientific Committee.

Key topics of the conference call are urban heat island studies; dynamic simulation tools to study pollutants dispersion and outdoor thermal comfort and building heating demand; blue-and-green technologies; air quality improvement strategies, etc. Researchers from many Countries have answered to the call sending papers, 28 of them have been (blind) reviewed and selected.

In this proceedings book selected papers are divided in four sections: Models and tools for urban climate studies, Urban comfort studies, Green and Blue strategies and technologies for urban environment, Heat energy demand and indoor comfort. They are a great example of multidisciplinary approach to complex and challenging problems of our society.

Keynote speakers are renowned international experts in the field of environmental quality and urban areas: Prof. Thomas Auer - Chair of Building Technology and Climate Responsive Design, Technische Universität München - and Prof. Bert Blocken - chair Building Physics and Urban Physics at the Unit Building Physics and Services (BPS) of the Department of the Built Environment at Eindhoven University of Technology in the Netherlands. The Organizing Committee acknowledges both for sharing their experience with the attendants, inspiring new development and research topics.

The Organizing Committee also wishes to thank all the authors and reviewers for their contribution, with the hope that this will be the first of a successful series.

MODELS AND TOOLS
FOR URBAN CLIMATE STUDIES

CFD simulations and field measurements of urban microclimate in a real compact heterogeneous urban area

N. Antoniou^{1,2}, H. Montazeri^{2,3}, M. Neophytou¹, B. Blocken^{2,3}

¹Department of Civil and Environmental Engineering, University of Cyprus, Nicosia, Cyprus

²Building Physics and Services, Eindhoven University of Technology, Eindhoven, The Netherlands

³Building Physics Section, Department of Civil Engineering, KU Leuven, Leuven, Belgium

Corresponding author: Nestoras Antoniou, antoniou.nestoras@ucy.ac.cy

Abstract

Considering the radical increase of urban population and the trend toward urbanization, the analysis of microclimatic conditions in the urban environment is getting more significant. In this perspective, this study analyzes microclimatic conditions in a real urban area. The real compact inhomogeneous urban area under study is located in Nicosia old town, in Cyprus. High-resolution Computational Fluid Dynamics (CFD) simulations are performed based on the 3D unsteady Reynolds-Averaged Navier-Stokes equations to assess the air temperature and wind speed distributions. The CFD results are compared with on-site measurements for the same area. The results show that CFD can predict air temperatures in compact real urban areas, with an average deviation of 6.8%. Based on the results, conclusions are going to be made regarding thermal comfort in the case study area.

1 Introduction

Because of the rapid trend toward urbanization around 54% of the world's population currently live in urban areas (UNFPA, 2007). The urbanized population is projected to increase and reach up to 66% by 2050 (United Nations, 2014). In addition, due to climatic changes phenomena like the Urban Heat Island (UHI) effect and heat waves are becoming more severe, with dramatic consequences for the urban population (Toparlar et al., 2015; Montazeri et al., 2017). In this perspective, the analysis of microclimatic conditions in urban areas is getting more significant. A detailed review of the literature indicates that a vast majority of studies on urban microclimate in complex urban areas has been performed using on-site measurements since data provided with this method can capture the real complexity of the microclimatic conditions. Nevertheless, a well-known problem of on-site measurements is that there is no or only very limited control over the boundary conditions. This is, however, very important given the wide range of parameters influencing microclimate conditions, which are not easily varied independently. Numerical simulation with CFD, as opposed to on-site experiments, provides whole-flow field data, i.e. data on the relevant parameters in all points of the computational domain. Similar to on-site experiments, CFD does not suffer from potentially incompatible similarity requirements because simulations can be conducted at full scale. This study, therefore, presents high-resolution CFD simulations using the 3D unsteady Reynolds-Averaged Navier-Stokes equations to assess urban microclimate in a real compact inhomogeneous urban area. The validation of the results is based on on-site measurements of air temperature performed by (Neophytou et al., 2011) for the same area.

2 Case study area

The selected urban area covers 0.247 km² and is composed mainly of low-rise and medium-rise buildings (Fig. 1). The average and maximum building height are about 8.1 m and 45.5 m (Shakolas Tower), respectively. The plan area density λ_p is 0.40, as derived from European Research Project TOPEUM (Towards Optimization of Urban Planning and Architectural Parameters for Energy Use Minimization in Mediterranean Cities, Neophytou *et al.*, 2011). The urban canopy is composed of narrow streets forming an organic, non-orthogonal structure. The street widths are ranging from 6 m to 10 m, where the aspect ratio of the street canyons (width to height) ranges from 0.5 to 1. Streets are covered with asphalt and buildings are constructed with concrete and bricks. There is a lack of green areas, which is considered a possible reason for increased temperatures inside the street canyons during the summer period.

3 Field measurements

A series of on-site measurements took place inside the case study area, under the field measurement campaign, which occurred in July 2010, within the TOPEUM project (Neophytou *et al.*, 2011). The air temperature was measured using four sensors. One sensor was located on top of a high rise building at the height of 26.8 m from the ground (point 2 in Fig. 1a), while the other three sensors were located inside the street canyons at the height of 5 m from the ground (points 1, 3, 4 in Fig. 1a). The measurements occurred from 7th to 21st of July 2010, taken every 30 minutes. Aerial thermographic images were also taken from a helicopter on 12th of July 2010, at 08:00, 15:00 and 22:00 using a FLIR -P640 thermographic camera. In addition, a satellite thermographic image was obtained from LST Landsat for 10th of July at 11:00, with a resolution of 30 m × 30 m. CFD Simulations

3.1 Computational domain and grid

The computational domain consists of a subdomain containing the explicitly modelled buildings (i.e. those included in the computational domain with their actual main dimensions) (Fig. 1c) and an additional downstream subdomain (not shown in this paper). The dimensions are selected based on the best practice guidelines (Franke *et al.*, 2007; Tominaga *et al.*, 2008). The computational grid is created using the surface-grid extrusion technique by van Hooff and Blocken (2010). The procedure is executed with the aid of the pre-processor Gambit 2.4.6, resulting in a grid with 14,670,517 hexahedral cells. The computational grid is shown in Fig. 1d.



Figure 1. (a) Top view and (b) aerial view of the case study. (c) high-resolution computational grid on the building surfaces (14,670,517 hexahedral cells).

3.2 Computational settings and parameters

The commercial CFD code ANSYS/Fluent 15.0 is used to perform the simulations. The 3D unsteady Reynolds-averaged Navier-Stokes equations are solved (URANS) in combination with the realizable $k-\epsilon$ turbulence model by Shih *et al.* (1995). The simulations are performed for four consequent days (9th to 12th of July 2010), with time steps of 1 hour. Meteorological data used in this study are obtained from the national meteorological station of Athalassa, which is located approximately 5 km away from the area of interest. Velocity inlets and pressure outlets are set to the four vertical sides of

the domain, depending on the wind direction. Symmetry conditions are set to the top of the domain. The ground and the building surfaces are set as walls. At the inlets, a logarithmic mean speed profile (Eq. 1) is imposed with $z_0 = 0.25$ m to 0.4 m, depending on the wind direction and with reference wind speed ($U(z)$) at 10 m height. The turbulence kinetic energy (k) and turbulence dissipation rate (ε) at height z from the ground is given by (Eq. 1 and Eq. 2), where u_{ABL}^* is the atmospheric boundary layer friction velocity, κ is the von Karman constant ($= 0.42$), z_0 is the surface roughness length (m), and z is the height coordinate (m).

$$U(z) = \frac{u^*}{\kappa} \ln\left(\frac{z+z_0}{z_0}\right) \quad (1)$$

$$k = \frac{u^{*2}}{\sqrt{C_\mu}} \quad (2)$$

$$\varepsilon(z) = \frac{u_{ABL}^{*3}}{\kappa(z+z_0)} \quad (3)$$

The standard wall functions by Launder and Spalding (1974) are used to the wall boundaries with roughness modifications by Cebeci and Bradshaw (1977). The values of the roughness parameters, i.e. the sand-grain roughness height (k_s) and the roughness constant (C_s) are determined using their consistency relationship with the aerodynamic roughness length z_0 introduced by Blocken *et al.* (2007):

$$k_s = \frac{9.793z_0}{C_s} \quad (4)$$

The internal air temperature inside the buildings is assumed to be 26 °C. The building walls are composed of brick materials with 0.25 m thickness. The ground plane is modelled implicitly as a 10 m thick layer composed of a layer of concrete with 0.5 m thickness and a layer of earth with 9.5 m thickness with a constant temperature of 10 °C at 10 m below ground. The roads are modelled with a layer of asphalt with 0.2 m thickness followed by a layer of earth with 9.8 m thickness. The roofs of the buildings are modelled as a layer of concrete with 0.25 m thickness. The total solar radiation is calculated with the solar calculator included in ANSYS/Fluent 15.0. The P-1 radiation model (ANSYS Inc, 2013) is used to solve the radiative heat transfer. Buoyancy is calculated using the Boussinesq approximation. More detailed information concerning the computational settings and parameters will be provided in the full paper.

4 Results and validation

Fig. 2 presents the comparison between the predicted and the measured air temperatures for point 2, shown in Fig. 1.

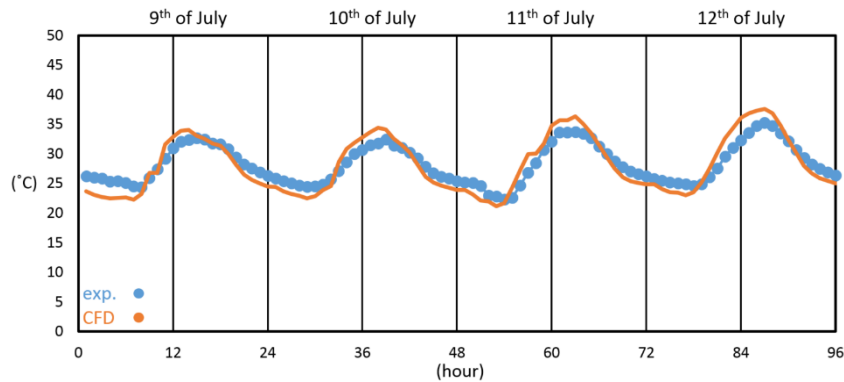


Figure 2. Comparison of predicted and measured air temperatures at point 2 (Fig. 1a)

The diurnal cycle is captured well for all of the four points. The average deviation from the measurements for points 1, 2, 3 and 4 is 7.5%, 5.9%, 6.5% and 7.4%, respectively. The maximum deviation is observed at points 1 and 4, which are placed in very narrow street canyons close to building walls. The best agreement is achieved at point 2 (Fig. 1a), which is located at the top of the second highest building, at 26.8 m from the ground (Fig. 2). More information about the validation study and the CFD results will be provided in a further paper, including the comparison with aerial and satellite images for better representation of the whole temperature field.

Acknowledgements

Hamid Montazeri is currently a postdoctoral fellow of the Research Foundation – Flanders (FWO) and is grateful for its financial support (project FWO 12M5316N). The authors gratefully acknowledge the partnership with ANSYS CFD.

References

- ANSYS Inc, 2013, ANSYS FLUENT User's Guide.
- Blocken, B., Stathopoulos, T., and Carmeliet, J. (2007). CFD simulation of the atmospheric boundary layer: wall function problems. *Atmospheric Environment* 41, 238–252.
- Cebeci, T., and Bradshaw, P. (1977). *Momentum Transfer in Boundary Layers* (H. P. Corp., Ed.): Washington.
- Franke, J., Hellsten, A., Schlünzen, H., and Carissimo, B. (2007). Best practice guideline for the CFD simulation of flows in the urban environment, *in* COST action 732, p. 1–52.
- Launder, B.E., and Spalding, D.B. (1974). The numerical computation of turbulent flows. *Computer Methods in Applied Mechanics and Engineering* 3, 269–289.
- Montazeri, H., Toparlar, Y., Blocken, B., and Hensen, J.L.M. (2017). Simulating the cooling effects of water spray systems in urban landscapes: A computational fluid dynamics study in Rotterdam, The Netherlands. *Landscape and Urban Planning* 159, 85–100.
- Neophytou, M.K.-A., Fokaides, P., Panagiotou, I., Ioannou, I., Petrou, M., Sandberg, M., Wigo, H., Linden, E., Batchvarova, E., Videnov, P., Dimitroff, B., and Ivanov, A. (2011). Towards Optimization of Urban Planning and Architectural Parameters for Energy use Minimization in Mediterranean Cities, *in* World Renewable Energy Congress, Sweden.
- Shih, T.-H., Liou, W.W., Shabbir, A., Yang, Z., and Zhu, J. (1995). A new $k-\epsilon$ eddy viscosity model for high reynolds number turbulent flows. *Computers & Fluids* 24, 227–238.
- Tominaga, Y., Mochida, A., Yoshie, R., Kataoka, H., Nozu, T., Yoshikawa, M., and Shirasawa, T. (2008). AIJ guidelines for practical applications of CFD to pedestrian wind environment around buildings. *Journal of Wind Engineering and Industrial Aerodynamics* 96, 1749–1761.
- Toparlar, Y., Blocken, B., Vos, P., Van Heijst, G.J.F., Janssen, W.D., van Hooff, T., Montazeri, H., and Timmermans, H.J.P. (2015). CFD simulation and validation of urban microclimate: A case study for Bergpolder Zuid, Rotterdam. *Building and Environment* 83, 79–90.
- UNFPA (2007). *Growing up urban*.

United Nations (2014). World Urbanization Prospects: The 2014 Revision, Highlights, *in* Department of Economic and Social Affairs.

van Hooff, T., and Blocken, B., 2010, Coupled urban wind flow and indoor natural ventilation modelling on a high-resolution grid: A case study for the Amsterdam ArenA stadium. *Environmental Modelling and Software* 25, 51–65.

The POR-FESR MEMORIA project: an integrated models-sensors approach for the air quality assessment

P.Brotto¹, L. Caponi¹, L. Brugnatti², F. Tarchino² and S. Frassetto²

¹PM_TEN srl, Genoa, Italy

²SIGE srl, Genoa, Italy

Corresponding author: P.Brotto, paolo.brotto@pm10-ambiente.it

Abstract

We present here the activity and preliminary results of the MEMORIA project, funded within the POR-FESR programme of Liguria Region, which supports industrial research and innovation actions on specific thematic areas. The project aims at the development and testing of a methodology for the air quality assessment that will integrate data from a low-cost sensors network with the results of atmospheric dispersion numerical simulations. Thus it will be provided an innovative tool for diagnostic analysis of urban pollution levels and potentially operational use for short-time forecast and early warning production, in view of the possible future application of for regulatory purposes.

1 Introduction

Air quality, especially in urban areas, is one of the most relevant environmental challenges of our time. Nowadays the harmful effects of various pollutants on human health are well known and both European (DE 2008/50) and national standards (D.Lvo 2010/155) set limits on atmospheric pollutant concentration to protect the population health. The same standards indicate and prescribe the methodologies for air quality monitoring: in the territory this is normally carried out with more or less extensive networks of monitoring stations. At the same time the standards themselves introduce the use of numerical simulation models to integrate or replace, where needed, the information provided by the networks.

It therefore appears necessary to pursue policies to protect public health and improve the quality of life and land, to put in place measures to reduce pollutant emissions and at the same time to carry out a careful and effective monitoring of the environmental impact of the most relevant emission sources.

The MEMORIA project described here is part of this context and, aims to develop an innovative approach to meet the needs described before.

The air quality monitoring by reference stations is available (and useful) in a limited number of sites and provide information that is necessarily representative of a limited portion of the surrounding area. On the other hand, numerical models simulations, which can evaluate, and possibly forecast, atmospheric pollutants concentrations on an entire geographic area, is carried out by processing statistical data calculated and cannot reproduce occasional events other than as a posteriori diagnostic analysis.

Usually the two different approaches described above (measurements and models) are adopted separately for air quality studies and evaluation (both diagnostic and predictive), choosing the one that best fit the specific case under investigation. The combined use of the two methodologies typically refers to the validation of models simulation and/or assimilation of observed data and to the use of numerical models for scenario analysis and complement of local (and sometimes partial) information provided by the measuring stations. The project aims to study a "hybrid" instrumental configuration (model-measurements) and develop a methodology to integrate in a structured way the information collected by a low-cost sensors network and the outputs produced by an urban scale atmospheric

dispersion model. The “MEMORIA tool” so obtained will be tested on a small domain (about 10 km²) located in the Genoa urban area to verify the limits of its application and to optimize its characteristics (sensors type) and configuration (station numbers and location, simulation model parameters...)

2 MEMORIA project activities and preliminary results

MEMORIA project started in September 2016 and will be concluded at the end of August 2018. It is structured in two work packages: the first (WP1), which will end within the summer 2017, includes the identification of the most appropriate configuration and the installation of the sensor network and the implementation of the simulation chain. The second (WP2) will consist in the implementation of the "instrument" as a whole, i.e. the collection and analysis of data from the sensor network, the of air quality simulations runs, and the development and application of the procedures to integrate models output and observations data.

2.1 The sensors network

Low-cost sensors represent an innovative approach to air quality monitoring based on the collection of real-time data from a large amount of monitoring sites able to describe the analysed area with higher spatial resolution. On the other side, low costs usually imply a low level of the technologies used for sensor production that affects the data reliability and stability over long time observation period.

There are currently two different configurations for the stations included in the sensor network:

- Configuration # 1 (5 stations)
 - Pollutants monitored: NO, NO₂, O₃, PM₁₀
 - Power supply: battery + mains connection
- Configuration # 2 (10 stations)
 - Pollutants monitored: NO, NO₂, O₃
 - Power supply: battery + solar panels

Considering the weak aspects of sensors measurements we decided to install the five stations in Configuration # 1 at some of the reference stations included in the Genoa Air Quality Monitoring Network currently operated by the Genoa Metropolitan City and soon transferred under Liguria Environmental Protection Agency (ARPA Liguria) management. Thus the "training" phase of sensors station, whose results are currently under analysis, will take advantage on benchmarking with more validated but consistently more demanding technologies in terms of initial and maintenance costs.

In Figure 1 we report the location of the nodes of sensors network and the area where the integrated procedure will be developed.

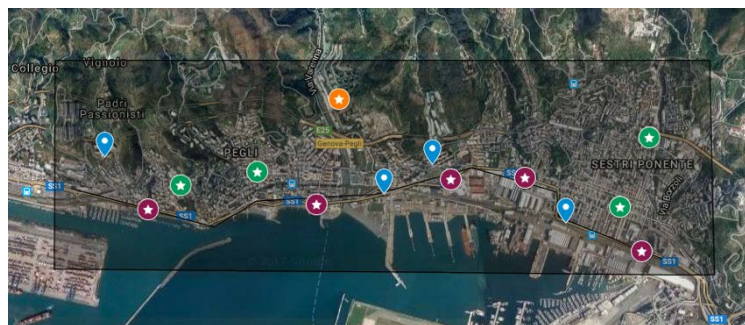


Figure 1. Sensors network (blue markers identify Configuration #1 stations; circled stars markers identify Configuration #2 stations)

Blue markers identify Configuration #1 stations. Circled stars markers identify Configuration #2 stations, whose location has been selected according to the most relevant emission sources expected to be observed, in particular:

- Purple markers sensors should be affected by road traffic emissions

- Green markers should be affected by road traffic, residential and harbour activities emissions
- Yellow marker should observe oil transport and stocking area emissions

2.2 The dispersion modelling chain

The modelling chain structure has been defined to meet the project needs. In particular, the simulation models configuration will have to provide a tool suitable for accurate diagnostic analysis (current as well as past or future scenarios evaluation) and ready to be upgraded to an operational forecasting use for the analysis of short-term pollution conditions.

The modeling chain is divided into two complementary and consequential modules:

1 – System for the assessment of the background conditions and the preservation of the atmospheric chemical balance (“background model”). The objective of the first module of the modelling chain is the definition of chemical composition and environmental background parameters. Global models with low spatial resolution can provide such kind of information with a reasonable accuracy. We are still considering the possibility to include regional scale model runs (WRF+CAMx meteo-dispersion chain) to obtain a more detailed background description.

2 - Modelling system for the simulation over high spatial resolution receptor grids to be integrated with sensor network measurement (“core model”). To obtain an air quality assessment with spatial resolution comparable to that of the sensor network described in the previous paragraph, you need to use Gaussian and / or Lagrangian models able to describe the atmospheric pollutant dispersion over a smaller scale.

The “core model” chain developed and implemented for MEMORIA project is described in the scheme below (see Figure 2) and includes:

- WRF-ARW [Skamarock *et al*] meteorological simulation code + meteorological preprocessor CALMET (U.S. EPA reference) for calculating wind flows and main boundary layer parameters
- Gaussian dispersion model CALPUFF (U.S. EPA reference) for calculating the transport and diffusion of atmospheric pollutant [Scire *et al*]

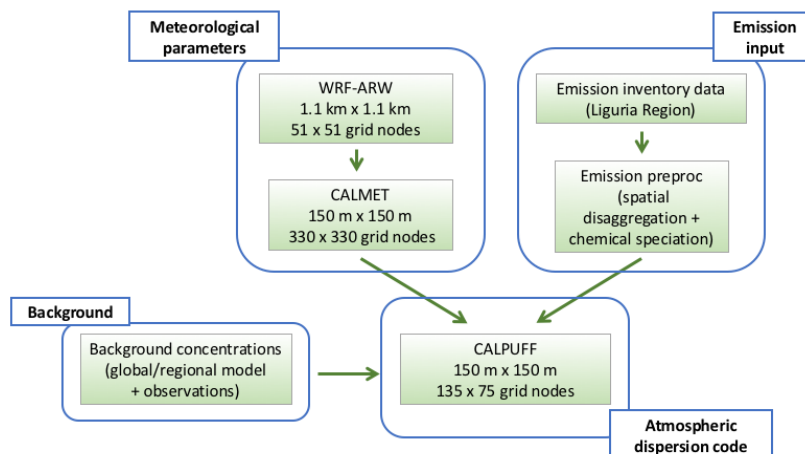


Figure 2 . The modelling structure

Emission data has been provided by Liguria Region and extracted over the analysed area from the Regional Atmospheric Pollutant Emission Inventory. Year 2011 hourly emission data are available for different sources type (1km x 1km gridded, area, linear and point) and for the main sources sectors (according to the SNAP classification).

In Figure 3 we report the simulation domain, whose overall dimension has been evaluated in accordance with the installation area and the density of the measuring points (see previous paragraph and Figure 1) balanced with the computational costs needed to perform high resolution runs.

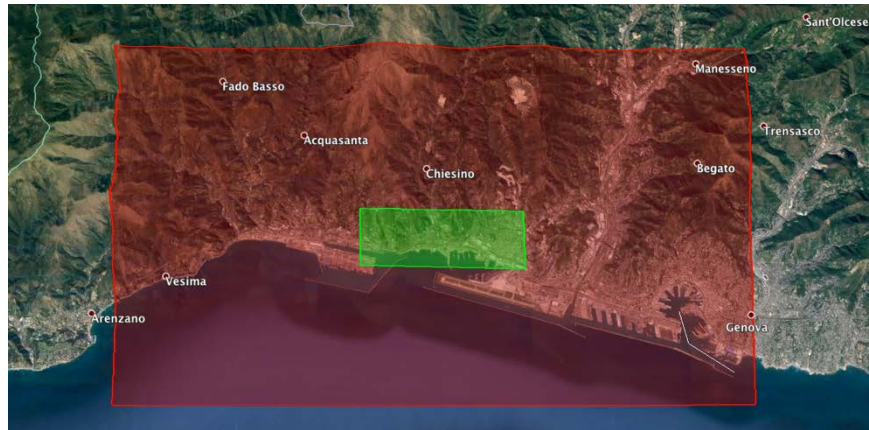


Figure 3. The modelling domain. Red area is the CALPUFF receptor grid. Green area indicate the sensors network area

3 MEMORIA expected results and future perspectives

The main results expected from the project are:

- 1) The development and in-field validation of an innovative method for assessing air quality structured in two integrated elements: a low-cost sensor network and a numerical simulation software for the atmospheric pollutant dispersion.
- 2) The development of an instrument (equipment, procedures and interface) that can exploit the above methodology to provide guidance to possible stakeholders. An “alert system” will be studied that will report in near-real-time any critical event and, within a certain degree of reliability, it may be expected to provide short-time forecast and possible early warning.

As a follow-up of the research activities we will be able to use innovative and validated technologies with two main competitive aspects:

- the ability to respond to existing demand with a greater degree of detail, more effectively classifying the nature of the issues raised
- the ability to provide, with no increase in infrastructure installation and / or management costs, more accurate and complete information than those currently available from air quality monitoring networks or operational simulation models (at regionale and/or urban scale)

Acknowledgements

The authors would like to acknowledge Dr. Zannetti and Mr Manni of the Genoa Metropolitan City for the installation of sensors on reference stations and Dr. Costi and Dr. Brescianini of Liguria Region for providing the emission inventory data.

Moreover, we would like to thank the research activity consultants for fruitful discussion and collaboration: Prof. Prati and Dr. Massabò of DIFI-Unige and INFN-Genoa, Dr. Fedi and Dr. Lima of CIMA, Prof. Capannelli and Dr. Cepolina of TICASS.

References

Skamarock W.C., Klemp J.B., Dudhia J., Gill D.O., Barker D.M., Huang X.Z., Wang W., Powers J.G. (2008). A Description of the Advanced Research WRF Version 3, Mesoscale and Microscale Meteorology Division, NCAR, Boulder, Colorado.

Scire, J.S.; Strimaitis, D.G.; Yamartino, R.J. A User’s Guide for the CALPUFF Dispersion Model (Version 5). Available online: <http://www.src.com>

Key Performance Indicators to assess the local climate potential of three passive cooling heat sinks

G. Chiesa

Department of Architecture and Design, Politecnico di Torino, Italy

Corresponding author: G. Chiesa, giacomo.chiesa@polito.it

Abstract

Energy consumption for space cooling and ventilation is a rising voice in National energy balances. The use of more efficient mechanical cooling systems may reduce, but not invert this trend. Nevertheless, possible passive cooling alternatives are able to reduce the fossil energy need for cooling. These natural solutions are based on the use of heat sinks in order to dissipate heat gains. Unfortunately, all these solutions are very local specific and need for a correct design process to be effectively applied. The paper introduces a series of comparable Key Performance Indicators (KPI) to easily assess the local climate potential of three heat sinks in reducing the “virtual” climate cooling demand calculated by using a well-recognized synthetic parameter: the cooling degree hours. The considered techniques are natural ventilation, both for comfort and structural cooling, direct evaporative system and earth-to-air heat exchanger. The paper allows to compare these solutions using local climate conditions even before the definition of a specific building in order to introduce KPIs able to be used in the definition of urban scale policies and regulations.

1 Introduction

Building stocks are responsible for more than 40% of total primary energy consumptions in industrialized countries (Cuce and Riffat, 2016). A huge amount of these consumptions are due for heating and cooling of internal spaces, a voice than in the U.S. was calculated to reach for the residence sector alone 11.5% of total energy consumptions (Logue et al., 2013). Between these two voices, the percentage of energy devoted to space cooling is rising quickly and is expected to overpass the heating one after 2050 (Isaac and Vuuren, 2009). Globally, the total consumption for cooling already reached in 2010 the impressive amount of 1.25 PWh (Santamouris, 2016). Furthermore, the air conditioner market is growing fast, both in industrialized and emerging countries (Daikin, 2015). As an example, the forecast for air conditioners installed in Chinese warm provinces is expected to overpass 120 millions of units by 2017 (source IEA, 2007).

These trends ask for alternative solutions to reduce the consumptions of not-renewable sources for space cooling, e.g. by using passive or hybrid technologies. Passive cooling, which is less diffused if compared to passive heating due to its very site specific nature based on a large amount of different solutions, is based on two main families of strategies: thermal control and natural cooling techniques (heat sinks) (Grosso, 2017). The first category refers to heat gain prevention (e.g. shading devices) and to heat gain modulation (attenuation and time lag of thermal waves). Differently, the second category includes solutions to the heat gain dissipation by using renewable sources to generate cooling inputs to reduce the space temperature below the external one and dissipate solar and internal gains (Givoni, 1994). Main passive cooling dissipative techniques refer to four thermal sinks: environmental air (Controlled Natural Ventilation - CNV including comfort, environmental and structural cooling); water (Direct and Indirect evaporative cooling); Ground (Earth-to-fluid heat exchangers); and night sky (Radiative cooling). Solutions relative to natural dissipative technologies are analysed in this paper. In Section 2 are introduced specific Key Performance Indicators (KPI) to assess the climate local potential of three different heat sinks (air, water and soil). Finally, in Section 3 these KPIs are applied to five sample locations in Europe (Berlin, Wien, Rome, Madrid, and Lisbon).

2 Proposed Key Performance Indicators to assess the climate potential of passive cooling solutions

This paper describes four KPIs to assess the local climate-related potential of respectively controlled natural ventilation for comfort ventilation (CNV), ventilation for structural night cooling (NV), direct evaporative cooling towers (DEC), and earth-to-air heat exchangers (EAHX).

The proposed methodology, which was demonstrated to be effective in a previous work (Chiesa and Grosso, 2015), analyses the climate potential of a passive heat sink by calculating its “virtual” effect on the reduction of the local climatic cooling demand. This climate-related demand may be effectively represented by the Cooling Degree Hours – CDH – indicator, considering, for the purpose of this paper, a base temperature of 22°C, calculated in an extended summer period (from May to October) in order to be applied in different climatic conditions (see Eq. 1). Nevertheless, considering specific conditions or standards, different base temperatures may be assumed (Mourshed, 2012).

$$CDH_{22} = \sum_{hr} (\vartheta_e - 22)^+ \quad (1)$$

Hence, the climate cooling potential of a passive solution can be described as the difference between the original CDH_{22} and the residual CDH_{22-res} calculated after the “virtual” effect of the considered heat sink on the external air by substituting the dry bulb external temperature (ϑ_e) with the treated air temperature (ϑ_{treat}). A possible source for local temperature data may be the Typical Meteorological Year (TMY) such as the ones used by dynamic energy simulation software (e.g. EnergyPlus and Trnsys) or included in devoted database (e.g. Meteonorm).

2.1 Controlled natural ventilation – Comfort ventilation and night ventilation

To assess the potential of ventilative cooling strategies several KPIs were developed – see e.g. (Kolokotroni and Heiselberg, 2015). Nevertheless, this paper will consider one recently developed KPI able to analyse the effect of air movements on the comfort perception considering the “virtual” perceived temperature reduction as a function of the airflow velocity as defined by ASHRAE in 1989 (Grosso, 2017). The treated air temperature ($\vartheta_{treat,CNV}$) can be calculated using Eq. 2, derived by regressing the ASHRAE mentioned relation and limiting the maximum air velocity to simulate a control strategy in window opening (Chiesa and Grosso, 2015).

$$\vartheta_{treat,CNV} = \vartheta_e - \begin{cases} 2.319 * v_{air} + 0.4816 \Rightarrow v_{air} \leq 1m/s \\ 2.319 * 1 + 0.4816 \Rightarrow v_{air} > 1m/s \end{cases} \quad (2)$$

Using the “virtual” treated air temperature, it is possible to calculate the CNV residual $CDH_{22-res,CNV}$ for comfort ventilative cooling.

Furthermore, a different indicator able to estimate the effect of structural ventilative night cooling (NV) can be calculated by analysing the daily temperature variations in order to calculate the residual $CDH_{22-res,NV}$ (Chiesa and Grosso, 2015) –see Eq. 2–.

$$CDH_{22-res,NC} = \sum_{day} \left(\sum_{hrs,cd} (\vartheta_e - 22)^+ + \left(\sum_{hrs,NC} (\vartheta_e - 22) \right) * \eta_{EF} \right)^+ \quad (2)$$

Where hrs,cd are the number of hours of the day in where cooling is needed ($\vartheta_e > 22^\circ C$), hrs,NC is the number of hours of the day in where a night cooling potential is present ($\vartheta_e < 22^\circ C$), and η_{EF} is an exploitation factor able to consider a “virtual” thermal capacity of building mass, here assumed as 0.5. In order to compare all KPIs and verify their combinations, the used KPI for ventilative cooling will be the one relative to comfort ventilation.

2.2 Passive draught evaporative cooling

To assess the potential of DEC systems, such as Passive Draught Evaporative Cooling towers (Ford et al., 2010), the treated air temperature ($\vartheta_{treat,DEC}$) can be fixed as the expected outlet temperature (Chiesa, 2016). The treated outlet temperature can be calculated using Eq. 3, see also

(Givoni, 1994), which was demonstrated to be the most effective in comparison to other simplified calculation expressions (Chiesa and Grosso, 2015b). The *slope* value may be assumed, for early evaluations, between 0.7 and 0.8, as was demonstrated in the same paper.

$$\mathcal{G}_{treat,DEC} = \mathcal{G}_e - slope * (\mathcal{G}_e - \mathcal{G}_{e,WBT}) \quad (3)$$

The evaporative cooling potential is due to the local wet bulb depression – the difference between the environmental dry bulb and wet bulb ($\mathcal{G}_{e,WBT}$) temperatures (see also Chiesa et al., 2017; Salmeron et al., 2012).

2.3 Earth-to-air heat exchanger

The treated air temperature ($\mathcal{G}_{treat,EAHX}$) to assess the potential of a EAHX system can be calculated by substituting, in the EAHX efficiency equation – see (Givoni, 1994) – the expected temperature of the soil at a given depth in the same instant of the year e.g. by using the Hadvig equation– see Eq. 4.

$$\mathcal{G}_{treat,EAHX} = \mathcal{G}_e - \varepsilon * \left(\mathcal{G}_e - \left(\mathcal{G}_{sf,av} + A_s \cdot \exp \left(-h \sqrt{\frac{\pi}{\alpha \cdot 31536000}} \right) \cos \left(\frac{2\pi}{t_0} \cdot (t - t_{max}) - h \sqrt{\frac{\pi}{\alpha \cdot 31536000}} \right) \right) \right) \quad (4)$$

Where ε is an efficiency factor assumed as 0.7 (Chiesa, 2017), $\mathcal{G}_{sf,av}$ is the yearly average temperature of the ground surface, A_s is the semi-variation of the annual ground surface temperature, h is the EAHX depth, α is the ground diffusivity, t is the instant of calculation from the beginning of the year in seconds, and t_{max} is the phase shift constant.

3 Sample applications

As mentioned in Section 1, for this paper five locations were analysed considering their climate-cooling requirements (CDH_{22}) and their “virtual” residual CDH_{22-RES} expected when CNV, PDEC and EAHX are used. A “virtual” optimisation algorithm was simulated by choosing, for each of the considered KPI, the better hourly condition between CDH_{22} and CDH_{22-res} . Furthermore, to calculate the EAHX KPI, a wet clay soil was assumed considering a ground diffusivity of $6.18E-07 \text{ m}^2/\text{s}$ and a depth for EAHX of 3m. Differently, to define the PDEC KPI a slope value of 0.7 was considered.

Figure 1 shows the values of CDH_{22} and CDH_{22-res} considering the “virtual” effect of each heat sinks on the expected climate cooling demand (EnergyPlus weather database).

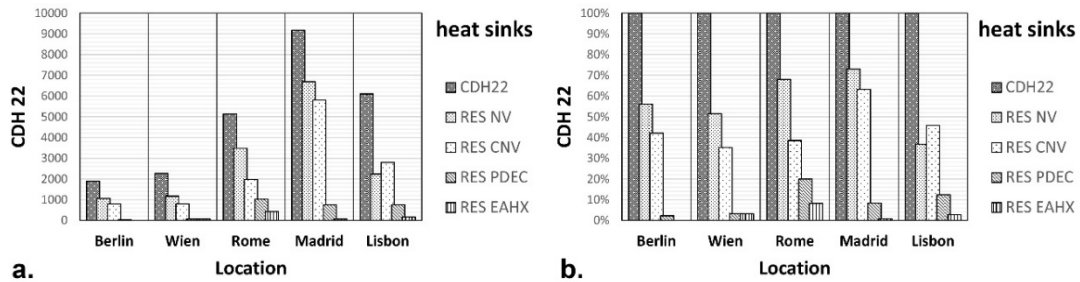


Figure 1. CDH_{22} and “virtual” CDH_{22-res} for each technique for the five considered locations both in (a) absolute values and (b) relative ones.

The graphs illustrate that ventilation alone may significantly reduce the climate cooling requirement especially in those locations in where a significant daily temperature fluctuation is registered. If a higher base temperature for calculating the climate cooling potential is considered (e.g. 26°C), in colder locations a higher potential for passive ventilative cooling is expected (see Chiesa and Grosso, 2015). Nevertheless, the other thermal sinks, able to reduce the air temperature further below the environmental one, show a very good “virtual” climate applicability. EAHX systems may constitute a good passive/hybrid source for low-energy cooling of spaces.

4 Conclusion and limitations

The paper proposes a simple methodology to assess the local cooling climate-related potential of three heat sinks. Results show that the proposed KPIs can be directly compared and/or combined (CNV, PDEC, and EAHX); while the one proposed for the night ventilation is based on a different time step (daily mean). The proposed KPIs differ for other indicators because they can be applied even before any building definition. Hence, they can be used at urban and territorial scales to define policies and incentives based on local climate issues. Nevertheless, further analyses have to be performed in order to better define boundary conditions and limits of the proposed methodology. Nevertheless, the proposed set of indicators has been partially validated in previous studies showing good correlations with monitoring data (EAHX, PDEC) and energy dynamic simulations (CNV). Finally, a more complete study is under development considering further KPIs, a larger comparison with monitored and simulated data, and applications by using Geographic Information Systems.

References

- Cuce, P.M., and Riffat, S. (2016). A state of the art review of evaporative cooling systems for building applications. *Renew. Sustainable Energy Rev.* 54, 1240-1249.
- Chiesa, G., and Grosso, M. (2015a). Geo-climatic applicability of natural ventilative cooling in the Mediterranean area. *Energy Build.* 107, 376-391.
- Chiesa, G. (2017). Climate-potential of earth-to-air heat exchangers. *Energy Procedia*, in press – accepted CISBAT 2017.
- Chiesa, G. (2016). Geo-climatic applicability of evaporative and ventilative cooling in China. *Int. J. Vent.* 15(3-4), 205-219.
- Chiesa, G., and Grosso, M. (2015b). Direct evaporative passive cooling of building. A comparison amid simplified simulation models based on experimental data. *Build. Environ.* 94, 263-272.
- Chiesa, G., Huberman, N., Pearlmutter, D., Grosso, M. (2017). Summer discomfort reduction by direct evaporative cooling in Southern Mediterranean areas. *Energy Procedia* 111, 588-598.
- Ford, B., Schiano-Phan, R., and Francis, E., eds, (2010). The architecture & engineering of draught cooling: A design sourcebook. PHDC press.
- Grosso, M. (2017). Il raffrescamento passivo degli edifici in zone a clima temperato. IV edn. Maggioli.
- Givoni, B. (1994). Passive and low energy cooling of buildings. Van Nostrand Reinhold.
- Isaac, M. and van Vuuren, D.P. (2009). Modeling global residential sector energy demand for heating and air conditioning in the context of climate change. *Energy Policy* 37, 507-521.
- Kolokotroni, M., and Heiselberg, P., eds, (2015). IEA ANNEX 62 - Ventilative Cooling: State-of-the-Art Review. Department of Civil Engineering, Aalborg University.
- Logue, J.M., Sherman, M.H., Walker, I.S., Singer, B.C. (2013). Energy impacts of envelope tightening and mechanical ventilation for the U.S. residential sector, *Energy Build.* 65, 281–291.
- Mourshed, M. (2012). Relationship between annual mean temperature and degree-days. *Energy Build.* 54 (12), 418-425.

Salmeron, J.M., Sánchez, F.J., Sánchez, J., Alvarez, S., Molina, L.J., & Salmeron, R. (2012). Climatic applicability of draught cooling in Europe. *Archit. Sci. Rev.* 55, 259-272.

Santamouris, M. (2016). Cooling the buildings – past, present and future. *Energy Build.* 128, 617-638.

Early-design method to localize outdoor activities on microclimate criteria

G. Chiesa and M. Grosso

Department of Architecture and Design, Politecnico di Torino, Italy

Corresponding author: G. Chiesa, giacomo.chiesa@polito.it

Abstract

A sustainable approach considering environmental parameters such as wind and solar access/protection has gaining increasing importance in urban design due to the urgent need to cope with the effects of global warming and urban heat island. An analytical method is presented here, based on the application of microclimate matrixes as evaluation tools for choosing the localisation of outdoor activities as well as new building construction placement. This approach, experimented in a didactical experience for architecture students, can also be applied by urban design professionals.

1 Introduction

Considering the large amount of primary energy consumed by the building sector, low energy and environmental strategies to reduce this voice of consumption are essential. Several actions were assumed to reduce the energy consumption in buildings – e.g. nZEB EU Directives as the 2010/31/EU on Energy Performance of Buildings (EPBD) for Europe. Furthermore, a great importance is recognised to low-energy, eco-friendly and environmental design strategies in the entire design process. Efforts have been exerted so far for reducing energy consumption in the winter season. This is obtained by: increasing the performance of building envelope; substituting low efficient with higher efficiency technical building systems; and applying passive/low-energy heating solutions, i.e., sunspaces, increased solar gains, thermal solar panels. Nevertheless, a lower number of actions have been applied for the summer season. It was demonstrated that air conditioners reached 25% of total electrical consumptions in the residential sector in industrialised countries (Daiking Industries 2015) and that the total amount of consumed energy for cooling is one of the most growing voices in building energy consumption (Santamouris, 2016). For these reasons, it is important to increase dissemination of environmental and technological strategies, tools, and solutions regarding not only solar heating, but also space cooling and controlled natural ventilation, adding as well interest in building design for users' comfort conditions.

Even if this introduction is principally focused on indoor spaces, a similar bioclimatic approach can be adopted also to design outdoor spaces around buildings. Especially from a microclimate point of view, the variables to be considered are comparable (e.g. solar and wind access) even if the requirement-driven localisation of activities may differ. This paper will discuss a simple method to assess, since early design stages, the optimisation of site localisation of activities both outdoor and indoor.

2 The proposed methodology

The method described in this paper is part of a more complex procedure able to introduce, evaluate and optimise environmental and technological criteria in the design process, considering a performance-driven approach and feed-back cycles. This process, also tested and implemented during didactical activities, is illustrated in (Chiesa and Grosso, 2017).

In order to define the design phases of site analysis and building programming, it is necessary to set specific indicators and requirements. These are related to standards, modal classification and related functional units, energy, materials and waste flows matrixes, and a virtual spatial configuration. See (Grosso and Chiesa, 2015) for a list of environmental, economic and social requirements related to sustainability in buildings according to ISO/DIS 21929-2.

Considering outdoor activities, several aspects may be taken into account to guarantee comfort conditions according to a specific framework of needs. In outdoor spaces, limited solutions may be assumed to control the environmental temperature and humidity (heat gain dissipation or increase) – even if some systems may be considered, i.e. for summer evaporative cooling systems as shower towers or porous media (Ford et al., 2010). Nevertheless, several design solutions may help to reduce possible discomfort, e.g., by using vegetation, adopting shading devices, and specific finishing materials and colours. See, for example (Dessi, 2007). Furthermore, the reduction of outdoor temperature in summer due to the effect of vegetation may also constitute a pre-cooling phase for naturally ventilated spaces (Perini et al., 2017). In this paper, a preliminary site analysis is presented and detailed for outdoor activities.

3 Site analysis for activities' localisation

According to the methodology shortly introduced in Section 2, a possible procedure to classify a plot area for activity localisation is the use of site microclimate matrixes. This approach was firstly described by (Brown and Dekay, 2001) and further implemented by (Grosso, 2017) including a procedure to evaluate wind calm zones due to obstacles. A site microclimate matrix evaluates a construction plot according to two Boolean variables: solar access and wind exposition. The four resulting classes subdivide the plot in zones that can be scored differently according to the specific environmental requirement framework of each considered activity. The analysis has to be implemented in representative days of the years and hours able to synthetize the environmental conditions of the plot. Hence, the calculation procedure can be subdivided in the following steps:

- definition of the plot, obstacles and activities to be localized;
- calculation of the shading profile on the plot due to obstacles in representative days and hours – i.e. 21st of December at 10:00 and 14:00; 21st of June at 8:00 and 16:00 (local solar time);
- calculation of the wind calm zones –wind velocity reduction of more than 50%– due to obstacles for the prevalent wind direction(s) considering at least seasonal variations, even if for specific locations and sites night and day cycles must be considered (e.g. coastal sites, valley sites);
- definition of the site microclimate matrix for each representative days and hours by overlapping the two previous analyses;
- scoring of each matrix according to the list of requirements related to the considered activities and consequent needs;
- yearly or seasonal sum of the score for each activity in order to define a priority suggestion for site design and activity planning.

The calculation of shading profiles may be done manually, or automatically using devoted software. Differently, the definition of calm zones needs a more complex analysis. This calculation may be conducted using Computational Fluid Dynamic software, which generally are expensive in terms of both time and costs, or by using a simplified procedure based on geometrical fitting (Chiesa and Grosso, 2015) of wind tunnel and CFD results (Boutet, 1987) – e.g. Fig. 1. This procedure, specifically described in the mentioned references, has been recently automatised by developing a code scripted in the Grasshopper™ environment in order to calculate the calm zones of a parallelepiped obstacle in the Rhinoceros® CAD environment (Chiesa and Grosso, 2017b).

The scoring system used to classify site microclimate matrixes has to be defined for each activity or typology of activities as well as for each building or type of building. In particular, a classification to localise correctly new buildings may be assumed using different sources, in relation to specific building aspects such as climate conditions, environmental activity needs, building typology, expected amount of internal and external gains (Grosso, 2008; Brown and Dekay, 2001). Figure 2 reports the

application of the method based on microclimate matrixes (Fig. 2a), to a building plot in Turin for the localisation of a student house (Fig. 2b), developed as a case study during the Environmental and Technological Design course at the Politecnico di Torino.

Wind wake core depth for different wind incident angles: H is the relative height of the obstacle (4x1x1H)

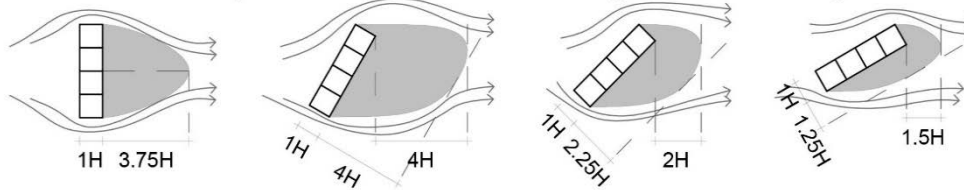


Figure 1. Sample wind wake core dimensions according to different wind incident angles (wind tunnel testing by Boutet, 1987) before the fitting analysis used in the proposed methodology (e.g. Chiesa and Grosso, 2015)

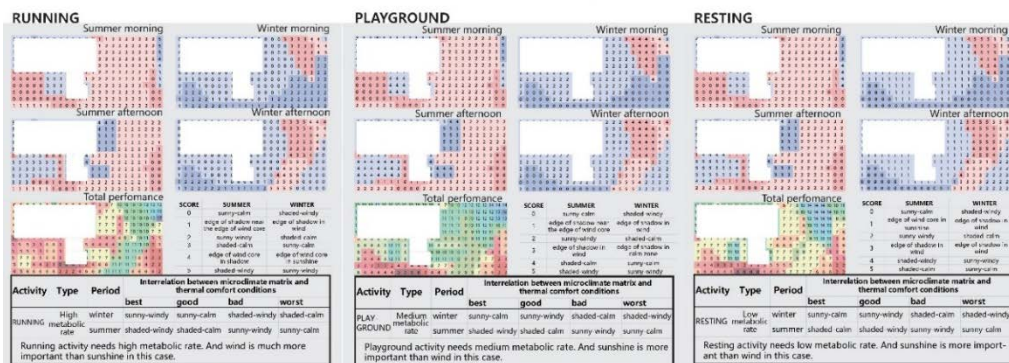


Figure 2. (a) Sample application of the site microclimate matrix tool to (b) environmentally score the building localisation in a plot and, after the definition of a virtual building configuration, to (c) score the virtual localisation of different outdoor activities (high metabolic rate – running; medium metabolic rate – playground; low metabolic rate – resting) (students: Group No. 5 Luyang, C., Yun, C. and Siyu, C., A.Y. 2016-17)

Table 1. A possible scoring system to define the optimum localisation of outdoor activities according to their metabolic rate (elaborated from Chiesa and Grosso, 2015; Grosso, 2008). Score values varies from 1 to 4.

Activity	Season	Site microclimate matrix classes of exposure [solar-wind] – exposed = 1; protected = 0			
		[0-0]	[0-1]	[1-0]	[1-1]
Winter (cold wind)		2 (3)	1 (1)	4 (4)	3 (2)
Summer (high RH%)		4 (2)	3 (4)	1 (1)	2 (3)
Winter (cold wind)		2 (3)	1 (1)	3 (4)	4 (2)
Summer (high RH%)		3 (2)	4 (4)	1 (1)	2 (3)
Winter (cold wind)		1 (3)	2 (1)	3 (4)	4 (2)
Summer (high RH%)		3 (2)	4 (4)	1 (1)	2 (3)

Differently, outdoor activities can be generally classified according to their relative expected metabolic rate: high, medium, or low (see Fig. 2c). Table 1 reports a possible scoring for each

metabolic class, although different scores may be applied for specific activities considering the peculiar framework of needs (e.g. a bar's dehors may differ from a bench for specific activities and environmental needs). Different comfort models may be assumed to define a scoring system to evaluate the two Boolean considered variables, even if the majority of the used charts and expressions are relative to indoor conditions (see for example Santamouris and Asimakopoulous, 1996; Pellegrino et al., 2016).

4 Conclusions

The proposed methodology is a simplified method to early define and include in the design process environmental needs. In this paper, it was demonstrated that the method can be easily applied also to early localisation of outdoor activities using a scoring system related to the activity metabolic rate. At present, the wind wake core calculation can be applied to simple building shapes (parallelepiped, L, T, U shapes) and in specific geometrical boundaries (e.g. for parallelepipeds $0.125 \leq \text{width/height} \leq 10$; $1 \leq \text{length/height} \leq 8$). Although, implementations are under development to increase present boundaries and to define an automatic system to optimise outdoor activity localisation according to environmental requirements including different comfort indexes.

References

- Boutet, T. (1987). Controlling air movement. A manual for architects and builders. McGraw-Hill
- Brown, G.Z., and Dekay, M. (2001). *Sun, Wind & Light*. John Wiley & Sons.
- Chiesa, G., and Grosso, M. (2017). Environmental and Technological Design: a didactical experience towards a sustainable design approach. *XV forum Le vie dei Mercanti, 15-17 June, Naples-Capri*.
- Chiesa, G., and Grosso, M. (2017b). A parametric tool for assessing optimal location of buildings according to environmental criteria. *IV Med Green Forum, 31 July-2 August, Florence*.
- Chiesa, G., and Grosso, M. (2015). Accessibilità e qualità ambientale del paesaggio urbano. La matrice microclimatica di sito come strumento di progetto. *Ri-Vista* 13(1), 78-91.
- Dessi, V. (2007). Progettare il comfort urbano. Sistemi Editoriali.
- Ford, B., Schiano-Phan, R., and Francis, E., eds, (2010). The architecture & engineering of downdraught cooling: A design sourcebook. PHDC press.
- Grosso, M. (2017). Il raffrescamento passivo degli edifici in zone a clima temperato. IV edn. Maggioli.
- Grosso, M. (2008). Progettazione bioclimatica. In Castelli, L., ed, *Architettura sostenibile*. UTET, 6-40.
- Grosso, M., and Chiesa, G. (2015). Environmental indicators for evaluating properties. *Territorio Italia* 15(2), 63-74.
- Pellegrino, M., Simonetti, M., and Chiesa, G. (2016). Reducing thermal discomfort and energy consumption of Indian residential buildings: Model validation by in-field measurements and simulation of low-cost interventions. *Energy Build.* 113, 145-158.
- Perini, K., et al. (2017). The use of vertical greening systems to reduce the energy demand for air conditioning. Field monitoring in Mediterranean climate. *Energy Build.* 143, 35-42.

Santamouris, M. (2016). Cooling the buildings – past, present and future. *Energy Build.* 128, 617-638
Santamouris, M., and Asimakopoulous D., eds (1996). *Passive cooling of buildings*. James and James.

Mathematical Generative Approach on Performance Based Urban Form Design

A.Chokhachian¹, K. Perini², S. Giulini², T. Auer¹

¹ Chair of Building Technology and Climate Responsive Design, Faculty of Architecture
Technical University of Munich, Germany

²Architecture and Design Department, University of Genoa, Italy

Corresponding authors: ata.chokhachian@tum.de, kperini@arch.unige.it

Abstract

The research proposes a mathematical generative methodology to identify performance linking urban forms and density indicators. Selected performance criteria for this preliminary study are shadow factor (on the public ground) and Urban Heat Island effect. The results are interpreted based on the mathematical correlation between building form factors and environmental qualities, depending on the building density, to identify the most performing cases by means of parametric design. The study shows that, in the case of buildings with square foot print, UHI is highly dependent on height of urban canyon and optimum shade factor is achievable with intermediate canyon width.

1 Introduction

Cities could be considered as live structures with complex metabolism including different scales changing over time. Solving this equation, designing and programming a liveable city could be achievable by rising quality of urban spaces. Talking about qualities in general could be a never ending discussion since qualities are always objective phenomena. However transforming quality into performance indicators could be a substitute translation to give more understandable sense and scale to measure assets of urbanity.

Thinking about environmental qualities will raise couple of keywords like: building shape factor, indoor solar access, outdoor comfort, urban heat island effect, sky view factor and etc. (Oke, 1982). Additional layer beside these qualities is the density, which has extremely direct exchange on the performance of the urban entities. Combining density factors with performance qualities will allow the designers and planners to understand and justify extreme bounds and consequences of rapid urbanization to look for optimized solution (Ng, 2010). To understand the correlation between urban form and performance through generic methods there are several directions to follow. Ratti, Raydan, and Steemers (2003) analyzed and compared the archetypes in terms of built potential and day lighting criteria as well as Surface to volume ratio, Shadow density and daylight distribution and Sky view factor with question of which building forms make the best land use? The suggestions indicate; larger surface area and high thermal mass, daylight via the courtyard and shallow plan form, narrow spaces for shade and improved thermal and comfort despite increased heat island. Balling, Taber, Brown, and Day (1999) used genetic algorithm was used to search for optimal future land-use and transportation plans for a high-growth city with the objective of minimization of traffic congestion and costs to control air pollution. Austern, Yu, Moral, and Jirathiyut (2014) suggested a framework for generating environmentally adapted urban tissue by using genetic algorithms as form-finding processes of environmental optimization considering solar exposure on the streets and facades, rate of wind flow on the pedestrian level and emergent pathways.

Looking back to the history and starting point of generative design, Mehaffy (2008) assesses the progress of generative methods in urban design and finds the roots in the ideas of Christopher Alexander about pattern language (Alexander, 1979). Alexander developed “laws of wholeness” with detailed structural logic, to propose a method by which this quality can be attained again in a

contemporary context – not through a conventional kind of master plan, but through a process involving the sequential collaboration of a series of participants, and such a method could be described as generative. However seems the fact is happening recently dependent on computer science achievements offering variety of tools and efficient computation power. Within such an approach the collaborating participants will together generate an evolving form that grows out of a complex transformation of the existing context, together with all its environmental, social, and cultural factors. Such a generative process is continuous, and cannot be frozen in a standardized master plan (Mehaffy, 2008).

Accordingly, the present study explores generative approach based on environmental and performance indicators measuring weight and value of each parameter on the final equation of the urban form. The aim of this approach is to focus on the form dependent performances criteria in urban context. The proposed and implemented parametric model could be used to generate desired set of urban forms to have holistic understanding performance and design proposal in the early stages of urban planning. In this study two main outdoor factors selected to simulate and measure performance. First, Urban Heat Island as temperature difference between urban and rural areas, and second shade factor with the definition of shade benefit on the pedestrian area on the public ground.

2 Methodology

2.1 Generative Approach & Rules

The concept of generative design is based on the incorporation of system dynamics into the production of experience and it offer a methodology to look to the facts in terms of dynamic processes and their outcomes. The generative methodology is an unconventional way of conceptualizing and working in design (McCormack, Dorin, & Innocent, 2004), However, generative systems are relevant to contemporary design practice in a variety of ways and intentions. The integration of generative concepts into the design process allows the development of novel design proposals through iterational workflows, which are not easy to achieve via other methods.

Application of generative approach for creating urban forms is not entirely new method however coupling it with performance indicators could be the added value. The current workflow is being developed in Grasshopper (visual programming interface) to generate parametric and iterative urban forms. Additional tool is scripted and implemented in Python to calculate urban heat island and shade factor from derived urban forms. Recording the output data was also important for each iteration, so the workflow after each generation and performance calculations, writes results to CSV files in real time. Afterward these outputs could be processed to generate visual map and also apply statistical methods to find correlations between inputs and outputs (Figure 1). In order to control amount of variants and to avoid specious outputs set of boundary circumstances are defined:

Simulation Area	Blocks	Block number	Floors	Window to wall Ration (WWR)	Height per floor
200 × 200 m	16 < x < 28 m	9-16-25	5 to 20	0.3 - 0.5 - 0.7	3.2 m

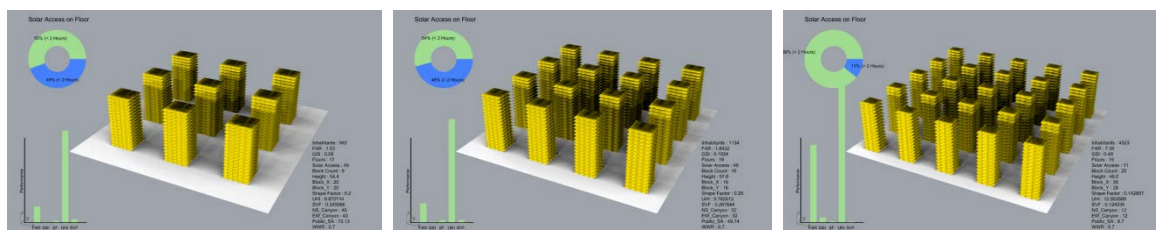


Figure 1: Visual interface of urban forms and simulation parameters

For building density factor, the floor area ration (FAR) is calculated which represents the relation between the total area and the floor area (Berghauser Pont & Haupt, 2010). For performance indicators the shadow factor (SF) for public ground is calculated considering the pedestrian area shaded at least 50% of the day on the 21st of each month of the year in Munich, Germany. The urban heat island (UHI) is calculated using formula(1), where W is the canyon width, H is the canyon height (Oke, 1981).

$$UHI = \Delta T_{u-r} = 7.45 + 3.97 \times \ln (H \div W) \quad (1)$$

2.2 Data analysis and statistical approach

In order to identify the correlation between performances (UHI and shadow factor) with geometric outputs (FAR, canyon height, width, building size, WWR and etc.) the recorded data is elaborated by means of a statistical approach. Due to high number of different configurations (600 cases), a valid interpolation between the parameters investigated, i.e. between UHI-FAR and SF-FAR, is not always obtainable. Therefore, three different groups are identified according to canyon width (w) and building size (x) and the results are analyzed consequently: $x + w = 40$, $x + w = 48$ and $x + w = 60$ m. In this manuscript, the results related to the $x + w = 60$ configurations with square building footprint are specifically presented.

3 Results and discussion

The geometric parameters, i.e. width of the canyon, buildings dimensions, and the relation between these two parameters (sum and ratio) highly influence shadow factor and urban heat island values (Table 1). Figure 2 shows that the shadow factor (SF) mainly depends on the canyon width (w). SF is higher when the width of the canyon is increasing, with a linear dependency and high reliability. For the same canyon width (w), the variability of SF is low for deep canyons (40-45 meters) and narrow ones (up to 20). Differently, the variability is higher with intermediate width canyon. Figure 3 focuses on the results related to the $x + w = 60$ m configurations. Results highlight that SF depends on the ratio between w and x. Thanks to this graph it will be possible to identify the most performing configuration for different FAR values, according to w/x ratio and number of floors, in terms of shadow factor. As shown in Figure 4, in a similar way it is possible to identify the most performing $x+w=60$ m configuration (canyon width and number of floors) in terms of UHI for different FAR. Indeed, UHI depends highly on the height of the canyon. Eq. (2) defines the relation between UHI and FAR.

$$UHI = 7,45 + 3,97 \log e \left(3,2 FAR \frac{\left(1 + \frac{w}{x}\right)^2}{w} \right) \cong 12,08 + 3,97 \left(\log e FAR + 2 \log e \left(1 + \frac{w}{x} \right) - \log e W \right) \quad (2)$$

Table 1. Geometric parameters and related SF (average and standard deviation) and UHI (range) values.

w Canyon (m)	x Block (m)	W + X (m)	W / X (m)	average SF (%)	STDEV-SF	UHI Range (°C)
12	28	40	0.43	8,83	0,23	8,59-14,10
16	24	40	0.67	14,02	1,76	7,45-12,95
20	20	40	1.00	21,57	6,17	6,56-12,07
24	16	40	1.50	33,19	12,25	5,84-11,84
20	28	48	0.71	24,16	4,66	6,56-12,07
24	24	48	1.00	32,23	8,13	5,84-11,84
28	20	48	1.40	44,00	11,27	5,23-10,73
32	16	48	2.00	63,37	11,50	4,70-10,20
32	28	60	1.14	53,06	8,49	4,70-10,20
36	24	60	1.50	64,80	0,04	4,23-9,73
40	20	60	2.00	77,72	5,42	3,81-9,32
44	16	60	2.75	89,14	1,57	3,43-8,94

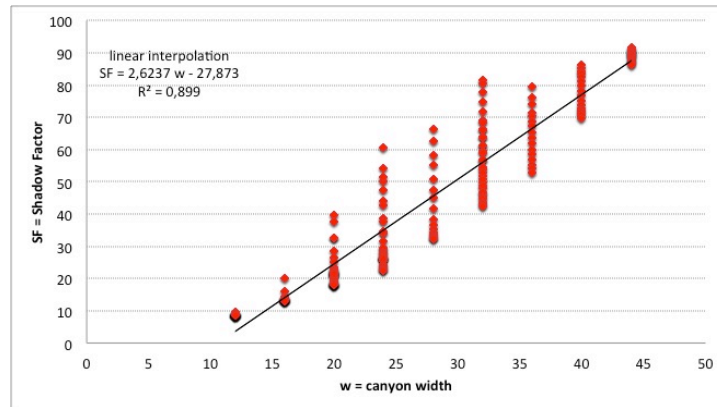


Figure 2: dependency of shadow factor on canyon width (all urban configurations analyzed)

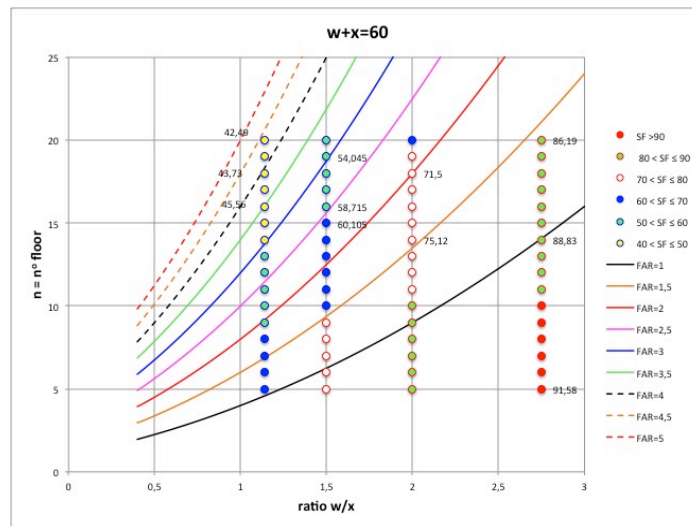


Figure 3: dependency of shadow factor and floor number on FAR for the cases where width of the canyon and size of the building is equal to 60 m.

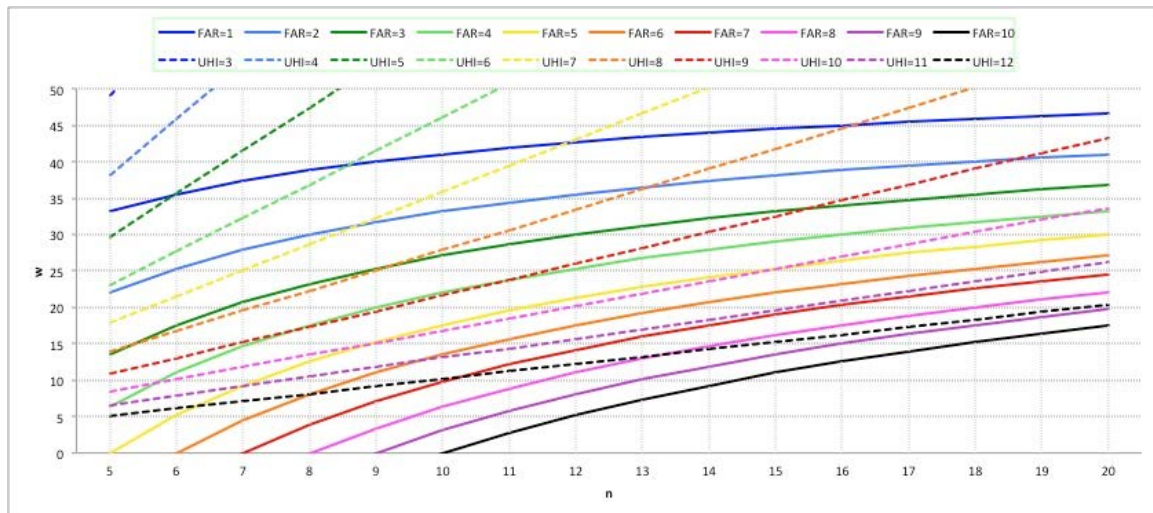


Figure 4: relation between canyon width (w) and number of floors (n) and FAR and UHI, for the cases where width of the canyon and size of the building is equal to 60 m.

4 Conclusions

Generative framework explained so far could clearly highlight dependencies of urban form on environmental performance criteria. This approach could be applied for any location to propose a guideline for optimum performing densities within each context. The mathematical dependency uncovers main role playing parameters in urban design and planning. As highlight, due to high correlation of UHI and density, the proposed equation can predict UHI potential based on floor area ratio of each neighborhood.

References

- Alexander, C. (1979). *The timeless way of building*. New York: NY: Oxford University Press.
- Austern, G., Yu, S., Moral, M., & Jirathiyut, T. (2014). *The Urban Genome*. Paper presented at the 19th International Conference on Computer-Aided Architectural Design Research in Asia (CAADRIA 2014), Kyoto.
- Balling, R. J., Taber, J. T., Brown, M. R., & Day, K. (1999). Multiobjective Urban Planning Using Genetic Algorithm. *Journal of Urban Planning and Development*, 125(2), 86-99. doi: doi:10.1061/(ASCE)0733-9488(1999)125:2(86).
- Berghauser Pont, M., & Haupt, P. (2010). *Spacematrix : space, density and urban form*. Rotterdam: NAI Publishers.
- McCormack, J., Dorin, A., & Innocent, T. (2004). *Generative design: a paradigm for design research*. Paper presented at the Futureground, Design Research Society, Melbourne.
- Mehaffy, M. W. (2008). Generative methods in urban design: a progress assessment. *Journal of Urbanism*, 1(1), 57-75.
- Ng, E. (2010). *Designing high-density cities: for social and environmental sustainability*. (E. Ng Ed.): Routledge.

Oke, T. R. (1981). Canyon Geometry And The Nocturnal Urban Heat-Island - Comparison Of Scale Model And Field Observations. *Journal of Climatology*, 1(3), 237-&.

Oke, T. R. (1982). The energetic basis of the urban heat island. *Quarterly Journal of the Royal Meteorological Society*, 108(455), 1-24. doi: 10.1002/qj.49710845502.

Ratti, C., Raydan, D., & Steemers, K. (2003). Building form and environmental performance: archetypes, analysis and an arid climate. *Energy and Buildings*, 35(1), 49-59. doi: [http://dx.doi.org/10.1016/S0378-7788\(02\)00079-8](http://dx.doi.org/10.1016/S0378-7788(02)00079-8).

Flow adjustment and turbulence in staggered high-rise building arrays by wind tunnel measurements and numerical simulations

Jian Hang¹, Yuguo Li², Riccardo Buccolieri³, Mats Sandberg⁴

¹School of Atmospheric Sciences, Sun Yat-sen University, Guangzhou, PR China

²Department of Mechanical Engineering, The University of Hong Kong, PR China

³Dipartimento di Scienze e Tecnologie Biologiche ed Ambientali, University of Salento, Italy

⁴Laboratory of Ventilation and Air Quality, University of Gävle, Sweden

Corresponding author: Riccardo Buccolieri, riccardo.buccolieri@unisalento.it

Abstract

This study investigates flow and turbulence within two arrays of staggered high-rise buildings. Each array is characterized by a packing density (λ_p) of 0.25 and a uniform building width B and height H , with $H=2B$ in one array and $H=2.67B$ in the other. Wind tunnel measurements and numerical simulations are performed to evaluate the wind reduction within the arrays, and explore the main mechanisms of rural wind flowing through such idealised arrays and how rural air distributes within them. Results show a quick wind reduction through the arrays. Wind strongly interacts with buildings producing downward motion near the leeward top corner of each building and upward motion near the windward top corner. These vertical flows across the street roof level mostly contribute to the air exchange and ventilation in such staggered arrays. The analysis also shows that increasing the building height does not have critical influence on flow and turbulence at pedestrian level.

1 Introduction

In urban areas, airflow is weak due to high drag force exerted by buildings. Traffic-pollutant releases are consequently not well dispersed, and it is thus crucial to improve air exchanges in the urban canopy layers. Experiments and numerical simulations have evaluated the effect of a wide range of features affecting pollutant dispersion, such as street aspect ratios, roof-shape, building packing density, wind direction (see for example recent reviews by Blocken, 2014; Lateb et al., 2016). Recently, Buccolieri et al. (2017) showed that, for regular aligned arrays of cubes, the drag force increases with increasing packing densities until it reaches a maximum at an intermediate packing density ($\lambda_p = 0.25$) followed by a slight decrease at larger packing densities when the array mostly behaves as one single unit.

Within this context we explore flow and turbulence within such intermediate packing density, when one can expect that the maximum drag force is attained, by a combination of wind tunnel and numerical simulations. We extend the previous work performed over aligned arrays by Hang et al (2011) to staggered arrays of high-rise buildings. Here we present results on staggered arrays and further investigation will be performed by comparing the impacts of aligned building arrays and staggered ones to evaluate the impact of building arrangement for urban planning purposes.

2 Description of physical models and measurement set-up

Wind tunnel experiments (model scale 1:1000) were performed in a closed-circuit boundary layer wind tunnel at the Laboratory of Ventilation and Air Quality, University of Gävle (Sweden). Models investigated were staggered arrays, with a building area density (represented by λ_p , i.e. the ratio between the plan area of buildings viewed from above and the total lot area) equal to 0.25. The

working section of the wind tunnel is 11m long, 3m wide and 1.5m tall. Velocity and turbulent kinetic energy were measured using hotwire anemometers. For further details please refer to Hang *et al.* (2011).

The building width was $B=3\text{cm}$ and the building height was $H=6\text{cm}=2B$ or $H=8\text{cm}=2.67B$, i.e. square building models at full scale are 60m or 80m high and 30m wide. Two staggered square arrays of uniform building height were studied. These cases are indicated as Case Staggered [2.67, 9-15, 0.25] and Case Staggered [2, 9-15, 0.25], which denote staggered square arrays of uniform building height $H=2.67B$ and $2B$, respectively, 9 rows and 15 columns of buildings, and $\lambda_p = 0.25$ ($l=5.5\text{cm}$, $d=1.25\text{cm}$) (Figure 1). In the figure, the location of the first upstream row of building arrays is at $x/B=0$. The plane $y/B=0$ is the symmetric plane in the middle street of building arrays. Points O1, O2, O3, O4 and O5 are centre points between buildings, i.e. the distance from these points to building surfaces is always 2.75cm ($l/2$).

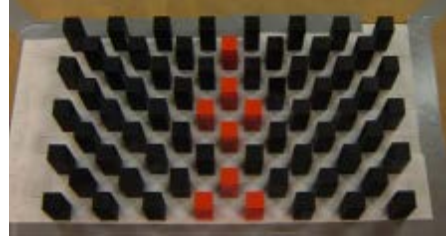
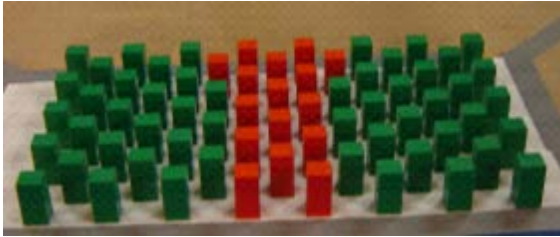
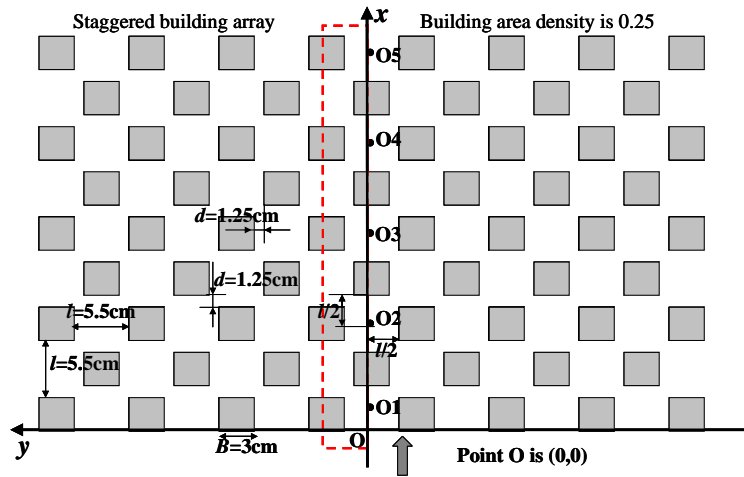


Figure 1. Building arrays of $\lambda_p = 0.25$ and uniform building height $H=2.67B$ (Case Staggered [2.67, 9-15, 0.25], bottom left) or $H=2B$ (Case Staggered [2, 9-15, 0.25], bottom right).

3 Numerical set-up

Numerical simulations were performed using the CFD code ‘Ventair’ (Hang *et al.*, 2011). The code employs the standard $k-\varepsilon$ turbulence model. The transport equations for the momentum and turbulence properties were discretized by finite volume techniques. The hybrid upwind/central differencing scheme was used to discretize the advection terms, with an option of second-order upwind scheme and QUICK scheme. The discretized differential equations were solved by the SIMPLE algorithm. No slip wall boundary condition at all the wall surfaces and a normal zero gradient boundary condition at domain outlet, domain top and all the symmetrical boundaries were employed. Approaching vertical profiles of stream-wise velocity (\bar{u}) and turbulence intensity (I) measured in the wind tunnel were used to provide inlet boundary conditions (Figure 2). At the domain inlet, the turbulent kinetic energy k and its dissipation rate ε were estimated by: $k=1.5(I\bar{u})^2$, $\varepsilon=C_\mu^{3/4}k^{3/2}/l_t$, with C_μ a constant ($=0.09$), $l_t=0.07D_h=0.14\text{m}$ the turbulent characteristic length scale and D_h the hydraulic diameter of the test section area of the wind tunnel. For further details please refer to Hang *et al.* (2011).

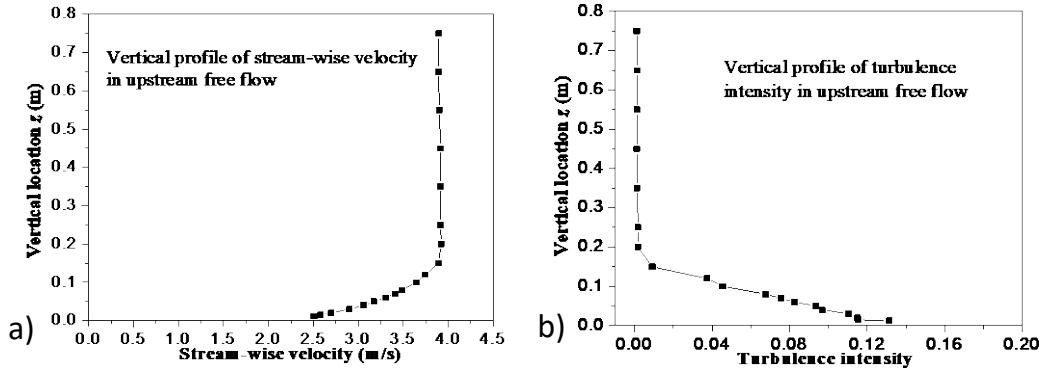


Figure 2. Upstream vertical profiles of (a) stream-wise velocity and (b) turbulence intensity measured in the wind tunnel.

Only the middle column of the building array was considered since the span-wise urban size is sufficiently large, and we only used half of this middle column which is surrounded by dots in Figure 1 to reduce computational time. So the width of computational domain in the lateral direction (y) was small, i.e. $0.75B$ (i.e. 2.25cm). The computational domain was 75cm high ($25B$) in the vertical direction (z). In the stream-wise direction (x), the distance from upstream domain inlet to the windward edge of the first building was $33.3B$, and that from the leeward edge of the final building to the downstream domain outlet was $121.3B$. A grid independence study allowed to select the final mesh of about 2.5 million cells. The cell sizes within the whole array volume were $\delta x=0.033B$, $\delta y=0.018B$ and $\delta z=0.013B$. The expansion ratio in the stream-wise direction from the first row of buildings to upstream domain inlet and from the last row of buildings to downstream domain outlet and in the vertical direction above the square buildings was 1.1 (Figure 3).

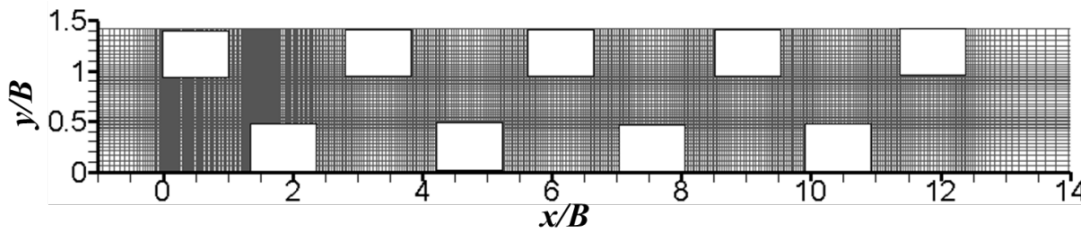


Figure 3. Sketch of the grid for Case Staggered [2.67, 9-15, 0.25].

4 Results

4.1 Wind reduction

To analyze the wind reduction through the staggered building arrays, vertical profiles of velocity and turbulent kinetic energy were taken at Points O1, O2, O3, O4 and O5 shown in Figure 1.

Figure 4 shows velocity and turbulent kinetic profiles at all points obtained from wind tunnel measurements. The figure shows that both velocity and turbulent kinetic energy decreases quickly from Point O1 to O5. The wind reduction (Figure 4a) from free (undisturbed) upstream flow to point O4 is very strong, while the velocity slightly increases from point O4 to point O5. Further the velocity gradients near the roof level ($z=H=2B=6\text{cm}$) are large. Figure 4b shows that the turbulent kinetic energy at points O1 and O2 is larger than that in free flow, confirming that strong turbulence is generated at the upstream region of the array. Then turbulence decreases from points O1 and O2 to points O3 and O4, especially turbulence below the roof level ($z=2B$) at points O4 and O5 is weaker than that in the free upstream flow.

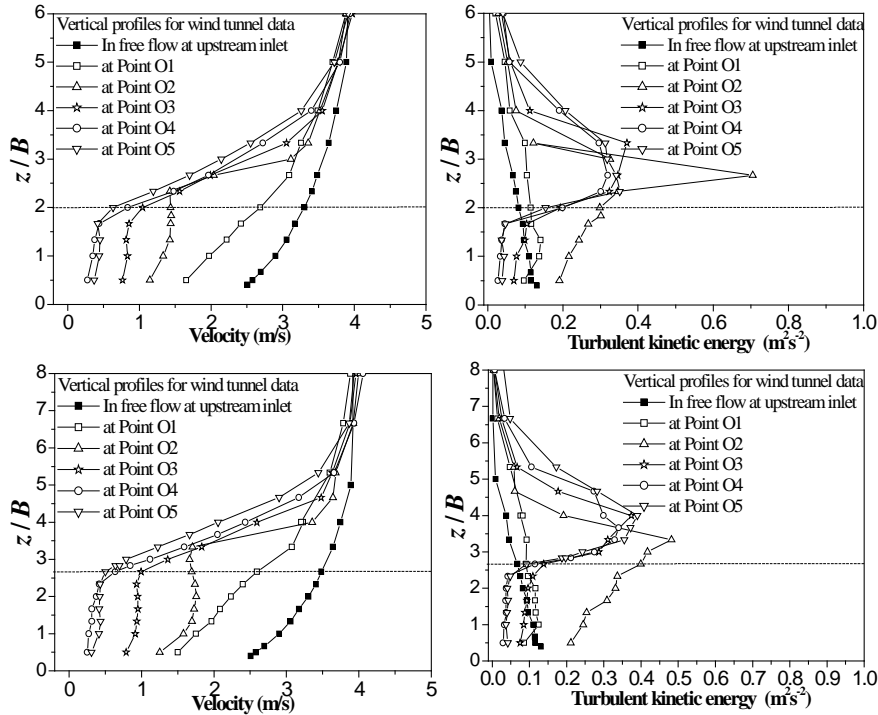


Figure 4. Measured vertical profiles of velocity and turbulent kinetic energy for (a) Case Staggered [2, 9-15, 0.25] and (b) Case Staggered [2.67, 9-15, 0.25].

To compare the influence of building height in the two staggered arrays, Figure 5 summarizes velocity and turbulent kinetic energy profiles obtained from wind tunnel experiments at all points. From $z/B=2$ to 2.67, velocity in Case Staggered [2, 9-15, 0.25] ($H/B=2$) is larger than that in Case Staggered [2.67, 9-15, 0.25] due to the different building height, but the wind profile below $z=2B$ is almost the same in both cases. It shows that the wind far below the roof level changes little when the building height increases from $2B$ to $2.67B$, suggesting that, for such kind of arrays, increasing the building height for residential purposes does not critically affect the flow and turbulence in the urban canopy layers.

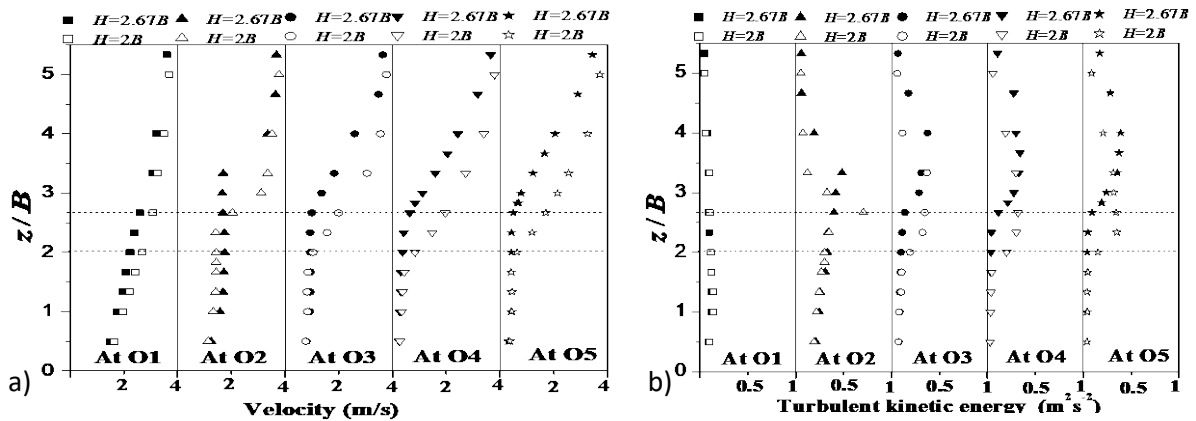


Figure 5. Comparison of velocity and turbulent kinetic energy vertical profiles for the Case Staggered [2, 9-15, 0.25] (empty symbols) and Case Staggered [2.67, 9-15, 0.25] (full symbols).

4.2 Flow pattern

Numerical simulations are used to spatially investigate the flow pattern across the array. First we compare numerical results with wind tunnel data for Case Staggered [2, 9-15, 0.25] ($H=2B=6\text{cm}$) at points O1-O5 (Figure 6). Numerical simulations well predicted velocity profiles (Figure 6a) at points

O4 (not shown here) and O5 (downstream region of the array), but under-predicted velocity profile at point O2 (not shown here) and O3 (middle of the array), and over-predicted at point O1 (upstream region of the array). This may be due to inability of the $k-\epsilon$ turbulence model to capture the strong separation flows which occurred at the upstream region. Vertical profiles of turbulent kinetic energy (Figure 6b) show that the shape was predicted generally well, but as expected turbulence at points O1, O2 (not shown here), O3 and O4 (not shown here) were over-predicted by numerical simulation, while a good prediction was found at point O5, showing that turbulence at the downstream region of the array was predicted better than at the upstream region. Similar results were obtained for Case Staggered [2.67, 9-15, 0.25] ($H=2.67B$). Results support the use of the CFD model to investigate mean flow pattern as reported below.

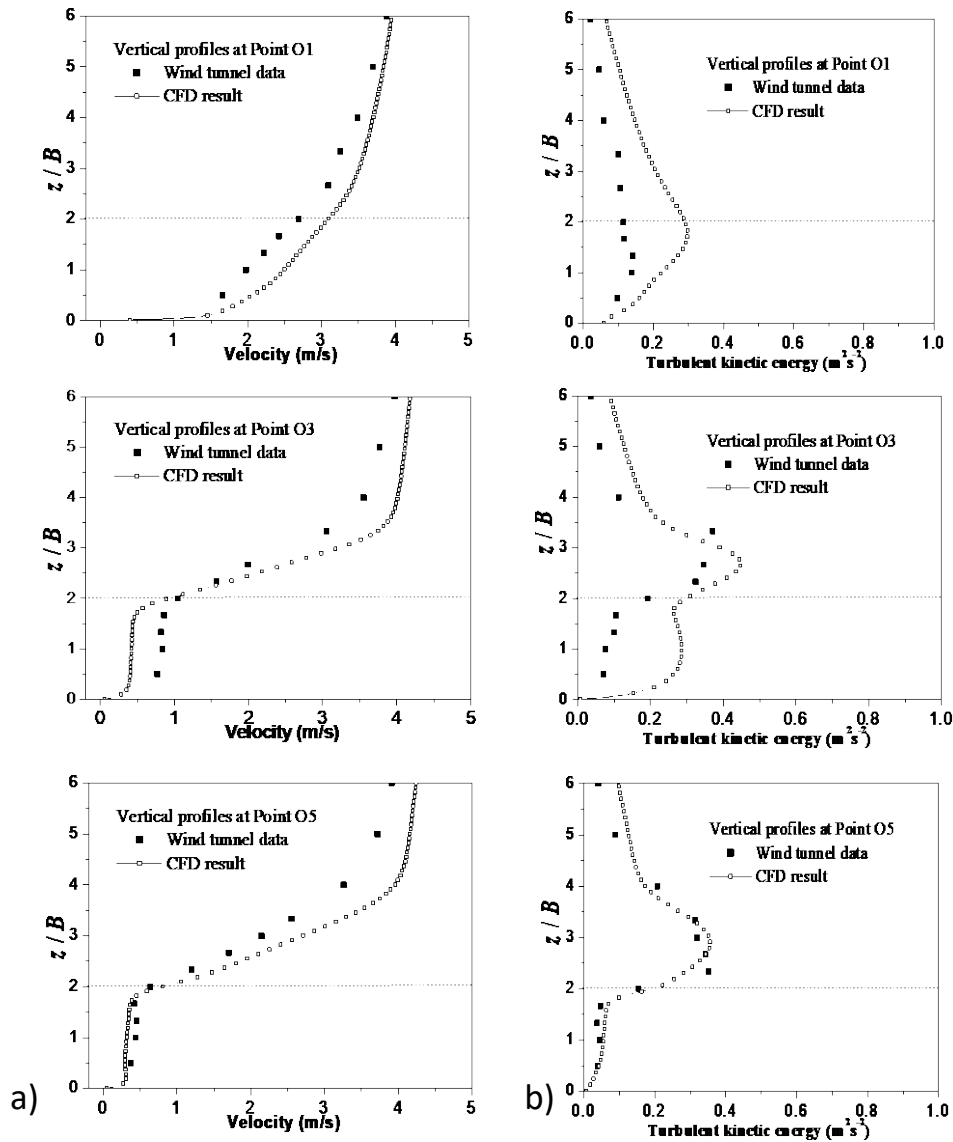


Figure 6. Vertical profiles of (a) velocity and (b) turbulent kinetic energy at points O1, O3 and O5 for Case Staggered [2, 9-15, 0.25].

The flow pattern in the Case Staggered [2, 9-15, 0.25] can be observed in Figure 7, which shows streamlines and flow variables at $z=B$. Overall, the pattern of streamlines is wave-shaped. The windward surfaces of buildings act as resistance to the wind and generate strong turbulence. So velocity components (Figure 7a,b) and turbulence (Figure 7c) decrease from upstream region to downstream region. Figure 7b shows large span-wise flows exists across locations of Plane A (plane

$y=0.92B$) and Plane B (at plane $y=0.5B$) at the height $z=B$ (defined in Figure 7d), which represents large momentum flow and mass flow across Plane A and Plane B at this height.

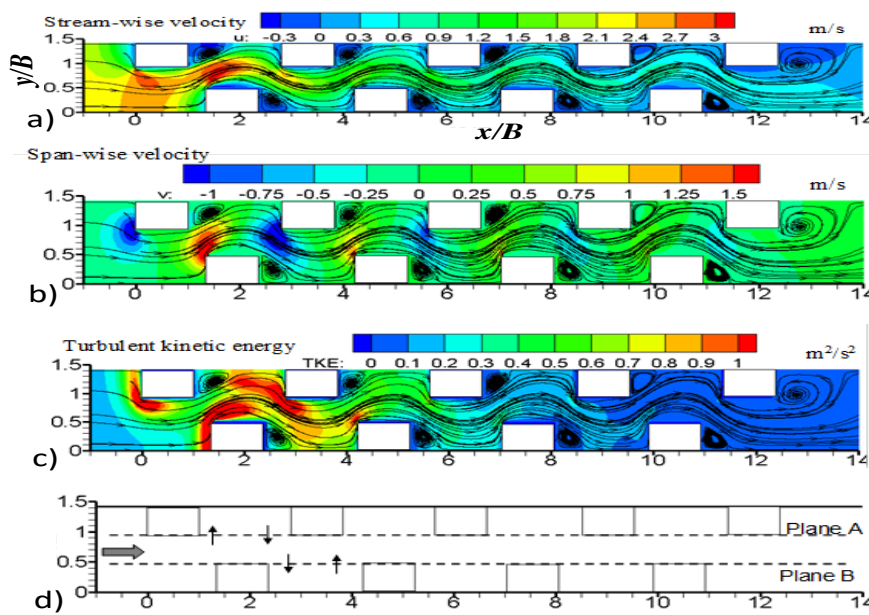


Figure 7. Case Staggered [2, 9-15, 0.25]. Flow pattern and contours of (a) stream-wise velocity, (b) span-wise velocity and (c) turbulent kinetic energy at $z=B$. (d) Location of Plane A ($y=0.92B$) and Plane B ($y=0.5B$).

To better display the span-wise exchange, Figure 8a shows distribution of span-wise velocity at Plane B. Large positive or negative span-wise velocity exists in the vicinity of each building (i.e. both behind and before the building height). Figure 8b shows the distribution of vertical velocity and turbulent kinetic energy at $y=0$. The figure shows that turbulence near the street roof level ($z=2B$) is larger than that far below the roof level. In addition, there are negative vertical velocity (downward motion) near the leeward top corner of each building and positive vertical velocity (upward motion) near the windward top corner of each building. The vertical flow across the roof level can be detected from Figure 8c, which shows distribution of vertical velocity at the street roof level. Negative vertical velocity mainly exists in the leeward vicinity of each building, in addition positive vertical velocity appears in the windward vicinity of each building and at the roof level of the narrow channel ($0.5 < y/B < 0.92$). These vertical flows across the street roof level contribute to the air exchange and ventilation in such staggered arrays.

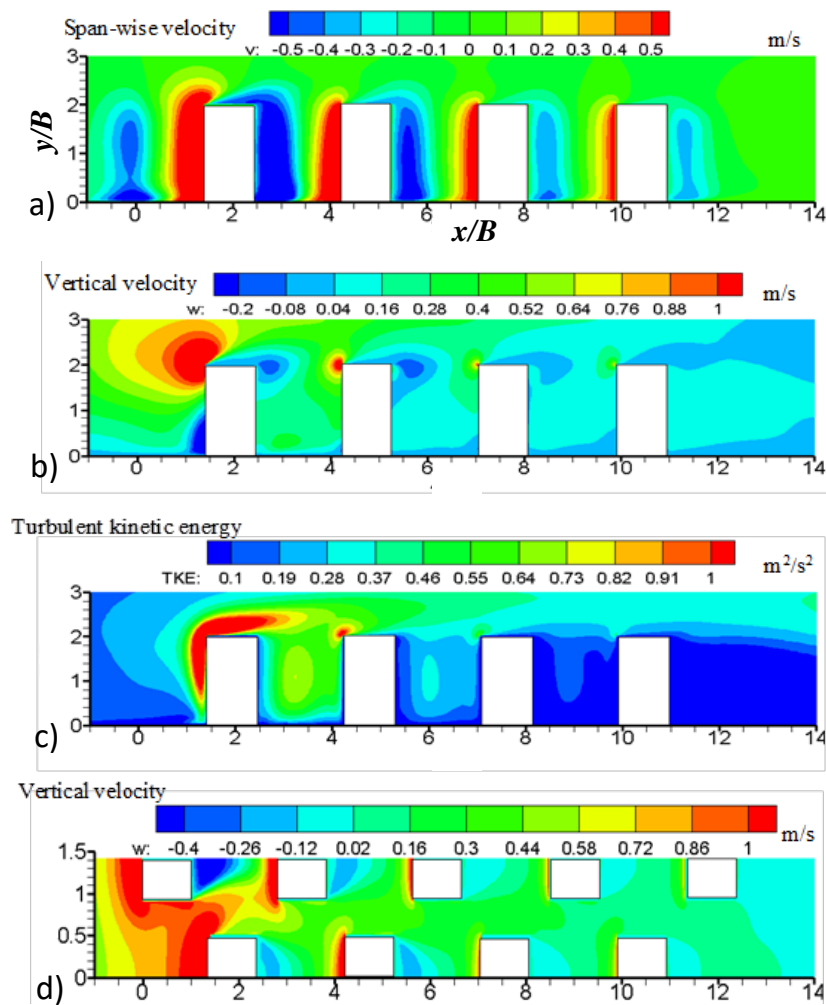


Figure 8. Case Staggered [2, 9-15, 0.25]. Contours of (a) span-wise velocity at Plane B, (b) vertical velocity and (c) turbulent kinetic energy at $y=0$, (d) vertical velocity at the street roof level $z=2B$.

5 Conclusions

This work numerically and experimentally investigated flow adjustment and turbulence within idealised staggered building arrays of building area density 0.25. Results show a strong wind reduction through the arrays and suggest that, for such a density of staggered arrays, (i) increasing the building height for residential purposes does not have critical influence on flow and turbulence at pedestrian level; and (ii) vertical flows across the street roof level mostly contribute to air exchange and ventilation. Future work will be devoted to the comparison with aligned building arrays investigated in Hang *et al.* (2011) to explore which kind of building array generates stronger resistances to the approaching wind.

Acknowledgements

This work is supported financially by a RGC CRF project (HKU9/CRF/12G) of the Hong Kong SAR government. The authors thank Mr. Leif Claesson (University of Gävle, Sweden) for his help in hotwire measurements in the wind tunnel.

References

Blocken, B. (2014). 50 years of Computational wind engineering: past, present and future. *Journal of Wind Engineering and Industrial Aerodynamics* 129, 69–102.

Buccolieri, R., Wigö, H., Sandberg, M., and Di Sabatino, S. (2017). Direct measurements of the drag force over aligned arrays of cubes exposed to boundary-layer flows. *Environmental Fluid Mechanics* 17, 373-394.

Hang, J., Li, Y., and Sandberg, M. (2011). Experimental and numerical studies of flows through and within high-rise building arrays and their link to ventilation strategy. *Journal of Wind Engineering and Industrial Aerodynamics* 99, 1036–1055.

Lateb, M., Meroney, R.N., Yataghene, M., Fellouah, H., Saleh, F., and Boufadel, M.C. (2016). On the use of numerical modelling for near-field pollutant dispersion in urban environments. A review. *Environmental Pollution* 208, 271–283.

A study of the pressure coefficient at a tunnel portal

T.Kubwimana¹, E.Bergamini², P.Salizzoni² and P.Méjean²

¹Centre d'Études des Tunnels, Bron, France

²Laboratoire de Mécanique des Fluides et d'Acoustique - École Centrale de Lyon, Écully, France

Corresponding author: T.Kubwimana, thierry.kubwimana@developpement-durable.gouv.fr

Abstract

The effect of the external wind on a road tunnel is the subject of the investigations reported here. The study aimed at evaluating the mean wind pressure coefficient at a tunnel portal through wind tunnel experiments together with numerical simulations. In addition to the incident wind direction, it is shown that the mean wind pressure coefficient depends largely on the presence of urban-like buildings. Similar conclusions could be drawn from the numerical investigations.

1 Introduction

Irrespective of the type of ventilation system to be installed in a road tunnel, the control over the airflow in the tunnel remains the key element to ensure appropriate conditions for self-evacuation and rescue operations in case of fire. In most cases, the ventilation design calls upon one dimensional modelling for the analysis of the general aerologic behaviour of a tunnel and the sizing of the mechanical ventilation system. The wind driven pressure difference ΔP_{wind} between the two tunnel portals provide the boundary condition for such 1D tunnel model. It is usually derived from a straightforward transposition of a velocity measurement:

$$\Delta P_{wind} = \frac{1}{2} k_p \rho V_{ref}^2 \quad (1)$$

where ρ is the air density, V_{ref} is a reference wind velocity and k_p is the pressure coefficient representing the wind exposure of the portal.

As in most of the times, extensive wind measurements on site are not available, V_{ref} is often issued from measurements at the nearest by meteorological station. And as for the wind coefficient k_p , it accounts under Eq. (1) for the possible changes in the wind field between the velocity measuring point and the actual portal. Consequently, k_p depends largely upon local aerological parameters such as the shape and dimensions of the portal itself and its surroundings (PIARC, 2007). Yet, a standard practice in the ventilation calculation procedure is to avoid the determination of the above-mentioned aerological parameters. A gross estimation of ΔP_{wind} is often obtained from the geometrical projection of the available velocity measurements onto the tunnel axis.

In this paper, we carry out a combined experimental and numerical analysis of the variation of the mean pressure coefficient k_p applied at the front section of an urban tunnel portal, which is idealized as an open cavity, with the ambient wind direction. Our investigations address the influence of the built-up areas for urban road tunnels as the cavity is then placed in urban like environments.

2 Wind tunnel setup

The experiments were performed in the atmospheric wind tunnel of the LMFA of the École Centrale de Lyon. The test section of this closed-loop wind tunnel was 14 m long, 2.5 m high and 3.7 m wide. It allowed the generation an atmospheric boundary-layer (ABL) whose depth δ was approximately 0.8 m.

The reference free-stream velocity U_∞ at the boundary-layer height was set at $5 \text{ m}\cdot\text{s}^{-1}$. In its lower part, the ABL vertical profile of the mean horizontal velocity could be modelled by a logarithmic law:

$$U(z) = \frac{u}{\kappa} \ln\left(\frac{z-d}{z_0}\right) \quad (2)$$

Where κ is the Von Karman constant, $u = 0.185 \text{ m}\cdot\text{s}^{-1}$ is the friction velocity, $z_0 = 1.14 \cdot 10^{-4} \text{ m}$ is the roughness length and $d = 0.0129 \text{ m}$ is the displacement height.

In a first series of experiments, the tests were confined to an isolated wooden cavity of dimensions of $80 \times 320 \times 1090 \text{ mm}^3$ ($h \times w \times l$). This configuration can be characterized as a reduced-scale model (1:100) of a standard two-tubes tunnel. A second series of tests addressed the aerodynamic response of the same cavity in urban-like environments. Two types of arrangements were tested: a dense and regular arrangement of 104 cubes on both sides of the isolated cavity (*Fig. 1a*), and a rather coarse and staggered arrangement of 52 cubes (*Fig. 1b*). In the dense arrangement, the distance between the cubes was taken equal to their height, which is 120 mm.

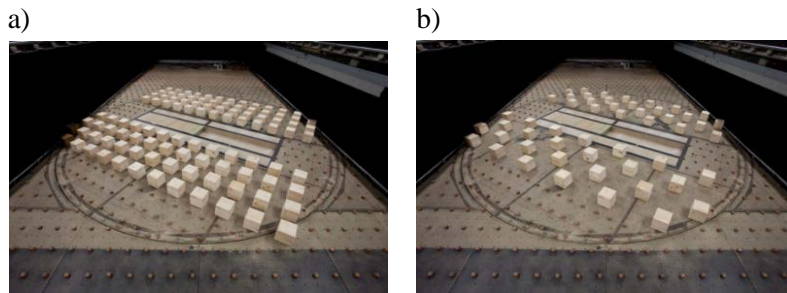


Figure 3: Cubes arrangement for the (a) dense and (b) coarse configurations.

The front section of the cavity placed at the centre of the test section represents the tunnel entrance, which implies that the longitudinal airflow through the tunnel was not reproduced. The entrance was covered with an aluminium plate pierced with 15 well-distributed pressure taps. Each tap was connected to a micromanometer that would measure the net pressure difference relative to the static pressure in the LMFA facilities. A stagnation pressure was thus measured at the entrance of the tunnel.

3 Numerical setup

ANSYS CFX was used to solve the Navier-Stokes equations under the RANS formulation. Steady conditions were considered in the simulations and the standard $k - \varepsilon$ turbulence model was used for the calculation of the turbulent characteristics of the flow.

The geometry was placed at the centre of a hexahedral domain. The same sized computational domain was used for the different cavity configurations. It had the following dimensions: $7200 \times 7200 \times 1200 \text{ mm}$ ($L \times W \times H$). The domain was meshed with a varying density grid which consisted of an unstructured hexahedron mesh. The finest elements were located in the cavity and had dimensions of $\Delta = 0.05h$, while the largest ones were near the domain boundaries and measured $1.5h$. The grid resolution was finer than that prescribed in the established guidelines for CFD simulations of urban flows (Franke *et al.*, 2007). The meshing procedure resulted in a number of elements ranging from 1 M for the isolated cavity to 3.5 M for the configuration with the dense cube arrangement.

The four lateral boundaries of the computational domain were treated differently depending on the wind incidence to be simulated. On inflow boundaries, the experimentally measured profiles of velocity, turbulent kinetic energy k and dissipation rate ε were prescribed. An outlet boundary condition was then specified on faces where the flow would be directed out of the domain. For the cases in which the ABL would flow parallel to two lateral faces, these would be treated as symmetry planes. At the upper boundary of the domain, a symmetry condition was invariably specified.

All the solid surfaces were treated with a no-slip wall boundary condition but with different roughness settings were made. The cavity walls, the cubes accounting for the buildings and the ground surface in the central part of the computational domain were considered as hydro-dynamically smooth walls.

Since the floor roughness elements of the wind tunnel were not modelled explicitly, their effects were taken into account through the specification of a sand-grain roughness parameter k_s on the ground surface of the outer part of the domain. Following Blocken's investigations (Blocken *et al.*, 2007), the sand grain roughness k_s was related to the wind tunnel roughness z_0 through a first order matching of the ABL profile with CFX wall function, yielding $k_s = 29.6 \cdot z_0$.

4 Results

Overall, the 360° range of possible incidences was covered with an angular step of 30° in the wind tunnel experiments. The incidence angle is denoted by θ and is zero when the tunnel entrance faces the incoming wind. Hence, from the 15 pressure taps set on the front section of the cavity, the area averaged pressure difference ΔP at the tunnel entrance was calculated for each configuration and wind angle θ . Since meteorological stations usually provide velocity measurements at 10 m above the ground, the non-dimensional pressure coefficient k_p was related to the reference dynamic pressure of the undisturbed ABL at $z = 10\text{cm}$:

$$k_p = \frac{\Delta P}{\frac{1}{2}\rho U_{ref}^2(z=10\text{cm})} \quad (3)$$

Where $U_{ref}(z = 10\text{cm}) = 3.1\text{ m/s}$. U_{ref} was kept constant throughout the experiments.

Figure 2 shows all together the curves of the experimental wind pressure coefficients versus the angle of wind incidence obtained for the three configurations. The maximum coefficient was invariably measured around the 0° angle, as the wind was blowing onto the cavities axis. For the isolated cavity, k_p is then reduced for oblique incident wind flow and goes eventually negative in the range $[90^\circ - 270^\circ]$. As the cavity was placed at the centre of the dense arrangement, the pressure curve was found similar to that of the isolated configuration, although its magnitude decreased faster. This could be readily explained by the shielding effect of the cubes. It is not possible however to extend this behaviour to the configuration with the coarse cube arrangement. For such arrangement, the pressure coefficient would not decrease monotonically with the incident angle. The coarse case curve shows indeed an increase around $\theta = 25^\circ$, which suggests a wind corridor amongst the cubes as the rotating table is set at this angle. Such investigation makes evident that the wind pressure difference depends largely on its immediate surroundings.

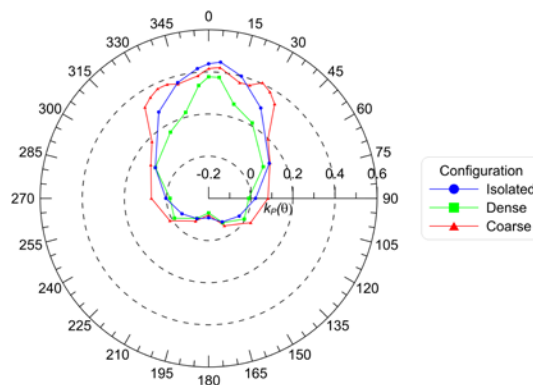


Figure 4: Mean wind pressure coefficient measurements for cavities in urban-like environment.

Figure 3 provides the comparison of the experimental and numerical wind pressure curves on a case-by-case basis. The numerical simulations took advantage of the CFD model flexibility so that a finer angular step could be considered around the incidence of particular interest, namely 0° , 90° , 180° and 270° .

The CFD code is found to perform better for the isolated cavities (Fig. 3a). For this first configuration, it is indeed found that the code leads to a virtually identical curve for k_p . The results show however that the accuracy of the CFD codes suffers with the complexity of the flow field. Firstly, regarding the dense cube array, a decent curve match could still be obtained (Fig. 3b). The simulations enabled to

analyse precisely the variation of the pressure coefficient around 90° and 270° as a transverse wind would be blowing. This numerical angular step refinement singled out a cusp-shaped variation of k_p in these angular sectors. Since measurements at the positions were not made, it is not possible, at this stage, to determine whether the code provided poor predictions there or if such behaviour could have been witnessed experimentally.

The simulation of the cavity in the middle of the staggered cube arrangement eventually provided the greatest discrepancies with the experimental measurements (*Fig. 3c*). Although the maximum pressure coefficient was reasonably well predicted, the $k - \varepsilon$ model was found here to somehow underestimate the wind pressure difference at the front section of the cavity. This may be related to the well documented poor predictions of the onset and the extent of flow separations by the standard $k - \varepsilon$ model (Pope, 2000). The numerical model may have difficulties in predicting accurately the dynamics of the large eddies in the wake of the cube blocks hitting the portal. Further investigations are to be made so as to determine if alternative turbulence closures, namely Reynolds Stress Models and Large Eddy Simulations, can overcome this $k - \varepsilon$ model limitation and provide better k_p predictions.

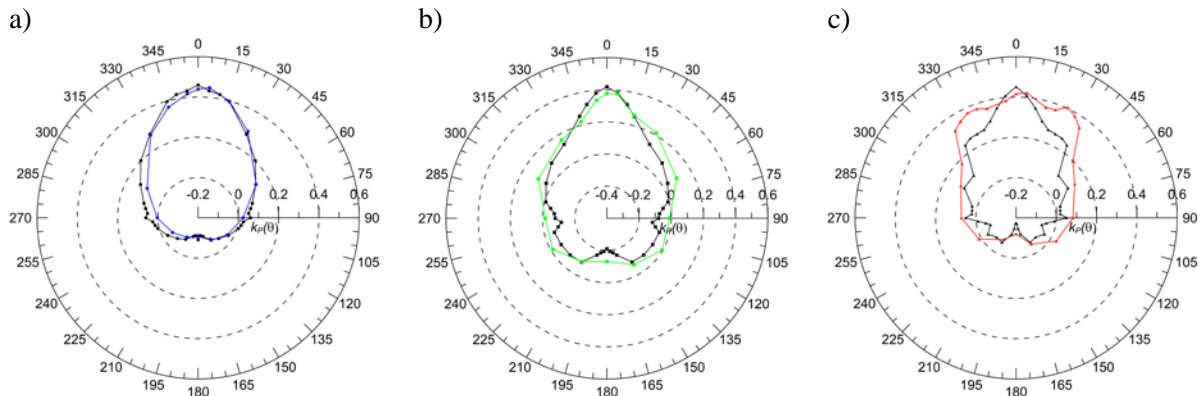


Figure 5: Numerical predictions of $k_p(\theta)$ for the isolated (a), dense (b) and coarse (c) configurations. Colour lines are wind tunnel results and black lines are issued from the standard $k - \varepsilon$ model

5 Conclusion and perspectives

Experimental and numerical investigations of the aerodynamic behaviour of reduced-scale models of generic configurations of a tunnel portal have been undertaken. These investigations covered isolated cavities but also urban-like arrangements. It is here confirmed that the net wind pressure difference at a tunnel portal depends largely on the incident wind direction and on the tunnel surrounding condition. For all the geometries, the highest pressure coefficients were measured as the cavity was more or less aligned along the incident wind direction. However, the magnitude of the coefficients, as a function of the wind direction, $k_p(\theta)$ could be significantly influenced by the possible presence of surrounding buildings. Similar conclusions could be drawn from the numerical investigations. The standard $k - \varepsilon$ model led to satisfactory predictions of the pressure profiles $k_p(\theta)$. Ultimately, the discrepancies between experimental and numerical models rose as the nature of the flow pattern was made complex. Urban-like geometries resulted in poorer performance of the numerical model.

References

- Blocken, B., Stathopoulos, T. and Carmeliet, J. (2007). CFD simulation of the atmospheric boundary layer – wall function problems, *Atmospheric Environment*, 41(2), pp. 238–252.
- Franke, J., Hellsten, A., Schlünzen, H. and Carissimo, B. (2007). Best practice guideline for the CFD simulation of flows in the urban environment, *COST Office Brussels*, ISBN 3-00-018312-4.

PIARC Technical Committee 5 Road Tunnels (2007). Systems and Equipment for Fire and Smoke Control in Road Tunnels.

Pope, S. B. (2000). Turbulent Flows, Measurement Science and Technology.

Modelling the effect of urban design on thermal comfort and air quality: the SMARTUrban Project

L. Massetti¹, M. Petralli^{2,3}, G. Brandani^{2,3}, M. Napoli², F. Ferrini², A. Fini^{2,4}, F. Torrini⁵, D. Pearlmutter⁶, S. Orlandini^{2,3}, A. Giuntoli⁷

¹Institute of Biometeorology, National Research Council, Florence, Italy

²Centre of Bioclimatology, University of Florence, Italy

³Department of Agrifood Production and Environmental Sciences, University of Florence, Italy

⁴Department of Agricultural and Environmental Sciences – Production, Landscape, Agroenergy,
University of Milan, Italy

⁵Florinfo S.n.c., Italy

⁶Ben-Gurion University, Israel

⁷Studio Bellesi Giuntoli, Florence, Italy

Corresponding author: Martina Petralli, martina.petralli@unifi.it

Abstract

More than half of the world population lives now in urban areas and therefore the quality of the urban environment has become a key issue for human health. In this context, it is important to evaluate and document any action that contributes to improvements in thermal comfort and air quality. The aim of this paper is to present a system for the design of urban spaces developed in the framework of the SMARTUrban project. Such a system aims at giving administrators and design professionals a strategic tool for the sustainable management and planning of urban areas. SMARTUrban is a prototype of an urban space design software that estimates the effect of design modification or of new design on thermal comfort, carbon sequestration and air pollutants removal.

1 Introduction

The strong contribution of cities to local and global warming is well documented (Grimmond, 2007). It is recognized by many international studies that the concentration of population and buildings in a small portion of territory alters its characteristics to the point of creating a significantly different local climate from surrounding rural areas (Oke, 1982). This affects weather variables including temperature distribution and intensity: cities, because of the materials from which they are constructed modify soil permeability and contribute to storing energy and re-dispersing it in the form of heat, and are by themselves warmer (Dirmeyer et al., 2010). One of the main drivers of global warming is CO₂, and cities are known to be major sources of this gas. Indeed, a compensation of CO₂ emitted by human activities is achievable through sustainable urban planning. Urban greening, in particular, can contribute effectively to CO₂ atmospheric reduction by assimilation and storage, as CO₂ is converted into organic carbon by photosynthesis then stored as woody biomass for long-term (Mori et al., 2016). Finally, urban sites are characterized by high pollution load, and close to 7 million premature deaths each year can be attributed to urban air pollution (WHO, 2014). It was estimated that in Italy, in 2010, 34143 inhabitants died because of exposure to transport-related pollution (Mori et al., 2015). Trees and shrubs have the potential to remove large quantities of gaseous and solid (i.e. PM) pollutants, with plant leaf area and density, as well as leaf anatomical characteristics playing a major role in determining the amount of pollutants sequestered (Mori et al., 2015).

In this general context of ongoing urbanization, the number of people experiencing stressful urban environmental conditions is increasing. At our latitudes, the negative impacts of urban climate on human health is stronger during the summer season. Among air pollutants, ozone reaches higher

concentrations during summer, while other pollutants like particulate matter, nitrogen and sulphur oxides peak during winter. Moreover, cities contribute to carbon dioxide emissions both locally and globally (Satterthwaite, 2008).

It is necessary to have spaces in the city that contribute to mitigating the negative effects of the urban environment on the health of the population and on the environment (Petralli *et al.*, 2014). All this means that knowledge of the urban environment and its peculiarities is the basis for the planning of future urban sustainable development (Brett, 2003). Although there are many studies in the literature on the environmental dynamics of the urban environment, there is a need to make this information easily accessible to urban planners and policymakers (Eliasson, 2000; Roth *et al.*, 2011; Massetti *et al.*, 2014; Ugolini *et al.*, 2015).

In this context the SMARTUrban project (Monitoring system and territorial urban research) was conceived. The aim of the project is to develop a prototype user-friendly system for the design of urban spaces and the evaluation of their environmental impacts. The evaluation of the environmental effects of these urban areas can be performed on different aspects: human thermal comfort, air pollution, CO₂ storage and sequestration and sensible heat evaluation.

This paper presents the prototype of a software tool, realized within the SMARTUrban project, that aims to facilitate the evaluation of the impact of an urban space design – providing an easy-to-use interface for both the design and the estimation phases.

2 Material and methods

The SMARTUrban software is composed of a graphic interface for the design of urban spaces, georeferenced through a GIS system and a set of functions to calculate indices of environmental performance. The user can work on a new layer or import the working area from Google Maps or from other GIS layers (including objects like buildings, plants and green infrastructure, and their characteristics, like colour, tree height, tree species, type of surfaces, etc.). This system gives the possibility of changing the characteristics of the objects or adding new objects to the work area (Figure 1). This is possible thanks to a database of materials and plants set up for this software. Each material is characterised according to its thermal and radiative properties (albedo, heat capacity, conductivity and emissivity), and also by permeability (permeable or impermeable). Tree species were clustered according to their similarity and characterized in terms of crown shape and size, leaf area index (LAI) and growth curves.

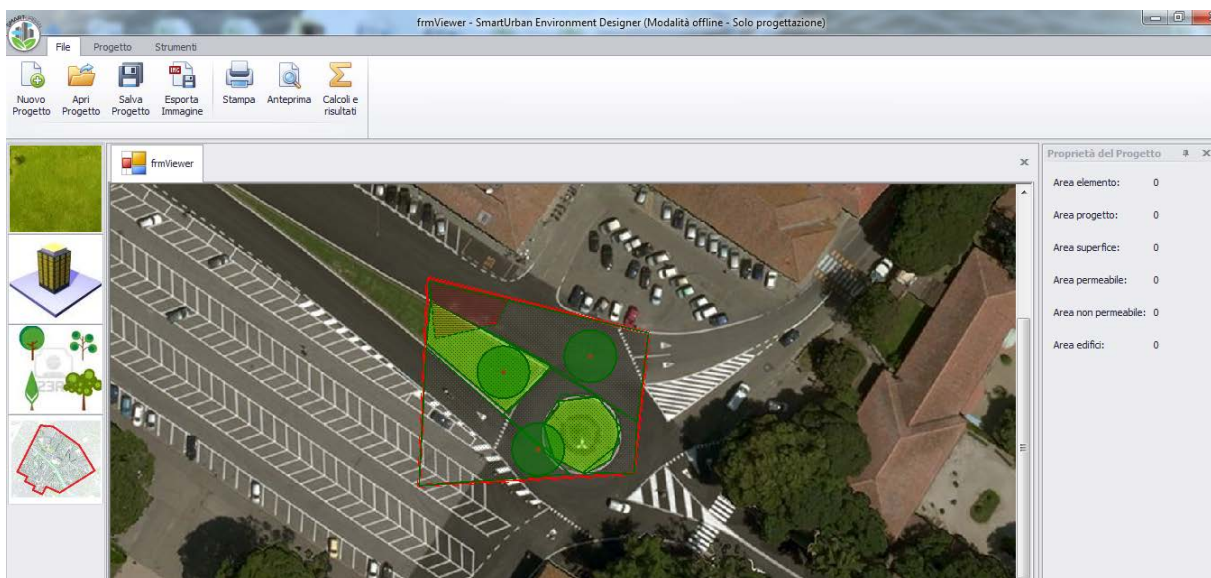


Figure 1: User interface of the prototype realized in the framework of the SMARTUrban project

Once the work area is designed and each element is defined, the user can proceed with the environmental indices calculation.

The environmental indices that the SMARTUrban software can calculate are:

- a) Thermal comfort:
 - ATI (°C) - Apparent Temperature Index (Steadman, 1994)
 - UTCI (°C) – Universal Thermal Climate Index (Jendritzky et al., 2012)
- b) Sensible heat – Q (W m⁻²): Computed through a one-dimensional energy balance model coupled with a routine for estimating the effect of plant canopies on surface heat transfer (Napoli et al., 2016). The model computes the shortwave and longwave radiation exchange by taking into account the shadow effects due to buildings and tall vegetation (tree, hedges, etc.) and the reflections on urban facets (pavements, walls, etc.). Mutual shading, heat emission and reflection between buildings, trees and pavements are included.
- c) CO₂ storage and sequestration: carbon storage was calculated after grouping tree and shrubs species into eleven classes based on growth rate, longevity, and final dimension at maturity. Average longevity and size at maturity were identified per each species. A growth curve relating age, diameter, and biomass was constructed per each vegetation class based on literature data. Carbon stored was calculated as 0.5 * estimated plant dry weight. Carbon assimilation was estimated as the annual increase in carbon storage, corrected for plant health status and irradiance.
- d) Air pollutant removal:
 - PM₁₀ and PM_{2.5}
 - NO₂, O₃ and SO₂

was calculated using the dry deposition model.

The calculation of all indices requires the following hourly environmental data. Meteorological and air pollutant data should be collected in a station representative of the study area (globe thermometer data must be collected in situ). For thermal comfort evaluation, the software includes coefficients of correction of air temperature related to different surfaces type and shading. These coefficients were empirically derived from a 2-year data monitoring and analysis (Brandani et al., 2016).

Table 2: list of input variables required for the calculation of the indices

Variable	Unit	Name	Index
Air temperature	°C	Ta	all
Wind speed	ms ⁻¹	v	all
Relative humidity	%	Rh	all
Global solar radiation	Wm ⁻²	rad	all
Rain	mm	p	PM ₁₀ , PM _{2.5} , O ₃ , NO ₂ , SO ₂ , Q
Black globe thermometer	°C	Tg	UTCI
Particulate Matter <10 microns	<10 µgm ⁻³	PM ₁₀	PM ₁₀
Particulate Matter <2.5 microns	<2.5 µgm ⁻³	PM _{2.5}	PM _{2.5}
O ₃	µgm ⁻³	O ₃	O ₃
NO ₂	µgm ⁻³	NO ₂	NO ₂
SO ₂	µgm ⁻³	SO ₂	SO ₂

Table 2: list of input variables needed for the calculation of CO₂ storage and CO₂ assimilation

Variable	Unit	Name	Index
Tree/shrub species	qualitative	Sp	CO ₂ storage and CO ₂ assimilation
Stem diameter at 1.3 m	cm	DBH	CO ₂ storage and CO ₂ assimilation
Tree health	qualitative	S	CO ₂ assimilation
Tree exposition	qualitative	E	CO ₂ assimilation
N days without frost per year	day	G	CO ₂ assimilation

The user can select the period of the simulation. ATI, UTCI and Q are calculated hourly for the selected period. Average values (from 1 pm to 3 pm) of UTCI and ATI are displayed in a map of the work area.

The energy balance results are expressed as the mean of hourly sensible heat of the whole period. Air pollution outputs are expressed by a value cumulated at the end of the selected period. The CO₂ outputs depict the actual storage and accumulation and allow predictive estimates of CO₂ storage after 10, 35, 75, and 100 years (or until predicted tree death if shorter than these time-spans).

The user can select one or more index and should provide only the input data required for the selected indices.

The SMARTUrban software was designed to compare the environmental performance of an existing situation with the design of a new urban area.

3 Results and discussion

In this section, an example of the environmental performance of an existing situation and a new design of an urban area located in Arezzo is presented (Figure 2).

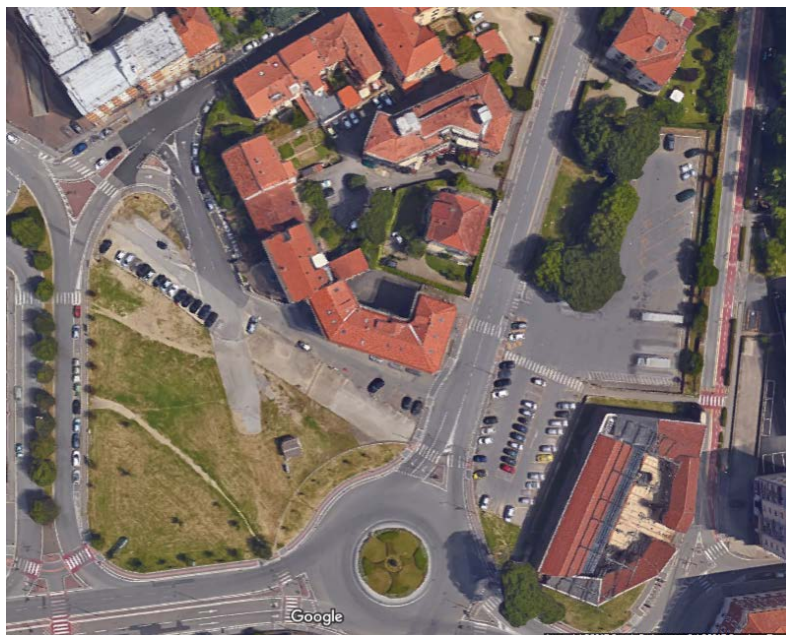


Figure 2: Google satellite image of the urban area selected for the case study in Arezzo

After the Google image is imported in the software, the study area is delimited and then the surfaces and features (buildings and trees) are classified by the user (Figure 3A). Now the designer can modify the study area to simulate different solutions by changing surfaces and adding trees or changing tree species. In our case study, the designer changed some areas covered by asphalt and bare soil with grass, and added some trees of different species and age (Figure 3B).

In this case study, the meteorological data inserted were related to summer 2014 and the results for ATI are presented in figure 4A (existing situation) and 4B (project situation). In this case, UTCI was not calculated because Tg data were not available.

The project of the study area gives a mean value for the ATI during the summer 2014 of approximately 2 °C less than the existing situation. The introduction of trees locally reduced the ATI by approximately 4 °C. This reduction refers to the average calculated between 1 pm and 3 pm.

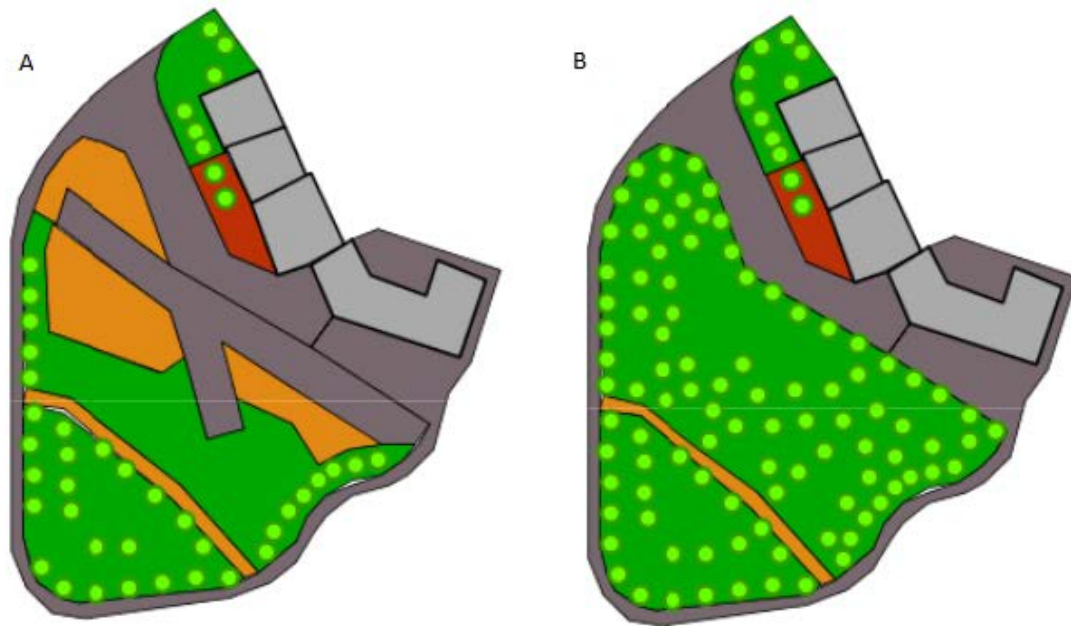


Figure 3: Study area: 2A) design of the existing situation; 2B) design of the project (gray: asphalt; orange: bare soil; green: grass; light green: trees; light gray: buildings; brown: bricks)

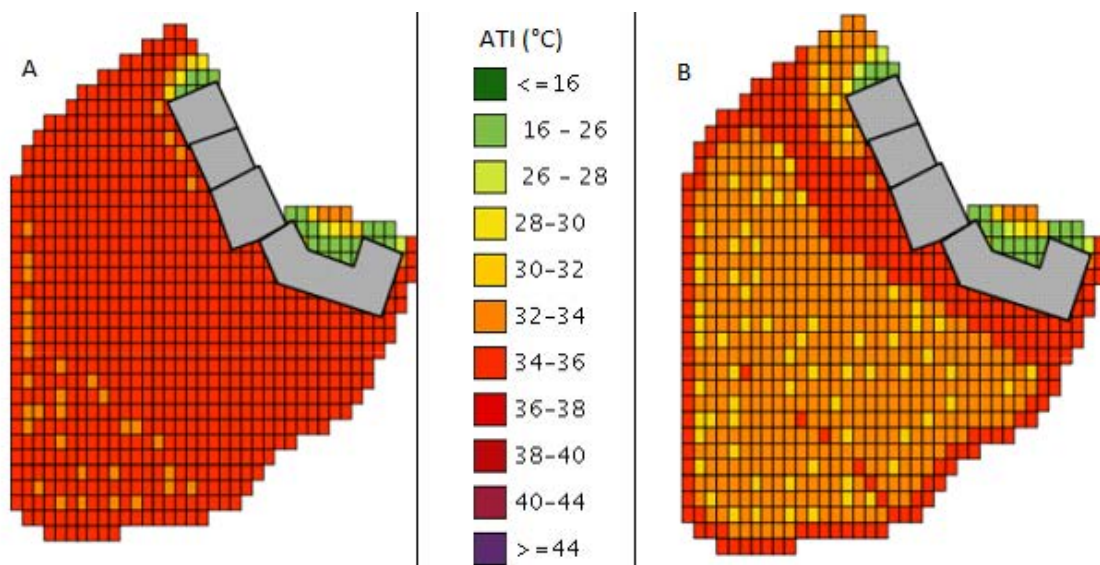


Figure 4: Average ATI (°C) during summer 2014 between 1 pm and 3 pm of the existing situation (A) and of the project situation (B).

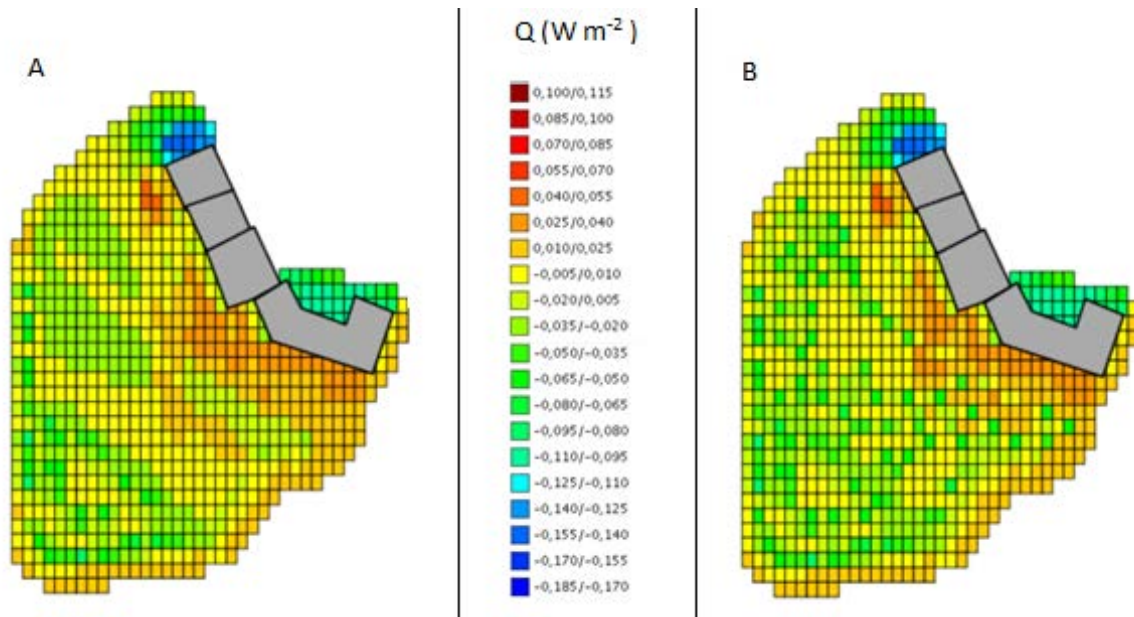


Figure 5: Average sensible heat (W m⁻²) per hour in Summer 2014 of the existing situation (A) and of the project situation (B)

Sensible heat results are presented in figure 5: figure 5A shows the existing situation and figure 5B the project situation. The project situation shows a reduction in mean summer sensible heat per hour of almost 1 W m⁻².

Results for air pollutant removal and carbon storage and sequestration are presented in Figure 6, comparing an existing industrial area in the suburbs of Florence with a proposed alternative design of the site.

It is possible to see how the planting of long-lived species, such as holm oak, may provide significant benefits in terms of carbon storage and pollution removal. In its current state, the site vegetation consists only of grass, with no trees, which results in the assimilation of about 700 kg C/year, but little carbon storage. Planting trees increases both CO₂ assimilation and storage, particularly after the 10th year since planting when trees are fully established and they approach maturity. Using long-lived trees assures that this benefit will increase progressively for over 100 years, whereas planting species with shorter life-span (e.g. poplar), may reduce benefits as soon as trees reach senescence and need to be replaced. Pollution removal increases proportionally with tree size and canopy area, with a larger impact seen for the projected tree plantings on O₃ and NO₂.

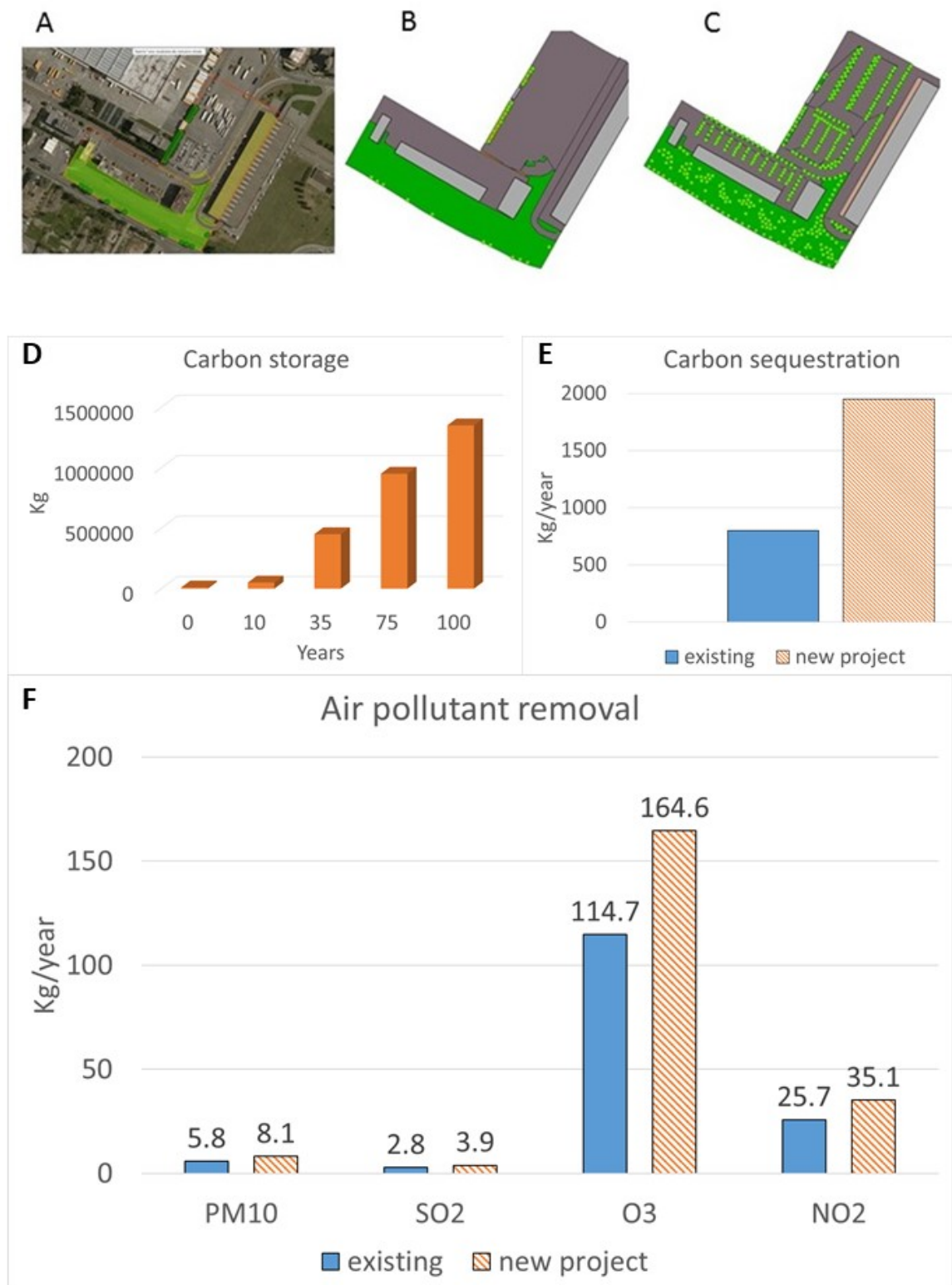


Figure 6: Industrial area in the suburbs of Florence (A) selected for estimating the environmental performance of the existing area (B) and the new projected area (C), and comparison between B and C in terms of carbon storage (D), carbon sequestration (E) and air pollutant removal (PM₁₀, SO₂, O₃ and NO₂) (F).

4 Conclusion

The SMARTUrban software is still a prototype, but it promises to be an easy-to-use tool that can provide quantitative results for sustainable urban environmental design. The system can calculate several performance indicators of thermal comfort, sensible heat, carbon sequestration and air pollutants removal. The system evaluates the environmental quality of an urban design by the total value of each indicator for the project and detailed maps for thermal comfort and sensible heat variability.

The maps of thermal comfort and sensible heat helps to immediately evaluate the impact of a design and identify critical points. Then, the user can revise, through a graphical interface, properties and position of any single element of the project.

The goals for the future are to improve the prototype by integrating it with other indices, such as the Index of Thermal Stress - ITS (Givoni, 1976; Pearlmutter et al; 2014), or other air pollutants – and finally, to transform the prototype into a complete software package.

Acknowledgements

This work was supported by “SMARTUrban - Monitoring System and Territorial Urban Research” Project cofinanced by the Regional Government of Tuscany (POR CReO Bando Unico R&S 2012) and the European Regional Development Fund (ERDF). We acknowledge for their technical contribution in the development of the system Geosystems srl and Netsens srl.

References

- Brandani, G., Napoli, M., Massetti, L., Petralli, M., Orlandini, S. (2016). Urban soil: Assessing ground cover impact on surface temperature and thermal comfort. *Journal of environmental quality*, 45, 90-97.
- Brett B.A. (2003). Physical environmental modeling, visualization and query for supporting landscape planning decisions. *Landscape. And Urban Planning*, 65, 237-259.
- Dirmeyer, P. A., Niyogi, D., de Noblet-Ducoudré, N., Dickinson, R. E., Snyder, P. K. (2010). Impacts of land use change on climate. *International Journal of Climatology*, 30, 1905-1907.
- Eliasson, I. (2000). The use of climate knowledge in urban planning. *Landscape and urban planning*, 48, 31-44.
- Givoni, B. (1976). *Man, Climate & Architecture. 2nd Edition, Applied Science Publishers, Ltd., London*, PP. 483.
- Grimmond, S. (2007). Urbanization and global environmental change: local effects of urban warming. *Geographical Journal*, 173, 83–88. doi:10.1111/j.1475-4959.2007.232_3.x.
- Jendritzky, G., De Dear, R., Havenith, G. (2012). UTCI - why another thermal index? *International Journal of Biometeorology*, 56, 421 – 428.
- Massetti, L., Petralli, M., Brandani, G., Orlandini, S. (2014). An approach to evaluate the intra-urban thermal variability in summer using an urban indicator. *Environmental pollution*, 192, 259-265.
- Mori, J., Saebo, A., Hanslin, H.M., Teani, A., Ferrini, F., Fini, A., Burchi, G. (2015). Deposition of traffic related air pollutants on leaves of six evergreen shrub species during a Mediterranean summer season. *Urban Forestry and Urban Greening*. 14:264–273.

- Mori J., Fini A., Burchi G., Ferrini F. (2016). Carbon Uptake and Air Pollution Mitigation of Different Evergreen Shrub Species. *Arboriculture & Urban Forestry*, 42: 329–345.
- Napoli, M., Massetti, L., Brandani, G., Petralli, M., Orlandini, S. (2016). Modeling tree shade effect on urban ground surface temperature. *Journal of environmental quality*, 45, 146-156.
- Oke, T. R. (1982). The energetic basis of the urban heat island. *Quarterly Journal of the Royal Meteorological Society*, 108, 1-24.
- Pearlmutter, D., Jiao, D., Garb, Y. (2014). The relationship between bioclimatic thermal stress and subjective thermal sensation in pedestrian spaces. *International Journal of Biometeorology*, 58(10), 2111–2127.
- Petralli, M., L. Massetti, G. Brandani, Orlandini, S. (2014). Urban planning indicators: Useful tools to measure the effect of urbanization and vegetation on summer air temperatures. *International Journal of Climatology* 34, 1236–1244. doi:10.1002/joc.3760.
- Roth, M., Emmanuel, R., Ichinose, T., Salmond, J. (2011). ICUC-7 Urban Climate Special Issue. *International Journal of Climatology*, 31(2), 159–161.
- Satterthwaite, D. (2008). Cities' contribution to global warming: notes on the allocation of greenhouse gas emissions. *Environment and urbanization*, 20(2), 539-549.
- Steadman, R.G. (1994). Norms of apparent temperature in Australia. *Australian Meteorological Magazine*, 43, 1–16.
- Ugolini, F., Massetti, L., Sanesi, G., Pearlmutter, D. (2015). Knowledge transfer between stakeholders in the field of urban forestry and green infrastructure: Results of a European survey. *Land Use Policy*, 49, 365-381.
- WHO, (2014) 7 million premature deaths annually linked to air pollution. *World Health Organization Regional Office for Europe*. <http://www.who.int/mediacentre/news/releases/2014/air-pollution/en/>.

Wind comfort analysis in urban complex area: the example of the new Erzelli Technologic District

M. P. Repetto, G. Solari, M. Burlando, A. Freda

Department of Civil, Chemical and Environmental Engineering, University of Genoa, Italy

Corresponding author: Maria P. Repetto, repetto@dicca.unige.it

Abstract

The paper analyses the wind comfort at pedestrian level in the new Technologic District of Genoa, at the top of the Erzelli Hill. The probabilistic analysis is based on the large historical database measured at the Genoa Airport. The anemometric database is transformed to the Erzelli site by means of suitable transformation coefficients which represent, for each direction, the ratio between the wind velocity at the site and at the Airport. Due to the complexity of the site, the transmission coefficients are derived by means of a multi-scale approach, involving numerical and experimental wind tunnel tests at two different scale models.

1 Introduction

The new Erzelli Technology District of Genova is part of a large urban expansion plan which includes a new technological centre, the new Faculty of Engineering and a large park. It will be realized at the top of the Erzelli Hill, situated in Liguria region in Italy, close to the west boundaries of Genoa city. Unfortunately, the Erzelli Hill is very exposed to strong winds, which can affect the human comfort of people living and working in the new urban areas. The present paper describes the analyses carried out by the wind engineering research group in University of Genoa, aimed at the complete probabilistic modelling of the Erzelli wind field and the assessment of the wind-induced comfort in the area. Because of the topographic and architectonic complexity of the site, the probabilistic assessment has been made possible through an integrated system of probabilistic analysis and wind field modelling and simulation at different scales.

The probabilistic analysis is based on the large historical database measured at the Genoa Airport, very close to the site. The information acquired at the anemometric station are transformed to the Erzelli site by means of suitable transformation coefficients which represent, for each direction, the ratio between the wind velocity at the site and at the Airport.

The transmission coefficients are derived by means of a multi-scale approach at three different scales. Firstly, a numerical model is used to simulate the wind field around the Erzelli Hill, taking into account the complex orographic effect of Apennines at a geographical scale. Then two wind tunnel test campaigns are carried out on two models. The first model represents the Erzelli Hill in 1:1000 scale, catching the topographic effect of speed up near the top of the Hill; the second model reproduces the new urban centre at the top of the Hill in 1:333 scale, taking into account the local wind flow modification generated by the buildings. In particular, wind tunnel tests on this latter model are designed to characterize the wind comfort at the site (ASCE, 2003) by providing information on the wind field at the pedestrian level. Each model is related to the wind field described by the model at a larger scale, and a probabilistic chain is derived to correlate the wind velocity at the airport to the wind velocity in the new urban centre.

The potentially critical zones for human comfort are identified and discussed. A series of possible solutions will be proposed and verified at a later stage by means of a new set of wind tunnel tests..

2 Multi-scale wind field simulation

2.1 Numerical simulation of wind fields on Erzelli Hill

The wind field at a geographical scale around the Erzelli Hill is simulated numerically, adopting the mass-consistent model WINDS (Burlando *et al.*, 2007). A macro-area is simulated at first, with a plan grid of 270 meters. A micro-area is then nested into the macro-area. The micro-area is modelled with a plan grid of 80 meters, in order to obtain a more reliable wind simulation in the relevant site.

The analyses assumes the hypothesis of neutral atmosphere, as usual in high wind velocity conditions, and imposes different scenarios of wind velocity and direction at gradient height. For each scenario, the mean wind velocity and direction are obtained at each point of the grid, including the anemometric position at the Airport station and the Erzelli Hill area. Figure 1a represent the mean wind field obtained in the micro-area; the circle identifies the perimeter of the physical Erzelli Hill model in 1:1000 scale Showed in Figure 1b). In particular, 12 points on the circle are considered, corresponding to 12 wind directions, with sectors of 30° (Fig. 1b). The wind profiles in the 12 points obtained from numerical simulation and showed in Figure 2 have been adopted to calibrate the input profiles of the wind tunnel tests on the Erzelli Hill model.

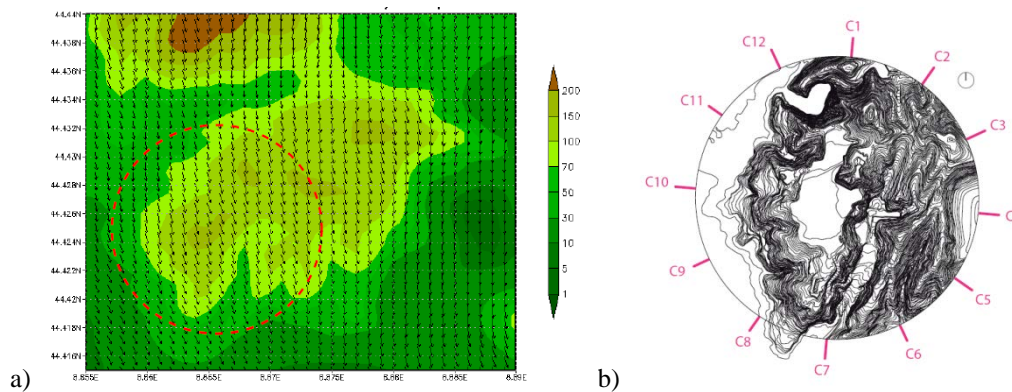


Figure 1. a) mean wind velocity scenario obtained with WINDS. The dotted line identify the Erzelli hill model in 1:1000 scale; b) scheme of the 12 considered points.

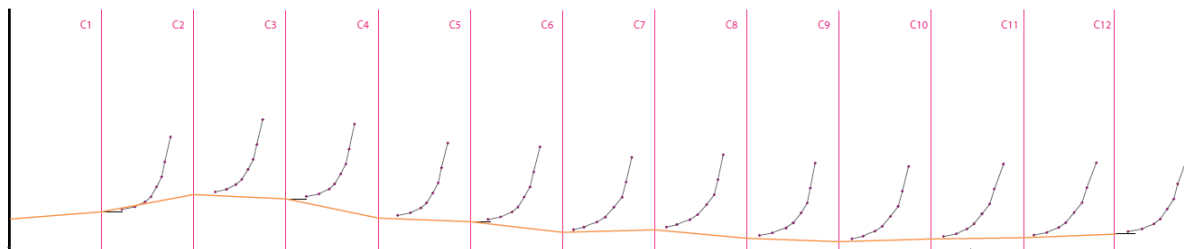


Figure 2. Wind velocity profiles approaching the Erzelli hill obtained with WINDS.

2.2 Wind tunnel test on Erzelli Hill model at scale 1:1000

The wind tunnel tests have been carried out in the closed-type wind tunnel DICAT-DIFI of University of Genoa, characterized by a test section of 1.7 by 1.35 m and an overall length of 8 m.

The first physical model reproduces the Erzelli Hill in scale 1:1000, and is designed to optimize the simulation of the local topographic effects (Fig. 3), disregarding the Erzelli Park buildings at the top. The wind tunnel tests are carried out reproducing the input wind profiles obtained with the numerical analysis and measures the wind profiles at the perimeter of the area at the top of the hill, which are strictly connected with the new Technologic Park plan. Fig. 4 shows, for some selected points, wind profiles obtained in the wind tunnel tests characterized by the maximum speed-up.

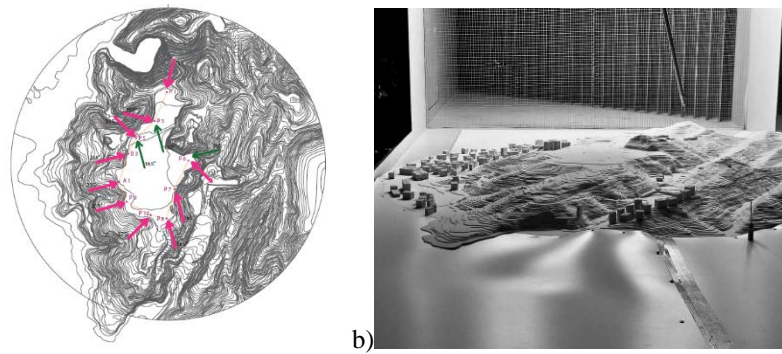


Figure 3. Erzelli Hill model in 1:1000 scale: a) scheme of the model with the considered points at the perimeter of the area and directions characterized by maximum speed-up; b) picture of the model during wind tunnel test.

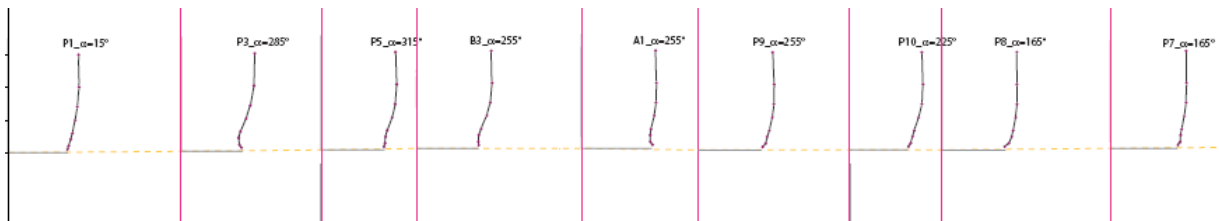


Figure 4. Wind profiles with maximum speed up obtained in wind tunnel tests on Erzelli Hill model in 1:1000 scale.

2.3 Wind tunnel test on Erzelli Hill model at scale 1:333

The second model describes the Erzelli Technologic Park in scale 1:333 and is designed to simulate the wind fields at pedestrian level taking into account the architectural features of the Park (Fig. 5a).

The wind tunnel input profiles have been calibrated considering the wind tunnel tests on the 1:1000 scale model; the pedestrian wind fields have been analysed through visualization, anemometric measurements of the wind profiles and wind velocity measurement at pedestrian level in 52 points using Irvin Probes instruments. Figure 5b shows an example of the maps of the measured wind velocity normalized with respect to the reference velocity of the wind tunnel. The dimension of the symbol is proportional to the measure. The maps for the 52 considered points put in evidence the critical points related only to the urban and architectural features of the site.

3 Wind comfort analysis

The anemometric station of the Airport of Genoa is close the Erzelli hill and is characterized by long-period records. The study considered 43 years of synoptic measurements of the 10-minute mean wind velocity, directions, and atmospheric pressure. The time series of the mean wind velocity and directions have been corrected and analysed in order to obtain the parent probability distributions at the anemometric site.

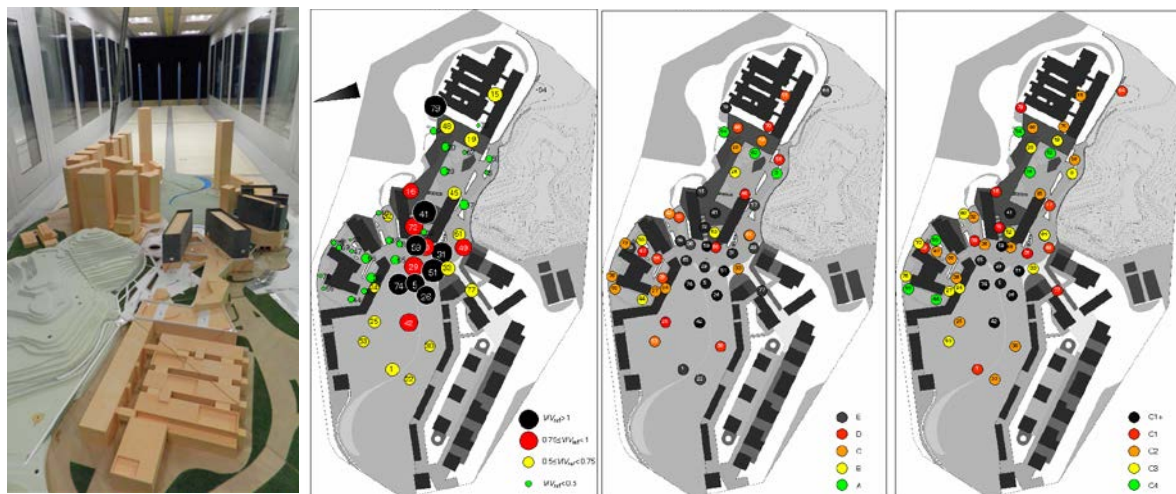
The long period series are then transformed at the grid points of Erzelli hill adopting transfer coefficients obtained by means of numerical and experimental simulations (Section 2). In particular, the first step transforms data from the anemometric site to the reference site, defined as a flat, homogeneous terrain, with uniform roughness $z_0=0.05$ m; the second step transforms data from the reference site to the selected points at the base of the Erzelli Hill; the third step transforms data from the selected points at the base of the Erzelli hill to the selected points at the perimeter of the area at the top of the hill; the final step transforms data from the selected points at the perimeter of the area at the top of the hill to the 52 points of analysis in the area of the Park. In this way, a set of 52 transfer coefficients is obtained

The database measured at the airport is transformed into 52 databases at the points of analysis in the area of the Erzelli Park and the statistical analysis is systematically repeated for each point of the analysis, obtaining the complete climatologic characterization of the area under exam.

The pedestrian wind comfort of the area is evaluated adopting two criteria proposed in literature. The former is reported in the new Dutch wind nuisance standard NEN 8100 (NEN, 2006, Wisse et al.2007). The comfort criterion establishes a threshold value for the hourly mean winds velocity of 5 m/s and defines five comfort classes (From A- comfortable to E - totally uncomfortable) on the basis of the exceedance probability of this threshold value of the local wind velocity. The latter comfort assessment procedure is provided by ASCE (ASCE, 2003). The comfort criterion establishes a threshold value for the exceedance probability of 20% and defines five comfort classes (from C4 – comfortable, to C1+ totally uncomfortable) on the basis of the range of the associated mean wind velocity. At each comfort class is associated a description of comfort activities. The class C1+ exceeds all the comfort criteria.

Figures 5c,d show the results of the wind comfort assessment according with the two adopted criteria. Both put in evidence a very critical condition of the whole area, with the most uncomfortable zone (black symbols) concentrated in the central square and in the neighbour of the new Faculty of Engineering.

The proposed multi-scale approach furnished information about a so unsatisfying results: the general orography and the local topographic speed up tend to accelerate the wind flow in the north sectors, which are also the most frequent directions for the high wind velocity, from a climatological point of view. In this unfavourable situation, the architectural features of the park increase the wind velocity, especially in the area of Engineering Faculty. A comfort analysis in the preliminary stage of the project would help the urban planning, in order to design architectural layout in a more efficient way.



a) b) c) d)
Figure 5. Erzelly Hill model at 1:333 scale (a), wind tunnel measurements for North-East direction (b); wind comfort assessment according to NEN8100 (c) and ASCE (d) criteria.

References

- ASCE, 2003. Aerodynamics Committee, Outdoor Human Comfort and its assessment, State of the Art Report, Task Committee on Outdoor Human Comfort, American Society of Civil Engineers, Boston, VA, USA.
- Burlando, M., Carassale, L., Georgieva, E., Ratto, C.F., Solari, G., 2007. A simple and efficient procedure for the numerical simulation of wind fields in complex terrain. *Boundary Layer Meteorology* 125, 417-439.

NEN, 2006. Wind comfort and wind danger in the built environment, NEN 8100 (in Dutch) Dutch Standard.

Wisse, J.A., Verkaik, J.W., Willemsen, E., 2007. Climatology aspects of a wind comfort code, in: Proceedings of the 12th International Conference Wind Engineering, 12ICWE, Cairns, Australia.

A numerical study of pressure coefficients distribution on high-rise buildings with balconies

X. Zheng¹, M. Montazeri^{1,2}, B. Blocken^{1,2}

¹ Building Physics and Services, Department of the Built Environment, Eindhoven University of Technology, P.O. box 513, 5600 MB Eindhoven, the Netherlands

² Building Physics Section, Department of Civil Engineering, KU Leuven, Kasteelpark Arenberg 40 - bus 2447, 3001 Leuven, Belgium

Corresponding author: X.Zheng, x.zheng.1@tue.nl

Abstract

Knowledge of the pressure distributions on building surfaces is essential for a complete understanding of infiltration, wind-induced ventilation and wind loads. Earlier studies have shown the influence of different façade appurtenances like balconies on the wind-induced pressure on building facades. However, a detailed investigation of the impact of facade appurtenances on the pressure distribution on building facade has not yet been performed. This is especially the case for high-rise buildings. This paper, therefore, presents a detailed study on mean wind pressure distributions on the windward façade of a high-rise building with and without façade appurtenances at wind direction of 0°. The realizable k- ϵ turbulence model in 3D steady Reynolds-Averaged Navier-Stokes (RANS) Computational Fluid Dynamics (CFD) is used for predicting. The evaluation is based on validation with wind-tunnel measurements. The results show that the presence of balconies can significantly influence the C_p distributions on the windward façade. This influence greatly depends on the size and geometry of balconies.

1 Introduction

Knowledge of the wind-induced pressure distribution on building walls is crucial to evaluate infiltration, wind-induced natural ventilation and wind loads. For example, exterior surface pressure coefficients are required as input parameters for analyzing natural ventilation and infiltration flow rates in Building Energy Simulations (BES) tools. The accurate prediction of natural ventilation can therefore significantly depend on the uncertainty involved in the pressure coefficients data (Cóstola, et al., 2005) (Ramponi, et al., 2005). Previous wind-tunnel measurements have shown the important influence of different appurtenances on wind-induced surface static pressure (Stathopoulos and Zhu, 1988) (Montazeri and Blocken, 2013) (Montazeri, et al., 2013). As many historical and contemporary building facades are characterized by protrusions and recessions such as balconies, knowledge of the impact of appurtenances on the pressure distribution on building walls is of significance.

A detailed review of the literature indicates that research on the impact of building appurtenances on wind-induced pressure distribution is very limited. This is especially the case for high-rise buildings. In addition, important parameters such as the geometry and the size of appurtenance have not yet been evaluated. Therefore, this study investigates the impact of different types of balconies on the wind-induced pressure distribution on the windward façade of a high-rise building.

The 3D steady Reynolds-Averaged Navier-Stokes (RANS) Computational Fluid Dynamics (CFD) is used. Three types of buildings are considered: (1) building without façade appurtenance (Case 1); (2) building including balconies with 4 m depth (Case 2); and (3) building including balconies with 4 m depth and 1 m height (Case 3). The evaluation is based on validation with the wind-tunnel measurements of surface pressure by Stathopoulos & Zhu (1988).

2 Wind-tunnel measurements

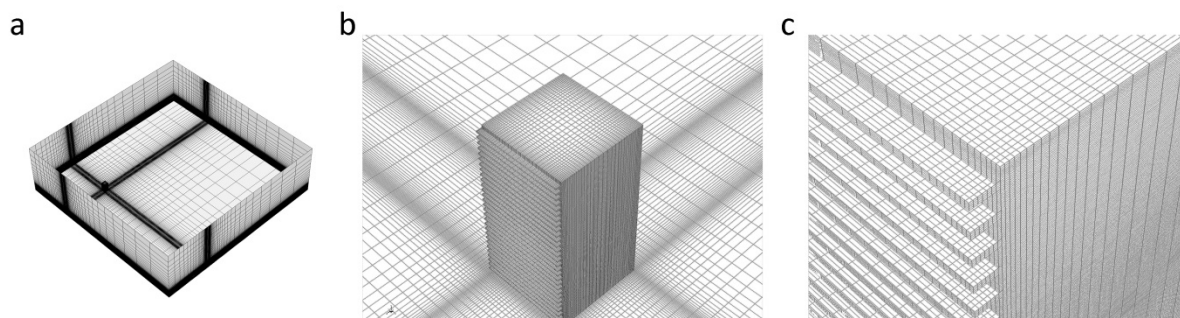


Fig. 1. Computational grid for Case 3. (a) Grid at the bottom and the side faces of the computational domain; (b) Grid at building surfaces; (c) Detail of grid near balconies.

Wind-tunnel measurements of wind-induced pressure coefficient on the facades of a high-rise building were conducted by Stathopoulos and Zhu (1988) in an atmospheric boundary layer open-circuit wind-tunnel. The wind tunnel was 12.2 m long with a cross-section of $1.8 \times 1.8 \text{ m}^2$. The mean velocity and longitudinal turbulence intensity profiles were taken at the center of the turntable, which represented by a log law with aerodynamic roughness length $z_0 = 0.0001 \text{ m}$ (model scale, corresponding to 0.04 m in full scale).

The building at scale 1:400 had dimensions width \times depth \times height = $0.152 \times 0.152 \times 0.3 \text{ m}^3$, corresponding to full-scale dimensions $60.8 \times 60.8 \times 120 \text{ m}^3$. Four types of building balconies were tested, which were different in size and geometry of balconies. Mean surface pressures were measured along lines located on windward façade of the models. In the present paper, the measured data along an “edge line” (0.15 cm to the edge of the building model) and a center line (6.1 cm to the edge of the building model) are used for validation purposes. The overall uncertainty of the C_p measurements was estimated to be less than 5%.

3 CFD simulation: computational settings and parameters

A computational model was made of the reduced-scale building models in the wind-tunnel measurements. The dimensions of the computational domain are $W \times D \times H = 6.15 \times 6.15 \times 1.8 \text{ m}^3$, which were chosen based on the best practice guidelines by Franke et al. (2007) and Tominaga et al. (2008). The surface-grid extrusion technique developed by van Hooff and Blocken (van Hooff and Blocken 2010) was applied to construct the computational grids, which only consists of prismatic cells, resulting in 5,240,496 cells. The computational grid was made in a way that it could be used for the three building models (Cases 1-3). Fig. 1 shows the grid for Case 3 (building including balconies with 4 m depth and 1 m height). The grid resolution resulted from a grid-sensitivity analysis (not shown in this paper). The distance from the center point of the wall adjacent cell to the wall, for the facade and ground plane is 0.0007 m and 0.0003 m, respectively. The standard wall functions are applied for modeling flow parameters in the near-wall region. The inlet vertical profiles (mean velocity U , turbulent kinetic energy k and turbulence dissipation rate ε) in the simulation were based on the measured mean wind velocity and longitudinal turbulence intensity. The 3D steady RANS equations were solved in combination with the realizable k - ε turbulence model, which has been proved its accuracy on similar cases in previous research (Montazeri and Blocken, 2013).

4 Validation study

The CFD results are compared with the wind-tunnel measurements for Case 1, Case 2 and Case 3 (Fig.2). The comparison is made for the edge line and the center line. A good agreement is achieved along the center line, where the average absolute deviations are 0.019, 0.047 and 0.045, respectively.

The agreement is less good for the edge line, as the deviations increase to 0.109, 0.083 and 0.149 for Cases 1, 2 and 3, respectively.

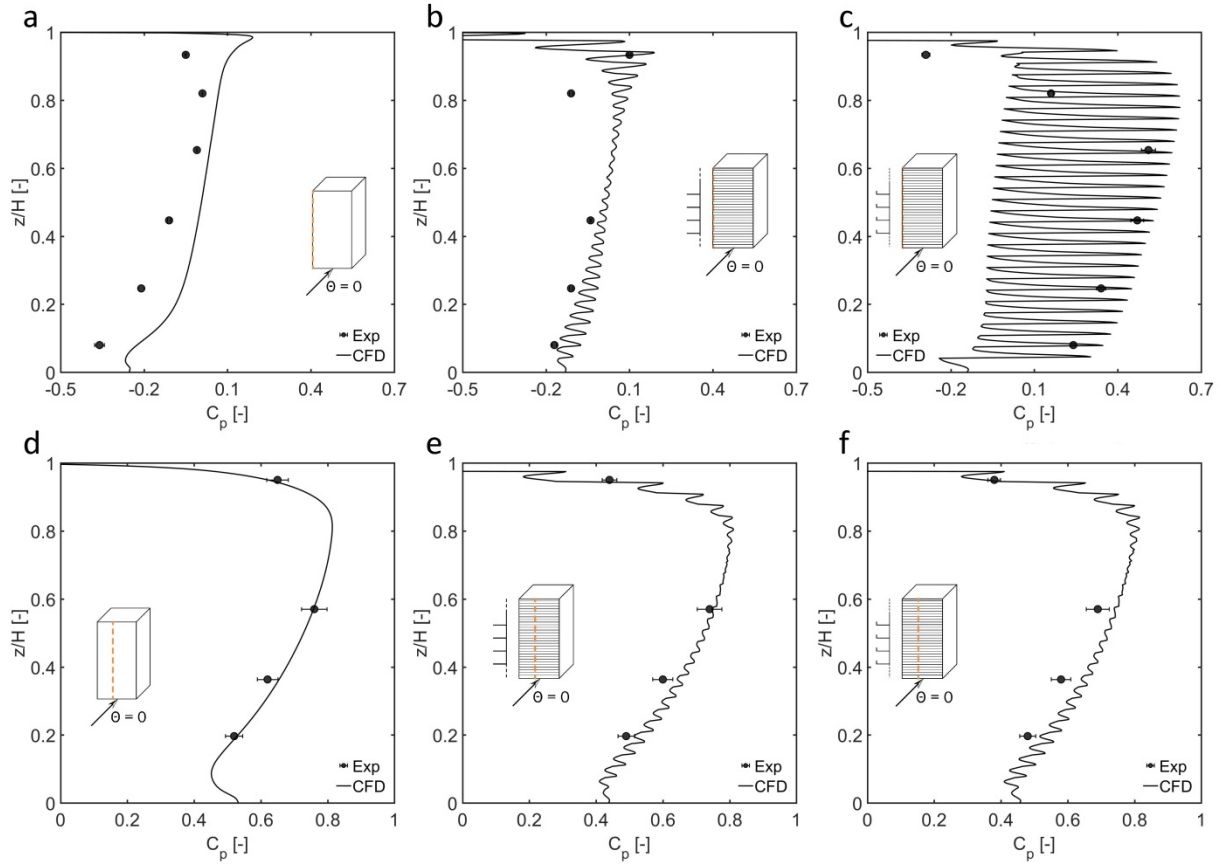


Fig.2. Comparison of C_p obtained by CFD and wind-tunnel experiments along the edge line for building (a) without façade appurtenance; (b) with 4 m balconies; (c) with 4 m balconies and 1 m walls; (d-f) same for the center lines.

5 Results

Figs. 2 a-c indicate that the presence of balconies with vertical walls (Case 3) can lead to very large vertical C_p gradients along the edge line. This is, however, less pronounced along the center line (Fig. 2 d-f). Fig. 3 shows the relative difference of the area-weighted average C_p for each balcony space between Cases 2 and 3 and the reference case (building without balcony), the value of the top balcony is removed because of large relative differences. It can be seen that the presence of the upper three balconies (close to the top one) and the first balcony close to the ground leads to a relatively high decrease in the area-weighted average C_p . The maximum reduction is 54% that occurs for Case 2. For Case 3, however, the presence of the second to the sixth balconies results in a growth in the area-weighted average C_p . The highest increase is 14% that occurs on the third floor. The impact of other balconies on the area-weighted average C_p of other floors is negligible (less than 5% for Case 2 and 7% for Case 3).

6 Conclusion

In spite of the limited data for validation, the results show that the 3D steady RANS CFD is capable of predicting the mean wind pressure distribution on the windward façade of high-rise buildings. In

addition, the presence of balconies can significantly influence the C_p distributions on the windward façade. This influence greatly depends on the size and geometry of balconies.

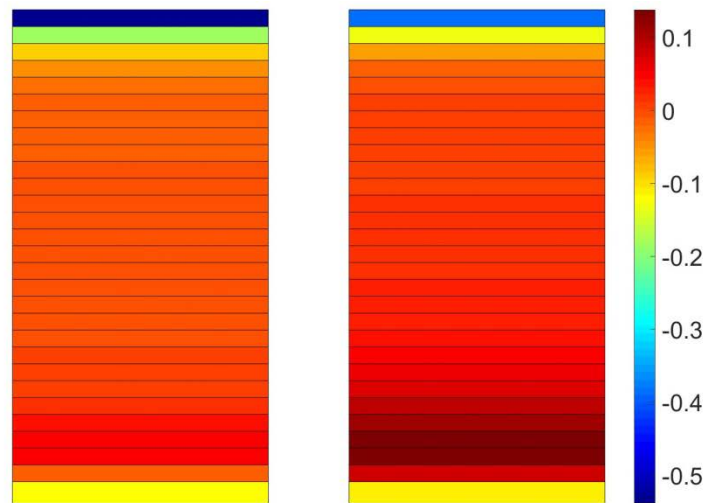


Fig.3. Relative difference of area-weighted average C_p between (a) façade with 4 m balconies; (b) façade with 4 m balconies with 1 m walls and reference case.

Acknowledgements

Hamid Montazeri is currently a postdoctoral fellow of the Research Foundation - Flanders (FWO) and is grateful for its financial support (project FWO 12M5316N). The authors also gratefully acknowledge the partnership with ANSYS CFD.

References

- Cóstola, D., Blocken, B., and Hensen, J. (2005). Overview of Pressure Coefficient Data in Building Energy Simulation and Airflow Network Programs *Building and Environment* 44: 2027–36.
- Franke, J. (2007). Best practice guideline for the CFD simulation of flows in the urban environment, *Meteorological Inst.*
- Montazeri, H., and Blocken, B. (2013). CFD Simulation of Wind-Induced Pressure Coefficients on Buildings with and without Balconies: Validation and Sensitivity Analysis. *Building and Environment* 60: 137–49.
- Montazeri, H., Blocken, B., Janssen, W.D., and van Hooff, T. (2013). CFD Evaluation of New Second-Skin Facade Concept for Wind Comfort on Building Balconies: Case Study for the Park Tower in Antwerp. *Building and Environment* 68: 179–92.
- Ramponi, R., Adriana, A., and Blocken, B. (2014). Energy Saving Potential of Night Ventilation: Sensitivity to Pressure Coefficients for Different European Climates. *Applied Energy* 123: 185–95.
- Stathopoulos, T., and Zhu, X. (1988). Wind Pressures on Building with Appurtenances. *Journal of Wind Engineering and Industrial Aerodynamics* 31 (2–3): 265–81.

Tominaga, Y., Mochida, A., Yoshie, R., Kataoka, H., Nozu, T., Yoshikawa, M., Shirasawa, T. (2008). AIJ guidelines for practical applications of CFD to pedestrian wind environment around buildings, *Journal of Wind Engineering and Industrial Aerodynamics* 96: 1749–1761.

URBAN COMFORT STUDIES

Dynamic Response of Pedestrian Thermal Comfort under Outdoor Transient Conditions

K. Ka-Lun Lau^{1,2,3}, Y. Shi⁴, Edward Yan-Yung Ng^{1,3,4}

¹Institute of Future Cities, The Chinese University of Hong Kong, Hong Kong

²CUHK Jockey Club Institute of Ageing, The Chinese University of Hong Kong, Hong Kong

³Institute of Environment, Energy and Sustainability, The Chinese University of Hong Kong, Hong Kong

⁴School of Architecture, The Chinese University of Hong Kong, Hong Kong

Corresponding author: Kevin Ka-Lun Lau, kevinlau@cuhk.edu.hk

Abstract

Outdoor thermal comfort studies have proved that urban design has a great influence on pedestrians' thermal comfort and its assessment helps to understand the quality and usage of the pedestrian environment. However, the majority of outdoor thermal comfort studies perceive pedestrian thermal comfort as "static". The dynamic multiple-use of urban spaces and the highly inhomogeneous urban morphology in high-density cities of the tropics are seldom considered. In high-density outdoor environment like Hong Kong, pedestrians experience highly variable microclimatic conditions within short distances. However, the application of the concept of transient thermal comfort in outdoor environment is rather limited and the use of longitudinal field surveys is relatively rare, which leads to a lack of understanding about how pedestrians respond to the changes of the outdoor environment. This study contributes to the understanding of the dynamic thermal comfort and the thresholds for tolerance to thermal discomfort. Findings of this study are expected to improve urban geometry design in order to mitigate the thermal discomfort and create a better pedestrian environment in high-density cities.

1 Introduction

Urban liveability and the well-being of urban inhabitants are associated with the outdoor thermal environment. One of the popular issues in this regard is pedestrianization since it promotes a healthier lifestyle and more sustainable urban environment (Castillo-Manzano et al., 2014). The level of thermal comfort experienced by pedestrians is influenced by the large variations in microclimatic conditions in urban areas owing to the complex urban geometry (Krüger et al., 2011). Therefore, the assessment of outdoor thermal comfort is important to ensure the quality of outdoor thermal environment and enhance the use of outdoor spaces (Maruani and Amit-Cohen, 2007).

In previous studies, the effect of subjects' thermal history on the dynamic response of thermal comfort is not sufficiently addressed since they focused on the effect of meteorological conditions on instantaneous subjective thermal sensation or comfort (Spagnolo and de Dear 2003; Pantavou et al. 2013). Mobile measurement system was previously employed to record the micro-meteorological conditions and individuals' physiological responses along a pre-defined pedestrian route covering a wide range of urban geometry and surface environment (Nakayoshi et al., 2015). It was suggested that thermal sensation was influenced by the cutaneous thermoreceptors responding to subtle environmental changes (de Dear, 2011), reiterating the importance of pedestrians' physiological response and thermal history.

The objective of this study is to compare the dynamic changes of pedestrians' thermal sensation and comfort between two designated routes in a high-density commercial area of Hong Kong. The effect of urban geometry and associated micro-meteorological conditions was also investigated. Findings of this study will provide information about how urban geometry design affects outdoor thermal comfort

and how people may tolerate the discomfort during their walk. Urban designers will then be able to design better outdoor spaces to enhance the walking environment in high-density cities.

2 Methods

In order to acquire information about the dynamic response of pedestrians when they are travelling within the urban environment, a longitudinal survey was conducted in one of the densest areas in Hong Kong with a variety of urban geometry. It aims to obtain information about how thermal sensation changes throughout the walking route and how it is affected by micro-meteorological conditions and urban geometry. Details of the instrumental settings and survey campaign are provided in the following sections.

2.1 Instrumentation

A backpack-type of mobile meteorological station was developed for the micro-meteorological measurements during the survey campaigns (Figure 1). It consists of a TESTO480 Digital Microclimatic Sensor Set for the measurements of air temperature (T_a), relative humidity (RH) and wind speed (v). Globe temperature was measured by a tailor-made globe thermometer composed of a thermocouple wire (TESTO flexible Teflon type K) held in the middle of a 38-mm black table tennis ball, which is designed for the purpose of decreasing the response time during mobile measurements (Humphreys, 1977; Nikolopoulou *et al.*, 1999). Mean radiant temperature (T_{mrt}) was then estimated according to Eq. (1) (Thorsson *et al.*, 2007):

$$T_{mrt} = \left[(T_g + 273.15)^4 + \frac{1.10 \cdot 10^8 \cdot v^{0.6}}{\varepsilon \cdot D^{0.4}} (T_g - T_a) \right]^{\frac{1}{4}} - 273.15 \quad (1)$$

where ε is emissivity (0.95 for a black globe) and D is globe diameter. Clothing of each subject was recorded and the level of metabolic activities is assumed to be 2.0 met which represents a slow walking speed of 3.0 km/h for pedestrian activities in commercial/shopping district (Fanger, 1973). Physiological equivalent temperature (PET) was then calculated from the above meteorological and human parameters and used as an objective indicator of pedestrian thermal comfort.

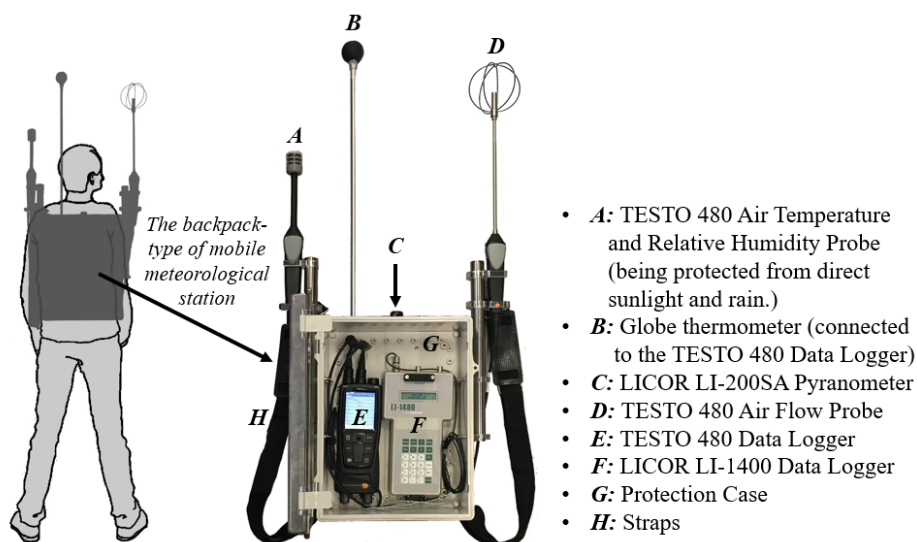


Figure 1. Instrumental settings of the mobile meteorological station.

2.2 Survey Campaigns

The survey campaigns were conducted in a high-density commercial area of Hong Kong. Two walking routes were designed to cover the variations in urban geometry and survey points were

designated to conduct thermal comfort survey (Figure 2a). They were instantaneously conducted in order to avoid temporal differences in background meteorological conditions. At each survey point, the subjects were asked for their thermal sensation vote (TSV) for the environment they were situated. Sky view factor (SVF) was used to represent the compactness of urban geometry and the SVF values were calculated for each survey point using Rayman model (Matzarakis and Rutz, 2010) based on fisheye photos taken during the survey (Figure 2b). Table 1 shows the meteorological conditions of the days when the survey was conducted. The data were based on the weather record of the ground-level meteorological stations operated by the Hong Kong Observatory, which is situated less than 1km away from the study area. The survey campaigns were conducted from 2pm to 4pm in order to represent the critical summer conditions. They were also carried out under three types of weather conditions, namely clear, partially cloudy and overcast sky.

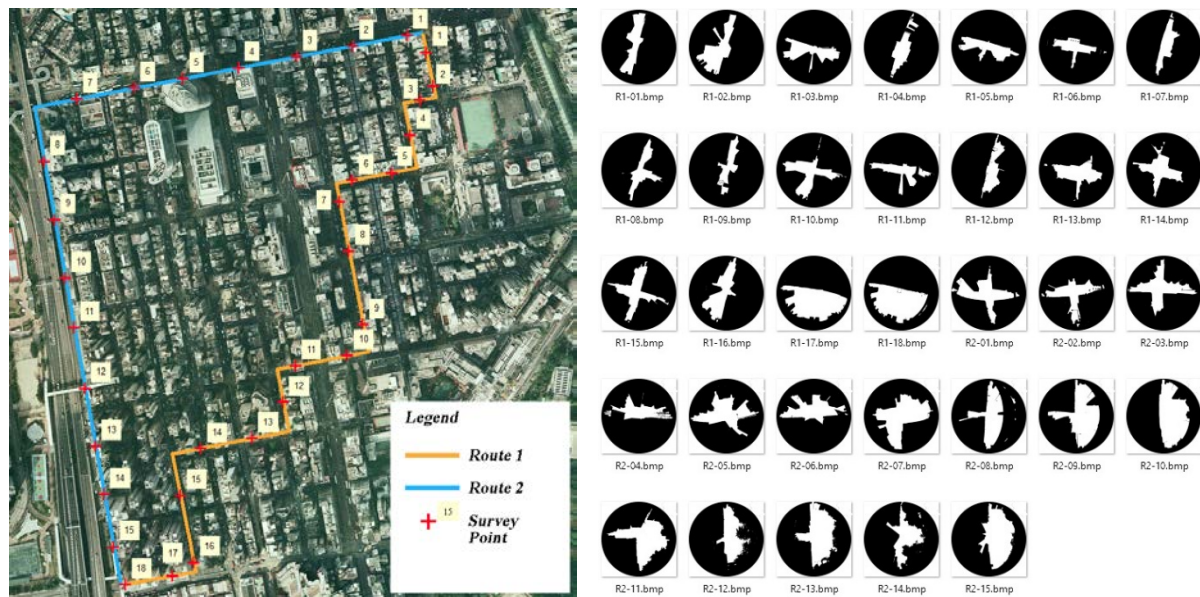


Figure 2. (a) Walking routes of this study; (b) fish-eye photos of each survey point.

Table 1. Meteorological conditions of the days when the survey being conducted.

Date	Air Temp (°C)	Relative Humidity (%)	Wind Direction	Mean Wind Speed (m/s)	Sky condition	Mean Amount of Cloud (%)
8-Aug-16	31.6-32.8	69-73	NW	3.6	Overcast Sky	83
22-Aug-16	31.3-31.8	64-72	SE	3.1	Clear Sky	27
13-Sep-16	29.5-30.5	70-76	SE	2.8	Partially Cloudy	61
14-Sep-16	31.7-32.8	50-60	N, W	1.9	Partially Cloudy	59
28-Oct-16	30.0-31.0	62-68	SE	1.4	Partially Cloudy	54
7-Nov-16	26.8-28.1	68-75	SE	3.3	Partially Cloudy	52

3 Results and Discussion

3.1 Micro-meteorological Measurements

There are considerable spatiotemporal variations in meteorological conditions along the two walking routes during the survey. Figure 3 shows the spatiotemporal variations in T_a , v , and T_{mrt} on 13 September 2016 (partly cloudy day). T_a is found to be higher in more open sections of the walking routes. For instance, higher T_a ($>32^\circ\text{C}$) is observed from the 10th to 22th minute in Route 1 when the subjects pass through a long section of N-S orientated street. High sun altitude results in direct exposure to intense solar radiation, which corresponds to the level of T_{mrt} . Higher level of pedestrian activities is also a reason for high T_a . The latter half of Route 1 covers mostly narrow streets which

provide sufficient shading. Lower T_a is found in this section except at the 45th minute when the subject reached an open intersection.

On the other hand, lower T_a and T_{mrt} were found in the first half of Route 2 because the subjects were walking along the shaded side of the E-W orientated main road. When the subjects turned to the N-S orientated road, T_a and T_{mrt} reached up to 33.8°C and 36.2°C respectively. However, roadside trees provide extensive shading to this particular section of the route, resulting a considerable decrease in T_{mrt} (by approximately 5°C). It reiterates the importance of shading to the microclimate of the street environment.

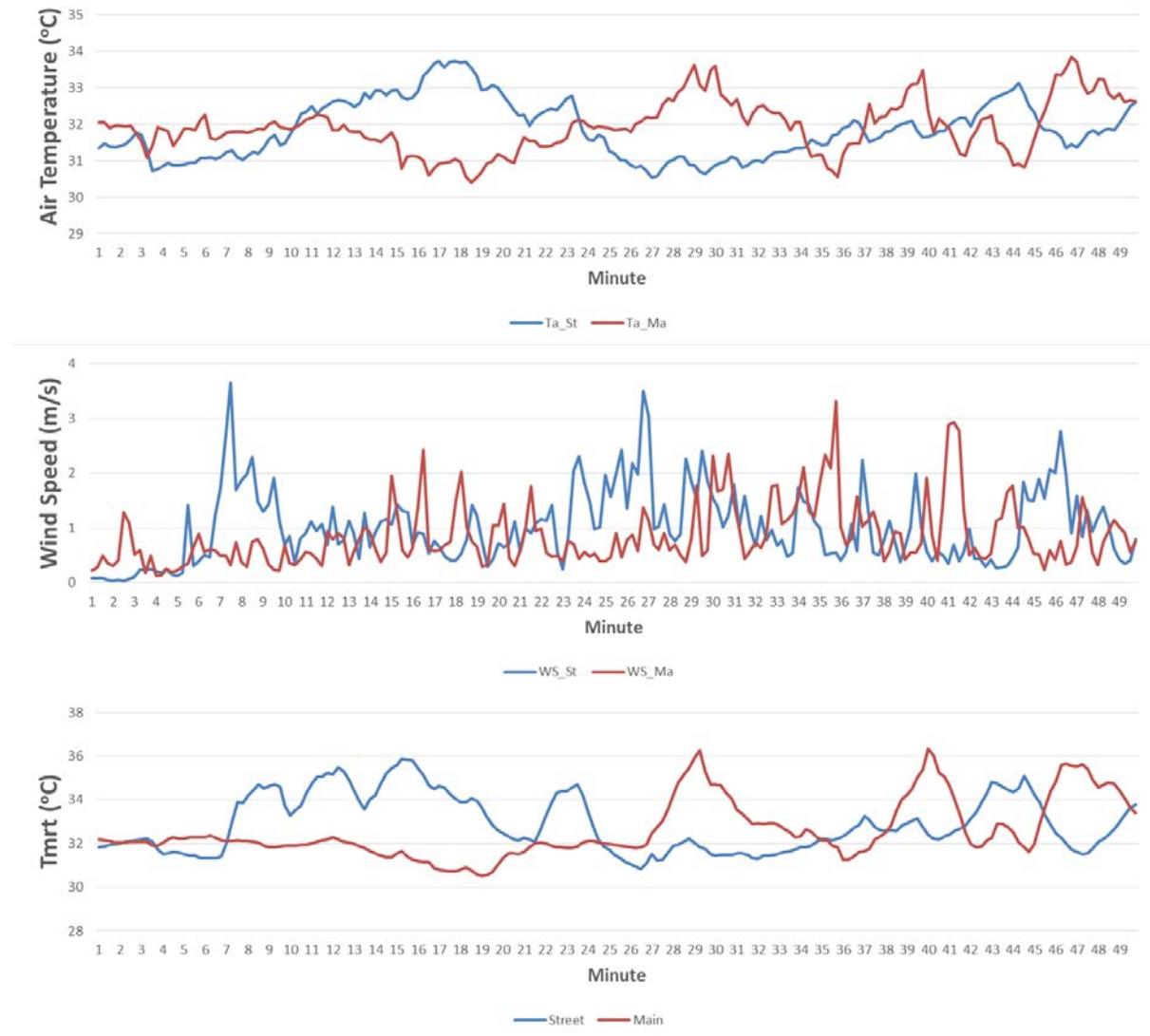


Figure 3. Temporal variations of air temperature, wind speed and mean radiant temperature.

3.2 Spatial variation of PET and subjective thermal sensation

Figure 5 shows the spatial variation of PET along the two designated routes under partially cloudy and clear sky conditions. Under partially cloudy conditions, PET values are up to 36°C along the main road (Route 2) where the subjects are largely exposed. The corresponding thermal sensation reported by the subjects is up to +2.5, indicating a thermally uncomfortable environment. Locations with trees present show lower PET values of about 28°C and serve as a “break” for urban dwellers to recover from the heat stress they experienced. PET values are consistently low in the narrow streets (Route 1)

due to the shading by surrounding high-rise buildings. The subjects reported mostly neutral thermal sensation throughout the entire route.



Figure 4. Street environment of Route 1 (left) and Route 2 (right).

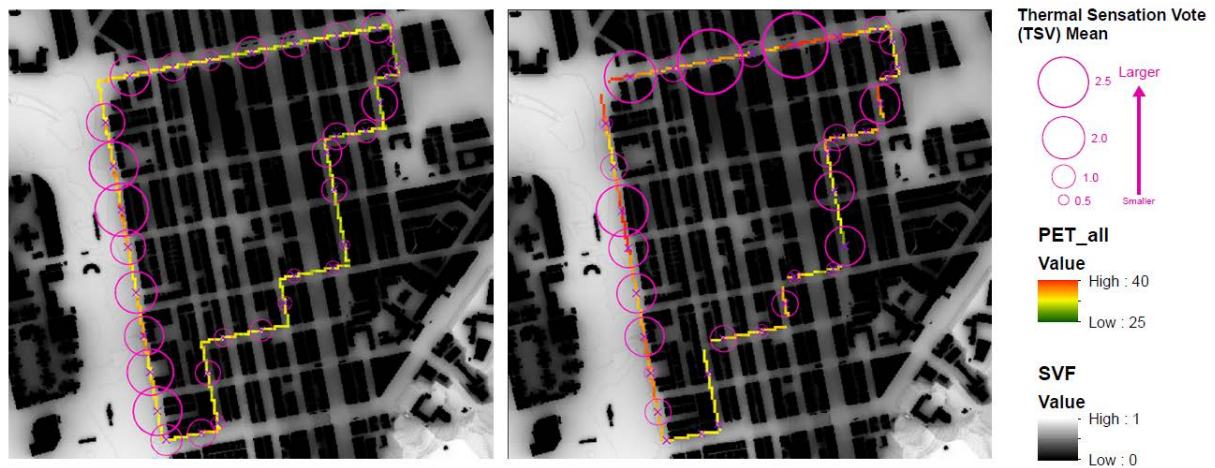


Figure 5. Spatial variation of PET for the two walking routes and the corresponding thermal sensation votes reported by the subjects.

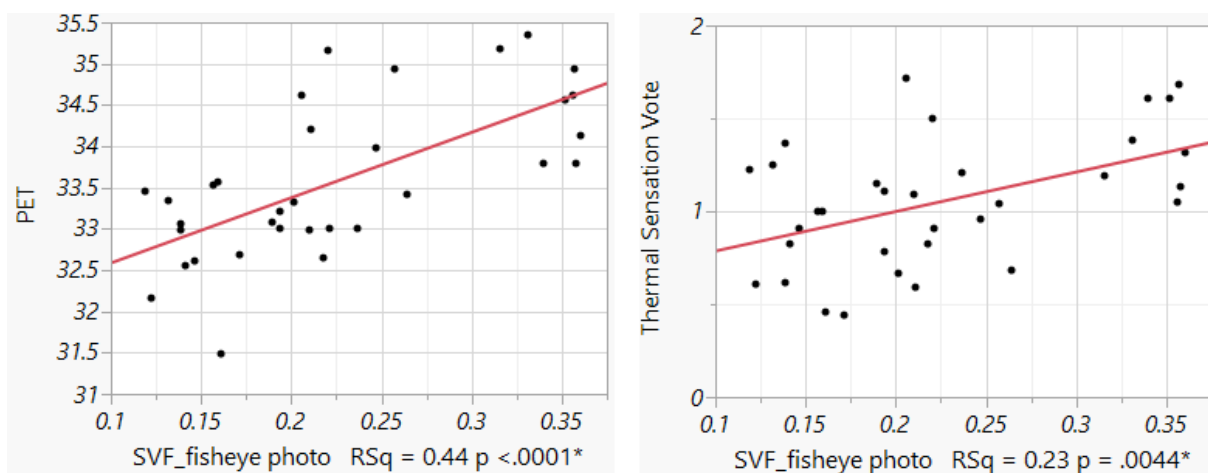


Figure 6. Scatterplots of (a) PET vs SVF and (b) TSV vs SVF.

Under clear sky conditions, PET values were found to be consistently high along Route 2 and most of the thermal sensation votes were warm (+2) to hot (+3). However, there were some lower TSVs reported between the higher TSV values. Such a large contrast is likely because of their immediate thermal history, resulting in much lower TSVs reported by the subjects. This phenomenon was previously suggested as “thermal alliesthesia” (Parkinson and de Dear, 2015). It implies that there are certain thresholds which pedestrians may be able to tolerate. Such information is important to the design of urban geometry since it offers greater flexibility to the design.

3.3 Effect of Sky View Factor on Outdoor Thermal Comfort

SVF has been used as an indicator to urban heat island phenomenon in previous studies (Lindberg, 2007; Chen *et al.*, 2012). In this study, it was used to represent the compactness of the built environment and examined for the relationship with PET and subjective thermal sensation. It was found that SVF is correlated with PET reasonably well with R^2 -value of 0.41. (Figure 6a). However, the R^2 -value for the relationship between SVF and TSV is 0.23 despite of the statistical significance (Figure 6b). It suggests that the non-directional nature of SVF may not be able to account for the thermal sensation reported by subjects. As such, the SVF measured was divided into eight sectors and a multiple linear regression is developed to examine which sectors are more influential to thermal comfort. It was found that the SW- and W-sector SVF together exhibit a R^2 -value of 0.71. It reiterates the importance of sun exposure in the afternoon in pedestrian-level thermal comfort so geometry design should pay attention to providing shading for this condition.

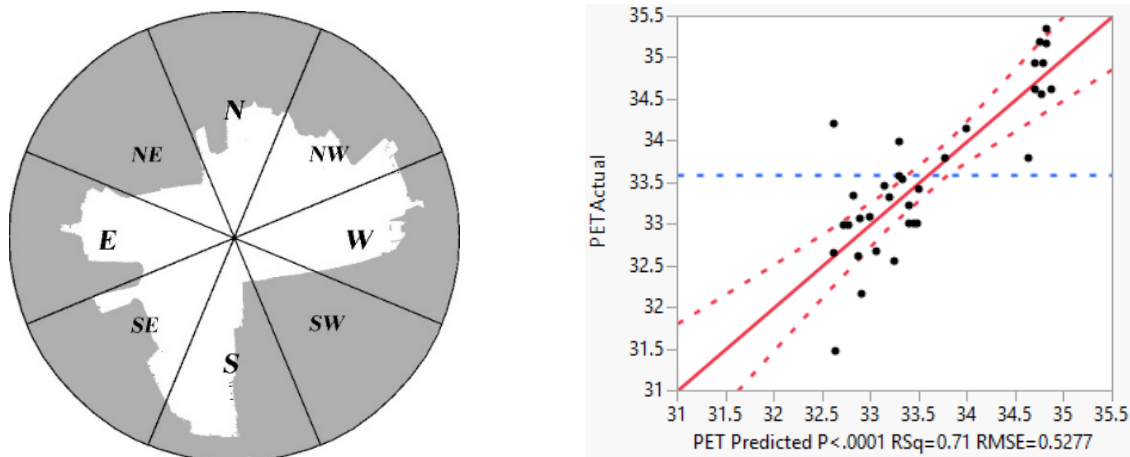


Figure 7. (a) The eight-sector SVF used in this study and (b) the performance of using SW- and W-sector SVF to predict PET for survey points.

4 Conclusions and Further Work

Survey campaigns were conducted in order to obtain information about the dynamic nature of pedestrian thermal comfort. Mobile measurement system was used to record the micro-meteorological data during the survey campaign. Results show that there are considerable variations in the meteorological conditions and the corresponding thermal sensation reported by subjects. Openness is one of the predominant factors influencing pedestrians’ thermal comfort. It was also shown that subjects felt more comfortable when moving from sunlit to shaded places. The improvement to thermal comfort is greater when the difference in PET is higher. It implies that more careful geometry design is important to pedestrian-level thermal comfort, taking into account the level of tolerance to thermal discomfort. Further study will be conducted to better understand such “rhythms” of tolerance and the physiological mechanism behind them.

References

- Castillo-Manzano, J.I., Lopez-Valpuesta, L., and Asencio-Flores, J.P. (2014). Extending pedestrianization processes outside the old city center: conflict and benefits in the case of the city of Seville. *Habitat International* 44, 194–201.
- Chen, L., Ng, E., An, X., Ren, C., Lee, M., Wang, U., and He, Z. (2012). Sky view factor analysis of street canyons and its implications for daytime intra-urban air temperature differentials in high-rise, high-density urban areas of Hong Kong: a GIS-based simulation approach. *International Journal of Climatology* 32(1), 121–136.
- de Dear, R. (2011). Revisiting an old hypothesis of human thermal perception: Alliesthesia. *Building Research and Information* 39(2), 108–117.
- Fanger, P.O. (1973). Assessment of man's thermal comfort in practice. *British Journal of Industrial Medicine* 30(4), 313–324.
- Humphreys, M.A. (1977). The optimum diameter for a globe thermometer for use indoors. *Building Research Establishment Current Paper* 78(9), 1–5.
- Krüger, E.L., Minella, F.O., Rasia, F. (2011). Impact of urban geometry on outdoor thermal comfort and air quality from field measurements in Curitiba, Brazil. *Building and Environment* 46, 621–634.
- Lindberg, F. (2007). Modelling the urban climate using a local governmental geo-database. *Meteorological Applications* 14, 263–273.
- Maruani, T., and Amit-Cohen, I. (2007). Open space planning models: A review of approaches and methods. *Landscape and Urban Planning* 81(1–2), 1–13.
- Matzarakis, A., and Rutz, F. (2010). *Application of the RayMan model in urban environments*. Freiburg: Meteorological Institute, University of Freiburg.
- Nakayoshi, M., Kanda, M., Shi, R., and de Dear, R. (2015). Outdoor thermal physiology along human pathways: a study using a wearable measurement system. *International Journal of Biometeorology* 59, 503–515.
- Nikolopoulou, M., Baker, N., and Steemers, K., (1999). Improvements to the globe thermometer for outdoor use. *Architectural Science Review* 42, 27–34.
- Pantavou, K., Theoharatos, G., Santamouris, M., and Asimakopoulos, D. (2013). Outdoor thermal sensation of pedestrians in a Mediterranean climate and a comparison with UTCI. *Building and Environment* 66, 82–95.
- Parkinson, T., and de Dear, R. (2015) Thermal pleasure in built environments: physiology of alliesthesia, *Building Research & Information* 43(3), 288–301.
- Spagnolo, J., and de Dear, R. (2003). A field study of thermal comfort in outdoor and semi-outdoor environments in subtropical Sydney Australia. *Building and Environment* 38, 721–738.
- Thorsson, S., Lindberg, F., Eliasson, I., and Holmer, B. (2007). Different methods for estimating the mean radiant temperature in an outdoor urban setting, *International Journal of Climatology* 27, 1983–1993.

Air movement representation as a tool for urban and architectural environmental quality

M. L. Germanà, S. Vattano and A. Tavalante

Department of Architecture, University of Palermo, Italy

Corresponding author: M. L. Germanà, marialuisa.germana@unipa.it

Abstract*

Air movement is a measurable physical phenomenon that produces indirectly measurable effects on people and on the environment. It is an essential prerequisite for the comfort and the hygiene of the built environment and it is highly relevant to the passive cooling strategies. The relationships between air movement and built environment have to be analysed under a multi-scale vision. They fall within the field of urban and architectural design because they can be influenced by artificial expedients, although they are always caused by natural factors. This paper discusses the need for a complete and objective representation of different kinds of air movement, to improve the urban and architectural design and to integrate the knowledge and the assessment of the built environment. The proposal for a graphic standard is partially described, aiming to contribute towards a codified and multi-scale representation of the air movements that can be considered as a tool for environmental quality, both in the maintenance or the conservation activities and in the transformation processes.

1 The role of the air movement in urban and architectural environmental quality: the need for graphic standard

Air is an essential environmental element for living beings, along with light, water and heat. *Exchange* and *Move* of air have been recognized as *functional convergences* between nature and buildings, focusing on the morphological adaptation (Badarnah, 2017). But air movement involves a wider field of interest, if seen as a measurable physical phenomenon that produces indirectly measurable effects on people (individuals or community) and on the environment (natural and built one). Many features of the vernacular architecture prove that the traditional approach to buildings was based on a shared awareness of these effects, which can be both beneficial and damaging.

Air movement is an essential prerequisite to achieve comfort and environmental quality of the built environment, both indoors and outdoors. Even if some natural physical factors (i.e. temperature and pressure) often increase and always cause air movement, it is a basic topic of architectural urban and environmental design, mainly because it can be influenced by artificial expedients. Although the multifaceted role of air movement has been studied from different perspectives (anthropocentric, environmental and engineering), a methodological synthesis is needed to face the concept of *breathing architecture* both in the existing settlements and in the new ones (Stavridou, 2015).

Two interlinked aspects in the role of the air movements in environmental quality can be underlined to contribute to this synthesis: the positive hygienic consequences and the energy-saving potential.

The exchange of air is the way to expel the pollutants and to avoid the formation of mould and dampness, preventing the *Sick Building Syndrome* (Apter *et al.*, 1994; Seppänen and Kurnitski, 2009). At a broader scale, the air movement could be a main factor in improving the urban air quality, contributing to the urban health (Kjellstrom, 2007), even if they aren't sufficient to reduce the global air pollution. At an urban level the natural ventilation is frequently identified (with vegetation and high albedo materials) as one of the basis of a concurrent approach in the mitigation of the *Heat Island*

* This paper reports some results of research and didactic activities driven under the scientific responsibility of M. L. Germanà. She has written the text; S. Vattano and A. Tavalante have contributed to the literature review and to the selection of the figures. The par. 2 has been improved by S. Vattano's skills in the architectural representation.

effect (Shahmohamadi, 2010). As the relationships between the geometry and density of the urban fabric and the wind flow affect the health and comfort conditions of the urban areas, the interventions on the built environment must focus on these features (Rajagopalan, 2014), even if the constraints of existing settlement may restrict the possibilities of action.

The air movement makes possible the air exchange that is a major contributing factor of the cooling strategies at an urban and building scales: the environmental cooling through air movement (in addition to the control of external thermal inputs through solar control, insulation and thermal capacity) characterizes the main passive cooling techniques (Santamouris, 2005). The natural ventilation, generated by outflow and inflow of air and increased by pressure and temperature differences, makes a sizable contribution to the NZEB (Nearly Zero Energy Buildings) goal, laid down by the European Community in 2010 (EU, 2010). In fact natural ventilation is 'passive' since it doesn't use equipment or engineering systems with energy consumption, and it is generally preferable to mechanical ventilation not only due to energetic issues, but also in consideration of the general well-being of occupants and users (Al horr, 2016).

For these reasons, hygienic and energetic performances are the features of cities and buildings in which the air movement plays the main role in attaining multiple Sustainable Development Goals (UN, 2015).

Air movement includes various phenomena with regard to the built environment that should be taken into account under a multi-scale vision, to be suitably directed and optimized for their better use in the urban and architectural design. The wider phenomenon of the prevailing winds (*territorial-scale winds* related to the macroclimate and *local-winds* related to microclimate) needs to be observed within a territorial area, considering some physical-geographical elements, as the specific geomorphological and hydrological features.

The urban and district levels need an intermediate scale, that focuses on the relationships between natural and artificial factors, which affect the urban climate: the air flows go across the urban fabric, meeting obstructions or being canalised and transforming their direction and intensity.

Within an organic vision, each building is featured by a different ability to breathe, that depends on several factors, as its shape and orientation and the characteristics of the openings (layout, size and typology). Every single building can be observed as a sort of air-system, in which the air movement follows a specific flow, dotted by elements that work in supply, distribution and extraction of the air, contributing both in terms of energy saving and of thermo-hygrometric comfort.

Finally, in a smaller scale, air movement plays an important role in improving the environmental performances of some main technological components, as in ventilated and micro-ventilated envelope. All these typologies of air movement, originated by external factors (winds) or by internal causes (stack effect), have consequences on the environmental and health performances of the urban areas and buildings. Their standard graphic representation is essential to integrate/update/improve the usual dimensions of the urban and architectural design, since the early and subsequent definition phases of the design solutions. A subjective or artistic representation of air movement does not encourage the exchange of experiences that is strategic in the general scientific advancement/upgrade. After decades of research in this field, the time has come to encode a graphic standard in the representation of air movement to obtain a more effective and shareable knowledge about it.

2 State of art in the representation of air movement

Many examples of air representation in artistic or graphical expressions lead to confirm that it is easier to represent the effects of the air than the air itself, without taking into account the metaphorical or mythological references (Nova, 2011). In fact, the air movements are not visible, even though their effects are well recognisable and permanent in the landscape and buildings (Fig. 1). Even the standardized scales to rate the wind (like the Beaufort Wind Force Scale) are based on their consequences, at sea and on land.



Figure 1. The recognisable and permanent effects of the wind on the landscape and on the built environment. Views of Favignana island (ph. by M. L. Germanà November 2016).

Since the air movement has become a part of the environmental architectural design, the need for their direct representation has arisen. The state of the art in the air movement representation includes more than fifty years of research and application efforts. In the second half of the 1950s Victor Olgay first proposed a scientific methodology in bioclimatic design, applicable case by case to each climatic zone, that still constitutes an important reference (Olgay, 1963). Olgay's ground-breaking methodological attempts were accompanied by very strong efforts in representing the effects of the wind on the built environment observed at territorial, urban and building scale, studying how the air flow affects the local microclimatic variables, therefore the contour conditions, and the actual impact of wind on buildings. These representations are very effective, especially if one refers to the technological advancement of that time (Fig. 2).

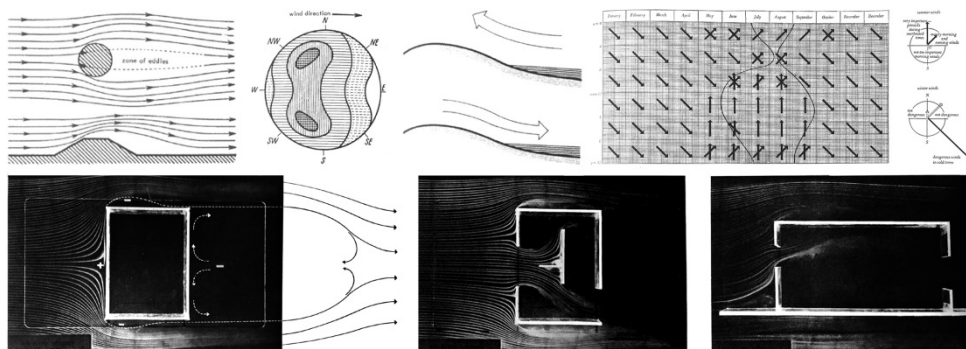


Figure 2. Above, the air representation at territorial scale (Olgay, 1963: figg. 97-98; 100; 183-184). Below, the air representation at building scale (Olgay, 1963: figg. 201; 214; 218).

In the last decades, many studies have been devoted to the on-going research of a generalizable method able to support the urban and architectural design solutions in pursuing sustainability. In the same time, an intense normative production and many training activities within the professional associations have approached the issues of environmental sustainability, energy saving and building energy performance certification. In most of these experiences, the air movements have been represented without a graphic standard: the literature review often shows, on one hand, the confirmation of Olgay's representation and, on the other hand, the application of his method to singular study cases. The suggestion for drawing the airflow diagram, by steps starting from the summer prevailing wind direction and proceeding through a trial-and-error process, is an interesting example of ventilation design guide based on simple graphic tools (Fig. 3).

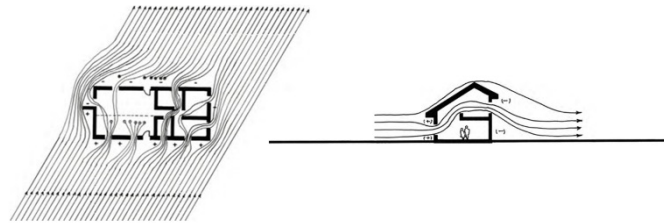


Figure 3. The Airflow Diagrams representing the air movement in plan and section (Lechner, 2015 p. 306).

The usual technical drawings (plans, sections and perspective or axonometric projections) have been commonly supplemented only by representations of airflows through arrows, larger outdoors and smaller indoors. In addition to the dimensional variation, which seems to indicate the mass of air, a colour variation (from green or blue to red) can be seen, which also allows to argue the temperature variation along the flow. The graphic representation attempts have included three-dimensional arrows placed in perspective or axonometric views in correspondence of changes in form or layout of the building (Fig. 4). Also at the urban scale, the schematic configurations of the interaction between ventilation and built context have shown the effort to represent the main aerodynamic trajectories of air around the built environment.

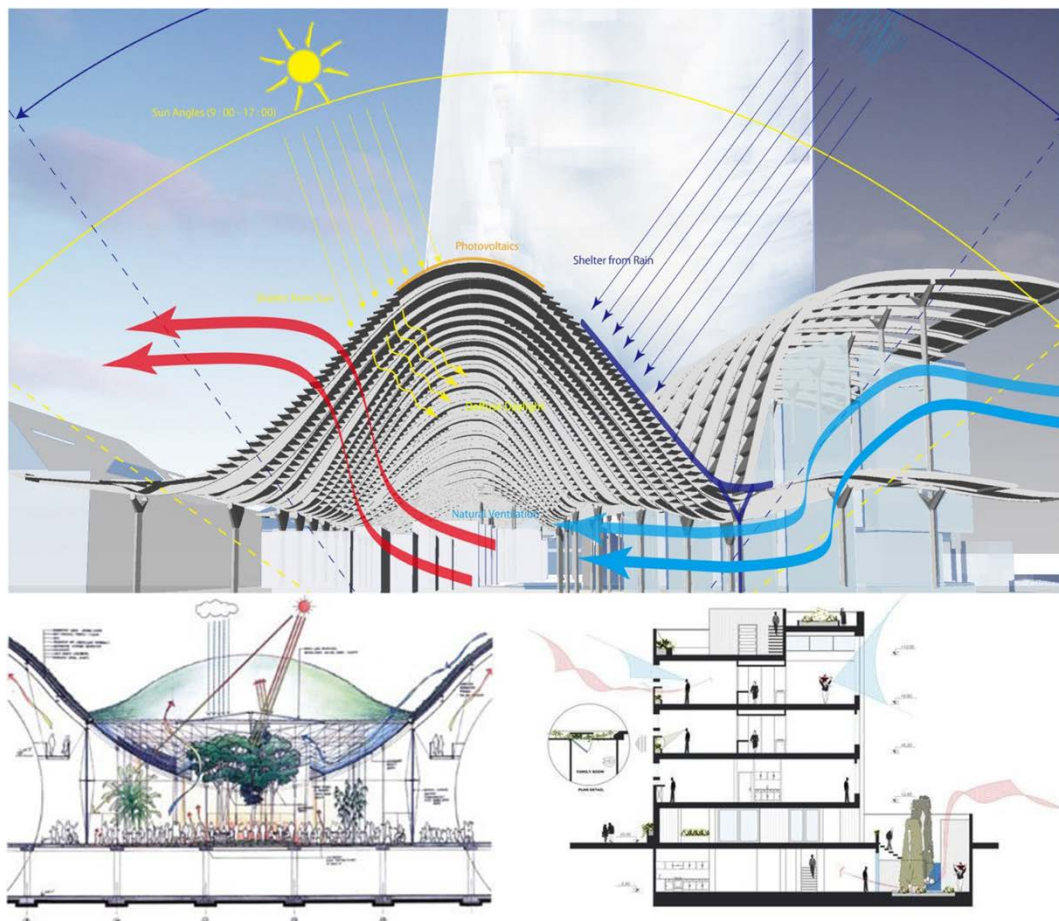


Figure 4. Examples of different air representation in contemporary architectural design. Above: *Singapore's New Eco-Complex, South beach*. Bioclimatic section. Project by Norman Foster 2007 (<http://inhabitat.com/foster-partners-new-green-complex-for-singapore/>). Below on the left: *California Academy of Sciences*. Piazza airflow. Project by Renzo Piano 2008 (<http://www.arcspace.com/features/renzo-piano-california-academy-of-sciences/>). Below on the right: *House no.2, Isfahan-Iran*. Bioclimatic section. Project by SarSayeh Architectural Office 2015 (<http://www.archdaily.com/787481/house-no-2-sarsayeh-architectural-office>).

Recently, the representation of the air movement has achieved previously inconceivable levels. Thanks to satellite images, geographical representation and meteorological data are available to everybody. For instance, the Air Quality Index and the wind velocity in every part of our planet are accessible for all in real time (Fig. 5).

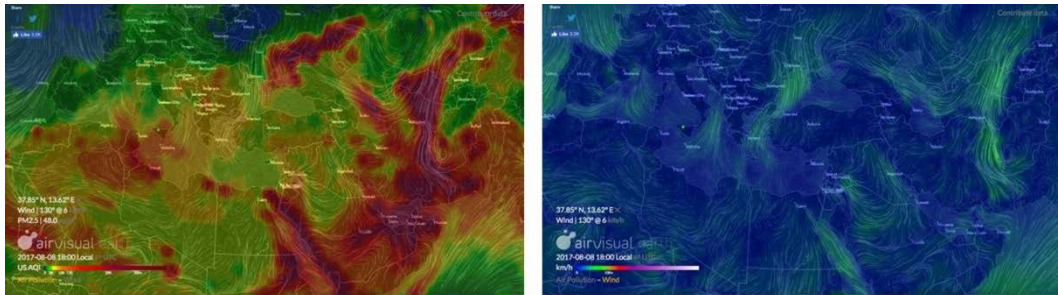


Figure 5. Air Quality Index and wind situation in Mediterranean Area in real time. August 8th 2017, 18:00.

(<https://airvisual.com/earth>).

Similarly, today the architectural design has many available digital tools that achieve a hyper-realistic representation in an apparently easy way. The current digital revolution has deeply changed the architectural drawings, both in an operational sense and in their use. The air movements, for instance, are widely represented in 2D or 3D models as fluids interacting with built environment at the different scales. The most common software products in the field of natural ventilation in buildings use Computational Fluid Dynamics to simulate airflows with the aim of assessing the effectiveness of the ventilation system in different conditions. This allows detecting air intakes through the configuration of irregular arrows or irregular surfaces that represent the direction and concentrations of air at certain points of the building. The fluid-dynamics study is also deepened through software that can control data from the urban scale to the detail of the single object. The simulations performed, albeit at different degrees of detail, show a single interactive symbol representing the airflows, with the chromatic distinction related to the variation of velocity. This kind of representation has been improved both in new design and in the assessment of existing settlement, also of historical interest (Pelliccio, 2016).

There is no doubt that these representations are very helpful in integrating the airflow analysis in the urban and architectural design process (Fig. 6). In fact, these newer representations are easily readable also without specialist skills and offer a useful synthesis of the phenomenon. However, these images cannot establish a unified relationship between data management and information provided. This makes the sharing of the knowledge and the interoperability between several fields of research difficult. In the same way as the general trend towards a hyper realistic representation increasingly confuses the observer (in fact the digital drawings look often more real than a picture), the representation obtained by specific software solutions poses the risk of an uncritical vision, unable to make understandable the complex and multi-scalar phenomenon of air movements.

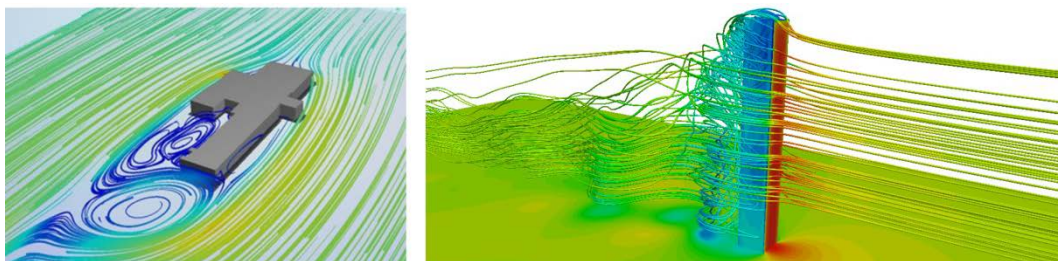


Fig. 6. Images of the *Wind & Airflow Strategies Course* (<http://auworkshop.autodesk.com/courses/wind-airflow-strategies-course>).

3 A methodology for a multiscale representation of the air movements

Some recent research and teaching experiences have given the opportunity for contributing to a graphic standard of air movements in a coherent multi-scale vision. A bioclimatic analysis has been done on diverse Sicilian cases of study (historical urban centres, archaeological sites, and single buildings of different epochs and uses) attempting to improve a repeatable method featured by multi-scale coherence, that allows a critical assessment of the air movements in a specific site, intending to increase the awareness of the design choices.

This analysing method aims to be repeatable regardless to the specific objective. Its results can be summarised in an improved understanding of the air movements useful to: a more complete knowledge and a more conscious intervention on the existing settlements; a more sustainable environmental design for the new buildings and urban areas. The theoretical basis of this aim is that the multifaceted architectural quality mostly depends on the relationships between the built environment and its context. The analysis of the environmental aspects, like the different kinds of air movement, is just a part of these relationships, important for some issue, as the hygienic and energetic performances of inhabited settlements, or the physical conservation of historical built heritage.

These experiences have allowed evaluating the urban and building characteristics, linking them to the action of dominant winds and offering a new interpretation that suggests original levels of understanding. The multi-scale analysis methodology starts with a series of geographic, topographic and meteorological data, taking into account the morphological features at the territorial scale. Through open access data obtained from the nearest meteorological stations, a graphical synthesis represents the general situation of the prevailing seasonal winds in the site. Different-coloured arrows are drawn in aerial photogrammetric views downloaded from <https://earth.google.com/web/>. A common caption, implemented referring to the Mediterranean wind rose, guides in the selection of the arrows' colour suggesting the temperature of the prevailing winds; the tip of the arrows indicates the speed, according to the Beaufort scale. The territorial scale analysis includes the altitudinal sections, where the arrows show the flow variation with respect to the local orography. A symbol distinguishes the reference season (Figg. 7-8).

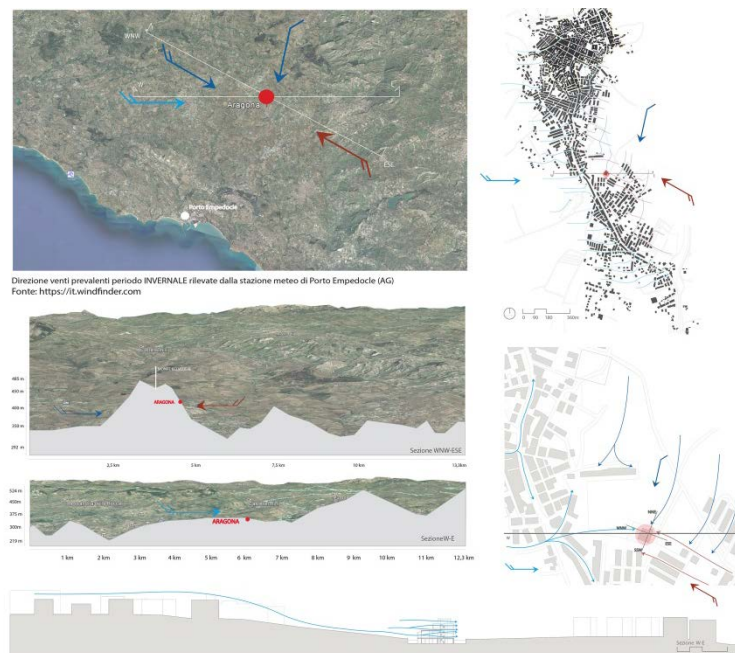


Figure 7. Air movements' multi-scale analysis: prevailing winter winds at territorial and district scale. Preparatory study for master diploma design of intervention on an unfinished building in Aragona, near Agrigento (F. Vella 2017).

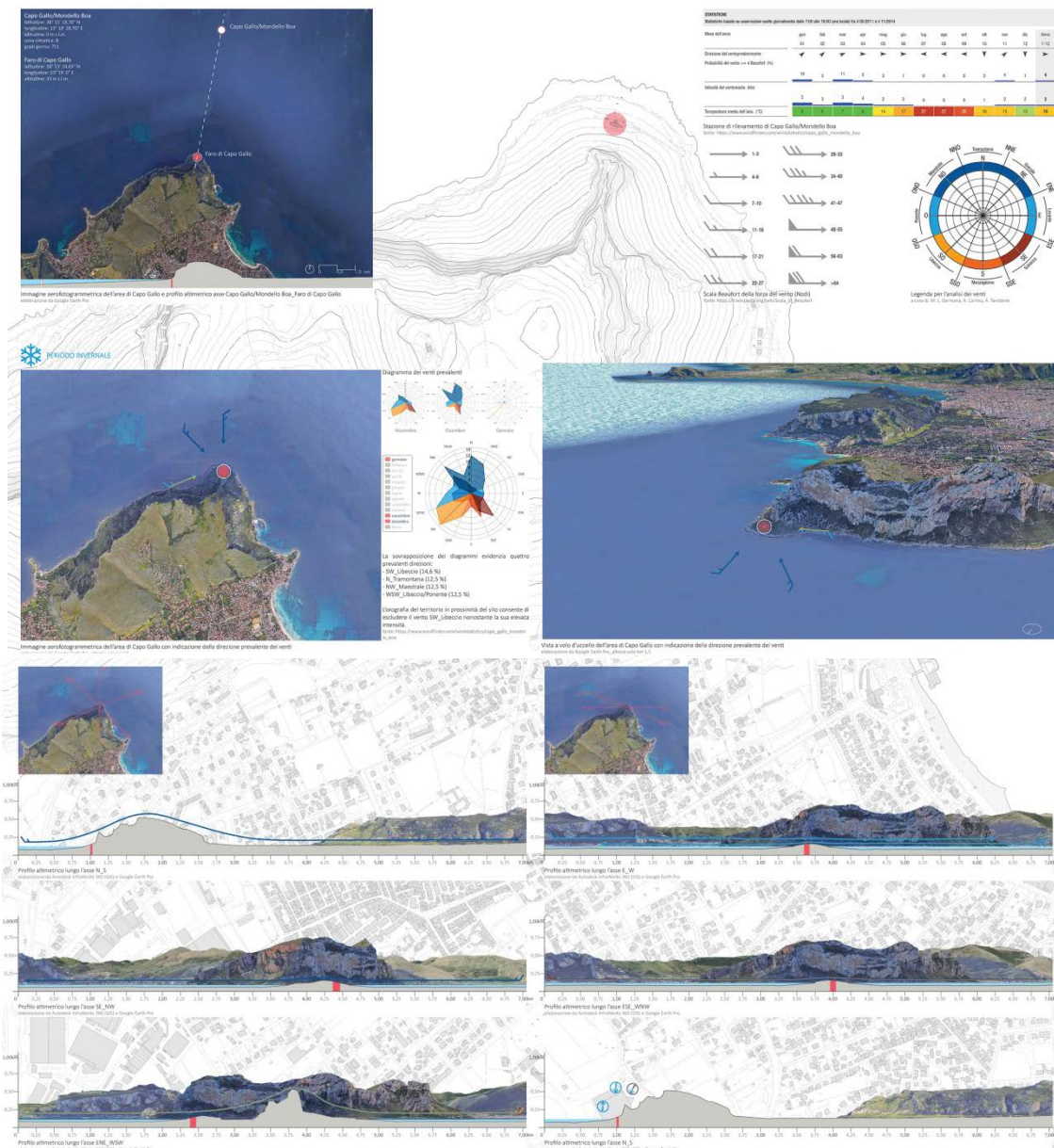


Figure 8. Air movements' multi-scale analysis. Above prevailing winter winds at territorial scale. Below altitudinal sections showing winter (on the left) and summer (on the right) winds. Preparatory study for master diploma design of intervention on the lighthouse of Capo Gallo a Palermo (C. Mendola, 2017).

The following analysis at urban and district scales considers only the wind that do not find any obstacle at the territorial scale. The arrows retain the same colour to remark the wind's direction; the straight lines became sinuous crossing the urban fabric or other barriers, in accordance to the known effects of variation of the airflow. At the building scale, the coloured arrows point out the spaces featured by a critical lack of natural ventilation. In the sections, the cross winds perpendicular to the plane of the representation are marked with a circular symbol that contains a little arrow, upward in case of following wind; downward in case of headwind (Fig. 9). In case of slope winds, thermally created winds that blow up or down in the same direction reversing the way by day and night, the graphical standard described above is not appropriate. In this case the arrows indicate the direction while the sun and moon symbols indicate the way (Fig. 10).

Further factors of air movement have their origin inside the building rather than outside. These kinds of air movements are also important in the health performances and in the passive cooling strategies, perhaps more than those have external origin. In fact, a careful solar design can contribute to the

natural ventilation, both indoors and outdoors, even in lack of external factors. Another graphic standard has been studied for these further air movements that is not covered by this paper, due to editorial limitations. It differs according to the air movement that is valuable in the spatial units or in the technical components (like the building envelope).

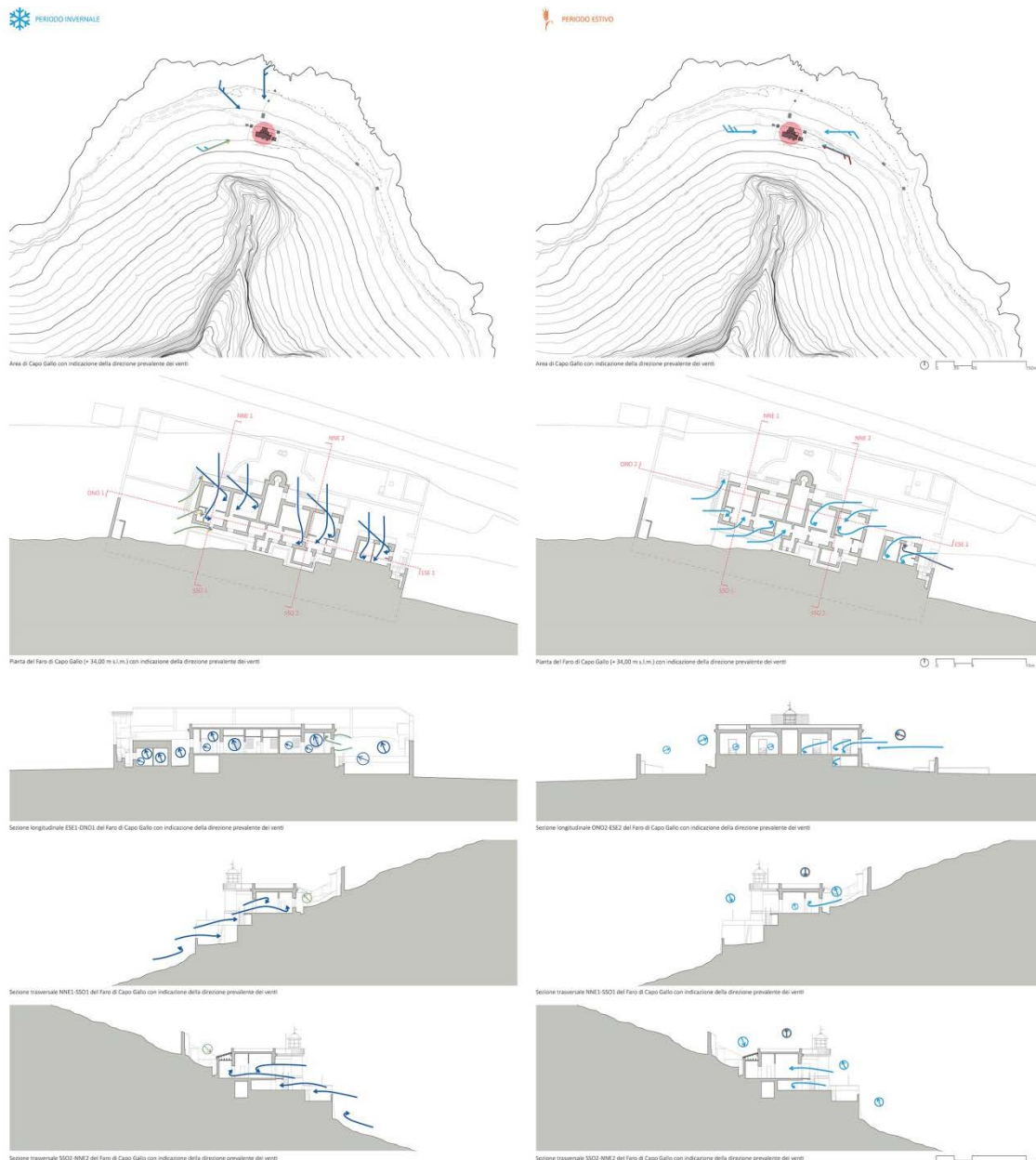


Figure 9. Air movements' multi-scale analysis: prevailing seasonal (winter on the left and summer on the right) winds at territorial scale at building scale. Preparatory study for master diploma design of intervention on the lighthouse of Capo Gallo a Palermo (C. Mendola, 2017).

4 Conclusions

Different kinds of air movement, featured by internal or external origins, relate to the built environment. There is a need of a multi-scale analysis for a comprehensive understanding of the interactions between the air movement and the architecture, within a wider vision of its contextual relationships. Two interlinked aspects in the essential role of the air movements in achieving urban

and architectural environmental quality, both indoors and outdoors, have been underlined: the positive hygienic consequences and the energy-saving potential.

A codified representation is required to include the air movement among the usual dimensions of the urban and architectural design, also in order to encourage the exchange of experiences that is strategic in the general scientific advancement. After decades of research and experiences in the environmental architectural design, the time has come to address the attempt to encode a graphic standard in the representation of air movement. This does not run counter the digitalization of the architectural representations, but it tries to eliminate the backlog comparing to the representation of other aspects, like the buildings materials.

An analysing and representing method has been partially described here, that aims to be repeatable, regardless to the specific objective. The results can be summarised in an improved understanding of the air movements, useful to: a more complete knowledge and a more conscious intervention on the existing settlements; a more sustainable environmental design for the new buildings and urban areas. It would be worth continuing the experimentation, applying this analysing and representing methodology to more study cases, in order to improve a graphic standard to the different kinds of air movement, bestowing therefore an image to something that is invisible in itself.

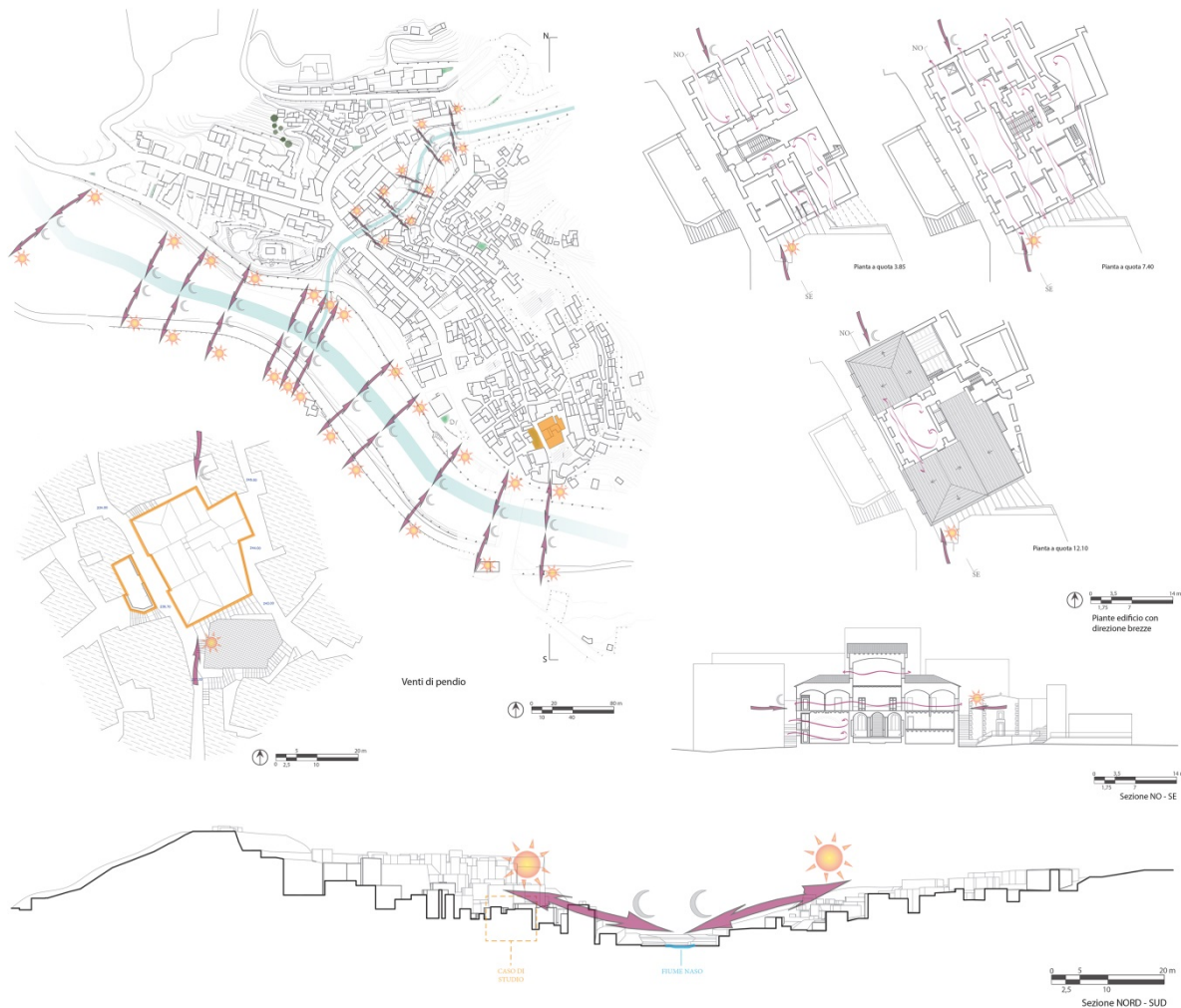


Figure 10. Air movements' multi-scale analysis: slope winds at district and building scale. Preparatory study for master diploma design of intervention on an historical building in Sinagra (M. Bonina, 2017).

References

- Al horr, Y., *et al.* (2016). Impact of indoor environmental quality on occupant well-being and comfort: A review of the literature. *International Journal of Sustainable Built Environment*, Vol. 5 Issue 1 pp. 1-11- June.
- Apter, A., *et al.* (1994). Epidemiology of the sick building syndrome. *The journal of Allergy and Clinical Immunology*, August 1994 Vol. 94, Issue 2, Part 2, 277–288; doi: <http://dx.doi.org/10.1053/ai.1994.v94.a56006>
- Badarnah, L. (2017). Form Follows Environment: Biomimetic Approaches to Building Envelope Design for Environmental Adaptation. *Buildings* 2017, 7, 40; doi:10.3390/buildings7020040
- EU (2010), Directive 2010/31/EU on the energy performance of buildings (available at <http://eur-lex.europa.eu/legal-content/EN/TXT/PDF/?uri=CELEX:32010L0031&from=EN>).
- Kjellstrom T., *et al.* (2007). Urban Environmental Health Hazards and Health Equity, *J Urban Health*; 84 (Suppl 1): 86–97 <http://doi: 10.1007/s11524-007-9171-9>.
- Lechner, N. (2009; 2015 4th edition). *Heating, Cooling, Lighting: Sustainable Design Methods for Architects*. John Wiley & Sons, Hoboken NY.
- Nova, A. (2011). *The Book of the Wind: The Representation of the Invisible*, McGill-Queen's University Press, Kingston.
- Olgyay, V. (1963). *Design with climate: bioclimatic approach to architectural regionalism*. Princeton University, New Jersey.
- Pelliccio, A. (2016). *Cognitive analysis for historical towns: digital representation and computational simulation to investigate the effects of solar radiation and wind exposure*. In Bertocci, S. and Bini, M. (eds), *The reasons of Drawing*, Gangemi Editore, Rome pp. 547-552.
- Rajagopalan, P., *et al.* (2014). Urban heat island and wind flow characteristics of a tropical city. *Solar Energy* 107 (2014) 159–170 <https://doi.org/10.1016/j.solener.2014.05.042>
- Santamouris, M. (2005). Passive cooling of building. *Advances of Solar Energy*. ISES, James and James Science Publishers, London.
- Seppänen, O. and Kurnitski, J. (2009). 3. *Moisture control and ventilation*. In WHO World Health Organization (2009), *WHO guidelines for indoor air quality: dampness and mould*, pp. 31-62 available at http://www.euro.who.int/__data/assets/pdf_file/0017/43325/E92645.pdf.
- Shahmohamadi, P. *et al.* (2010). Reducing urban heat island effects: A systematic review to achieve energy consumption balance. *International Journal of Physical Sciences* Vol. 5 (6), pp. 626-636, June, 2010 available at <http://www.academicjournals.org/journal/IJPS/article-stat/DBB8AC426195>.
- Stavridou, A. D. (2015). Breathing architecture: Conceptual architectural design based on the investigation into the natural ventilation of buildings. *Frontiers of Architectural Research* 4, 127–145 <http://dx.doi.org/10.1016/j.foar.2015.03.001>.
- UN United Nations (2015). *Transforming our world: the 2030 Agenda for Sustainable Development*, Resolution adopted by the General Assembly on 25th September 2015 70/1 available at http://www.un.org/ga/search/view_doc.asp?symbol=A/RES/70/1&Lang=E.

Urban comfort evaluation in an Italian historical district: the impact of architectural details in wind tunnel and CFD analysis

A. Ricci^{1,2}, A. Freda¹, M.P. Repetto¹, M. Burlando¹, B. Blocken^{2,3}

¹Department of Civil, Chemical and Environmental Engineering, University of Genoa, Italy

²Department of the Built Environment, Eindhoven University of Technology, The Netherlands

³Department of Civil Engineering, KU Leuven, Belgium

Corresponding author: A. Ricci, a.ricci@tue.nl

Abstract

In the present study the impact of the architectural details of the urban texture on the experimental and numerical evaluation of the pedestrian wind comfort is investigated. An Italian historical district, the so-called “*Quartiere La Venezia*” in Livorno (Italy), was selected as case study where wind tunnel (WT) tests and Computational Fluid Dynamics (CFD) simulations were performed at the same reduced-scale (1:300) and for the same inflow wind direction (WSW). Two types of geometrical CFD models, with different level of simplification with respect to the WT model are herein considered, referred to as the *simplified* and *approximated* geometrical models. The CFD results are compared to the WT measurements, in terms of mean wind velocity ratios, at 8 positions of “*Piazza del Luogo Pio*” in order to understand to which extent the architectural details are important to simulate properly the urban comfort. As far as the mean wind speed ratios between the experimental and both the geometrical CFD models are concerned, the results show not negligible differences.

1 Introduction

The fabric of cities and the complexity of their morphology make the analytical description of wind flow in urban areas extremely difficult. The urban boundary layer (UBL) is usually affected by the local-scale forcing due to the geometry of various details of buildings, bridges, trees and street furniture. In the last decade a wide research has been performed in which different aspects of urban wind flows were analyzed by means of wind tunnel (WT) tests and CFD simulations (e.g. Fernando et al., 2010). The joint use of these two techniques has allowed a better understanding of such flow complexity and has enhanced the performance of both (Blocken, 2014; Stathopoulos and Blocken, 2016). However, the creation of geometrical models for numerical and experimental tests must face considerable difficulties due to the extreme complexity of the urban contexts. Simplifications of architectural details, as balconies and pitched roofs, are therefore generally required and the question arises about how different levels of simplification affect the results (e.g. mean velocity, pressure coefficient or global forces). In order to understand how these details affect the wind flows in urban areas, WT tests and CFD simulations at the same reduced scale (1:300) were performed on a selected case study, the so-called “*Quartiere la Venezia*” in Livorno city (Italy). This area was chosen because the nearby port is monitored by several instruments at different locations, which will provide a further benchmark for the present study. In particular, five anemometric stations and one LiDAR wind profiler were placed in the framework of two European projects “*Wind and Ports*” and “*Wind, Ports, and Sea*” (Solari et al., 2012). The present contribution is organized as follows. Sections 2 and 3 contain a short description of the WT tests and CFD simulations setting, respectively. Section 4 quantifies the level of agreement between WT and CFD results. Finally, some conclusions and remarks are reported in Section 5.

2 Wind tunnel tests: the benchmark

WT tests were performed in the atmospheric boundary layer (ABL) wind tunnel of the University of Genoa (Italy). The wind tunnel at DICCA is a closed subsonic circuit with a test section of 8.8 m long and a cross section of 1.70 m (width) \times 1.35 m (height). The model of the case study - *Quartiere la Venezia* in Livorno city - was created at a scale of 1:300 using medium density fiberboard (MDF) of different thicknesses for the ground plates and buildings, and 3 mm closed cell PVC foam board panels for roofs and bridges (Fig. 1a). The tests were performed for the western wind direction WSW, corresponding to the prevalent wind directions for the strongest winds, and always maintaining the blockage ratio below 3.5 %. The mean wind velocity scenarios obtained during the European project *Wind and Ports* were adopted as reference for the choice of the incoming flow profiles. An ABL profile with aerodynamic roughness length $z_0 = 0.1$ m (at full scale) and friction velocity $u^* = 0.89$ m/s was used for the WT tests (Ricci *et al.*, 2017). The inlet wind speed was checked by means of fast response multi-hole probes. In order to investigate the pedestrian wind comfort in the central square of the selected urban district, the so-called *Piazza del Luogo Pio*, mean wind velocity values were measured at 8 different positions (P1 – P8) at 0.0067 m above the bottom, corresponding to 2 m above the ground plane at full-scale (i.e. the standard height considered for pedestrian wind comfort analysis) (Fig. 1b). The wind speed was measured by omni-directional Kanomax thermistors with temperature compensation. The aforementioned measures were successively used to validate the CFD simulations performed on the same urban model, as described in Sections 3 and 4.

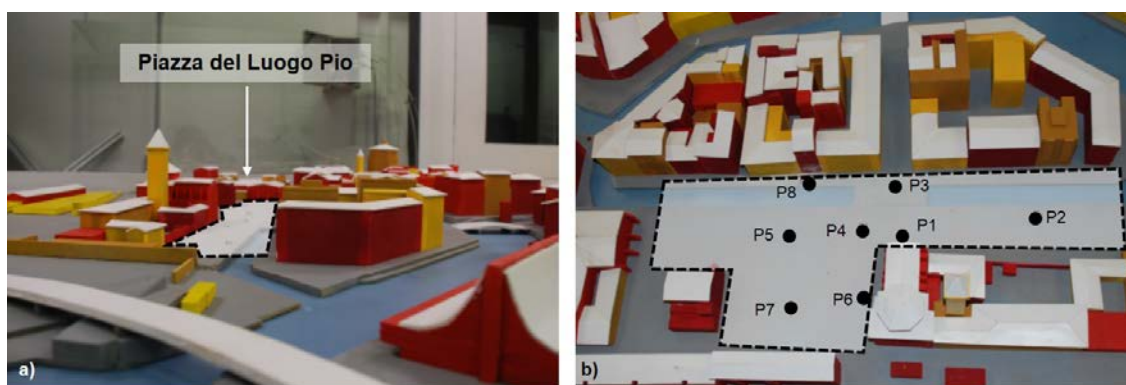


Figure 1. Picture of WT model at reduced-scale 1:300: (a) overview of the district *Quartiere La Venezia* and (b) *Piazza del Luogo Pio* with the measurements positions (P).

3 CFD simulations: computational settings

In order to facilitate the comparison between experimental and numerical results (in terms of mean wind velocity), a portion of the wind tunnel test section was reproduced by the computational domain. In particular, the size adopted for the domain was $L \times W \times H = 5.5 \times 1.70 \times 1.35$ m³, where the width (W) and height (H) are coincident with the WT cross-section while the length (L) represents the downstream part of the WT test-section. In order to understand to which extent the architectural details of the buildings, bridges and other fabrics can affect the numerical results, two geometrical models with different levels of precision were constructed. The first model, so-called *simplified model*, was obtained by approximating groups of buildings as single bluff bodies with a height equal to the arithmetic average height of that building group. The second model, so-called *approximated model*, was obtained by modelling the group of buildings with their real plan frame and heights, but replacing pitched roofs with flat ones (Fig. 2). For both geometries, meshes were generated using only hexahedral and prismatic cells, avoiding tetrahedral and pyramidal ones. The resulting meshes had 13.2 million cells for the simplified geometrical model and 23.2 million cells for the approximated geometrical model. The boundary conditions were defined in order to reproduce the input flow conditions measured during the WT tests as closely as possible. The experimental inflow conditions are reproduced at the inlet face by prescribing the mean wind velocity profile $U(z)$ detected

approximately 1 m upstream of the WT model. The turbulent kinetic energy $k(z)$ and the turbulence dissipation rate $\varepsilon(z)$ profiles were calculated using the equations proposed by (Tominaga *et al.*, 2008). At the bottom, sides and top of the domain as well as on the building and bridge surfaces, the standard wall functions with roughness modification were used. At the bottom of the computational domain, an equivalent sand grain roughness height k_s equal to 0.0013 m was imposed. This value was calculated as $k_s = 9.793 z_0/C_s$, where C_s (the roughness constant) was taken equal to 2.5 in order to comply with the necessary condition $y_p > k_s$, where y_p is the distance of the centroid of the first cell from the wall. The size of the first near wall cell was chosen in order to obtain dimensionless wall unit values y^+ in the logarithmic layer range. CFD simulations were performed using OpenFOAM 2.3.0, adopting a steady-state RANS approach and employing the realizable $k-\varepsilon$ turbulence model.

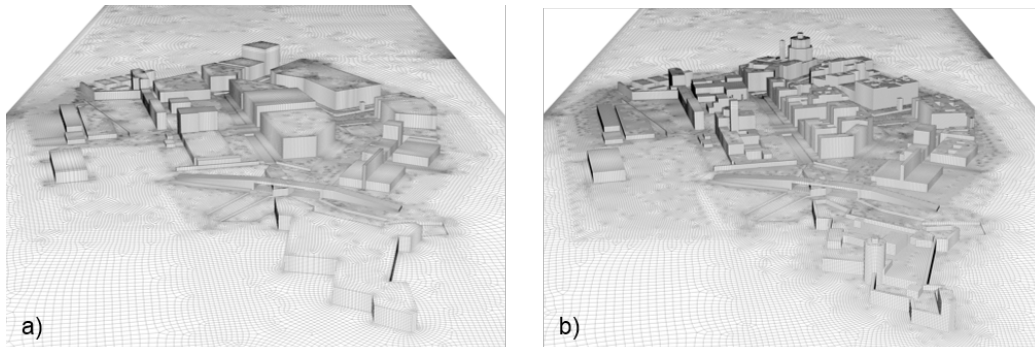


Figure 2. Computational grids of *simplified* (a) and *approximated* (b) geometrical models for the incoming wind direction WSW.

4 Experimental and numerical results

In order to better understand the whole flow field distribution inside the selected district, numerical results of both geometrical CFD models were initially analyzed in terms of velocity contours. Fig. 3 shows the contours of amplification factor made at 0.0067 m above the ground plane (corresponding to 2 m above ground plane at full-scale) of both geometrical CFD models. The contours were normalized by the inlet wind velocity magnitude at the same reference height, ($U_{ref} = 11$ m/s), as the WT results. Overall, the comparison between the *simplified* and *approximated* geometrical CFD model shows higher amplification factors for the simplified case with respect to the approximated one both at *Piazza del Luogo Pio* and along the main water canal of the district, the so-called “*Canale Rosciano*”.

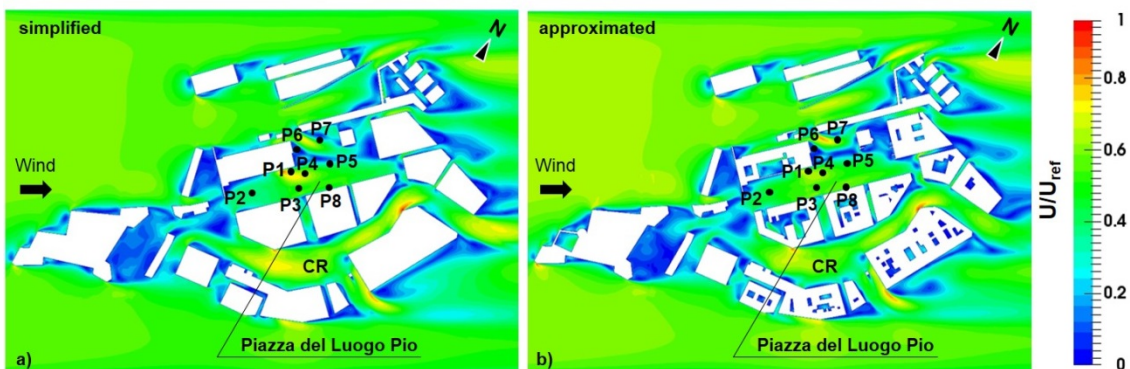


Figure 3. Contours of amplification factor: comparison between *simplified* and *approximated* geometrical models (a, b) - horizontal sections made at 0.0067 m above the ground plane (2 m above the ground plane at full-scale). *Canale Rosciano* is indicated by “CR”.

A comparison between experimental and numerical results, of both geometrical CFD models, is given in Table 1 in terms of wind velocity ratio (U/U_{ref}). A better agreement between the approximated

geometrical model and WT results, compared to the simplified one, are found at positions where separation of flow occurs (P1 and P4) and in the more open area (P3) (Table 1). Conversely, the simplified geometrical model outperforms the approximated one at the positions P2, P5, P6, P7 and P8. However, both geometrical CFD models showed noticeable discrepancies with respect to the experimental results.

Table 1. Comparison of wind velocity ratio (U/U_{ref}) between WT and geometrical CFD models, i.e. *simplified* (CFD sim) and *approximated* (CFD app), at 8 measurement positions (P1 - P8) and 0.0067 m above the ground plane (2 m above ground plane at full-scale).

<i>Point</i>	<i>WT</i>	<i>CFD app</i>	<i>CFD sim</i>	<i>CFD app vs WT (%)</i>	<i>CFD sim vs WT (%)</i>
P1	0.46	0.63	0.67	37.5%	47.2%
P2	0.31	0.44	0.40	43.1%	28.1%
P3	0.34	0.53	0.54	57.9%	58.7%
P4	0.45	0.61	0.69	37.8%	53.9%
P5	0.35	0.41	0.33	18.9%	-4.2%
P6	0.16	0.08	0.10	-48.1%	-36.6%
P7	0.37	0.55	0.25	48.6%	-32.6%
P8	0.36	0.58	0.49	60.0%	35.4%

5 Discussion and conclusions

This paper describes the wind comfort evaluation of a historical district in Italy, obtained by means of WT tests and CFD numerical simulations. The geometrical models adopted in the WT (one model) and for the CFD simulations (two different models) have a decreasing level of accuracy of the architectural details of the area under study (see Figure 1 and 2). The comparison between the results obtained with the three models (resumed in Table 1) show that the architectural details can have a strong impact in the overall wind comfort analysis of the area.

References

- Fernando, H.J.S. (2010). Fluid dynamics of urban atmospheres in complex terrain. *Annual review of fluid mechanics* 42, 365–389.
- Blocken, B. (2014). 50 years of Computational Wind Engineering: Past, present and future. *Journal of Wind Engineering and Industrial Aerodynamics* 129, 69-102.
- Stathopoulos, T., Blocken, B., (2016). Pedestrian wind environment around tall buildings. In: *Advanced Environmental Wind Engineering*. Editors: Tamura, Y. and Yoshie, R. Springer, Tokyo.
- Solari, G., Repetto, M.P., Burlando, M., De Gaetano, P., Parodi, M., Pizzo, M., Tizzi, M. (2012). The wind forecast for safety management of port areas. *Journal of Wind Engineering and Industrial Aerodynamics* 104-106, 266-277.
- Ricci, A., Burlando, M., Freda, A., Repetto, M.P. (2017). Wind tunnel measurements of the urban boundary layer development over a historical district in Italy, *Building and Environment* 111, 192-206.
- Tominaga, Y., Mochida, A., Yoshie, R., Kataoka, H., Nozu, T., Yoshikawa, M., et al. (2008). AIJ guidelines for practical applications of CFD to pedestrian wind environment around buildings, *Journal of Wind Engineering and Industrial Aerodynamics* 96, 1749-1761.

Mapping outdoor comfort for increasing environmental quality: a design proposal for Munich's *Viktualienmarkt*

D. Santucci¹, G. Volpicelli², A. Battisti², T. Auer¹

¹Technische Universität München, Chair for Building Technology and Climate Responsive Design, Munich, Germany

²Dept. PDTA Planning Design Technology of Architecture Sapienza Università di Roma, Italy

Corresponding author: Daniele Santucci, daniele.santucci@tum.de

Abstract

The environmental quality of public space is of determining importance for generating attractive urban spaces. The center of European historical cities is usually structured along market places that during the last centuries have partially shifted their function, still maintaining a high level of spatial quality and attractiveness. The present study investigates on the micro-climatic conditions that occur at present in the *Viktualienmarkt* in Munich's city center and the impact of improving measures prefigured through simulation, designed to mitigate extreme climatic phenomena and to preserve livability through guaranteeing environmental qualities of such spaces.

1 Introduction

Outdoor spaces are important in promoting the quality of life in cities. The thermal experience in an urban environment is a complex issue with multiple layers of concern. The environmental stimulus (i.e., the local microclimatic condition) is the most important factor in affecting the thermal sensations and comfort assessments of people: these assessments are both dynamic and subjective (Nikolopoulou and Steemers, 2003). In addition to the climatic aspects of thermal comfort, a variety of physical and social factors that influence perceptions of urban space come into play when people are outdoors. The challenge for designers and urban planners is not only how to collect, process or interpret such huge arrays of information, but to develop an integrated understanding of dependencies to prefigure vibrant urban environments (Santucci et al., 2017).



Figure 1. The *Viktualienmarkt* in Munich – Image by G. Volpicelli

The *Viktualienmarkt* in Munich is one of the most attracting places of the city. For centuries it has been used as a marketplace; nowadays, besides its original function, it is known for being one of the

most frequented public places. The present study has the dual aim of understanding local microclimate at a pedestrian level and of proposing design interventions to increase comfort levels to mitigate extreme climatic conditions.

Mapping comfort over time (i.e., physical and physiological characteristics) has been modeled effectively to provide “climatic knowledge”. Although people’s subjective perceptions and responses to the urban environment are various and not yet well understood, simulation and scenario-testing tools are always of particular importance in an assessment framework because they provide a platform for the integration of knowledge from various perspectives and comparisons of various design scenarios (Martinelli *et al.*, 2014). Givoni already addressed the need for “predicting tools” in the research for how changes in design details influence outdoor thermal comfort (Ng and Ren, 2015).

The human-biometeorological assessment of the thermal environment at urban open spaces has become increasingly important due to different reasons (Lee and Mayer 2013, 2015). Besides the need of a deeper understanding of the contemporary urban space, climate projections have foreseen both global warming, sea level rise and an increase in the frequency and intensity of extreme events, such as heavy rain and storm events, desertification, and giant forest fires (IPCC, 2013). Besides these extreme climatic phenomena, Central European cities suffer from the intensification of severe heat caused by regional climate change as neither their structures nor their residents are adapted to this meteorological hazard (Carter *et al.*, 2015).

The exposure to heat waves, exacerbated by the formation of heat islands (UHI), strongly affects health conditions and causes often many deaths. The character and intensity of urban heat island formation has been exhaustively documented through the field of urban climatology since the 1960s: the maximum intensity of the effect has been measured between 2 and 12 °C, suggesting that most large cities have already experienced a magnitude of warming roughly equivalent to that projected to occur through the global greenhouse effect this century (Stone *et al.*, 2012). In this context, urban planning faces the huge challenge to develop and apply measures, which may lead to a local reduction of human heat stress under regionally predetermined heat. As these measures have to be focused on citizens, they need a human-biometeorological basis (Lee *et al.*, 2016). Therefore prefiguring adaptation measures for societies to a new climate context is of prime importance (Masson *et al.*, 2014).

2 Methodology

The following section will focus on the methodologies used to gather information regarding microclimatic conditions and thermal comfort. Three main sections compose the methodology:

- Mesoclimate analysis

In the first phase, we have analyzed climate data of four years (2012-2015) in a hourly interval from the nearby LMU (Ludwig Maximilian Universität) weather station in Munich, selecting the most representative days for each season in terms of Air Temperature, Relative Humidity, Wind speed and Wind direction that are considered typical in relation to the season’s averages. This selection was done basing on the occurring frequency during each season during the four years period. July 18th 2015 was chosen as a representative extreme hot summer day due to high air temperatures combined to low relative humidity and typical wind direction, registered in the four years period; January 28th 2014 was chosen as a typical cold winter day. Following days were selected for the simulations:

	Winter	Spring	Summer
Average	March 2 nd 2014	April 2 nd 2016	July 30 th 2013
Extreme	January 28 th 2014		July 18 th 2015

- Microclimate

Those datasets were used to create a simulation model of the *Viktualienmarkt* with the ENVI –

MET software (Bruse, 2004). The model has an hourly timeframe resolution over a grid of 4 meters. The model, that includes the place has an area of 280m on 280m, provides air temperature, mean radiant temperature, water vapor pressure, relative humidity, and wind speed in a height of 10 meters as a result.

- Outdoor comfort

The simulation model has generated the input information to map outdoor comfort using the UTCI: Universal Thermal Climate Index (Bröde *et al.*, 2013). This index was chosen as it has shown to be the most suitable system to represent outdoor conditions basing on the equivalent temperature and is used by meteorologists across the globe (Jendritzky *et Tinz*, 2009). The model accounts for clothing using correlations derived from observations of human adaptive behavior in the outdoors. All other personal factors such as age, height, and weight are averaged over the population. The UTCI mapping was processed with Grasshopper and is expressed as an equivalent temperature (ET). The building geometry file has been provided by the *Referat für Stadtplanung und Bauordnung* (data were processed by SynerGIS web office).

3 Simulation settings

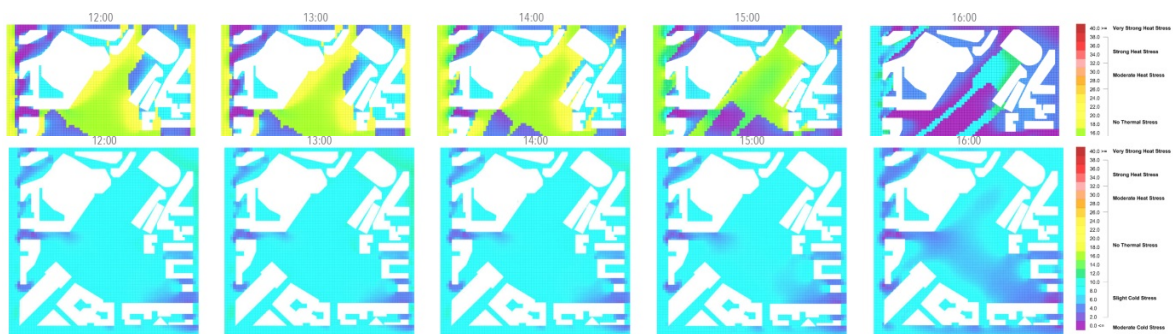
The simulations aim to obtain a detailed mapping of the UTCI values. The used UTCI scale has been applied to all the results in order to obtain a spatially distributed mapping of comfort levels. The analyzed area is located in Munich's historic center (48° 8' 7" N, 11° 34' 34" E). The simulations evaluated the main microclimate parameters in cells with a resolution of 4m x 4m for a total surface of 7,84 ha. The area is composed for 37,6% by buildings, 11% by road asphalt, 51,4% by pavement and has no soil surface. Each simulation starts at 7 a.m. but considers values starting from noon and ran for 24 hours for each simulated day. Cloud coverage was considered as non-occurring.

4 Simulation results

After all factors were plugged into the UTCI model, several high resolution maps of UTCI were generated on an hourly basis for the four previously-mentioned typical days for the present status.

4.1 Winter

Figure 2. Simulation results – Winter days, respectively Jan 28th (top) and March 2nd (bottom)



Winter days have shown a slight cold stress over 90% of the market's surface between noon and 4 pm. This means that comfort conditions are acceptable even when air temperatures are just above 0°C. The extreme cold day – January 28th (air temp. max 3,7 °C, min 0, RH max 100 min 68 avg 85) has slightly worse comfort conditions due to the increase of the relative humidity.

4.2 Spring

Spring days have no thermal stress conditions during the entire observed time period. The marketplace guarantees optimal comfort conditions.

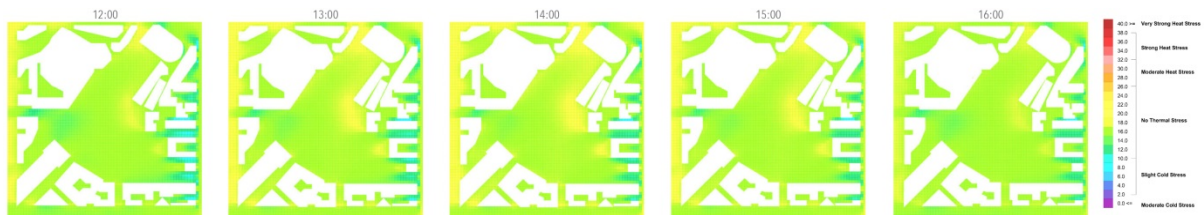


Figure 3. Simulation results - UTCI mapping for a typical spring day: April 2nd

4.3 Summer

Summer days show moderate heat stress over at least 35% of the surface while more than 50% undergoes to strong heat stress.

Looking at hot summer days, the percentage of strong heat stress goes up to 60% at 12 am while very strong heat stress rises up to 35% at 3 pm corresponding to equivalent temperatures of 40°C.



Figure 4. Simulation results – UTCI mapping for July 30th (above) and July 18th (below).

5 Microclimate manipulation

Basing on the outlined analysis, the mitigation strategies were selected primarily to reduce heat stress in summer, for both average- and hot days, since comfort conditions in winter and off-season can be considered acceptable or even very good.

As a first step, the existing tree coverage, composed by 74 chestnut trees, has been increased by 73%: 34% of it consists of deciduous trees added in the area facing northeast, and 39% of evergreen trees in the southern part of the place (Fig. 5).

Furthermore, for an additional heat stress reduction, we proposed to introduce a water surface along the marketplace: the water basin has a surface of 790 m² that corresponds to 2.7% of the place's surface. Both measures can be easily implemented and modeled in the ENVI-met model.

The water surface area was located at the southern border of the place in correspondence of the existing most congested road. This choice was done considering the prevailing wind direction during summer (east, occasionally south-east) and the main access to natural ventilation, to increase the effect of evaporative cooling during hot days. Besides aesthetic and microclimatic reasons, historical maps and pictures supported this location also: for centuries, Munich has been characterized by the presence of several water channels that were used for powering mills and for transporting goods. They were essential for Munich's development from the 14th century. During the 20th century almost all channels were closed to facilitate car circulation and to improve hygienic conditions, by strongly reshaping the appearance and the environmental qualities of the city center (Anlauf, 2013).



Figure 5. The *Viktualienmarkt*: current status and proposed interventions



Figure 6. Munich's city center: plan of the proposed water channels system with the highlighted market area.

The proposed river is considered a segment of a wider system, a circle, that includes Munich's entire city center that is, at present, mainly a pedestrian area (Fig.6). This intervention could contribute in promoting advantageous conditions for walking and biking, aiming at creating a more livable and *walkable* city: a healthy city that is built for people.

6 Limitations and future work

Although the simulation results show significant values, it has to be kept into consideration that the ENVI-met software has some not negligible limitations. Recent studies have shown that this tool gives higher influence of trees with about 1 K temperature difference, since this software is designed to model trees in detail. Furthermore, comparisons between ENVI-met results with those of other tools (such as TRNSYS) show that short wave radiation has a major influence on mean radiant temperature calculations, resulting in a high difference between sunny and shadowed areas (Perini *et al.*, 2017). This means, that the UTCI values could be not completely corresponding to the occurring conditions. In general, further studies on this specific case will focus on validating the simulations with field measurements, including acoustics and air pollution.

Besides microclimatic conditions, mapping people's presence and relating it to the microclimatic mapping, could integrate the present study with even more persuasive information about comfort perception and its influence on the use of public space.

7 Conclusion and Outlook

The comparison of the simulations' results show evident improvements in terms of heat stress reduction, especially during hot days. The UTCI score difference between July 18th 2015 and the design proposal – that was simulated with the same climatic conditions – is about 8K equivalent temperature difference in peak. Besides the significant heat stress reduction, the proposed design solution, that combines additional vegetation to the presence of an urban river, will provide several benefits in terms of acoustic comfort and air pollution that were not yet analyzed in this study.



Figure 7. UTCI-mapping with the proposed interventions for July 30th (above) and July 18th (below).

In conclusion, the design proposal contributes in combining a new image for the city with increased microclimatic conditions, especially during hot days and continuing heat waves. Through the reduction of peaks, the market could become not only a more comfortable place, but also a “cold spot” that assures more attractiveness in general and more specifically a place to recover and to compensate extreme heat stress during hot summer days. In Munich's climate, air-conditioners are rarely used in residential buildings where overheating phenomena occur frequently: the combination of a large presence of thermal mass, a dense urban environment and a low temperature shift during summer nights is therefore often fatal for elderly and sick people. This research project finds and validates

significant associations between design proposals and their effects on outdoor comfort improvement. Nevertheless, this approach, integrated with further analyses and measurements, opens new opportunities to understand the more challenging aspects of the urban environment and its impact on individuals' health. Through the use of tracking devices, data could be applied to a broader level to share data for public health and city planning purposes. Contributing to create more healthy and resilient cities.

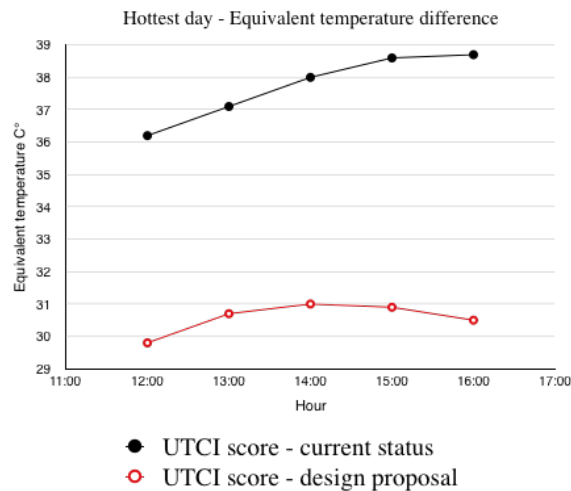


Figure 8. Equivalent temperature difference for the hottest day in an exemplary point of the place.

Acknowledgments

The authors would like to express their gratitude to Dr. Katia Perini, visiting DAAD research fellow and Ata Chokhachian of the Chair for Building Technology and Climate Responsive Design at TUM, for their support to the simulations of this research project.

This paper is based on research collaboration between the University of Rome “La Sapienza” and the Technische Universität München: Cand Arch. Giulia Volpicelli, who is a co-author of this paper, carried out simulations and data analysis presented in this study.

References

- Anlauf, T. (2013) <http://www.sueddeutsche.de/muenchen/baeche-in-muenchen-so-koennte-muenchen-wieder-ein-kleines-venedig-werden-1.3532836> - retrieved on June 3rd 2017.
- Bruse, M. (2004). ENVI-met 3.0: updated model overview. University of Bochum.
- Bröde, P., Błażejczyk, K., Fiala, D., Havenith, G., Holmér, I., Jendritzky, G., Kuklane, K., Kampmann, B. (2013). The Universal Thermal Climate Index UTCI compared to ergonomics standards for assessing the thermal environment, *Industrial Health*, 51(1):16-24.
- Carter, J. G., Cavan, G., Connelly, A., Guy, S., Handley, J., Kazmierczak, A. (2015).^[11]_{SEP} Climate change and the city: Building capacity for urban adaptation in *Progress in Planning* 95 (2015) 1–66.
- Chen, L., & Ng, E. (2012). Outdoor thermal comfort and outdoor activities: A review of research in the past decade. *Cities*, 29(2), 118-125.

Gulyas, A., Unger, J., & Matzarakis, A. (2006). Assessment of the microclimatic and human comfort conditions in a complex urban environment: Modelling and measurements. *Building and Environment*, 41, 1713–1722.

IPCC, Climate Change, (2013). The Physical Science Basis. Contribution of Working Group I to the Fifth Assessment Report of the Intergovernmental Panel on Climate Change. Cambridge University Press, Cambridge, United Kingdom and New York, NY, USA (pp. 2216).

Jendritzky, G., Tinz, B. (2009) The thermal environment of the human being on the global scale in *Glob Health Action*. 2009 Nov 11;2. doi: 10.3402/gha.v2i0.2005.

Lee, H., Mayer, H. (2016) Validation of the mean radiant temperature simulated by the RayMan software in urban environments in *International Journal of Biometeorology* 60(11) DOI: 10.1007/s00484-016-1166-3.

Ng, E., & Ren, C. (2015). The urban climatic map: a methodology for sustainable urban planning, Routledge Oxon, UK.

Masson, V., Marchadier, C., Adolphe, L., Aguejdad, R., Avner, P., Bonhomme, M., Bretagne, G., Briottet, X., Bueno, B., de Munck, C., Doukari, O., Hallegatte, S., Hidalgo, J., Houet, T., Le Bras, J., Lemonsu, A., Long, N., Moine, M.-P., Morel, T., Nolorgues, L., Pigeon, G., Salagnac, J.-L., Viguié, V., Zibouche, K. (2014). Adapting cities to climate change: A systemic modelling approach, *Urban Climate* 10, 407–429.

Martinelli L., Battisti A., Matzarakis A. (2015). Multicriteria analysis model for urban open space renovation: An application for Rome. *Sustainable Cities and Society*, vol. 14, February 2015, p. 10-20
Nikolopoulou, M., & Steemers, K. (2003). Thermal comfort and psychological adaptation as a guide for designing urban spaces. *Energy and Buildings*, 35(1), 95–101.

Perini, K., Chokhachian, A., Dong, S., Auer, T. (2017). Modeling and Simulating Urban Outdoor Comfort: Coupling ENVI-Met and TRNSYS by Grasshopper, *Energy and Buildings* <http://dx.doi.org/10.1016/j.enbuild.2017.07.061>.

Santucci, D., Mildenerger, E., Plotnikov, B. (2017). An investigation on the relation between outdoor comfort and people's mobility: the *Elytra Filament Pavilion* survey, *Powerskin conference proceedings*, TU Delft Open, 97-107, ISBN 978-94-92516-29-9.

Santucci, D., Auer, T., Chokhachian, A. (2017). Impact of environmental quality in outdoor spaces: dependency study between outdoor comfort and people's presence, in *S.ARCH 2017 I Sustainable Architecture Conference Proceedings*, ISBN 978-3-9818275-4-5.

Stone, B., Vargo, J., Habeeb, D. (2012). Managing climate change in cities: Will climate action plans work? In *Landscape and Urban Planning* 107, 263–271.

Relationship between city size, coastal land use and summer daytime air temperature rise with distance from coast

H. Takebayashi¹, T. Tanaka², M. Moriyama³, H. Watanabe⁴,
H. Miyazaki⁵ and K. Kittaka¹

¹Department of Architecture, Kobe University, Japan

²Department of Architecture, Hiroshima University, Japan

³Department of Living and Environmental Design, Setsunan University, Japan

⁴Department of Architecture, Tohoku Institute of Technology, Japan

⁵Department of Architecture, Kansai University, Japan

Corresponding author: Hideki Takebayashi, thideki@kobe-u.ac.jp

Abstract

The relationship between city size, coastal land use and air temperature rise with distance from coast is analysed by using mesoscale Weather Research & Forecasting (WRF) model, in five cities with different sizes; Tokyo, Osaka, Nagoya, Hiroshima, Sendai. There is no relationship between city size and air temperature rise. Coastal land use has a large influence on air temperature rise.

1 Introduction

Urban heat island intensity is defined by the air temperature difference between an urban area and its surrounding suburbs. Oke (1973) revealed that urban heat island intensity is proportional to the logarithm of the population, based on observations in a number of cities in North America and Europe. The population was used to indicate the degree of urbanization. An increase in population, for example, was associated with high-rise buildings and land use change, as well as with an expansion of the urban area. More specific indicators, such as urban area, artificial land coverage, and average building height, should be used to implement more effective heat island countermeasures.

Moriyama et al. (2014) have reported that air temperature is more influenced by the building coverage rate than the building height. When the building coverage rate is small or the building height is low, air temperature is low. In this study, for the purpose of actual recognition of urban heat island phenomenon, as the target five coastal cities in Japan with different sizes and coastal land use (Tokyo, Osaka, Nagoya, Hiroshima, Sendai), we have analysed the relationship between city size, coastal land use and air temperature rise with distance from coast during summer day.

2 Outline of calculation

We used mesoscale Weather Research & Forecasting (WRF) model (version 3.0.1.1-ARW). The objective study areas are shown in Figure 1. The outer square is domain 1 (3 km grid, 360 km square) and the inner filled square is domain 2 (1 km grid, 103 km square). The nesting technique was used in each region. The calculation results of air temperature at 2 m high and wind velocity at 10 m high in domain 2 were used for the analysis.

Calculation conditions are shown in Table 1. The period for which calculations were done was from August 1 - 31, 2010. Based on digital national land information (spatial resolution of 100 m) and a normalized vegetation index created from Landsat7 ETM+ data, urban areas were classified into three

categories according to the previous study (Kitao *et al.*, 2009): high-rise and high-density, middle-rise and moderate-density, and low-rise and low-density.

Land use conditions number of urban meshes in Tokyo, Osaka, Nagoya, Hiroshima and Sendai are shown in Figure 2. The numbers of urban land use meshes are 3,698 in Tokyo, 1,271 in Osaka, 1,416 in Nagoya, 364 in Hiroshima and 239 in Sendai. Frequency of urban land use in the five cities is larger in the coastal area and decreased gradually in the inland area. The number of urban land use meshes along the coastal area in Nagoya and Sendai is slightly smaller compared to those for Tokyo, Osaka and Hiroshima.

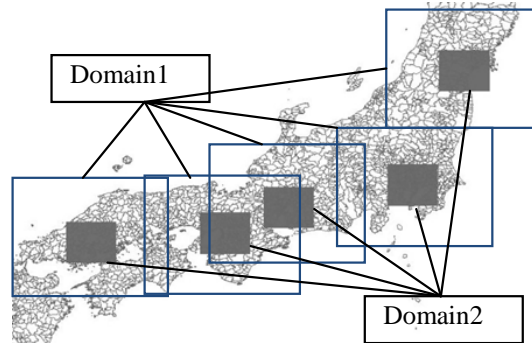
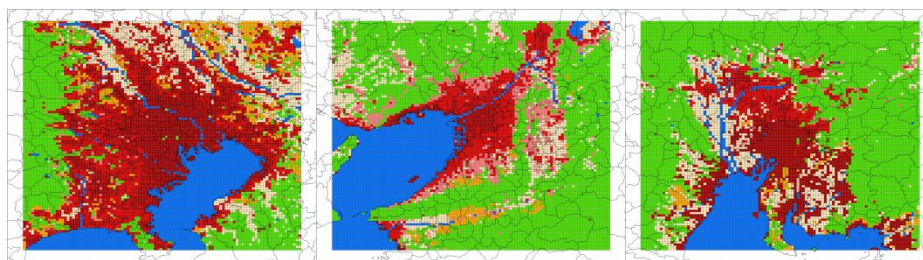


Figure 1. Objective study areas (Tokyo, Osaka, Nagoya, Hiroshima, Sendai).

Table 2. Calculation conditions for WRF model.

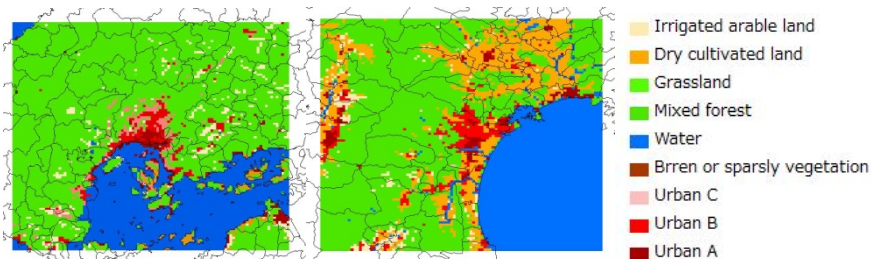
Calculation period		1-31, August, 2010
Vertical grid		28 layer (surface-100hPa)
Horizontal grid		Domain1: 3km (120×120 grids) Domain2: 1km (103×103 grids)
Meteorological data		JMA: Meso-scale Analysis (3 hourly, 10km grid, 20 layer) NCEP: final analysis (6 hourly, 1 degree grid, 17 layer)
Geographical data	Terrain height	Digital Map (50×50 resolution)
	Land use	Digital National Land Information (about 100×100 resolution) + NVI
Microphysics process		Purdue Lin <i>et al.</i> scheme
Radiation processes	Long wave	RRTM Longwave scheme
	Short wave	Dudhia Shortwave scheme
Planetary boundary layer process		Mellor-Yamada-Janjic PBL scheme
Surface processes	Urban area	UCM (Urban Canopy Model)
	Non urban area	Noah LSM
Cumulus parameterization		None
Four-dimensional data assimilation		None



(a) Tokyo (3,698)

(b) Osaka (1,271)

(c) Nagoya (1,416)



(d) Hiroshima (364) (e) Sendai (239)

Figure 2. Land use conditions and number of urban meshes (Tokyo, Osaka, Nagoya, Hiroshima, Sendai).

3 Calculation accuracy

Fine days and sea breeze conditions were selected according to weather conditions. The calculated values and observed values, which are instantaneous values every hour, are compared using observation station data in domain 2 of Tokyo, Osaka, Nagoya, Hiroshima and Sendai. The calculation accuracies of air temperature and wind velocity at Tokyo, Osaka, Nagoya, Hiroshima and Sendai observatories are shown in Table 2. For the five cities, calculation accuracy is comparable to previous studies (Kitao *et al.*, 2009 and Moriyama *et al.*, 2014).

Table 2. The calculation accuracies of air temperature and wind velocity.

	Temperture	Bias[°C]	RMSE[°C]	Correlation	Wind speed	Bias[m/s]	RMSE[m/s]	Correlation
Tokyo area	Tokyo	0.50	0.72	0.92	Tokyo	-0.38	0.54	0.78
	Nerima	0.72	0.79	0.92	Nerima	1.74	1.85	0.63
	Futyu	1.80	2.14	0.90	Futyu	0.01	0.72	0.70
	Saitama	1.13	1.19	0.91	Saitama	0.41	0.72	0.69
	Tukuba	0.82	0.88	0.94	Tukuba	0.73	0.95	0.74
	Chiba	-0.24	0.28	0.90	Chiba	-0.97	1.03	0.78
Osaka area	Osaka	0.20	0.31	0.92	Osaka	-0.13	0.43	0.67
	Kobe	0.30	0.45	0.89	Kobe	-1.14	1.19	0.59
	Sakai	0.40	1.15	0.91	Sakai	0.28	0.71	0.58
	Toyonaka	0.43	0.54	0.91	Toyonaka	-0.18	0.52	0.62
	Yao	0.92	0.98	0.92	Yao	-0.71	0.92	0.56
	Hirakata	0.42	0.63	0.87	Hirakata	0.86	0.94	0.47
Nagoya area	Nagoya	0.71	0.80	0.90	Nagoya	-0.46	0.56	0.64
	Toukai	0.24	0.48	0.89	Toukai	0.97	1.02	0.53
	Aisai	-0.18	0.32	0.93	Aisai	1.37	1.52	0.62
	Toyota	0.59	0.75	0.93	Toyota	0.42	0.58	0.33
	Gifu	0.97	1.01	0.90	Gifu	-0.29	0.40	0.64
	Tajimi	0.47	0.84	0.93	Tajimi	0.46	0.59	0.53
Hiroshima area	Hiroshima	0.01	0.02	0.91	Hiroshima	-0.56	0.77	0.56
	Kure	-0.05	0.06	0.93	Kure	0.04	0.55	0.59
	Otake	0.05	0.05	0.86	Otake	-0.70	0.74	0.41
	Higashihiroshma	-0.08	0.08	0.94	Higashihiroshma	-0.50	0.77	0.30
	miiri	0.03	0.03	0.89	miiri	-1.38	1.68	0.01
Sendai area	Sendai	-0.03	0.04	0.90	Sendai	-0.19	0.44	0.46
	Watari	-0.06	0.06	0.81	Watari	-0.36	0.62	0.31
	Shiogama	0.47	1.08	0.91	Shiogama	1.38	1.45	0.32
	Zaou	-0.02	0.04	0.83	Zaou	-0.82	0.90	0.12
	Ishimaki	-0.05	0.06	0.83	Ishimaki	-0.74	0.82	0.57

4 Analysis on air temperature distribution

Relationship between distance from coast and air temperature is shown in figure 3. In all five cities, as the distance from the coast increases, air temperature rose. The curve of air temperature rise varies in five cities. It is also different from day to day in a city. It is considered that the cause is the cloud amount during the night and the sea surface temperature during the day. There is no relationship between city size and air temperature rise. City size is indicated by the distance from the coast to the inland edge of each city as shown in Figure 3; Tokyo 60 km, Osaka and Nagoya 35-40 km, Hiroshima and Sendai 20 km. In Hiroshima, urban area is spreading along coastal line as in Tokyo and Osaka, and inland urban area is less than these cities, where air temperature is a little higher. As a result, the curve of air temperature rise in Hiroshima is smaller than those in Tokyo and Osaka.

Frequencies of air temperature at 14:00 on August 25 and 7, 2010 are shown in figure 4. In these days the cities indicated in the figure were fine and sea breeze condition. In Nagoya and Sendai, the number of urban land use in coastal areas is less than the other three cities, where air temperature is a little lower. As a result, air temperature difference between coastal and inland urban area is small and the

curve of air temperature rise is smaller than those in Tokyo and Osaka. In Sendai, air temperature in the inland urban area is the same as in the other cities, but air temperature in the coastal urban area is a little lower than the other cities, due to about 1 degree lower sea surface temperature influenced by the latitude. As a result, air temperature difference between coastal and inland urban area is large and the curve of air temperature rise is larger than those in Tokyo and Osaka. As described above, coastal land use has a large influence on air temperature rise.

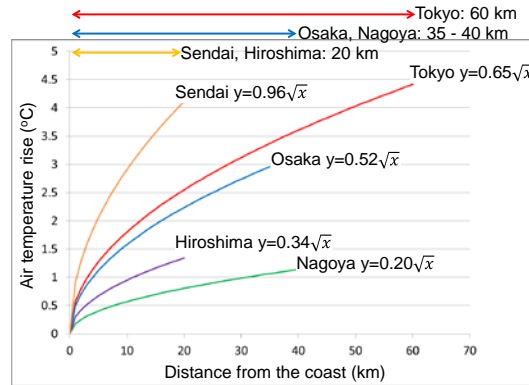


Figure 3. Relationship between distance from coast and air temperature.

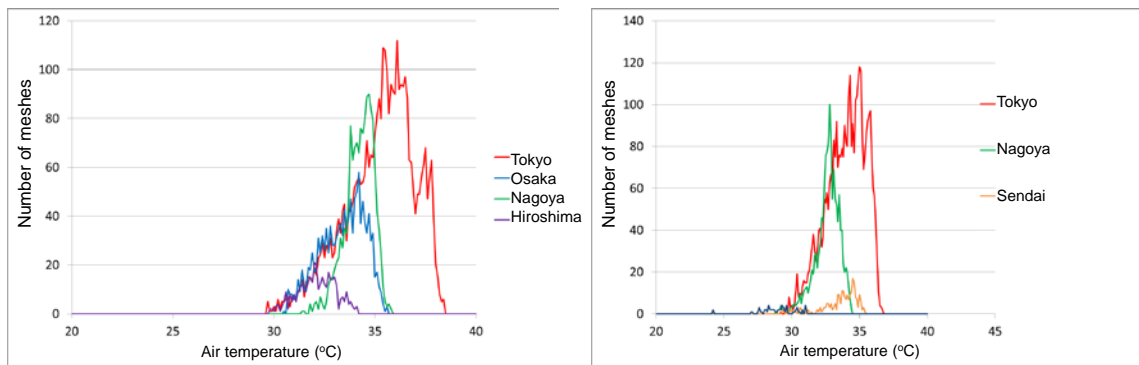


Figure 4. Frequencies of air temperature at 14:00 on August 25 (left) and 7 (right), 2010.

5 Conclusions

The relationship between city size, coastal land use and air temperature rise with distance from coast during summer day is analysed in five coastal cities in Japan with different sizes and coastal land use (Tokyo, Osaka, Nagoya, Hiroshima and Sendai). Air temperature rise increases with distance from coast and they are nearly the same in a giant city Tokyo and a big city Osaka. There is no relationship between city size and air temperature rise. Coastal land use has an influence on air temperature rise.

Acknowledgment

This work was supported by JSPS KAKENHI Grant Number 16H04464.

References

Kitao, N., Moriyama, M., Nakajima, S., Tanaka, T., and Takebayashi, H. (2009). The characteristics of urban heat island based on the comparison of temperature and wind field between present land cover and potential natural land cover, *Proc. Seventh International Conference on Urban Climate*.

Moriyama, M., Inui, Y., and Takebayashi, H. (2014). Study on Thermal Environmental Mitigation Effects Caused by Changes of Urban Form on a Large Scale Area, *Proc. 7th Japanese-German Meeting on Urban Climatology*.

Oke, T. R. (1973). City size and the urban heat island, *Atmospheric Environment* **7**, 769-779.

GREEN AND BLUE STRATEGIES
AND TECHNOLOGIES FOR
URBAN ENVIRONMENT

Improving Outdoor Thermal Comfort in Masdar City, Abu Dhabi, UAE.

L. Bande¹, M. Jha², Y. S. Pasha², A. Afshari², K. Alawadi²

¹Politecnico di Milano, Italy

²Masdar Institute of Science and Technology, UAE

Corresponding author: lindita.bande@polimi.it

Abstract

The outdoor thermal comfort (in this research represented by PET) is an important parameter to measure the quality of life in a metropolitan city such as Abu Dhabi. The hot arid climate of Abu Dhabi requires stronger measures toward the urban planning, orientation of the buildings, treatment of the different surfaces in order to improve the outdoor thermal conditions. (Pérez-Lombard, Ortiz, and Pout 2008)(Welcome to The Municipality of Abu Dhabi City n.d.)(Nikolopoulou and Steemers 2003) (Gaitani, Santamouris, and Mihalakakou n.d.) Considering the above, the proposed strategies have a crucial role in the city development plan. One district with 20 buildings, part of Masdar City is taken into consideration. The focus of the Computational Fluid Dynamics (CFD) models are eight different scenarios. The particular selection of these zone is due to the information gathered (building and environment properties), the site access, and the representative typology of the district (a sustainable city developed with its own building sustainable system). The main software used for this research is ENVI-met. The models have a medium size since there is a large number of scenarios but the models have a high scale of details 180x180. The different scenarios include the base case and the Masdar case. The first one refers to only buildings and the second one refers to the proposal of the Urban Planning Department in Masdar city. The other six scenarios have a different percentage spread of the shading devices and the trees. The shading devices are oriented toward the prevailing wind and the trees are selected considering their adaptation to the climate of Abu Dhabi. (masdar n.d.)(Limor Shashua-Bar, Pearlmutter, and Erell 2011)(Akbari, Pomerantz, and Taha 2001) Making small interventions in each district can bring about a considerable improvement in the quality of life of the citizens by improving the outdoor comfort therefore the walkability. The new districts developing outside Abu Dhabi Main Island need a detailed analysis in order to give a good example of city according to the UPC (Urban Planning Council) guidelines. By implementing a proposed strategy that combines shading, vegetation and cool materials, the city can reach its goals toward the Abu Dhabi 2030 sustainability plan. (Abu Dhabi Urban Planning Council - Abu Dhabi Vision 2030 n.d.)(Estidama n.d.)

1 Introduction

Physiological equivalent temperature (PET) is an index that measures the thermal comfort of a human body. It is defined to be as a standardized person with a work metabolism of 80W of light activity, in addition to basic metabolism and 0.9 clo of heat resistance because of clothing. The different levels of PET vary according to the levels of temperature into: very cold, cold, cool, slightly cool, comfortable, slightly warm, warm, and hot. (Höppe 1999)(Matzarakis and Amelung n.d.)

There are several studies done on the outdoor thermal comfort and the conditions that improve it. The urban design and the attention paid to the internal spaces is connected to such parameter. The impact of the building environment is different in different climates. There are several softwares developed to improve such parameters such as RAYman, which is mainly used in this research to process the air temperature, wind speed, relative humidity, and mean radiant temperature measured in the real site downtown Abu Dhabi. (table 6) (Nikolopoulou and Steemers 2003)(Matzarakis and Amelung n.d.)

Other softwares used in calculating and simulating the PET are : ENVI-met, Fluent etc. Despite the defects that the software has in calculating the mean radiant temperature, the results of the PET before and after an intervention are close to the real measured data. Several different studies show the effect

of the vegetation and shading. The PET can be decreased by several degrees in hot arid climate. The wind analysis is also an important factor in these CFD softwares and impacts the PET results.(Setaih et al. 2014) (Carfan, Galvani, and Nery 2012)

As regards a research conducted in Shanghai, an increase of 0.4 in the ground surface albedo generally reduces the thermal comfort by 5-7°C in PET. The tree canopy can reduce daytime PET by up to 15°C if dense. The measurements are done in two different residential areas and the models are developed with ENVI-met. The effect of the vegetation has a bigger impact on reducing the PET than the cool surfaces.(Yang, Lau, and Qian 2011)

The Green areas impact on the improvement of the outdoor thermal comfort is analysed in the city of Hong Kong. From the measurements taken, it is shown that the green roofs can reduce the air temperatures of the district by 0.4-0.7 °C. This improves the outdoor thermal comfort and also reduces the energy use of the buildings analysed in this research.(Peng and Jim 2013)

Several studies focused on human behaviour towards outdoor thermal conditions. The perception of different people and their physiognomy is the one to define the personal outdoor thermal comfort. In a research done in Athens during summer, the use of architectural solutions to improve the OTC by an average of 6% was shown. Another research done in Algeria during the summer season showed that the PET under the trees in a canopy are several degrees lower than the same scenario without trees. The air temperature could be reduced by 1.5°C. (Gaitani, Santamouris, and Mihalakakou n.d.)(Fazia and Helmut n.d.)

A study done in Fez, Morocco showed that the air temperature in the narrow streets of the city have a difference of 6-10K from the shallow areas. This showed that during the summer the narrow areas of the city were more comfortable for the inhabitants to walk in. (Johansson 2006)

Table 1. Physiological equivalent temperature (PET) ranges. Internal heat production 80W, heat transfer resistance of the clothing 0.9 clo. (Matzarakis and Amelung n.d.)

PET	Thermal perception	Grade of physiological stress
4°C	Very cold	Extreme cold stress
8°C	Cold	Strong cold stress
13°C	Cool	Moderate cold stress
18°C	Slightly cool	Slight cold stress
23°C	Comfortable	No thermal stress
29°C	Slightly warm	Slight heat stress
35°C	Warm	Moderate heat stress
41°C	Hot	Strong heat stress
	Very hot	Extreme heat stress

2 Methodology

This study aims to propose different scenarios of urban features in outdoor space in Masdar City. The base model is referring to the plan proposal with the minimum building heights. The Masdar City is a town currently under construction that takes place near the Abu Dhabi Airport. The reference plans have been modified in terms of the outdoor space. Shading device and green areas are added to the initial plans in different percentage with the aim of understanding the best impact into improving the PET values in the area. This particular case study is selected due to the recent developments in the area and the high attention the sustainability program has brought in the public. The outdoor thermal comfort is of a great interest for the citizens of Abu Dhabi. The rural data is taken in the borders of the study area. Since currently there is no construction then this particular locations can be considered as the rural or the boundary conditions. In this study are included the first range of the ENVI-met models done with the minimum building height specified in the developing plan of the city.(masdar n.d.) (Abu Dhabi Public Realm Design Manual n.d.)(<http://www.f-in-d.com/stories/abu-dhabi-guide-2014-introduction> n.d.)

The main sections of this study continue as follows:

- 2.1.The Case study
- 2.2.The rural data
- 2.3.The ENVI-met models

2.1 The case study



Figure 1: Masdar City aerial view. (masdar n.d.)

In this study the district taken into consideration is part of Masdar City Abu Dhabi. Masdar City is part of the expansion of Abu Dhabi towards the desert. It has a strategic position as its closer to the airport and to Dubai. There is limited traffic and more open areas. However, Masdar has a mix use of buildings between residential and offices. This mix use is visible from the different building typology. The first city core of Abu Dhabi was in the main island, near to the end of and near to the port that was also an important economical part. As the years passed by due the economic growth the city started to develop within the island and then towards the desert. In the map of 1968, 1972, 1978 can be seen this growth within the island. Starting from 1980 the city started to expand toward the desert with an initial

industrial area. In the 1990 and then 2015 the city goes further more into the south east direction. (Old and Rare Pictures of Dubai and Abu Dhabi - 1966, 1954 | Living Life in UAE | Life in UAE, Dubai, Abu Dhabi, Sharjah, Universities, college, education, banks, jobs, business, expats life, working in dubai n.d.) (The man behind Abu Dhabi's master plan | The National n.d.) (Cassano et al. n.d.) (<http://www.f-in-d.com/stories/abu-dhabi-guide-2014-introduction> n.d.)

Masdar city is part of this expansion. Masdar city has a different concept of a city. The idea was to have a vertical city in order to have pedestrian areas only. The initial plan of Masdar city has been modified several times, but no matter the modifications the concept is kept the same. The centre of the city was planned a park with opening shading structures to maximise the outdoor thermal comfort. This Proportion creates a low H/W factor in Masdar city is very high creating shading for the pedestrians and improving the outdoor thermal conditions In Masdar city the identifying objects are the central park that as per the latest modifications will include also the last pavilion of UAE exposed in Milan EXPO 2015. The pavilion turned out a success in Milan due to the materials used (the same terracotta used for the first zone of Masdar City), the shape of the structure (sandy curves), the information offered inside (the history of UAE). (Expo Milano 2015 - Feeding the Planet, Energy for Life n.d.) (Ali-Toudert and Mayer 2006)

However, other identifying Buildings are the Masdar institute Library, the wind catcher, the Irena building etc. Masdar City tends to create a different building typology in each block to diversify the use of the blocks. The difference of the building blocks is related also to the façade treatment. Although there are new policies in conserving the previous architecture and façade treatment. A general impression after visiting the full island is the missing element of the arcades. The city of Masdar tends to give each building a value by selecting carefully the façade materials in order to achieve not only the aesthetic parameters but also the sustainable goals settled for each building typology. The main materials used in Masdar City are the terracotta and innovative wall packages by combining the tradition with the new innovative materials. Regarding the architectural elements the most notable elements are the shading devices placed in the centre of the area, the mashrabiya screens and the wind catcher. Each one of this elements has a sustainable function. (Middle East Sustainable Cities n.d.) (Cities : architecture and society : 10. Mostra internazionale di architettura, la Biennale di Venezia. 2006) (Stone and Rodgers 2001)

2.2 *The rural data*

The rural data refers to two weather stations located in Masdar City. The stations are close to the Irena Building and Masdar Institute of Science and Technology. The data recorded is used for the boundary conditions in the ENVI-met models simulations. The area in Masdar city is being developed recently. Almost 90% of the buildings are at the foundation construction phase or they will shortly enter in that phase. The area taken into study is near to Airport, 50km from the Abu Dhabi centre where the dense build-up area is located. Figure 2 shows the locations of the weather sensors. Figure 3 and table 2 shows the different components of the weather stations. Each unit has three main components located at a height of 2 meters: the air and relative humidity sensor, the wind speed sensor, the wind direction sensor. The units have a solar panel that supplies the battery with energy. The logger box is well protected and resistant to high air temperatures. (testo 435-3 multi-function climate measuring instrument | Pressure measurement - Filter | Pressure measurement | Air-conditioning systems maintenance | Operations/ maintenance and service | Applications | Testo® India n.d.)

The units are more than 300 meters from the closest barrier that might impact the wind speed or the wind direction. The soil around the measurement is mainly sand. Few asphalted streets are located on both sides of the sensors. There is a green path on the east side of the first node at a distance of 150 meters. However the trees composing the green path have a four meter height and they don't impact the wind speed or the wind direction. The decision to use this data instead of the TMY (Typical Meteorological Year) data from the station near the airport is because of the large average taken while composing the file. Meanwhile the site data taken from the two stations refers to the spring 2017. Three weeks of data are averaged in a 24H profile and used in models simulation. His because ENVI-met makes calculations referring to a single day.

Table 2. Weather station components.

Weather Station Components	
Sensor 01	Air temperature and relative humidity
Sensor 02	Wind speed
Sensor 03	Wind direction



Figure 2: Site measurements equipment (Gianinetto et al. 2014)



Figure 3: Location of the weather stations in Masdar City.

2.3 The ENVI-met models

The ENVI-met models have a size of 180x180. The study area includes a block of 20 buildings within the Masdar City. The main focus is in the area where most of the outdoor activities are concentrated. In this district are included: one mosque, one museum (the UAE pavilion exposed to the EXPO 2015 in Milan) and one mall (the only one in the Masdar City area). (Expo Milano 2015 - Feeding the Planet, Energy for Life n.d.) (Bruse and Fleer 1998)

Table 3-4 show the different scenarios proposed in this study. The base case refers to the 20 buildings and the paved area only. The Masdar case refers to the proposal done from the Urban Planning department of Masdar City. The six other proposals refer to the different percentage of distribution of the shading devices and the trees. The ‘cool’ shading device has the properties of a cool surface and a reflectance of 0.85, assuming that it is a white tent. The thickness is considered 0.1 m or 10 cm, as this was the smallest size that would be allowed to build the model at this scale. Even though in the 3D it seems that the height is one meter, it is not the real size. In the 3d model the size depends on the pixel sizes. The dimensions of the shading devices are 300 cm x 400 cm x 500cm and 300 cm x 400 cm x 600cm. The soil is more detailed. The asphalt is recreated, as the one in the template did not consider the heat fluxes in the different layers. The walls of the buildings do not have window division; however, there is a new wall with average characteristics. The type of tree used in this simulations is Albizia Julibrissin. This is a type of tree mentioned in the Abu Dhabi Realm Guidelines. It requires a considerable amount of water. The selection of this tree is done after comparing with palm trees and populous Alba. The shading devices in this model are not linear but interrupt in order to improve the air circulation and bring the model closer to the real conditions. (Ozkeresteci et al. 2003)(Santamouris n.d.)(Paolini et al. 2014)

Table 3. Area distribution 01

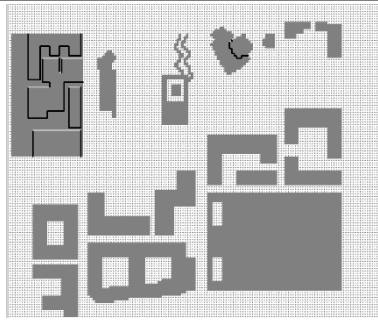
	Total Area (m2)	Built-up area (m2)	Asphalt Area (m2)	Non-Asphalt Area (m2)
1 Base Case	242,057.00	78,243.00	26,829.00	136,985.00
2 Masdar Case	242,057.00	78,243.00	26,829.00	136,985.00
3 Scenario 01	242,057.00	78,243.00	26,829.00	136,985.00
4 Scenario 02	242,057.00	78,243.00	26,829.00	136,985.00
5 Scenario 03	242,057.00	78,243.00	26,829.00	136,985.00
6 Scenario 04	242,057.00	78,243.00	26,829.00	136,985.00
7 Scenario 05	242,057.00	78,243.00	26,829.00	136,985.00
8 Scenario 06	242,057.00	78,243.00	26,829.00	136,985.00

Table 4. Area distribution 02

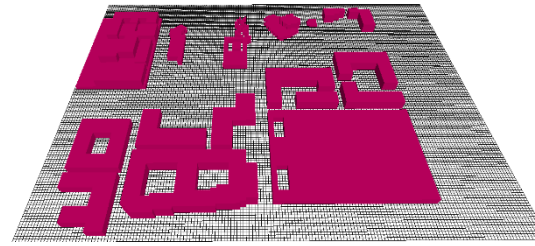
	Intervention Area (m2)	Shaded Area (m2)	%	Green Area (m2)	%
1 Base Case	30,798.00	-	0%	-	0%
2 Masdar Case	30,798.00	2,162.00	7%	28,636.00	93%
3 Scenario 01	44,182.00	-	0%	44,182.00	100%
4 Scenario 02	44,182.00	44,182.00	100%	-	0%
5 Scenario 03	44,182.00	8,389.00	19%	35,793.00	81%
6 Scenario 04	44,182.00	35,793.00	81%	8,389.00	19%
7 Scenario 05	44,182.00	16,610.00	38%	27,572.00	62%
8 Scenario 06	44,182.00	27,572.00	62%	16,610.00	38%

Table 5. ENVI-met models 1-4. (Bruse 2004)

Base Case Plan	Base Case 3D
----------------	--------------



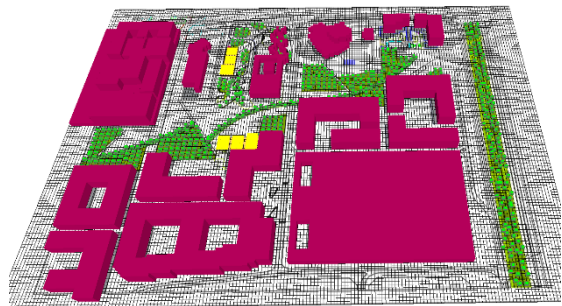
Masdar Case Plan



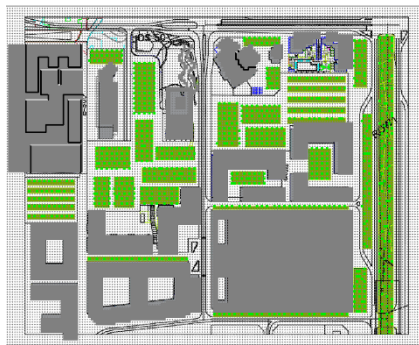
Masdar Case 3D



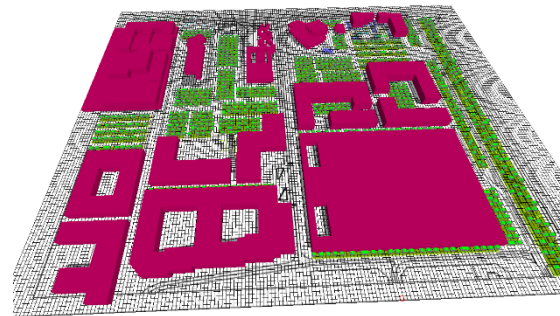
Scenario 01 Plan



Scenario 01 3D



Scenario 02 Plan



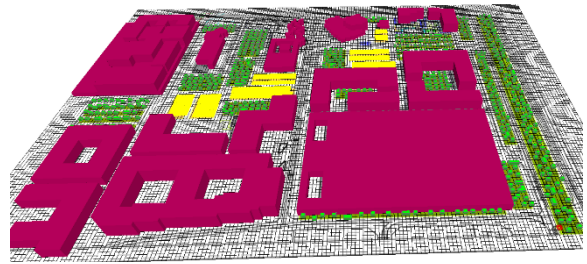
Scenario 02 3D

Table 6. ENVI-met models 5-8. (Huttner, Bruse, and Dostal n.d.)

Scenario 03 Plan



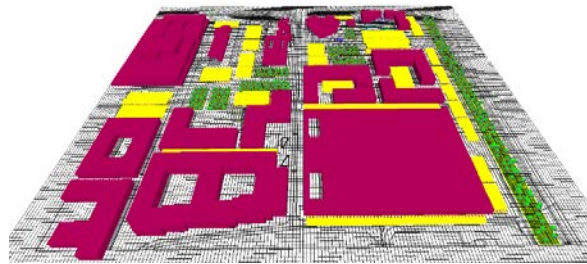
Scenario 03 3D



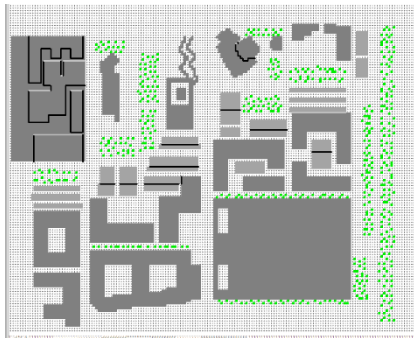
Scenario 04 Plan



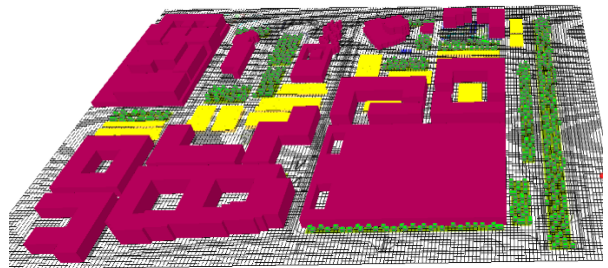
Scenario 04 3D



Scenario 05 Plan



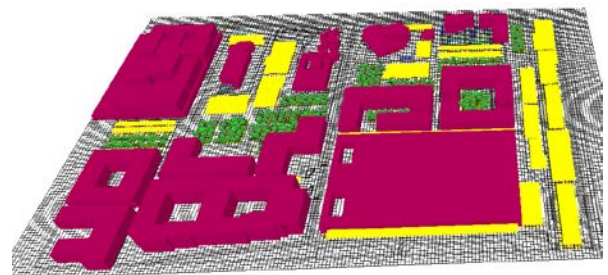
Scenario 05 3D



Scenario 06 Plan



Scenario 06 3D



3 Results

The PET (described in the previous sections) results are listed in this paragraph. Tables 7-8 show a comparison of the base case with the different scenarios. Respectively the highest difference of the Base case versus Masdar city case PET is 2.06 °C, base versus scenario 01 is 3.47 °C, base versus scenario 02 is 3.29 °C, base versus scenario 03 is 3.56 °C, base versus scenario 04 is 3.31 °C, base versus scenario 05 is 3.44 °C, base versus scenario 06 is 4.05°C.

Table 7. Shade and Trees distribution in the ENVI-met models.

	Masdar	SC01	SC02	SC03	SC04	SC05	SC05
% Shading	7	0	100	19	81	38	62
% Trees	93	100	0	81	19	62	38

Table 8. The results of the ENVI met simulations for the peak hours 12.00-17.00.

Hour	Masdar	SC01	SC02	SC03	SC04	SC05	SC06
12	1.23	2.1	2.8	2.32	2.46	2.4	3.21
13	1.4	2.36	2.91	2.56	2.64	2.61	3.4
14	1.83	3.07	3.23	3.22	3.12	3.2	3.89
15	2.1	3.47	3.29	3.5	3.31	3.44	4.05
16	2.06	3.32	2.69	3.22	2.93	3.15	3.54
17	1.75	2.57	2.2	2.51	2.31	2.5	2.87

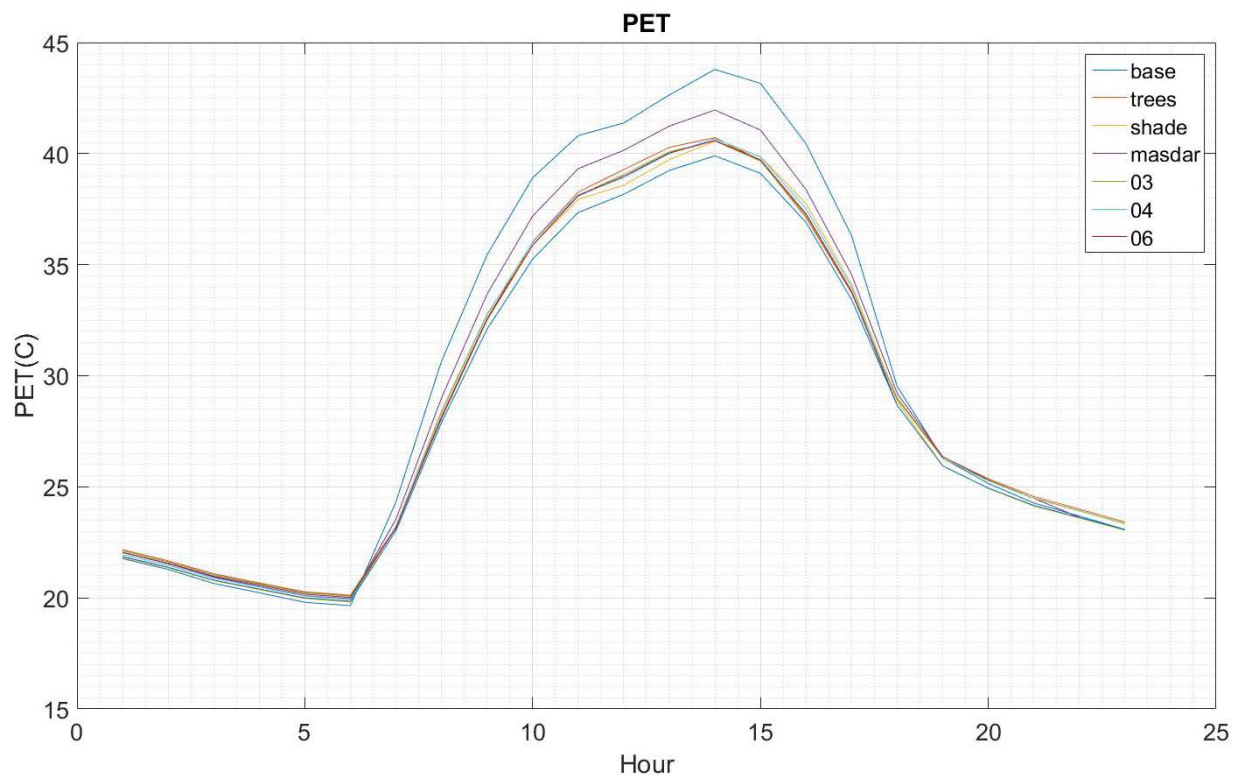


Figure 4. Base case and Masdar City proposal comparison.

The best result achieved in average is the mix between shading devices and trees at a value of 62% and 38% for the reference hours between 12.00- 17.00. This timing is taken into consideration since it has a bigger impact into improving the OTC. People tend to walk outside during the lunch time and after their work time. Scenario 03 and 05 behave in a similar way, while scenario 04 has slightly different. PET values. Figure 4 shows the difference in a graphic form between all the cases taken into study. The graphs visualize a bigger difference during the time of 12.00- 17.00pm.

4 Conclusions and future work

The results of the first two scenarios, the 100% tree coverage and 100% shade coverage are similar. However the shading devices behave slightly better since the relative humidity decreases the perceived outdoor thermal comfort. The combination of the trees and shade location impacts the PET values. Prevail direction of the wind has an impact into the CFD simulations.

This results show that not necessarily using one strategy 100% over the other can bring better results. A combination of both shading and trees has a better impact in reducing the PET values. However, choosing one option over the other in terms of sustainability is connected to the cost and lifecycle of the materials used into this process.

Future work

Part of the future work is analysing the same models but with the maximum number of floors as programed in the plans of the Masdar City. Observing the difference of the PET between an additional 08 scenarios will help building up some guidelines for the city management since the construction phase is still in the initial phase. (Yuan and Chen 2011)(Zhang, Gao, and Zhang 2005)

The ENVI-met software with the dimension 180x180 is time consuming therefore its recommended that future simulations to be done in the format 90x90. Also its important mentioning that in this study we discuss the difference between one scenario and the other. Since there is no anthropogenic heat involved then each simulation can't be compared directly with hypothetical site measurements of PET. (Oke n.d.)

Further studies must be conducted in understanding the change of the shaded area compared to the full district analysed. A mean radiant analysis in other softwares such as Grasshopper is ingoing. This would help understand the importance of the shading devices and vegetation in terms of shading. (Tutorials - Grasshopper n.d.)(honeybee example files - Grasshopper n.d.)

The impact of the different regional trees for the same coverage areas might be important to understand in order to make the best selection during the execution phase. There is an ongoing study that analyses the difference of the PET related to palm trees and other regional trees. (Boukhabl and Alkam 2012)(Sakai et al. 2012)(L Shashua-Bar and Hoffman 2000)

Acknowledgment

This work was supported from the Masdar City team: Gaurish Wagle, Dirk Booyesen.

Annex

Boundary Conditions in ENVI-met for the spring season:

```

Output interval main files (min)           =60.00
Output interval log files (min)           =30.00
Include Nesting Grids in Output (0:n,1:y) =0
[SOLARADJUST] _____
Factor of shortwave adjustment (0.5 to 1.5) =0.90
[CLOUDS] _____
Fraction of LOW clouds (x/8)              =1.00
Fraction of MIDDLE clouds (x/8)           =2.00
Fraction of HIGH clouds (x/8)             =1.00
[SOILDATA] _____
Initial Temperature Upper Layer (0-20 cm) [K]=301.15
Initial Temperature Middle Layer (20-50 cm) [K]=297.50
Initial Temperature Deep Layer (below 50 cm)[K]=293.00
Relative Humidity Upper Layer (0-20 cm)   =95.00
Relative Humidity Middle Layer (20-50 cm) =90.00
Relative Humidity Deep Layer (below 50 cm) =85.00
[SIMPLEFORCE] _____
Hour 00h [Temp, rH] = 300.16, 60.28
Hour 01h [Temp, rH] = 299.20, 61.48
Hour 02h [Temp, rH] = 298.94, 61.10
Hour 03h [Temp, rH] = 298.14, 62.25
Hour 04h [Temp, rH] = 297.81, 62.09
Hour 05h [Temp, rH] = 297.34, 62.53
Hour 06h [Temp, rH] = 297.43, 62.79
Hour 07h [Temp, rH] = 299.84, 57.95
Hour 08h [Temp, rH] = 302.92, 50.29
Hour 09h [Temp, rH] = 305.72, 42.04
Hour 10h [Temp, rH] = 308.27, 33.97
Hour 11h [Temp, rH] = 310.32, 28.79
Hour 12h [Temp, rH] = 311.40, 25.84
Hour 13h [Temp, rH] = 311.99, 25.55
Hour 14h [Temp, rH] = 312.22, 25.19
Hour 15h [Temp, rH] = 311.17, 28.20
Hour 16h [Temp, rH] = 309.68, 32.95
Hour 17h [Temp, rH] = 308.10, 38.05
Hour 18h [Temp, rH] = 306.01, 44.81
Hour 19h [Temp, rH] = 304.20, 50.72
Hour 20h [Temp, rH] = 303.18, 55.56
Hour 21h [Temp, rH] = 302.35, 57.12
Hour 22h [Temp, rH] = 301.87, 56.61
Hour 23h [Temp, rH] = 301.18, 56.33

```

References

- “Abu Dhabi Public Realm Design Manual.” <http://www.upc.gov.ae/prdm/index.asp>.
- “Abu Dhabi Urban Planning Council - Abu Dhabi Vision 2030.” <http://www.upc.gov.ae/abu-dhabi-2030.aspx?lang=en-US> (February 1, 2017).
- Akbari, H, M Pomerantz, and H Taha. 2001. “Cool Surfaces and Shade Trees to Reduce Energy Use and Improve Air Quality in Urban Areas.” *Solar Energy* 70(3): 295–310.
- Ali-Toudert, Fazia, and Helmut Mayer. 2006. “Numerical Study on the Effects of Aspect Ratio and Orientation of an Urban Street Canyon on Outdoor Thermal Comfort in Hot and Dry Climate.” *Building and Environment* 41(2): 94–108.
- Boukhabl, Moufida, and Djamel Alkam. 2012. “Impact of Vegetation on Thermal Conditions Outside, Thermal Modeling of Urban Microclimate, Case Study: The Street of the Republic, Biskra.” *Energy Procedia* 18: 73–84.
- Bruse, Michael. 2004. “ENVI-Met 3.0: Updated Model Overview.”
- Bruse, Michael, and Heribert Fleer. 1998. “Simulating Surface–plant–air Interactions inside Urban Environments with a Three Dimensional Numerical Model.” *Environmental Modelling & Software* 13(3): 373–84.
- Carfan, Ana Claudia, Emerson Galvani, and Jonas Teixeira Nery. 2012. “Study of Thermal Comfort in the City of São Paulo Using ENVI-Met Model Estudio Del Confort Térmico En La Ciudad de São Paulo Utilizando El Modelo ENVI-MET.” *Núm* 78: 188–4611.
- Cassano, Simona et al. “Atlas Environmental Abu Dhabi Emirate of.” www.ead.ae (October 7, 2016). *Cities : Architecture and Society : 10. Mostra Internazionale Di Architettura, La Biennale Di Venezia*. 2006. Rizzoli.
- “Estidama.” <http://estidama.upc.gov.ae/>.
- “Expo Milano 2015 - Feeding the Planet, Energy for Life.” <http://www.expo2015.org/archive/en/index.html> (June 26, 2017).
- Fazia, Ali-Toudert, and Mayer Helmut. “Thermal Comfort in Urban Streets with Trees under Hot Summer Conditions.”
- Gaitani, N, M Santamouris, and G Mihalakakou. “Thermal Comfort Conditions in Outdoor Spaces.” Gianinetto, Marco et al. 2014. “Remote Sensing Urban Analysis.” In, 101–12. http://link.springer.com/10.1007/978-3-319-02117-1_8 (October 6, 2016).
- “Honeybee Example Files - Grasshopper.” http://www.grasshopper3d.com/group/ladybug/forum/topics/honeybee-example-files?xg_source=activity (February 16, 2017).
- Höppe, P. 1999. “The Physiological Equivalent Temperature - a Universal Index for the Biometeorological Assessment of the Thermal Environment.” *International Journal of Biometeorology* 43(2): 71–75. <http://link.springer.com/10.1007/s004840050118> (February 2, 2017).
- <http://www.f-in-d.com/stories/abu-dhabi-guide-2014-introduction>. “Introduction.” <http://www.f-in-d.com/stories/abu-dhabi-guide-2014-introduction>.

Huttner, Sebastian, Michael Bruse, and Paul Dostal. "Full 3D Editor Numerical Modelling of the Urban Microclimate – a Preview on ENVI-MET 4.0."

Johansson, Erik. 2006. "Influence of Urban Geometry on Outdoor Thermal Comfort in a Hot Dry Climate: A Study in Fez, Morocco." *Building and Environment* 41(10): 1326–38.

"Masdar." <http://www.masdar.ae/>.

Matzarakis, Andreas, and Bas Amelung. "Physiological Equivalent Temperature as Indicator for Impacts of Climate Change on Thermal Comfort of Humans."

"Middle East Sustainable Cities." <http://www.carboun.com/sustainable-design/passive-cooling-responding-to-uae's-soaring-electricity-demand/> Journal.

Nikolopoulou, Marialena, and Koen Steemers. 2003. "Thermal Comfort and Psychological Adaptation as a Guide for Designing Urban Spaces." *Energy and Buildings* 35(1): 95–101.

Oke, Tim. "NOTE The Thirteenth Session of the Commission for Instruments and Methods of Observation (CI-MO) Recognized the Need to Include in the WMO Guide to Instruments and Methods of Observation, WMO-No.8 (CI-MO Guide) a New Chapter on Urban Observations. Professor."

"Old and Rare Pictures of Dubai and Abu Dhabi - 1966, 1954 | Living Life in UAE | Life in UAE, Dubai, Abu Dhabi, Sharjah, Universities, college, education, banks, jobs, business, expats Life, Working in Dubai." <http://blog.idubai.info/2012/11/old-and-rare-pictures-of-dubai-and-abu.html> (December 13, 2016).

Ozkeresteci, I, K Crewe, A J Brazel, and M Bruse. 2003. "Use and Evaluation of the ENVI-Met Model for Environmental Design and Planning. An Experiment on Lienar Parks." *South Africa*: 10–16.
Paolini, Riccardo, Andrea G. Mainini, Tiziana Poli, and Lorenzo Vercesi. 2014. "Assessment of Thermal Stress in a Street Canyon in Pedestrian Area with or without Canopy Shading." *Energy Procedia* 48: 1570–75.

Peng, Lilliana, and C. Jim. 2013. "Green-Roof Effects on Neighborhood Microclimate and Human Thermal Sensation." *Energies* 6(2): 598–618. <http://www.mdpi.com/1996-1073/6/2/598/> (December 8, 2016).

Pérez-Lombard, Luis, José Ortiz, and Christine Pout. 2008. "A Review on Buildings Energy Consumption Information." *Energy and Buildings* 40(3): 394–98.

Sakai, S. et al. 2012. "Sierpinski's Forest: New Technology of Cool Roof with Fractal Shapes." *Energy and Buildings* 55: 28–34.

Santamouris, M. "USING Cool Pavements As A Mitigation Strategy To Fight Urban Heat Island – A Review Of The Actual Developments."

Setaih, Khalid et al. 2014. "CFD Modeling as a Tool for Assessing Outdoor Thermal Comfort Conditions in Urban Settings in Hot Arid Climates." *Journal of Information Technology in Construction (ITcon)* 19(19): 248–69. <http://www.itcon.org/2014/14> (January 25, 2017).

Shashua-Bar, L, and M E Hoffman. 2000. "Vegetation as a Climatic Component in the Design of an Urban Street An Empirical Model for Predicting the Cooling Effect of Urban Green Areas with Trees." *Energy and Buildings* 31: 221–35. www.elsevier.com/locate/enbuild (October 7, 2016).

Shashua-Bar, Limor, David Pearlmutter, and Evyatar Erell. 2011. "The Influence of Trees and Grass on Outdoor Thermal Comfort in a Hot-Arid Environment." *International Journal of Climatology* 31(10): 1498–1506. <http://doi.wiley.com/10.1002/joc.2177> (December 11, 2016).

Stone, Brian, and Michael O. Rodgers. 2001. "Urban Form and Thermal Efficiency: How the Design of Cities Influences the Urban Heat Island Effect." *Journal of the American Planning Association* 67(2): 186–98. <http://www.tandfonline.com/doi/abs/10.1080/01944360108976228> (December 8, 2016).

"Testo 435-3 Multi-Function Climate Measuring Instrument | Pressure Measurement - Filter | Pressure Measurement | Air-Conditioning Systems Maintenance | Operations/ Maintenance and Service | Applications | Testo® India." <https://www.testo.com/en-IN/Applications/Operations-maintenance-and-service/Air-conditioning-systems-maintenance/Pressure-measurement/Pressure-measurement---Filter/testo-435-3/p/05604353> (February 12, 2017).

"The Man behind Abu Dhabi's Master Plan | The National." <http://www.thenational.ae/uae/heritage/the-man-behind-abu-dhabis-master-plan#page3>.

"Tutorials - Grasshopper." <http://www.grasshopper3d.com/page/tutorials-1>.

"Welcome to The Municipality of Abu Dhabi City." <http://www.adm.gov.ae/en/home/index.aspx> (February 1, 2017).

Yang, Feng, Stephen S.Y. Lau, and Feng Qian. 2011. "Thermal Comfort Effects of Urban Design Strategies in High-Rise Urban Environments in a Sub-Tropical Climate." *Architectural Science Review* 54(4): 285–304. <http://www.tandfonline.com/doi/abs/10.1080/00038628.2011.613646> (December 9, 2016).

Yuan, Chao, and Liang Chen. 2011. "Mitigating Urban Heat Island Effects in High-Density Cities Based on Sky View Factor and Urban Morphological Understanding: A Study of Hong Kong." *Architectural Science Review* 54(4): 305–15. <http://www.tandfonline.com/doi/abs/10.1080/00038628.2011.613644> (December 9, 2016).

Zhang, Aishe, Cuilan Gao, and Ling Zhang. 2005. "Numerical Simulation of the Wind Field around Different Building Arrangements." *Journal of Wind Engineering and Industrial Aerodynamics* 93(12): 891–904.

Assessment of Bioclimatic Comfort of Residential Areas to Improve the Quality of Environment by Using Urban Greening and Hard Landscaping

I.V. Dunichkin ¹, O.I. Poddaeva ¹, K.S. Golokhvast ²

¹Educational, scientific and industrial laboratory for aerodynamic and aeroacoustic tests of building structures, Moscow State University of Civil Engineering (National Research University), Russia

²Department of life safety in technosphere, Far Eastern Federal University, Russia

Corresponding author: Dunichkin I.V., ecse@bk.ru

Abstract

The actual issues of settlement and experimental studies of wind effects of residential complexes in Moscow are considered on the examples of project building objects for justification of design solutions. The further development of scientific school of architecture and construction aerodynamics is presented as well as its research on the aeration, air quality of urban spaces and aerodynamic comfort. The results of these studies are different comfort criteria currently used in most developed countries as a guide in the design of residential buildings. As an integrated research in implemented project practice the results of research in the physical Big gradient wind tunnel of the Educational and scientific and industrial laboratory for aerodynamic and aeroacoustic tests of building structures as well as numerical simulation of wind effects and bioclimatic comfort are given. The method of numerical-experimental researches of wind effects on the areas of urban buildings with the development of design solutions for complex land improvement to compensate bioclimatic discomfort is also considered as well as design and research products.

1 Introduction

Attempts to increase the efficiency of the use of urban areas entail the development of multi-storey complexes, increasing the number of storeys and density of housing. When considering design solutions for site designs and build projects for housing of micro-districts and blocks, in addition to issues related to insolation and noise protection, it is necessary to take into account the distribution and velocity and direction of wind flows in the development area, which in turn is directly related to the bioclimatic comfort for pedestrians. The wind is the most important factor. Oliveira, S., & Andrade, H. (2007) wrote that wind perception largely depended on the extreme values of wind speed and wind variability. The study of the aeration of urban space allows us to take into account the above-mentioned impacts when assessing the location of objects of land improvements and urban greening.

2 Methods for Studying Wind Effects for Assessing Bioclimatic Comfort

The study based on the testing method of the model in the Large gradient wind tunnel (Figure 1) as well as on verified numerical modeling of wind fields at a height of 2 meters from the surface of the territory. Dunichkin I. V., Zhukov D. A. and Zolotarev A. A. (2013) wrote that methods of microclimatic conditions forecasting for urban environment and assessment of aeration of the territory and aerodynamics of the development had been verified. The optimal and most reliable method of investigation study is a numerical-experimental simulation with refinement of turbulence model. Verification is also necessary because there are no codes of wind regime and bioclimatic comforts. Poddaeva, O.I., Buslaeva, J.S. and Gribach, D.S. (2015) demonstrated that the current Russian and international building codes did not contain recommendations of the appointment of the aerodynamic coefficients required to determine design wind loads on structures for the tall buildings with complex shape. Climatic analysis, based on the statistics of weather stations on the frequency and direction of

winds, calms, taking into account warm and cold seasons, provides the initial data of numerical-experimental studies, the result of which are aggregate wind velocity fields for cold and warm seasons. The assessment of bioclimatic comfort by seasons is based on the method of solving of a heat-balance equation and the method of maximum permissible level of wind pressure on a human visual vision system and the method of maximum permissible concentrations of repugnant substances and biologically dangerous microorganisms during the calm.

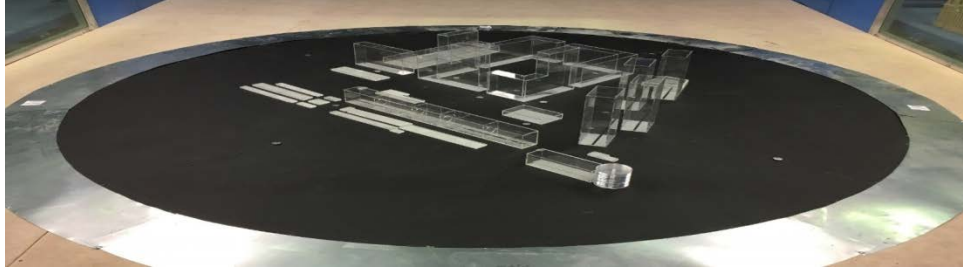


Figure 1. - Model of the high-rise residential complex (141, Varshavskoye Highway, Uzhnoe Chertanovo, Moscow) on an automated rotary table in the working area of the wind tunnel of the Educational, scientific and industrial laboratory for aerodynamic and aeroacoustic tests of building structures

3 Criterion for Assessing Bioclimatic Comfort

Conditions for the dispersion of repugnant substances are getting worse in the areas of air blanketing, that can lead to the increase in their concentrations by several times in comparison with the open areas. Veremchuk L.V., Yankova V.I., Vitkina T.I., Nazarenko A.V., Golokhvast K.S. (2016) stated that the content of suspended particulate components of pollution remained more stable, due to the features of atmospheric circulation, rugged terrain and residential development. According to the research of urban environment, the probability of occurrence of asthmatic diseases increases when a person is in the zones of air blanketing, with the velocity of air mass movement below 0.5 m/s. In the zones of increasing wind velocity, pulsations of air currents occur and the wind velocity can reach 10 m/s and more, even at average climate velocities of the background wind. This wind velocity is dangerous for pedestrians and causes deflation from the surface of the ground cover, causing an increase in dustiness of the air in the surface layer. It is especially dangerous when zones of air blanketing and zones of wind velocity increase are formed at a close distance from each other.

Temperature accounting allows defining criteria for a more detailed assessment of people's comfort in the street.

Gaitani N., Mihalakakou G., & Santamouris M. (2007) demonstrated that the used indices for assessment of comfort were the following: (a) "Comfa", which was based on estimating the energy budget of a person in an outdoor environment and (b) "thermal sensation", based on the satisfaction or dissatisfaction sensation under the prevailing climatic conditions of the outdoor spaces. Thus, on the basis of these and other studies on the heat balance of human body, for the climatic conditions of the middle lane of Russia, the range of winter breezes is 0.5 m/s to 3.0 m/s, and during the summer period is from 1.0 m/s to 5.0 m/s.

Based on the experimental results obtained in the wind tunnel and verified numerical simulation, it is possible to draw conclusions for a background wind velocity of 2.2 m/s on the presence of zones with low wind velocities (Zones of air blanketing) in which repugnant substances and chemically active dust can accumulate (Figure 2a). Cetin, M. (2015) said that bioclimatic comfort mapping methods were useful to urban managers and planners. The compilation of seasonal schemes of Bioclimatic comfort mapping methods with the imposition on the master plan has made it possible to move from research to design practice and justify the design solutions for the territory of the projected construction (Figure 2b).

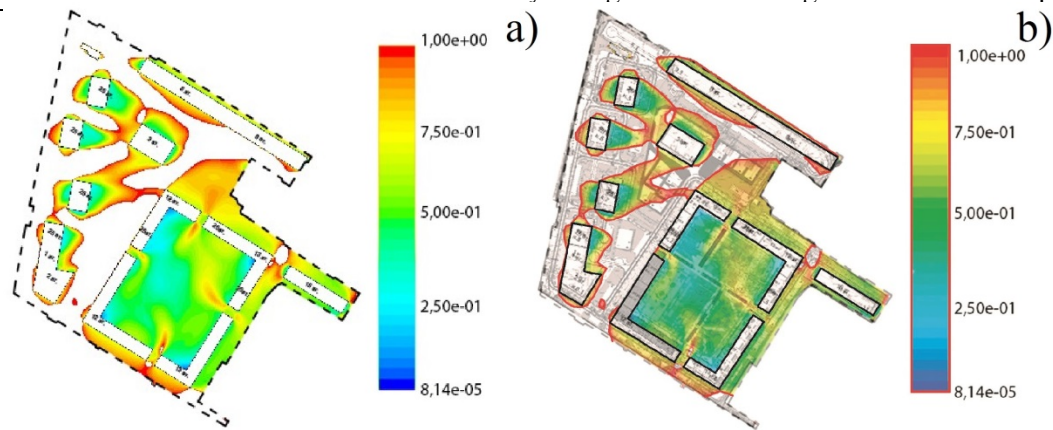


Figure 2. –Zones of air blanketing. Aggregate cartogram for summer (the zone marked with color has a velocity of less than 1 m / s with the most repeated wind directions) (a). Scheme for the location of blanketing air zones (highlighted in color) with respect to facilities for the development of design measures for ventilation and protection against overheating (b).

4 Analysis of the Evaluation Findings of Bioclimatic Comfort

The parameters of the bioclimatic comfort will correspond almost everywhere to the environment excess temperature. Only in the proximate vicinity of buildings walls, where the supply of solar radiation is limited, comfortable parameters will be provided. Especially strong overheating will be observed in the open areas of the courtyard. In January at the average north wind velocity 3.2 m/s and the average air temperature of the heating period (-15°C) in the courtyard, there is practically no chance for frostbite on open skin area. Time restriction of static stay of an adult person in the adjoining area for up to 30 minutes at the average monthly wind velocity occurs only if the air temperature drops to 18 degrees below zero or lower. In winter due to the seasonal insolation decrease for astronomical reasons and denser clouds, the temperature contrast between the different areas of housing, which is necessary for thermal convection, is getting lower. The winds of medium strength are observed more often, and in the case of their lack thereof, as a rule, or we can see an inversion state of the atmosphere, suppressing vertical convection. The described winter processes make it possible to reduce significantly the local concentration of repugnant substances in the air and at this require wind protection for the entrance groups and resting places.

5 Development of Design Solutions for Landscaping and Urban Greening for Compensating of Bioclimatic Discomfort

The territory of the land improvement areas and people's long-term stay (more than 10 minutes) are recommended to be landscaped in two ways, based on the results of zoning of zones of air blanketing and discomfort zones.

I) For benches in resting places and at children's playgrounds in areas of discomfort, it is necessary to plant around the perimeter, at least, one row of shrubberies (shrubby bushes), while the second row is planting trees (horse chestnut, rowanberry, bird cherry).

II) For benches in resting places and at children's playgrounds in zones of air blanketing, it is necessary to make dense groups of trees at a distance of 3 meters (horse chestnut, common rowanberry, bird cherry, clear stem) to organize a shadow and ensure micro ventilation at the expense of the effect of temperature convection, (Figure 3b);

Also for the draft master plan, it is recommended to provide for the installation of landscaping areas for more than 70 square meters of hard landscaping, made of windproof structures with a spatial grating serving as a diffuser for damping gusts of wind. The recommended design parameters have the arrangement of columns and rails in the form of a spatial grating serving as a diffuser for damping

gusts of wind. The distance from the edge of the area of land improvements is at least 3 meters. The overall dimensions of the diffuser are not less than - 2m x 2m, $h \geq 3m$. The cell size of the spatial grating is 0.2-0.4 m.

6 Conclusion

Solutions of the current problem of discomfort from high wind speeds, and environmental problems of excess temperatures and zones of air blanketing with increasing concentrations of harmful substances are presented as a real example in the research of the bioclimatic comfort of residential housing. Analysis of the results of the assessment of bioclimatic comfort, considering to the temperature regime of the season allowed developing design solutions for the placement of hard landscaping and urban greening. The presented methodology and project approach give opportunity to ensure the creation of the living environment that is functionally organized and well-maintained in accordance with the requests of various socio-demographic groups and favorable for sanitary and hygienic conditions for real natural and climatic conditions. The placement of windproof structures, green strips and individual trees in accordance with the town planning standards and in places recommended by the assessment of bioclimatic comfort compensates wind discomfort, the effect of summer excess temperatures and local accumulation of harmful substances in the atmosphere at the ground surface in the courtyard space.

References

- Oliveira, S., & Andrade, H. (2007). An initial assessment of the bioclimatic comfort in an outdoor public space in Lisbon. *International journal of biometeorology*, 52(1), 69-84.
- Dunichkin, I. V., Zhukov, D. A., & Zolotarev, A. A. (2013). The effect of aerodynamic parameters of high-rise buildings on the microclimate and aeration urban environment. *Promyshlennoe i grazhdanskoe stroitel'stvo*, 9, 39-41.
- Poddaeva, O. I., Buslaeva, J. S., & Gribach, D. S. (2015). Physical model testing of wind effect on the high-rise. In *Advanced Materials Research* (Vol. 1082, pp. 246-249). Trans Tech Publications.
- Veremchuk L.V., Yankova V.I., Vitkina T.I., Nazarenko A.V., Golokhvast K.S. (2016). Urban Air Pollution, Climate and its Impact on Asthma Morbidity. *Asian Pacific Journal of Tropical Biomedicine. B. 6. № 1.*, 76-79.
- Gaitani, N., Mihalakakou, G., & Santamouris, M. (2007). On the use of bioclimatic architecture principles in order to improve thermal comfort conditions in outdoor spaces. *Building and Environment*, 42(1), 317-324.
- Cetin, M. (2015). Determining the bioclimatic comfort in Kastamonu City. *Environmental monitoring and assessment*, 187(10), 1.

Mitigation technologies for counteracting the UHI effects and for improving outdoor thermal comfort in mediterranean urban open spaces: a study of vegetation and cool materials effects on pedestrian comfort in Rome

F. Laureti, A. Battisti

Department of Planning, Design and Technology of Architecture, La Sapienza University of Rome,
Italy

Abstract

The present study investigates the influence of building materials, traditional as well as innovative, and vegetated urban surfaces on the urban microclimate and on pedestrian outdoor thermal comfort in a typical Mediterranean city: Rome. It focuses the attention on selected mitigation technologies aiming to increase the albedo of cities: high reflective materials called *cool colored materials*, and the use of vegetative surfaces: *green roofs*, *green walls* and trees, with the main purpose to test, verify and quantify the overall microclimate mitigation and thermal performance of the aforementioned strategies,

The study proposes and analyses, through CFD calculations (ENVI-met v.4.0), five renovations scenarios: applying cool materials and vegetation on roofs, walls and pavements of the selected square. In order to support planning authorities and researches by going beyond the traditional way of urban heat island studies, the present study aims to highlight the multiple effects of cool colored materials on human comfort and to investigate which could be the best combination materials in terms of mitigation of ambient temperatures and pedestrian thermal stress. Therefore, air temperature as well as the physiologically equivalent temperature (PET) were applied to take into account the effect of the variations of urban materials on human comfort, the studies focus the attention and draw its conclusions through the comparison of the Envi-met thermal maps and the values of the different scenarios in terms of delta variations. The results show the negative effect of cool colored materials on human thermal comfort when applied isolated to surfaces in direct contact with pedestrians, such as pavements and urban façades, nevertheless it underlines the benefit associated with a mixed combination of cool materials and trees, setting the path for further research in this direction.

1 Introduction

There is a strong public interest in creating liveable and comfortable urban open spaces, because of their role played as social aggregator and in supporting the urban metabolism (*Martinelli et al., 2014*). As heat stress is expected to occur more frequently, more intense and long-lasting in the Middle Europe in the 21st century (*Meehl & Tebaldi, 2004*), mitigation and adaptation strategies for the improvement of urban *climate (Santamouris, 2014)* are necessary to enhance health, comfort and to follow the latest communal agreements concerning climate change (*Cop 21, 2015*). With these regards, a resilient city is low risk to natural and man-made disasters, it reduces its vulnerability by building on its capacity to respond to climate change challenges, disasters and economic shocks (*ICLEI, 2013*). Concerning the mitigation strategies two are the most important cooling measures: increase of vegetated surfaces and of urban albedo (*Shashua-Bar & Hoffman, 2000*). According to *Akbari et al. (2001)* most of the summer heat islands are created by the lack of vegetation and the high solar radiations absorptions at urban surfaces. Even though there are a solid body of researches that point out the mitigation effect that vegetation and cooling surfaces might have, (*Akbari et al., 2001; Synnefa et al., 2008; Kolokotsa et al., 2013*), there remain some unsolved issues that require further research. Especially concerning the reflective materials: whereas their use on roof has proved to an efficient technologies for the improvement of outdoor microclimate conditions as well as indoor, their use on grounds and buildings façades can be seen as contributing positively or negatively to pedestrian comfort and building energy balances (*Erell, Boneh, Pearlmutter, & Bar-Kutiel, 2013*). Therefore, the present study focuses on the materials' characteristics of the urban open spaces surfaces in terms of

physical characteristics, such as albedo and permeability, and thermal characteristics, such as emissivity and thermal transmittance, and compare variations the ambient temperatures and surface temperatures as well as on mean radiant temperature and Pet values. The study investigates the influence of building materials and vegetated surfaces on pedestrian outdoor comfort. In particular the main interest is to assess the multiple effects that cool materials might have on pedestrian comfort not only on the mitigation of UHI, in order to deepen the knowledge related to these advanced materials technologies and to understand the peculiar behaviour of innovative and vegetated surfaces depending on their different combinations and applications on the urban surfaces of the built environment.

2 Case study: Piazza San Silvestro, Rome (Italy)

2.1 Study area

The study analyses a specific urban square in the city of Rome: Piazza San Silvestro, selected for its morphological, typological and social features. Its relevance has been assessed by a recent requalification intervention (Portoghesi, 2011) and an interesting microclimatic study assessing the influence of daily shading pattern on human thermal comfort and attendance in the square (Martinelli, Lin, & Matzarakis, 2015). Even though the initial design proposed an integration of trees and green lawn as well as the insertion of a fountain in the elliptical square, the final construction didn't include those elements and proved to have no concerns for the microclimatic conditions and the thermal behaviour of the place (Martinelli *et al.*, 2015). The surrounding buildings, representing the urban interface of the open space and its main interacting surfaces, are about 4-5 floor height, with a H/W ratio equal to 0.36. Thus, the square doesn't offer a natural or shaded environment during the hot season, especially during the summer when the low albedo and the high emissivity of the materials of pavements doesn't mitigate the heatwaves effects.

1.2 Methods

Five urban renovation scenarios are proposed, based on bioclimatic and energy efficiency criteria, with the specific aim to examine the isolated as well as the combined effects that vegetation and 'cool' materials have on the outdoor comfort, focusing on design aspects such as: position, distribution and ratio of different outdoor materials. The tools used in the simulation are the numerical microclimate model ENVI-met 4 and BIOMET (Huttner & Bruse, 2009), for assessing thermal comfort in terms of PET index. The methods used in this study consist of the following: (i) the selection and modelling of specific renovation interventions, (ii) the selection of specific cool materials already object of investigations in previous researches (Santamouris *et al.*, 2011; Gobakis *et al.*, 2015) as test reference, (iii) the evaluation stage. The square is near one of the main street of the historic centre (Via del Corso) close to relevant tourist attractions, shopping boulevards, offices and the related public transport hub, its relevance has been assessed by a recent requalification intervention (Portoghesi, 2011). The square is a quadrangular paved open space measuring approximately 80 x 60 m², the surrounding buildings are about 4-5 floor height, with a H/W ratio equal to 0.36. The roof average albedo is 0.40, the walls' albedo is 0.45 and the pavements measures about 0.30 whereas the Sky View Factor (SVF) is 0.7. Thus, it doesn't offer a natural or shaded environment during the hot season, especially during the summer when the low albedo and the high emissivity of the materials of pavements exacerbate the heatwaves effects. The simulations were carried out from the 21st of June 2015 at 6.00 a.m. to the 6.00 a.m. of the 22nd of June 2015 (24 hours), in order to stabilize the calculations and to analyze the nocturnal effects of the upgraded surfaces. For validating the accuracy of the model the weather data input (Tab.1) were selected from a near weather station (Ciampino) and from the *ItMeteoData Test Year Reference Database* (2013): wind speed measures 4.5 m/s with a direction of 225°, T air is equal to 292.75 K – 19.6 °C, specific humidity measures 11.5 g/kg, relative humidity is 83%. The first stage was the selection of the most interesting combinations in terms of vegetated and cool surfaces that could be applied in an historic urban square, the five mitigation scenarios were modelled according to three criteria: the selection of those combinations that maximize the cooling effect of singular materials, the combination of mixed materials (cool and green), the minimal intervention. The 1st scenario, 'total

green scenario, aims to increase the green surfaces applied to the whole urban open space it includes *green roofs*, *green walls* and trees, the 2nd scenario, focuses on the minimal intervention and on the principal surfaces interacting with the pedestrian level: the urban pavement. It aims to analyze the combined cooling effect of trees and cool pavements. The 3rd scenario aims to convert building roofs and façades into green surfaces while applying cool materials on the urban pavements, the 4th scenario called '*total cool colored*' aims to the upgrade of the surfaces albedo through the substitution of traditional roof, wall and pavement material with *cool colored* ones, lastly the 5th scenario on the other hand apply *cool colored coatings* on roofs and walls and increase the vegetated surfaces and trees on the urban pavements. The second stage was the selection of cool materials database: the asphalt (albedo=0.20) was renovated with a cool colored thin layer asphalt (a=0.45), the basalt pavement (a=0.22) with a white Portland cement coating mixed with dolomitic marbles (a=0.89), flint blocks with cool colored concrete tiles (a=0.65); for the walls façade, the entire surfaces of pastel plaster and bricks (a=0.30-0.45 ca.) have been renovated with a yellow cool coating with TiO₂ (a=0.73), finally for the roofs surfaces: concrete tiles (a=0.30) have been upgraded with cool dark colored concrete tiles (a=0.60), brick tiles (a=0.50) with cool red brick tiles (a=0.65). Regarding the cool materials' database they were selected from previous scientific studies (Santamouris et al. 2011), whereas regarding the trees and grass they were selected from the ENVImet default database (Table 1, Table 2).

Initial material	Initial albedo	Final upgraded material	Final albedo	Delta Upgrade
Pavements				
Asphalt	0.20	Cool colored thin layer asphalt	0.45	+ 0.25
Basalt	0.80	White Portland cement with dolomitic marbles plaster	0.89	+ 0.09
Flint blocks	0.40	Cool colored pigmented concrete tiles	0.65	+ 0.25
Walls				
Areated brick block with lime plaster	0.40	Yellow cool coating with TiO ₂	0.73	+ 0.33
Roofs				
Ceramic gres tiles	0.45	Cool dark colored tiles	0.60	+ 0.20
Clay Brick tiles	0.40	Cool red brick tiles	0.65	+ 0.25

Table 1. Materials database

Name	Leaf Type	Albedo
Lemon Tree (Citrus x limon)	Decidous	0.40
Judas Tree (Cercis siliquastrum)	Decidous	0.70
Koelreuteria paniculata	Decidous	0.60
Grass (Luzerne)	Evergreen	0.20

Table 2. Trees and vegetated surfaces

The third stage was the modelling in ENVI-met of the different configuration scenarios for the environmental upgrade of the urban historical square, during this phase some adjustments have been made in order to correct some limitations within the CFD software, exposed in the next paragraph.

2.2 1.3 Limitations of the ENVI-met software

In order to understand the process supporting materials digital modelling, the microclimatic results and make valid comparisons among the different scenarios it is important to underline the limitations of the ENVI-met software used in this study (ENVI-met v.4.0, summer 2016). ENVI-met is a valid CFD software for the evaluation of thermal factors (air temperature, mean radiant temperature, etc), nevertheless some limitations related to the resolution of the space model and to the accuracy of some default materials have to be considered in order to put the results in proper perspective. First, regarding the model resolution, ENVI-met allows a minimum grid cell dimension of 1m therefore it was impossible to model a thin green wall and green roof, thus the green wall and green roof tested in the study measure 1 m in depth, resulting in a likely increased effects and values of the green surfaces to take into account. In addition, another relevant limitation linked to the material characterization of the surfaces concerns the 3d-mode, which represents the only way to apply and modify the materials of roofs and walls: the software doesn't support a detailed and easy application of the materials, thus for solving the problem it was modelled for walls and roofs only those materials most present to best approximate the real ante-operam condition. Therefore, since the majority of the walls characterising the urban square are in brick covered by light pastel colors of lime plaster, it has been selected a medium value plaster material (pastel yellow lime plaster, $a=0.45$), and for the roofs there have been selected red clay tiles ($a=0.40$) and ceramic gres tiles ($a=0.45$). Secondly, some of the materials contained in the default database need to be implemented or in some case corrected: for the basalt pavement used in this study the corresponding albedo presented in the default database has an albedo of 0.80 which is according to the scientific manual too high for a dark stone, thus all the deltas related to the pavement between the different scenarios and the default scenario with the default basalt stone need to be considered bigger than they appear. Thirdly, it is likely that the software can't calculate the heat release from walls at night which effects the air temperature at night, hence increasing the urban heat island intensity and the pedestrian thermal perception, and resulting in some computations stability problems.

3 Results and findings

In order to make comparison among the different scenarios, four main time steps were analysed: 8.00 a.m., 12.00 p.m., 6.00 p.m. and 12.00 a.m. CET, and four microclimatic parameters were taken into account for their influence on local microclimate and outdoor comfort: the air temperature (T_{air}), the surfaces temperature ($T_{surfaces}$), the mean radiant temperature (T_{mrt}) and finally the Physiologically Equivalent Temperature index (PET) (Höppe 1999; Matzarakis *et al.* 1999) in order to assess the outdoor pedestrian comfort. In the interest of underline the variations among the different scenarios, a specific point of the square was selected for its position and for the solar radiation hours to which it is exposed (equal to 9 hours of solar radiation during the day): point A (Fig. 1).

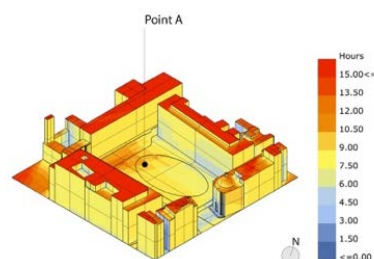


Figure 1. Point A, solar hour analysis calculated with Grasshopper software.

3.1 Observations

Concerning the air temperature values (T_{air}) the results at 12.00 a.m., described in Figure 2 (refer to the end of the document), show that the most efficient scenarios are the 1st (*total green*) and the 2nd (*cool pavement + trees*) in which the T_{air} values decrease between 0.6-1°C, whereas the others shows a decrease between 0.2-0.3°C. The deltas of the mitigation scenarios, in comparison with the initial condition, during the night time (12.00 p.m.) are moderate between -0.2-0.5°C. If we consider the T_{surfaces} values (Fig.3), the 1st scenario (*total green*) shows a value of +23.7°C, the 2nd scenario (*cool pavement + trees*) shows a value of +23.1°C, the 3rd scenario (*green wall, green roof and cool pavement*) measures +25°C, the 4th (*total cool materials*) measures +25.5°C, finally the 5th scenario (*cool roof, cool wall, trees*) shows a value of +24.8°C whereas the initial condition measures +27.1°C. The most efficient solution is represented by the 2nd scenario that combines a *cool pavement* with trees, the data appears to suggest that the reflective capacities of the materials collaborates within the shading effect of the trees, as if the reflected ratio of solar radiation is captured and moderated by the shading influence of the tree itself. It is interesting to observe that the highest value among the renovation scenarios in terms of T_{surfaces} is represented by the 5th solution (the mixed *cool colored scenario+trees*) that measures +24.8°C in comparison with the initial condition of +27.1°C. Regarding the mean radiant temperature values (T_{mrt}), as shown in Figure 4, the 1st scenario at 12.00 a.m. shows a value of +38.6°C, the 2nd shows a value of +30°C, the 3rd (*green roofs, green walls, cool pavements*) measures +61.4°C, the 4th (*total cool colored materials*) shows a T_{mrt} value of +64°C, and the 5th scenario (*cool roof, cool wall and trees*) shows a value of +39.5°C whereas the initial condition at 12.00 a.m. measures + 61.20°C. It appears that the most efficient scenarios are represented by the 2nd and the 1st scenarios measuring respectively + 30°C and +38.5°C at 12.00 a.m., whereas the 3rd and 4th scenarios show a worsening of the T_{mrt} with a delta of +0.20°C and +7.3°C compared with the +61.2°C of the initial condition. This is a considerably interesting result since it shows the multiple effect that high reflective materials could have in an urban environment while considering the ‘radiative landscape’ (Rogora & Dessì, 2005) and the radiative exchanges between man and urban surfaces. Finally, a thermal comfort analysis was carried out to define environmental performance in terms of people wellbeing. Thermal comfort was considered in terms of PET index. The PET graphs (Fig.5) show an initial condition value of +36.4°C at 12.00 a.m., the 1st scenario (*total green surfaces*) measures +29.6°C, the 2nd scenario (*cool pavement + trees*) measures + 29.6°C and the 5th scenario (*cool roof, cool wall, trees and grass*) shows a value of +29.4°C, whereas the 3rd and 4th scenarios show a worsening of the PET value at 12.00 a.m. that measures respectively + 37.30°C and +40.32°C. During the night time the initial condition measures +14.4°C, the 1st scenario and the 2nd show increased value of +16.7°C and + 16.5°C respectively, whereas the 3rd, the 4th and the 5th solutions show values of +14.6°C, +14.2°C and 16.4°C. The PET increased values of those scenarios that present an upgrade in terms of trees is probably related to the high LAI index of the trees that decrease considerably the SFV thus limiting the dissipation of the heat stored during the day by the surfaces. It is important to observe that increasing the albedo without considering the principal radiative exchanges of a surfaces and its predominant behaviour in the urban open space may contribute to a decrease of the ambient air temperature as well as of the surfaces temperature, but on the other hand, it could increase considerably the mean radiant temperature values and worsen deeply the outdoor comfort for pedestrians. Therefore, the scenarios in which the principal upgrade was in terms of albedo of roofs, walls and pavements, show poor results in terms of comfort index. This situation occurs most likely because a *cool material* with a high reflective factor reflects most of the incoming radiation towards the surrounding environment, thus increasing the radiative landscape and creating a sort of ‘glass effects’ of the infrared radiation that eventually is absorbed by the human beings, as underlined in *Erell et al. (2014)* and *Chatzidimitriou & Yannas (2015)*. Nevertheless, two interesting combined scenarios between natural and cool materials need further reflection: the 2nd scenario and the 5th scenario. Particularly the 2nd scenario, takes advantages from the reflective capacities of the innovative materials and the shading effect and evaporative cooling guarantee by the tree natural behaviour, hence it may represent a good basis for further applications. Figure 6 shows the changes in terms of materials, surfaces’ area that undergone changes and configurations in 3d models, Table 3 shows the temperatures and Pet values variations of each scenario for the reference point A, whereas

Table 4 shows a graphic synthesis of the renovation scenarios, the materials upgrade in terms of albedo, and the resulting thermal values.

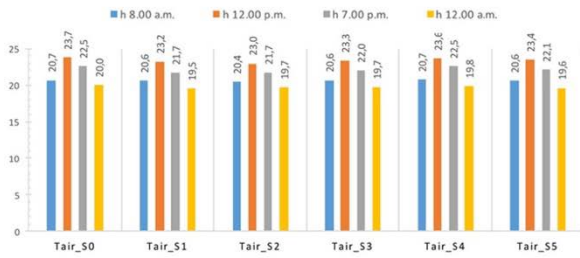


Figure 2. Air Temperature values

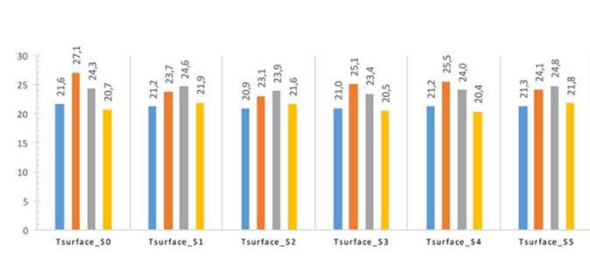


Figure 3. Surface Temperature values

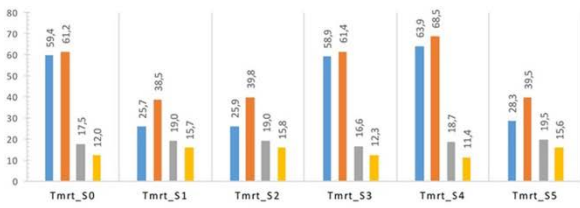


Figure 4. Mean Radiant Temperature values

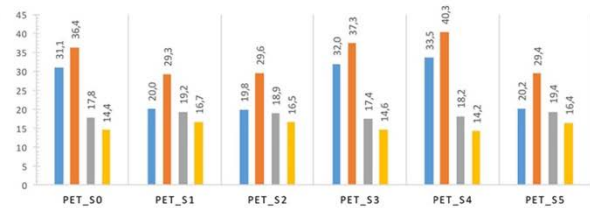


Figure 5. PET values

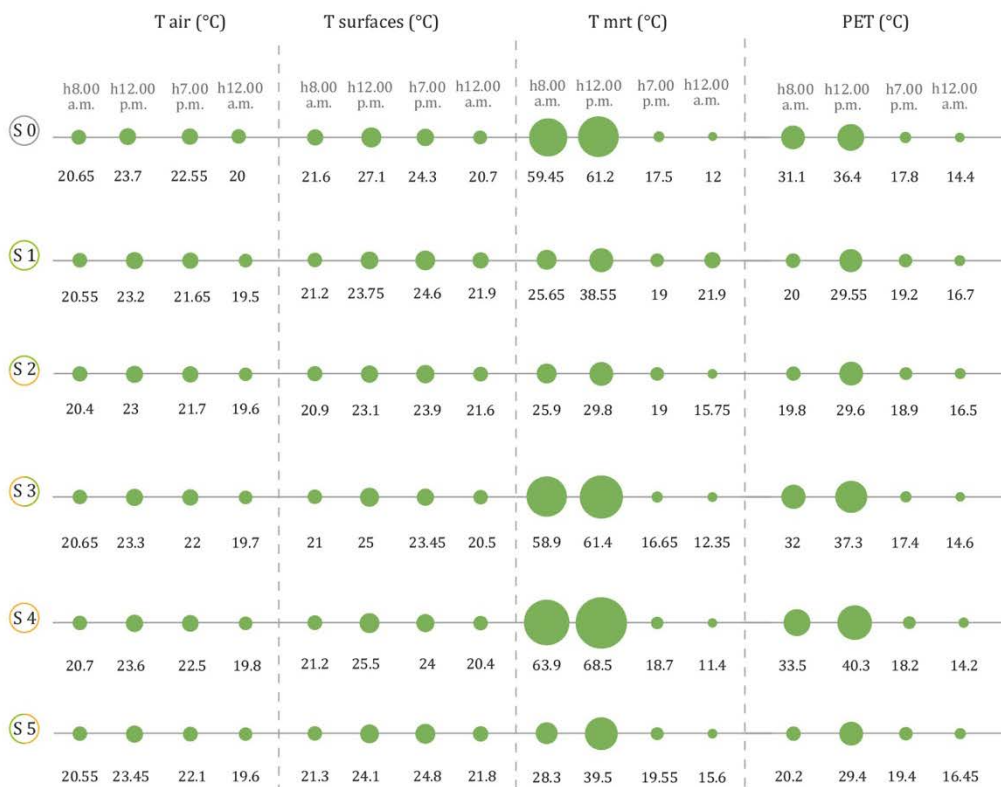
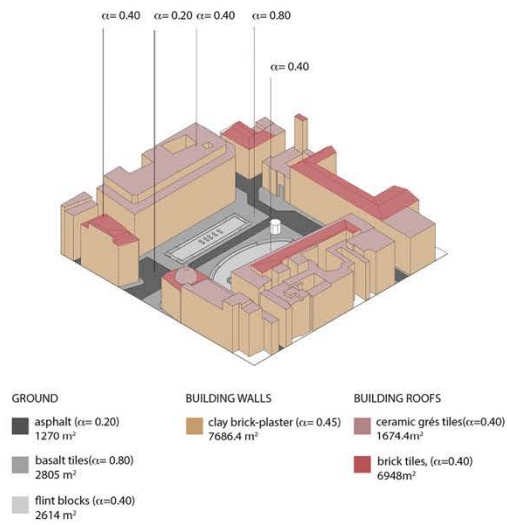
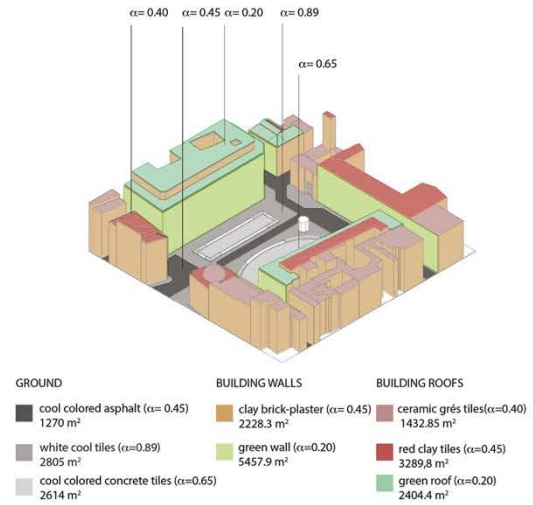


Table 3. Graphic representations of the variations among the different scenarios and the temperatures trends.

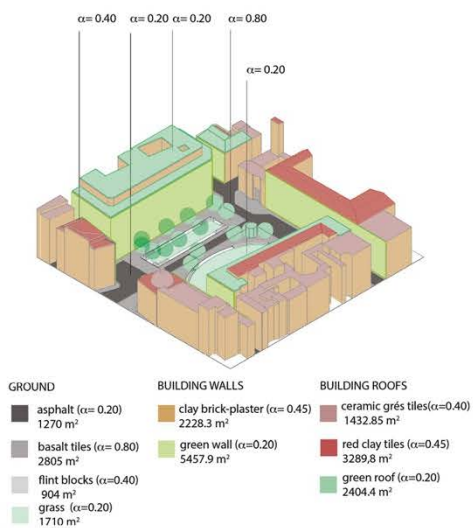
Scenario_0 (ante-operam)



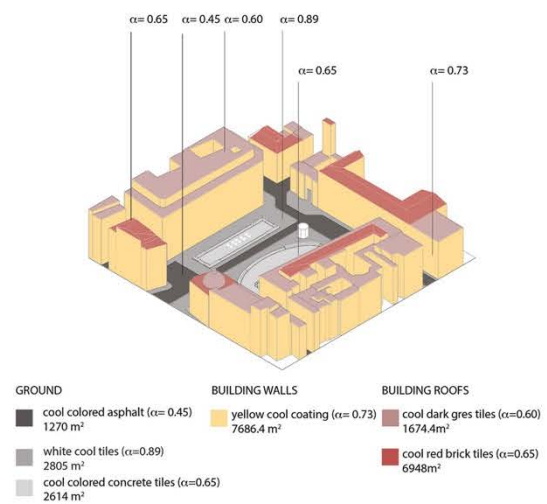
Scenario_3 (green roofs+green walls+ cool pav.)



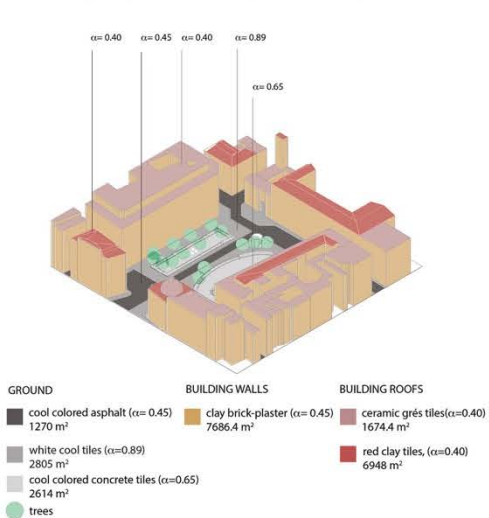
Scenario_1 (total green)



Scenario_4 (total cool colored materials)



Scenario_2 (cool colored pav. + trees)



Scenario_5 (cool roofs + cool walls + green pav.)

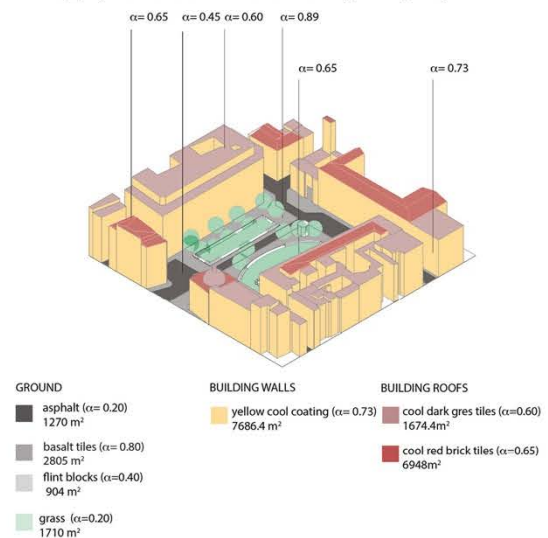


Figure 6. Ante-operam and renovation Scenarios models.

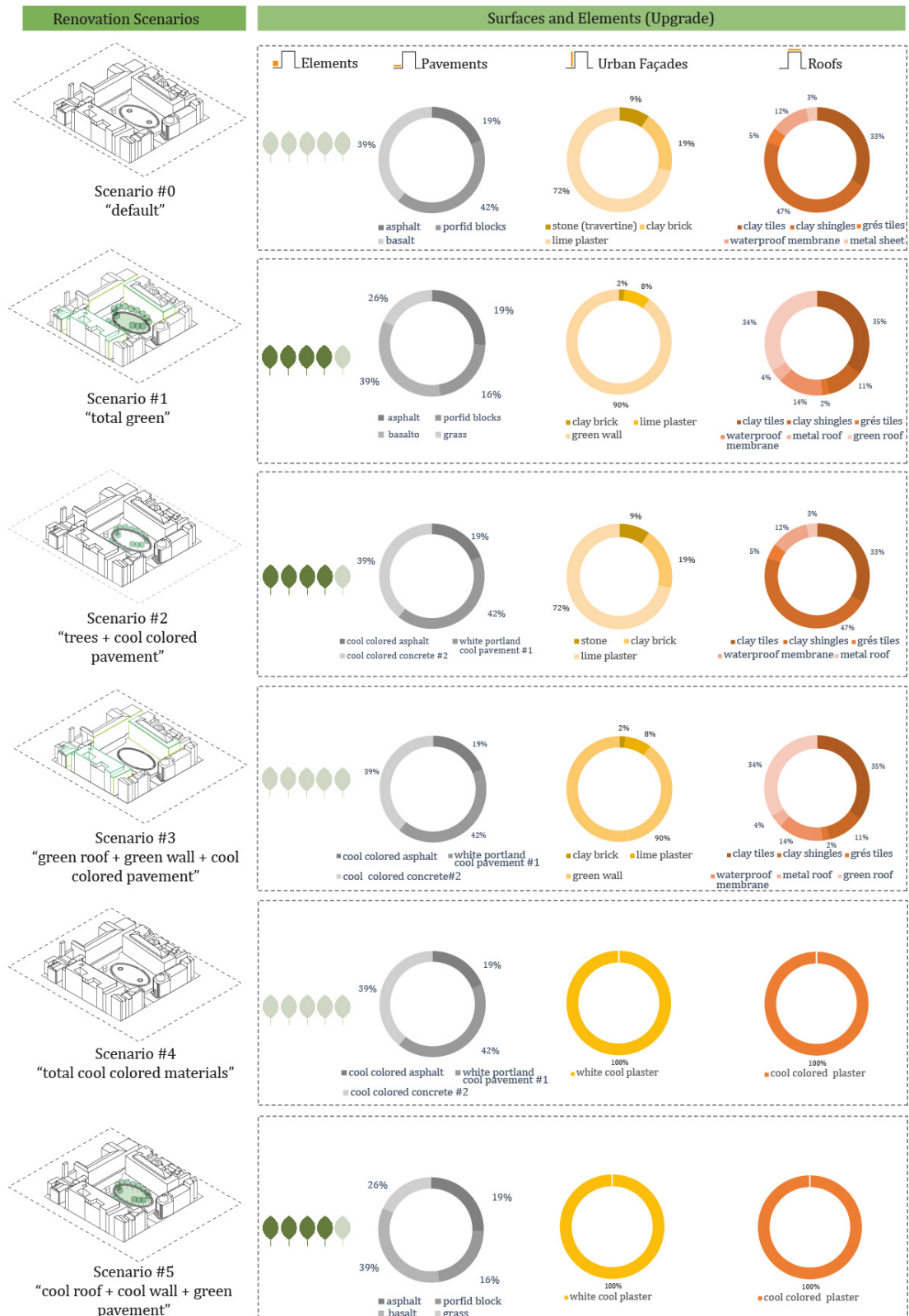
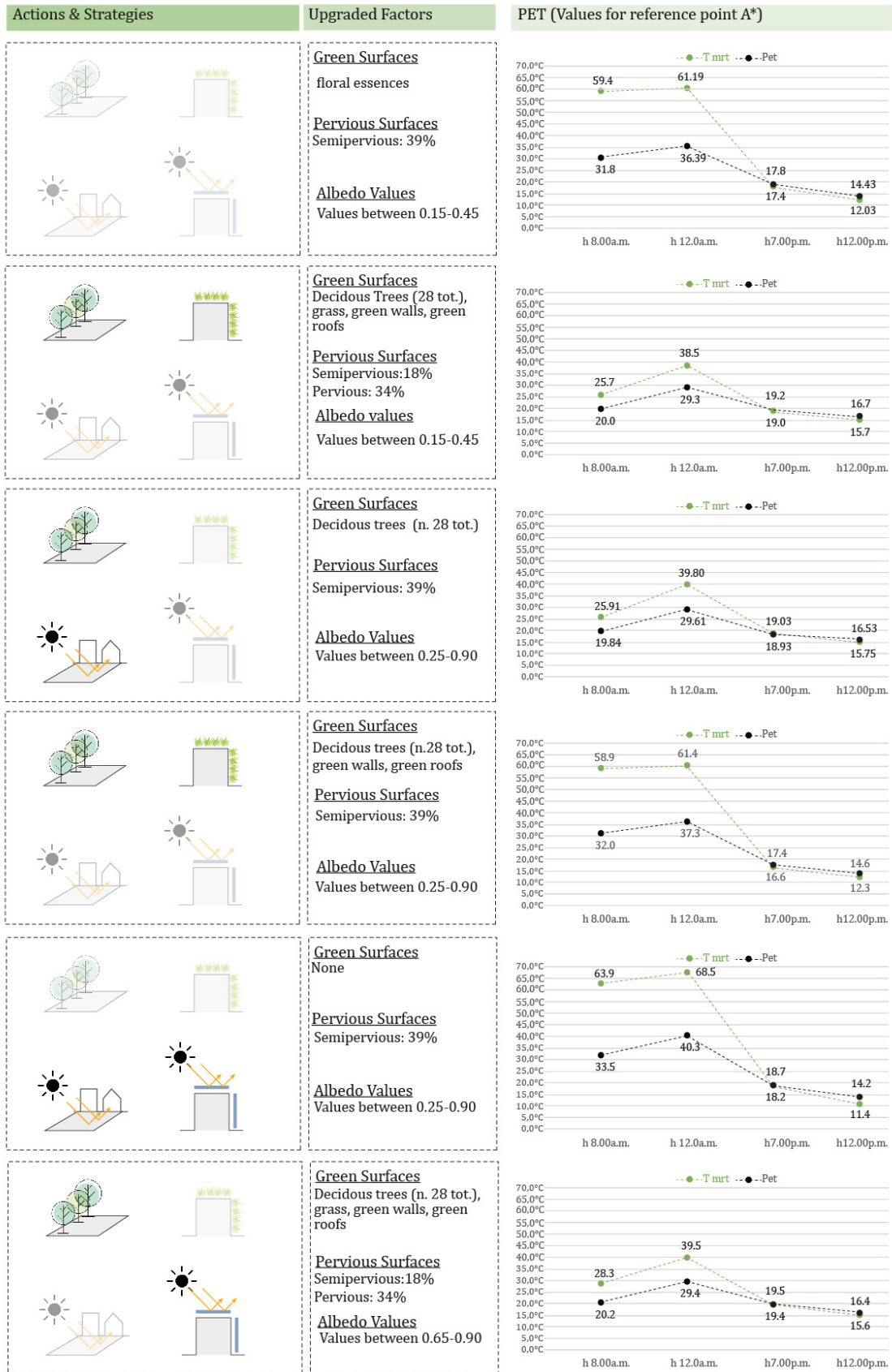


Table 4. Synthesis of the Ante-operam and Renovation Scenarios: percentages, actions, albedo variations, temperature trends.



4 Conclusions

Although use of high albedo materials for urban surfaces may reduce the air temperature and the surface temperature to which pedestrian are exposed, this reduction of the long-wave emission is offset by increased reflection of solar radiation. If applied on the roof surfaces it dissipates and reflects towards the sky sphere in a ‘win—win situation’ as stated by *Erell* (2014), whereas if applied on those urban surfaces that mostly interact with pedestrian, such as pavements and walls, it doesn’t represent a good solution for outdoor wellbeing. Regarding the vegetation, further simulations are needed in order to assess the performance of different roof and wall technologies, since the cooling effect on the outdoor environment, as well as their performance on the indoor, vary considerably in green typology, location, orientation and building construction.

References

- Chatzidimitriou, A., & Yannas, S. (2015). Microclimate development in open urban spaces: The influence of form and materials. *Energy and Buildings*, 108, 156-174.
- Erell, E., Boneh, D., Pearlmutter, D., & Bar-Kutiel, P. (2013). Effect of high-albedo materials on pedestrian thermal sensation in urban street canyons in hot climates. Proceedings of the PLEA2013—Sustainable Architecture for a Renewable Future, Munich, Germany, 10–12.
- Gobakis, K., Kolokotsa, D., Maravelaki-Kalaitzaki, N., Perdikatsis, V., & Santamouris, M. (2015). Development and analysis of advanced inorganic coatings for buildings and urban structures. *ENB Energy & Buildings*, 89, 196–205.
- Höppe PR (1999) The physiological equivalent temperature – a universal index for the biometeorological assessment of the thermal environment. *Int J Biometeorology*.
- Huttner, S., & Bruse, M. (2009). Numerical modeling of the urban climate—a preview on ENVI-met 4.0. In 7th International Conference on Urban Climate ICUC-7, Yokohama, Japan (Vol. 29).
- Martinelli, L., Battisti, A., & Matzarakis, A. (2014). Multicriteria analysis model for urban open space renovation: An application for Rome. *Sustainable Cities and Society*, 14, 10-20.
- Matzarakis, A., Mayer, H., & Iziomon, M. G. (1999). Applications of a universal thermal index: physiological equivalent temperature. *International journal of biometeorology*, 43(2), 76-84.
- Meehl, G. A., & Tebaldi, C. (2004). More intense, more frequent, and longer lasting heat waves in the 21st century. *Science*, 305(5686), 994-997.
- Rogora, A., & Dessi, V. (2005). Il comfort ambientale negli spazi aperti. Edicom Edizioni.
- Santamouris, M., Synnefa, A., & Karlessi, T. (2011). Using advanced cool materials in the urban built environment to mitigate heat islands and improve thermal comfort conditions. *Solar Energy*, 85(12), 3085–3102.
- Santamouris, M. (2014). Cooling the cities – A review of reflective and green roof mitigation technologies to fight heat island and improve comfort in urban environments. *Solar Energy*, 103, 682–703.
- United Nations, Framework Convention on Climate Change (2015) Adoption of the Paris Agreement, 21st Conference of the Parties, Paris: United Nations.

Environmental and energetic assessment of a vertical greening system installed in Genoa, Italy

F. Magrassi¹, K. Perini²

¹Department of Civil Engineering, University of Genoa, Italy

² Architecture and Design Department, University of Genoa, Italy

Corresponding authors: fabio.magrassi@edu.unige.it; kperini@arch.unige.it

Abstract

Greening systems for the building envelope are often considered as an environmentally sound choice regardless of specific characteristics and context. Anyhow, every construction requires a specific contribution in terms of energy, materials, and resources; this results in pollution and generates an environmental burden. Thus, it is of paramount importance to evaluate the expected environmental score of a system. The objective of this study is to understand the environmental burden of a vertical greening system using the Life Cycle Assessment methodology. The results of monitoring activities of a real case study and an experimental elaboration of two scenarios allow assessing the real benefit generated by a greening system. Results show that the adoption of the greening system is a sustainable option, in terms of GHG and energy efficiency, highlighting the importance of LCA for measuring the environmental sustainability of construction components.

1 Introduction

Sustainability can be defined as the property of a material or product that indicates whether and in which measure the main requirements are met in a specific application respecting the three equally important pillars of the triple bottom line (Social pillar, Economy pillar, and Environment pillar). Air, water and soil impact on the living environment, on raw material and energy consumption, on waste generation, and on damage to the surrounding environment (Hendriks, 2002). Life cycle assessment (LCA) is a useful tool for measuring the environmental sustainability of a building component. LCA is a methodology regulated by the ISO 14040:2006 that gives the measure of the balance between environmental load and possible benefits, considering the environmental costs of production, transport, use, maintenance and disposal of all components. Ottel  et al. (2011) conducted the first life cycle assessment of four vertical green systems: a comparative assessment of the environmental impact, in relation to the energy savings obtainable for heating and air conditioning. The study is based on simulations and data obtained from other studies. With a similar approach, Feng and Hewage (2014) compare air pollution and energy consumption in the material production, construction, maintenance, and disposal stages, with air purification and energy savings in the operation phase. Both LCA conclude that the living wall system based on felt layers is not environmentally sustainable. According to Ottel  et al. (2011) the environmental burden highly depends on durability and material used.

The present research aims at assessing the environmental sustainability of a vertical greening system built in Genoa, Italy in 2014 in order to conduct an LCA study based on monitoring data (Perini et al., 2017).

2 Methodology

This study quantifies the environmental burden of a vertical greening system using the Life Cycle Assessment methodology. The Life Cycle Assessment (LCA) methodology, is used to understand the impact on the environment of various types of products and is regulated by ISO 14040.

The LCA structure is divided into four main phases:

- Definition of objectives and scope
- Inventory Analysis (LCI)
- Impact Assessment (LCIA)
- Interpretation.

The vertical greening system (VGS) under investigation is installed at the INPS headquarters in Sestri Ponente (called INPS Green façade pilot project). The life time frame of the vertical greening system under analysis is assumed to be 25-year. Bibliography shows studies presenting longer time frames, the choice here is therefore to be understood as a conservative one, thinking of the possible arise of different critical conditions after 25 years. The functional unit of the study is defined as: the environmental score for a VGS with a surface area of 129 m² with a lifetime of 25 years.

Figure 1 shows the system boundaries considered in the study. The cultivation of vegetation that has been inserted into the VGS is beyond the limits of study for lack of data and also the end of life with the disposal of the wall. The impact of these two parts of the life cycle is not considered to compromise the validity of the results.

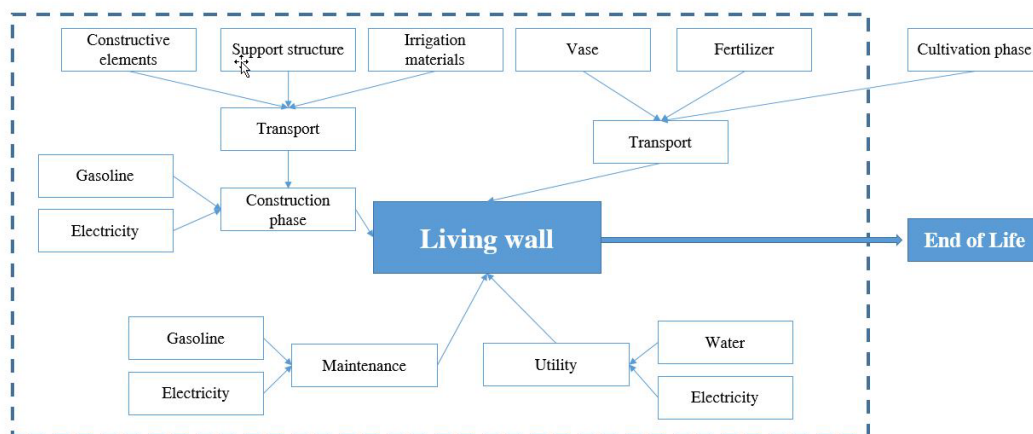


Figure 5. System boundaries of the system under investigation

The considered Impact assessment has been produced taking into account two impact categories:

- Glimmering gases, following the IPCC 2013 Global Warming Potential (GWP) method at 100 years
- Energy consumed throughout the life cycle with the Cumulative Energy Demand (CED) method

Vertical greening systems provide several benefits. In this preliminary study the improvement of thermal insulation of buildings was considered. This improvement is reached thanks to the green layer that avoids the direct radiation of the sun's rays on the wall, which does not heat up and does not radiate the heat inside. Perini et al. (2017) performed an experimental investigation to evaluate the cooling potential INPS Green Façade during summer. Based on the monitoring data, in this study the VGS is assumed to cool the air supplied to AC system, with an energy demand reduction of about 60%.

The improvement was then analysed by evaluating two scenarios:

- Scenario 1: Imaginary scenario where the wall has never been installed, therefore there have been no improvement of the wall and no impacts related to the construction of the vertical greening system
- Scenario 2: The real scenario in which the VGS have been build

These two scenarios were compared using the two impact methods presented earlier to evaluate the CO₂ Pay Back Time and Energy Pay Back Time. These indicators take into account only the energy and environmental balance and do not refer to any economic evaluation.

This was possible by comparing, thanks to parallel measurements, a green and an non-green situation.

3 Result and discussion

Table 1 shows the results of the analysis per m² of wall for 25 years of lifetime according to the two impact assessment method selected.

Table 8. Impacts calculated per 25 years of life time.

Impact category	Result	Unit
IPCC 2013 100y	0,15	t CO ₂ eq/m ²
CED	2957,89	MJ/m ²

In Figure 2, annual GHG emissions are presented for 25 years of useful life considered for the scenarios under investigation. According to Scenario 1, the scenario without the VGS (represented by the blue-colour in the image), the emissions considered are related to the only electricity used during the year. It can be noticed that for the Scenario 2, the one with the VGS (represented by the red colour in the image) the emissions for the first year are the highest, since all stages of construction and installation are considered. For the years following the first, the emissions for this scenario are constant, except for a non visible peak, which is too small to be appreciated in the figure, eight and sixteen year after the construction, in coincidence with the planned maintenance and replacement of the irrigation system, which has a useful life of about 8 years. Other impacts can be attributed to ordinary maintenance, electricity used for irrigation and fertilizer use. In addition to this, as with the other scenario, emissions from electricity consumption during the year are considered. However, the amount of electricity used is different, thanks to the energy efficiency improvements introduced by the construction of the vertical greening system.

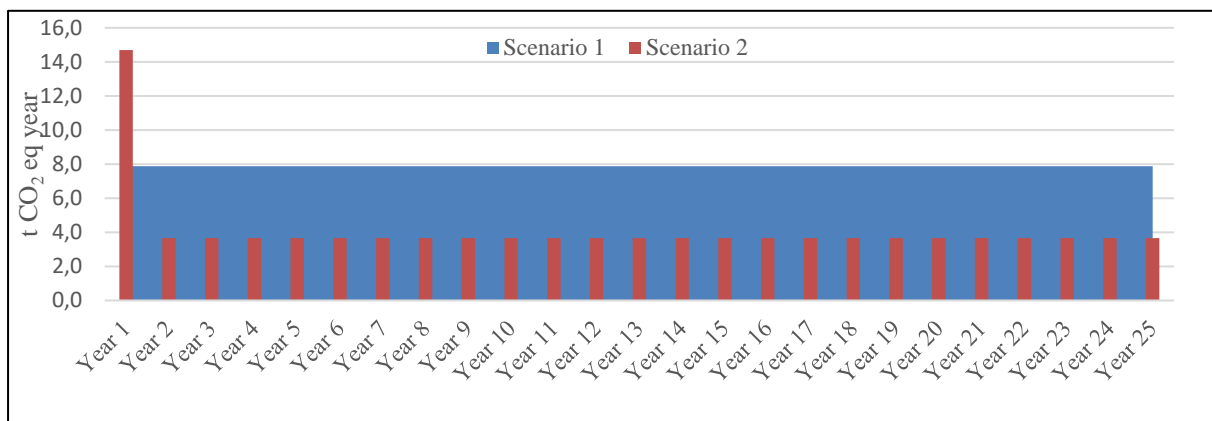


Figure 6. Comparison of GHG emissions over 25 years of useful life between the two scenario under investigation. Scenario 1 in blue, represents the case in which the vertical greening system does not exist. Scenario 2 in red, represents the case with the vertical greening system

An analysis has been carried out to determine when the environmental debt due to the construction of the green wall is repaid by a decrease of the emissions due to the energetic improvements and to understand whether these emission differences generates a positive environmental score for the Scenario 2. This analysis is called payback time and results in a very favourable result for the vertical greening system scenario. The environmental debt is repaid in about 3 years and take into account all the emissions along the 25 years of life cycle of both scenarios.

The same analysis has also been made with regard to energy impacts following the Cumulative Energy Demand methodology (CED). The results are comparable to the GHG emission analysis. Figure 3 shows the total energy consumption for both scenarios. Even in this case, the green building scenario presents a very high energy cost in the first year, due to the construction and the first phase of the vertical wall lifecycle. This, however, results in a very low energy consumption in the years following the first when compared with the scenario without a green wall.

A further analysis of the energy time payback. Again, the result obtained is excellent for the vertical greening system scenario, resulting in a payback time of just over 3 years and in an enormous amount of energy saved in the 25 years of time frame.

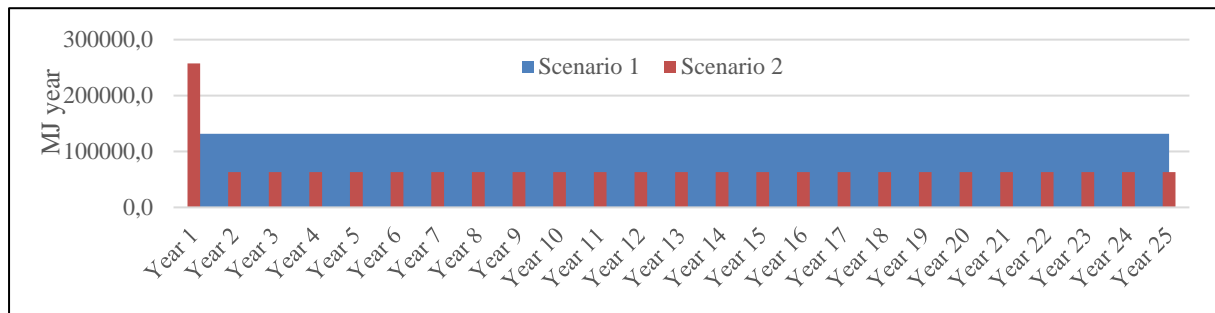


Figure 3. Comparison of CED over 25 years of useful life between the two scenario under investigation. Scenario 1 in blue, represents the case in which the vertical greening system does not exist. Scenario 2 in red, represents the case with the vertical greening system

4 Conclusion

This research has investigated the life cycle of a vertical greening system, comparing its GHG and energetic burdens using a LCA methodology. The analysis, based on data retrieved from real case study and field measurements, was conducted on two scenarios one with and one without VGS. The local energy and environmental advantages have been assessed in the previous sections, highlighting the possibility of reducing the building energy consumption, thanks to the greening system. At the level of global impacts, thanks to this analysis, it can be concluded that the adoption of the greening system is a sustainable option both with regard to the effects of GHG and the enhanced level of energy efficiency reached by the building after the VGS installation. The lack of data on cultivation and end-of-life is assumed to extend the payback time, but because we are abundantly within the life cycle of the green wall, they will not change the positive end result.

References

- Feng, H., Hewage, K., (2014). Lifecycle assessment of living walls: air purification and energy performance. *J. Clean. Prod.* 69, 91–99. doi:10.1016/j.jclepro.2014.01.041
- Hendriks, C.F., (2002). *Durable and Sustainable Construction Materials and the Building Cycle: Additions and Corrections.* Aeneas.
- Kosareo, L., Ries, R., (2007). Comparative environmental life cycle assessment of green roofs. *Build. Environ.* 42, 2606–2613. doi:10.1016/j.buildenv.2006.06.019
- Ottel , M., Perini, K., Fraaij, A.L.A., Haas, E.M., Raiteri, R., (2011). Comparative life cycle analysis for green faades and living wall systems. *Energy Build.* 43, 3419–3429. doi:10.1016/j.enbuild.2011.09.010

Perini, K., Bazzocchi, F., Croci, L., Magliocco, A., Cattaneo, E., (2017). The use of vertical greening systems to reduce the energy demand for air conditioning. Field monitoring in Mediterranean climate. *Energy Build.* 143, 35–42. doi:10.1016/j.enbuild.2017.03.036

Smart filters of particulate matter: plants in urban areas

E. Roccotiello, S. Romeo, L. Cannatà, M. G. Mariotti

Department of Earth, Environmental and Life Sciences (DISTAV), University of Genoa, Italy

Corresponding author: enrica.roccotiello@unige.it

Abstract

Plants can help restoring the environmental quality of dense urban areas realizing a trap-effect on air pollutants, specifically particulate matter (PM_x) that causes cardiopulmonary diseases for long-term exposure. Plant characteristics (e.g., species used, plant shape, leaf surfaces, leaf area index, porosity, etc.) play a key role in potential air quality improvement.

The goal of the present study was to evaluate the interactions between PM and leaf epidermis, the plant photosynthetic performance under pollutants stress and estimate the potential ability of PM removal in plant species commonly used for greening urban areas in Genoa (NW Italy).

The evaluation of PM deposition by ESEM-EDS analysis revealed a removal ability species-specific and depending on leaf epidermis, morphology and disposition and an early ecophysiological response to PM in sensitive/tolerant plant species.

Our results show the importance of choosing the right species to plan a functional, smart, mitigation in urban areas through nature-based solutions.

1 Introduction

Plants can significantly improve the environmental quality of dense urban areas by providing several ecosystem services, i.e. reducing the Urban Heat Island (UHI) effect, improving air quality and energy performance of buildings, fostering biodiversity, etc. (Perini et al. 2011; European Commission, 2016) Perini et al. 2017).

Air quality in urban areas is strongly affected by the noteworthy presence of traffic-induced emissions like nitrogen oxides (NO_x), carbon monoxide (CO) and dioxide (CO₂), hydrocarbons (HC), and particulate matter (PM_x) (EEA, 2016). Specifically, fine and ultrafine dusts with a diameter of less than 2.5 μm are among the most dangerous pollutants for human health (Powe and Willis, 2004) and represents an inhalable suspended fraction which can cause cardiopulmonary diseases, especially for long-term exposure (WHO 2013). This latter is getting a growing interest thanks to the potential ability of plant species to decrease PM_x level. Fine dust particles adhere to the plant surfaces, therefore plants are a perfect anchor for airborne particles at different heights (Ottel  et al., 2010). Plant characteristics (e.g., species used, plant shape, leaf surfaces, etc.) play a key role in potential air quality improvement (EEA, 2016). Leaves with different micromorphology are proven to be effective in collecting PM_{2.5} (Roccotiello et al. 2016; Perini et al., 2017), as a consequence, the collecting capacity of plant species significantly varies depending on specific leaf characteristics (i.e., leaf cuticle, and waxes on epidermis, leaf area index, leaf area density, porosity, etc.) (Lin et al., 2016; Tong et al., 2016; Tonneijck and Blom-Zandstra, 2002). Those leaf characteristics can influence and interact with PM deposition and dispersion, playing a key role in potential air quality improvements (K hler, 1993; Janh ll, 2015). In addition, plants species can strongly vary the ability to subtract air pollutant from the atmosphere even if arranged in the same way (e.g., in the same nature-based solutions).

However, care should be taken when choosing plant species for urban areas to avoid both O₃ damage in sensitive species (Gao et al., 2016), and Volatile Organic Compounds –VOCs- emission, which increase O₃ level (Leung et al., 2011; Churkina et al., 2015).

Finally, the species phenology and physiology can change the plant species performances considering that air pollutants can cause the closing of stomata, the structure responsible of plant transpiration (Xu *et al.*, 2016). In addition PMx can specifically bind to leaf cuticular waxes resulting in a “barrier effect” on leaf surfaces with a consequent decrease of photosynthetic efficiency (Roccotiello *et al.*, unpublished).

The goal of the present study was to evaluate the interactions between PM and leaf epidermis, assess the ecophysiological response of plants to PMx (in terms of photosynthetic efficiency) and estimate the potential ability of PM removal in plant species commonly used for greening urban areas in Genoa (NW Italy).

2 Materials and Methods

2.1 Sampling site and plants

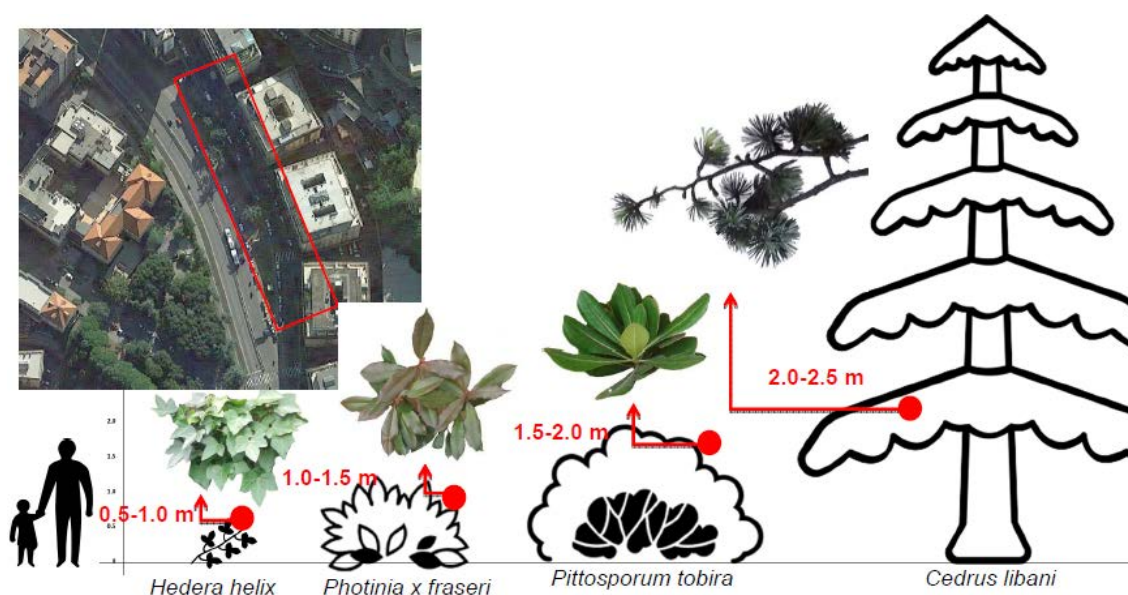


Figure 1. Sampling site in Genoa city centre at different sampling height

The study site, Corso Europa, traffic island between corso Europa and Via San Martino (Genoa, Italy) was in one of the most polluted areas of Genoa. Four plant species at different sampling height respect to ground level were selected: *Hedera helix* L. (0.5 m), *Photinia × fraseri* (*P. glabra* (thumb) Maxim. × *P. serratifolia* (Desf.) Kalkman (1 m), *Pittosporum tobira* (Thumb) W. Aiton (1,5 m), and *Cedrus libani* A. Rich. (2.5 m).

For each of the four plant species analysed, 5-10 leaves were randomly chosen from the same height, i.e., 0.5 ± 2 m, to allow the sampling through the windows at a reasonable distance from traffic source (i.e., 2 m) (Fig. 1).

2.2 Semi-quantitative ESEM-EDS analyses

All the leaves were analysed within one week after sampling at the DISTAV lab, University of Genoa with scanning electron microscope with X-ray analysis (ESEM-EDS). To evaluate PM disposition, dimension and composition of the particles on the leaves the Energy Dispersive X-ray Spectrometry-analysis (EDS-analysis) or elemental-mapping technique was done according to Ottel  et al. (2010). In total 4 positions per leaf (upper leaf epidermis were analysed with ESEM, while for chemical (elemental) analysis For counting methods magnification of 100X and 500X were used, while for EDS

analysis 5000X magnification was used. Surface area and spot analyses were done, the first on the whole leaf surface at 5000X magnification was strongly influenced by the “organic matrix effect” determined by the leaf that “dilute” the , the second choosing 20 particles to limit or exclude 3D errors.

2.3 *Plants' photosynthetic efficiency and performance*

The photosynthetic efficiency of leaves were recorded in field for each randomly selected branch of the target species. Before measurements leaves were dark adapted for 10 min using dark leaf clips. The fluorescence induction of chlorophyll a (Chl a) was measured by a fluorimeter (Handy PEA, Hansatech Instruments, UK). The source of excitation light was a 1-s pulse of ultrabright continuous red radiation (650 nm peak wavelength), provided by an array of three light-emitting diodes (LEDs), focused on a leaf surface of 5 mm at an intensity of 3500 mmol photons m⁻² s⁻¹. Chl a fluorescence transients (Kautsky curve) exhibited upon an illumination of dark adapted leaves by saturating red light (650 nm) were obtained through the “JIP test”. The analysis of the transient was focused on fluorescence values at 50 ms (F₀, step 0), 2ms (stepJ), 30ms (stepI) and maximal fluorescence (FM, step P) (Strasser and Tsimilli-Michael, 2001; Strasser *et al.*, 2004).

2.4 *Data elaboration and analysis*

The software Image J (<http://imagej.nih.gov/ij/>) was used to count the particles found on each magnification (100×, 500×, 1000×). Image J allows creating binary images (i.e., black and white) and distinguish particles from the leaf epidermis (background), with the function threshold. Once particles overlapping are separated, thanks to the function watershed, size and number are analysed, without boundary to the circularity. Image J counts particles and the related area. In this experiment particle diameter was calculated afterwards.

For all the cases analysed a surface of 1 mm² was considered to compare amount and size of particles. Considering all the particles counted on each magnification (100%), the amount of particles of different size were counted, e.g., >20m or <2.5m. The 5000× magnification was used only for qualitative comparison, since such a small area of a leaf can not provide reliable results for quantification.

3 **Results and Discussion**

The evaluation of PM deposition revealed a different removal ability by the considered species: *C. libani* > *P. × fraseri* > *H. helix* > *P. tobira* (Fig. 2). *C. libani* has more particles on leaf surface despite the highest sampling height, this could be linked to the thick cuticle and waxes and let us suppose a direct interaction between fine and ultrafine dust (PM<1) and leaf epidermis. Hwang *et al.* (2011) described similar ability for pine needles; they proved the higher ability to subtract PM_x from the atmosphere by conifers respect to broadleaves species. Other authors demonstrated that particles smaller than 10 μm were encapsulated into the leaf/needle cuticle (Terzaghi *et al.*, 2013).

The photosynthetic performance is high in all the selected species (photosynthetic efficiency F_v/F_m ≥ 1), but showed a significant difference between young and old leaves of *C. libani* because of the longer deposition time for PM_x on old needles and complexation with needles' waxes creating a "barrier effect" to light with an overall decrease in plant performances (performance index PI < 1). This is in accordance with Terzaghi *et al.* (2013) who demonstrated that three-year-old needles had more polycyclic aromatic compounds (PAH) transferred into the needle wax, showing an age effect on the wax in the needle surface.

Even if *Hedera helix* has a good performance In other studies, Przybysz *et al.* (2014) found greater deposition on pine than on yew, and even less deposition on ivy (*Hedera helix* L.). Our findings agree with Sternberg *et al.* (2010) who show that ivy acts as a ‘particle sink’, absorbing particulate matter, particularly in high-traffic areas with high level of fine (<2.5 μm) and ultrafine (<1 μm) particles. This could probably be related to the thick leaf epidermis, specifically high level of waxes and leaf micromorphological alterations (Rai, 2016).

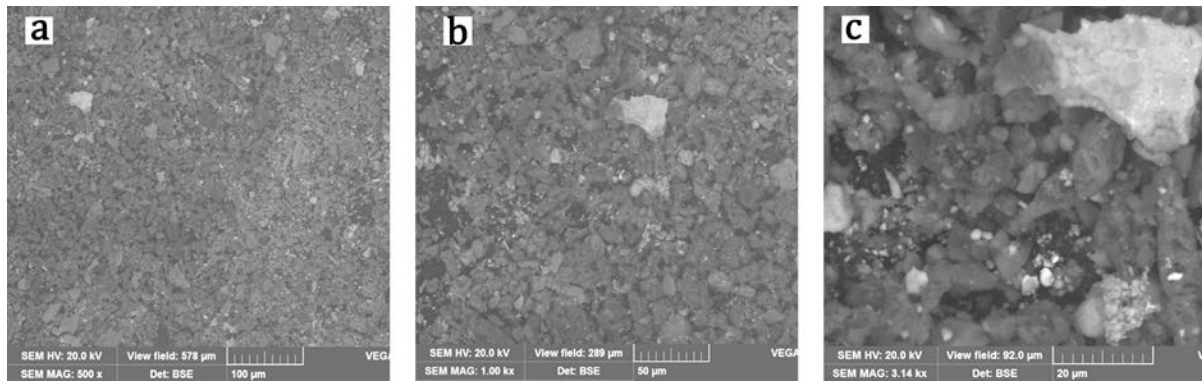


Figure 2. PMx specifically binds to leaf epidermis at 100× (a), 500× (b) and 1000×(c) magnification in *C. libani*. ESEM micrographs.

Our results show the mitigation potential of plants in limiting urban PM exposure.

On the other hand, further studies are necessary to clarify the plant response to air pollutants and to provide reliable and realistic input parameters for numerical simulations. In addition, for future greening solutions several plant factors can be taken into account: plant photosynthetic performance and its adaptability and resilience to climate change (i.e., low water requirements), high biomass with a good LAI and LAD and adequate leaf micromorphology for air pollutants capture (Perini *et al.*, 2017), limited production of Volatile Organic Compounds (VOCs), low allergenicity, high resistance to plant pests, low cost of maintenance, and ability to act as a strong atmospheric CO₂ sink.

References

- Churkina, G., Grote, R., Butler, T.M., Lawrence, M. (2015). Natural selection? Picking the right trees for urban greening. *Environmental Science & Policy* 47, 12–17.
- European Commission (2016). Nature-Based Solutions <https://ec.europa.eu/research/environment/index.cfm?pg=nbs> (accessed 10.3.16).
- European Environment Agency (2017). Air Quality in Europe – 2016 Report.
- Gao, F., Calatayud, V., García-Breijo, F., Reig-Armiñana, J., Feng, Z. (2016). Effects of elevated ozone on physiological, anatomical and ultrastructural characteristics of four common urban tree species in China. *Ecological Indicators* 67, 367–379.
- Hwang, H.-J., Yook, S.-J., Ahn, K.-H. (2011) Experimental investigation of submicron and ultrafine soot particle removal by tree leaves *Atmospheric Environment* (1994) 45, 6987-6994.
- Janhäll, S. (2015). Review on urban vegetation and particle air pollution – deposition and dispersion. *Atmospheric Environment* 105, 130–137.
- Köhler, M. (1993). Fassaden- und Dachbergrünung. Ulmer Fachbuch Landschafts- und Grünplanung, Stuttgart.
- Leung, D.Y.C., Tsui, J.K.Y., Chen, F., Yip, W.-K., Vrijmoed, L.L.P., Liu, C.-H. (2011). Effects of Urban Vegetation on Urban Air Quality. *Landscape Research* 36, 173–188.
- Lin, M.-Y., Hagler, G., Baldauf, R., Isakov, V., Lin, H.-Y., Khlystov, A. (2016). The effects of vegetation barriers on near-road ultrafine particle number and carbon monoxide concentrations. *Science of the Total Environment* 553, 372–379.

- Ottel , M., van Bohemen, H.D., Fraaij, A.L.A. (2010). Quantifying the deposition of particulate matter on climber vegetation on living walls. *Ecological Engineering* 36, 154–162.
- Perini, K., Ottel , M., Fraaij, A.L.A., Haas, E.M., Raiteri, R. (2011). *Building and Environment*, 46, 2287–2294.
- Perini, K., Ottel , M., Giulini, S., Magliocco, A., Roccotiello, E. (2017). Quantification of fine dust deposition on different plant species in a vertical greening system. *Ecological Engineering* 100, 268–276.
- Powe, N.A., Willis, K.G. (2004). Mortality and morbidity benefits of air pollution(SO₂ and PM₁₀) absorption attributable to woodland in Britain. *Journal of Environmental Management* 70, 119–128.
- Przybysz, A., S eb , A., Hanslin, H.M., Gawronski, S.W. (2014). Accumulation of particulate matter and trace elements on vegetation as affected by pollution level, rainfall and the passage of time. *Science of the Total Environment* 481, 360–369.
- Rai, P.K. (2016). Impacts of particulate matter pollution on plants: implications for environmental biomonitoring. *Ecotoxicology and Environmental Safety* 129, 120–136.
- Roccotiello, E., Perini, K., Cannat , L., Mariotti, M. (2016). Air Pollution Mitigation via Urban Green Interactions with Particulate Matter. III international Plant Science Conference, Rome.
- Sternberg, T., Viles, H., Cathersides, A., Edwards, M. (2010). Dust particulate absorption by ivy (*Hedera helix* L.) on historic walls in urban environments. *Science of the Total Environment* 409, 162–168.
- Strasser, R.J., Tsimilli-Michael, M. (2001). Stress in plants from daily rhythm to global changes, detected and quantified by the JIP test. *Chimie Nouvelle (SRC)* 75, 3321–3326.
- Strasser, R.J., Tsimilli-Michael, M., Srivastava, A. (2004). Analysis of the Chlorophyll a fluorescence transient. In: Papageorgiou, G.C., Govindjee (Eds.), *Chlorophyll a Fluorescence: A Signature of Photosynthesis*. Springer, pp. 321–362.
- Terzaghi, E., Wild, E., Zacchello, G., Cerabolini, B.E.L., Jones, K.C., Di Guardo, A., 2013. Forest Filter Effect: role of leaves in capturing/releasing air particulate matter and its associated PAHs. *Atmospheric Environment* 74, 378–384.
- Tong, Z., Baldauf, R.W., Isakov, V., Deshmukh, P., Max Zhang, K., 2016. Roadside vegetation barrier designs to mitigate near-road air pollution impacts. *Science of the Total Environment* 541, 920–927.
- Tonneijck, M.B.-Z.A.E.G., Blom-Zandstra, M. (2002). *Landschapselementen ter verbetering van de luchtkwaliteit rond de Ruit van Rotterdam: eenhaalbaarheidsstudie*. Wageningen Plant Research International 152.
- World Health Organization -WHO (2013). Health effects of particulate matter.
- Xu, Z., Jiang, Y., Jia, B., Zhou, G. (2016). Elevated-CO₂ response of stomata and its dependence on environmental factors. *Frontiers in Plant Science* 7, 657.

A general overview on urban adaptation strategies to climate change and sea level rise.

G. E. Rossi, C. Lepratti, R. Morbiducci

Department of Architecture and Design, University of Genoa, Italy
Corresponding author: Rossi Guido Emilio, guido.e.rossi.unige@gmail.com

Abstract

The impacts of climate change increase the vulnerability of urban areas who meet a global trend of increasing inhabitants and hosted in 2015 the 53% of the world population (UN-Habitat 2016). It has been estimated that 23% of the world's population lives both within 100 km distance of the coast and <100 m above sea level, population densities in coastal regions are about three times higher than the global average (Neumann 2015), and a growing population will be exposed to the impacts of sea level rise (Neumann 2015). Adaptation strategies and measures are required in order to face the adverse impacts of climate change in general and those related to sea level rise (SLR). Few frontrunner cities already developed and implement adaptation plans, although a great number of cities are still lacking a systemic approach to face the challenge.

1 Introduction

According to the Fifth Assessment Report of the Intergovernmental Panel on Climate Change (Stocker 2014), global warming since the mid-20th century is primarily a consequence of greenhouse gas emissions due to human activities (Stocker 2014). However, even though strong mitigation actions are put into practice to maintain climate change impacts under a threshold that still allows the main services to function reasonably well, even if global greenhouse gas emissions would end nowadays, climate would continue to change as a consequence of emissions of the last decades and the inertia of the climate system, and the sea level would continue to rise. Mitigation by itself is not able to avoid the impacts of climate change. Thus, in order to face the adverse impacts of climate change, mitigation and adaptation actions should be brought about in a harmonised approach.

2 Impacts and vulnerability of cities to climate change and sea level rise

The report “*Climate change, impacts and vulnerability in Europe 2016*” (EEA 2017) presents an indicator-based assessment of former and expected climate change, impacts and the related vulnerabilities and risks to ecosystems, human health and society in Europe, taking into account a broad range of model simulations. The report identifies key detected and predictable changes in climate and their impacts for the main biogeographic regions in Europe. All over Europe coastal zones cope with rising of the sea level and the consequent increasing risk of flooding as well as a possible intensification in storm surges (see fig. 1. Key observed and projected climate change and impacts for the main biogeographical regions in Europe).

Global mean and extreme sea level augmented worldwide and along most of the European coasts. According to the IPCC Fifth Assessment Report (Stocker 2014) sea level in the 21st century will rise by 26–81 cm, varying on the emissions scenario, and assuming that the Antarctic ice sheet remains stable. Other recent model-based researches and expert assessments have foreseen an upper bound for global mean SLR in the 21st century in the range of 1.5–2.0 m (Horton 2014) (Zecca 2012). Some

coastal cities need to face also the impact of subsidence, the gradual sinking of landforms to a lower level often as a result of human activities like mining operations and underground water exploitation.

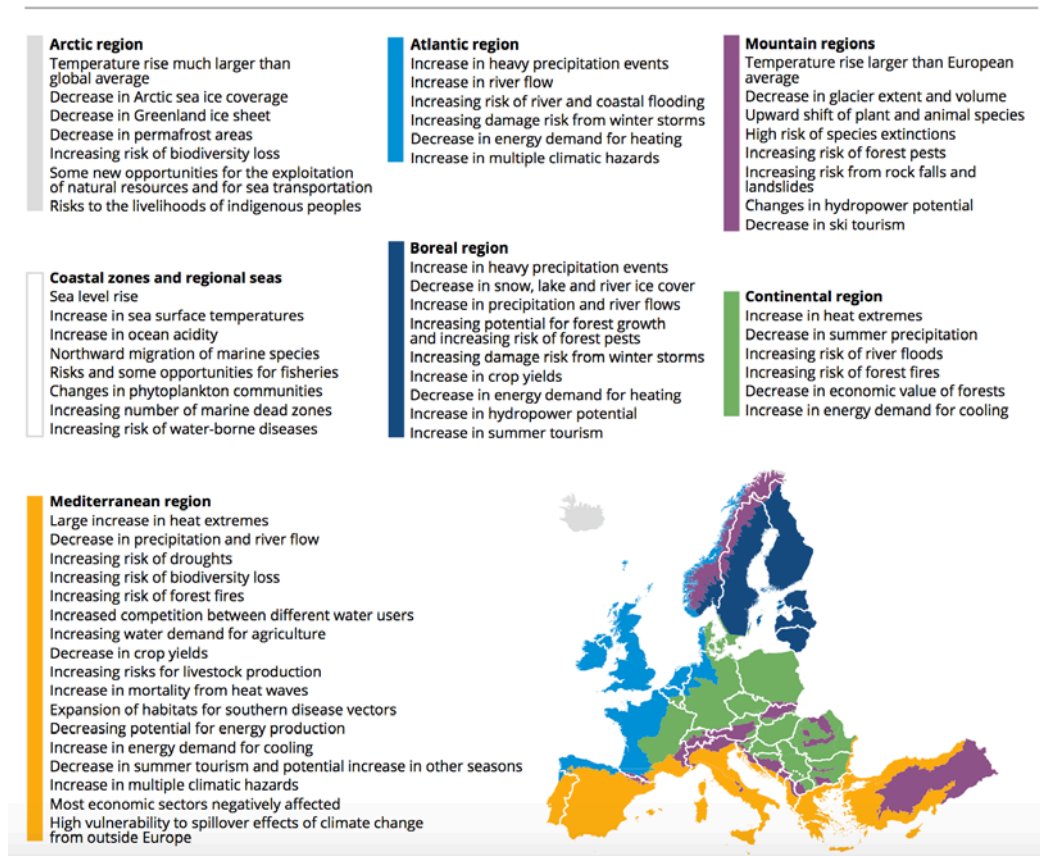


Fig. 1. Key observed and projected climate change and impacts for the main biogeographical regions in Europe – Source: “Climate change, impacts and vulnerability in Europe 2016” (EEA 2017)

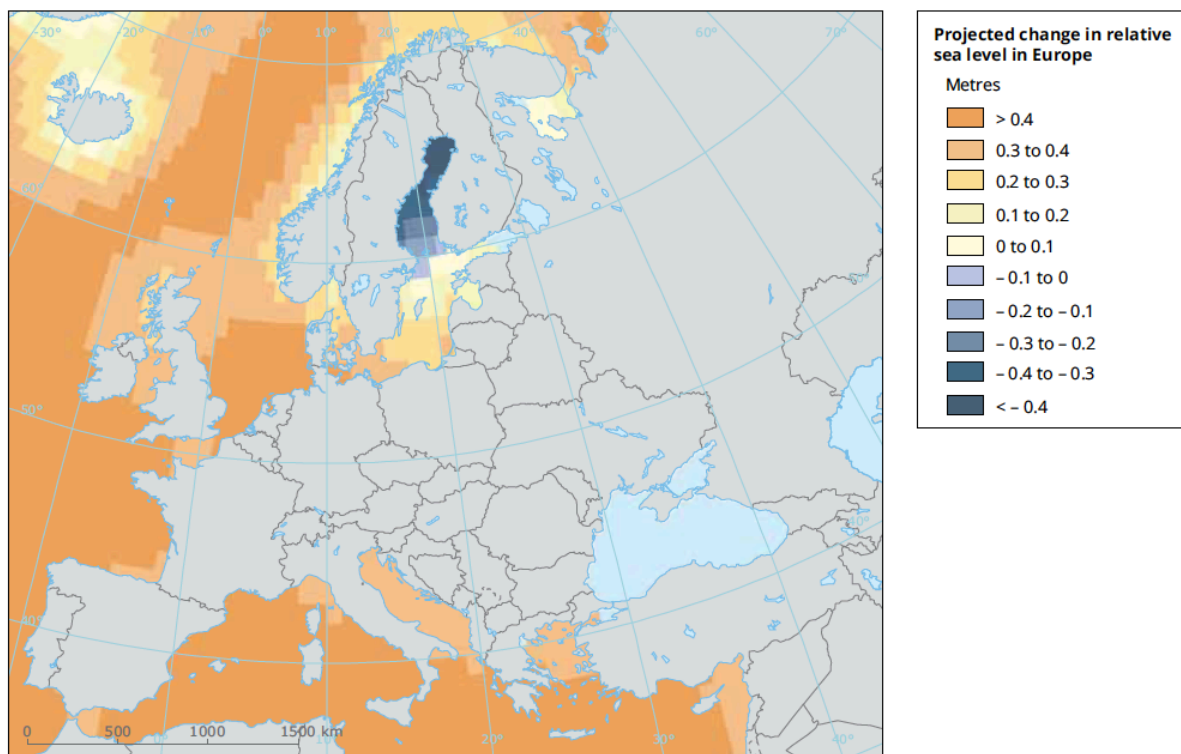
UN Habitat reports estimates that 550 million people will live in coastal cities in 2050 (UN-Habitat 2016). According to data from the National Oceanic and Atmospheric Administration, US government agency, about 100 million people live at an altitude between 0 and 180 cm from the average sea level (NOAA 2017). In terms of the overall cost of damage, the cities at the greatest risk are: Guangzhou, Miami, New York, New Orleans, Mumbai, Nagoya, Tampa, Boston, Shenzhen and Osaka (Weltbank 2013). In Europe the most affected cities will be those facing the Atlantic Ocean and the North Sea, but also Mediterranean such as those Italian ones of the north Adriatic like Ravenna and of course Venice will be strongly touched (see fig. 2. Projected change in sea level rise in Europe). Some of the

mentioned areas (e.g. the city of Ravenna and its surroundings) will have to cope also with the phenomenon of subsidence that greatly increases the impact of the SLR.

3 The need of adaptation plans to face climate change impacts in European cities

Over 70% of people in Europe live in cities and the predicted trend is increasing (Perks, Horrocks 2011) more than 80% by 2050 (EEA 2016a). European cities are facing demographic changes, technological innovations and socio-economic transitions. These changes, together with the additional pressure of the impacts of climate change may increase the vulnerability and challenges to cope with, however, they can also be an opportunity for enhancing quality of life, economic competitiveness, health and urban biodiversity (EEA 2016). European cities, as a task given by the National Government are progressively required to face the threats of climate change and meet the planned goals even if they often lack the needed resources.

Cities have always been struggling to tackle the problems of unforeseen climatic events that sometimes may change the existing balance and urban structure in a tragic and irreparable way. Cities mostly reacted to past catastrophic events, such as flooding, droughts or heat waves, trying to adapt in order to escape the disasters in the future. The unexpected event most commonly became a part of water, health or disaster risk management and the measures taken are a starting point, even if few cities followed the path towards adapting to future climate changes.



Note: This map shows projected change in relative sea level in the period 2081–2100 compared with 1986–2005 for the medium-to-low emissions scenario RCP4.5 based on an ensemble of CMIP5 climate models. Projections consider gravitational fingerprinting and land movement due to glacial isostatic adjustment, but not land subsidence as a result of human activities. No projections are available for the Black Sea.

Fig. 2. Projected change in sea level rise in Europe – Source: “*Climate change, impacts and vulnerability in Europe 2016*” (EEA 2017), Adapted from IPCC, 2013 (Figure TS.23 (b)).

The European Union, through its reports and funding programs, has been supporting climate change urban mitigation actions for several years, while adaptation is still recent. However, the number of

cities that begin to engage in the process of drafting and implementing adaptation plans is growing in the last few years. Most of them are in the phase of assessing the vulnerability of their territories in order to draft adaptation plans and strategies. Few cities well along in the process are already implementing adaptation actions and fostering monitoring and reporting measures.

The European Union set up an Adaptation Strategy developed in the Covenant of Mayors for Climate and Energy, an adaptation initiative. Moreover, the Paris climate conference (COP21) defined an action plan for adaptation in December 2015. Furthermore, the UN Sustainable Development Goals underline the necessity for cities to take action. Climate change is a systemic challenge that is strictly linked to socio-economic dynamics and regional and global aspects and tendencies.

4 An overview of the European path towards adaptation plans

The need of adaptation plans for European cities is clearly stated in the report “*Urban adaptation to climate change in Europe 2016*” (EEA 2016) that provides an overview of the measures and strategies that may be used in order for European cities to adapt to climate change, the improvements and advances already pursued in the latest years and the future challenges to be faced so to reach the goal of well-adapted and climate-resilient cities for a climate-resilient Europe. The report describes the path to adapt and convert cities into attractive, climate-resilient and sustainable places defining three main different approaches that city administrations can pursue towards adaptation depending on the the circumstances, starting points and key actors involved. Often planners and/or the decision-making bodies have to respond to an unforeseen tragic event and they put into practise existing adaptation measures and knowledge gained, for example in disaster risk management, coping with the emergency with a relatively quick and not extremely expensive solution, thus implementing a *coping approach* focused on solving the problem rather than addressing complex issues and interdependencies of climate change. When existing adaptation measures are incrementally improved and increased in efficiency and implemented in order to follow the requirements of vulnerability assessment and adaptation plans a second approach named *incremental adaptation* is set, thus following an approach based on opportunity. Incremental adaptation may be appropriate and efficient to cope with short and medium-term challenges. However, coping and incremental adaptation implemented through “soft”, “low-regret” and “low-cost” measures may be useful in a short term, but it may not be sufficient to respond in the long-term. As an example, the city of Vác, near Budapest, needs to face severe flooding almost every four years as a result of the increasing impacts of climate change and the flood defences built in cities upstream, including in Slovakia, Austria and Germany which worsen the flooding in Vác. A plan to build a mobile dam to protect the city was set, however the dam is only 1 m higher than the 'last worst' flood and the flood level is increasing thus the problem will not be solved in long-term. As adaptation measures locally implemented can have considerable impacts on other places a regional perspective is essential to face the problem as well as a long-term perspective using future climate projections instead of relying on past experience in order to avoid subsequent events from producing damage over and over again, requiring costs that could otherwise be avoided.

Moreover, the *coping approach* and *incremental adaptation* are often only applied locally, while the impact of climate change may involve large areas also including different countries. An example is the Elbe river valley and the Dresden region where in the past years, several severe flooding events have caused huge damage to the region and the city. Dresden is only some 50 km away from the border with the Czech Republic; thus the river and flood management across the border upstream is of immediate importance for Dresden. A regional and transnational approach to address flooding, involving Czech institutions in flood protection and forecasting helped Dresden to be much better prepared, to a large extent also because of the increased level of information and aided to face a severe flooding event in 2013 lowering the damage.

Taking into account that extreme climate-driven events are foreseen to be more intense and recurrent a long-term vision should be aimed. In order to address the systemic challenge of climate change a third approach should be applied, described as *transformational adaptation* which is a wider and systemic approach that investigates and deals with the causes, frequently linked to human actions, e.g. settlements set in risk-prone areas, inadequate building design or other human activities that may

increase the impact of climate change. Transformational adaptation promotes a change of approach towards the challenges, trying to provide new and innovative solutions with the aim of transforming problems in opportunities and support the path to a resilient and sustainable city. This approach is intended to combine adaptation with other aspects of urban development in a long-term systemic perspective, starting from the state of the art of the current city and trying to organise it in a different, more efficient and sustainable way. Transformational adaptation needs a longer time to be implemented and probably higher investments, on the other hand it considers the city in its many interwoven aspects, with the aim and vision of a better and more liveable city for the future (see fig. 3. Examples of different adaptation approaches and complementary benefits at different water levels due to flooding).

An adaptation plan often needs to combine a *coping approach* with *incremental adaptation* and *transformational adaptation* in order to face the climate change impacts and the specific local and regional conditions. Few cities already implemented adaptation plans combining the three adaptation approaches, however, cities like Copenhagen, Rotterdam, Bologna, the Emscher valley in Germany, Bilbao in Spain, Eferdingen in Austria and some others, are engaged in transformative steps (EEA 2016).

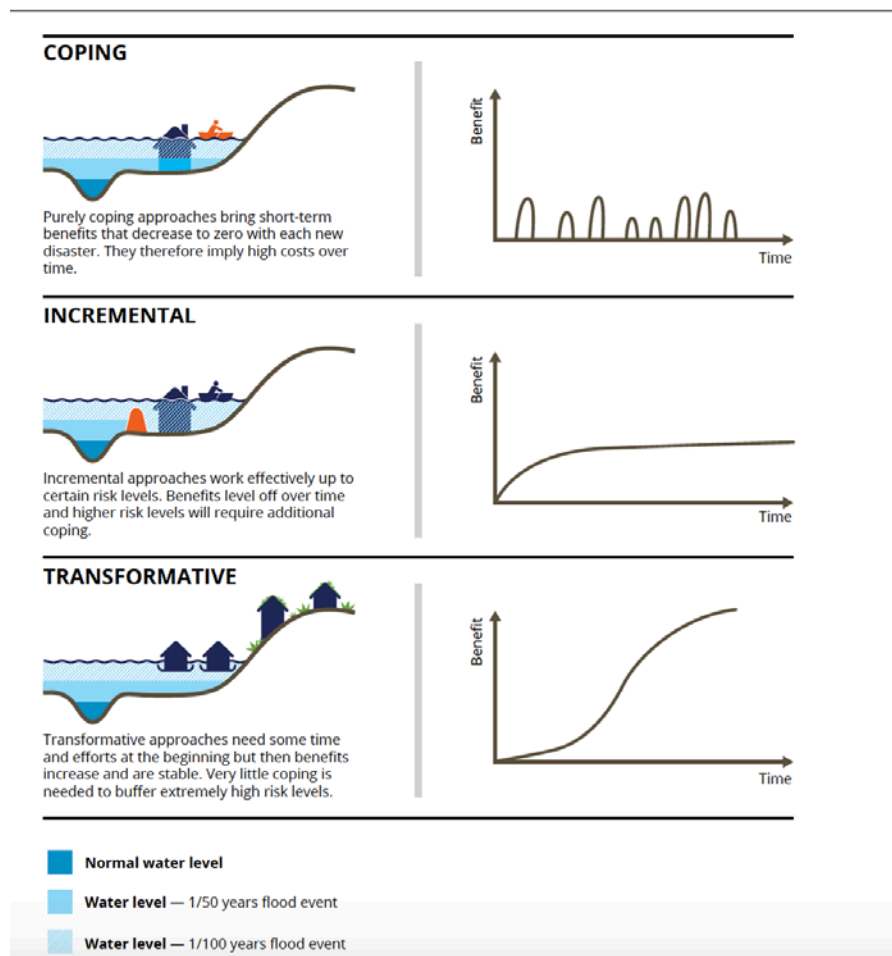


Fig. 3. Examples of different adaptation approaches and complementary benefits at different water levels due to flooding – Source: “*Urban Adaptation to Climate Change in Europe 2016*” (EEA 2016)

5 Adaptation plans and sea level rise

The rising of the sea level is already affecting some European coastal areas, however, its impact, together with the effect of subsidence in some cases, will grow more and more as clearly stated by predictions on global warming and sea level (Neumann et al. 2015) (Stocker 2014). Although adaptation plans at local or national level has been developed for some territories, they generally do not take into account the impact of SLR and subsidence. Adaptation to climate change is a rather new question for cities, thus only few European cities such as Copenhagen and Rotterdam developed wide-ranging and highly visionary plans that include also the impact of SLR. The lack of awareness and knowledge among local authorities, politicians and decision-makers often prevents actions and measures intended to pursue climate adaptation plans that includes the impact of SLR. Although already striking some areas, SLR rise will have a major impact over the years to come (Hallegatte 2013). Local administrations often do not have a clear picture about the assessment on future impacts and vulnerability at local level and are engaged at solving actual issues without a sound vision of the future assets and threats of their city.

An example of a transformational approach related to SLR applied in Europe are the the amphibious houses in Maasbommel in the Netherlands (see fig. 4, 5). Much as 60 % of the country is below sea level, thus The Netherlands has a long history of mitigating flood damage and adapting to flood risk (EEA 2016). Some river floods in the '90s led to a more restrictive legislation and the implementation of a new government programme, *Ruimte voor de Rivier* (room for the river), in 1997. Under the new programme natural flood areas, which could store water temporarily if water levels rose were implemented with a substantial effect on urban developments as permanent buildings were not permitted in flood areas like Maasbommel. A project for houses based on floating foundations was brought about and in 2005 Maasbommel became the first site with amphibious houses. A new approach was pursued instead of the usual flood-resilient infrastructure and a change of attitude has been brought about with an attempt to live with different water levels instead of keeping the water out (Pötz 2014).





Fig. 4, 5 Amphibious houses in Maasbommel in the Netherlands – Source: www.urbangreenbluegrids.com

All over the world experiences and projects dealing with the leverage of sea level are multiplying. At present, they are mostly thought of for hurricanes, flash floods and tsunamis, but these actions are already interpreted as solutions that can be used to adapt to SLR, the main difference being in fact related to time and not to strategies. As examples New York developed a plan to enhance coastal resiliency producing a sort of manual for retrofitting buildings for flood risk, mainly intended for flash floods, but also useful in case of SLR impact (The City of New York 2014); Miami is facing the problem of SLR and subsidence and already developed incremental transformation solutions in order to adapt (City of Miami Beach 2015) (Miami-Dade County 2016); Vancouver developed the research “*A Public Engagement Toolkit for Sea Level Rise*” (Barisky 2015) about climate communication best practice as well as policy directions from the Greenest City 2020 Action Plan and the City’s 2012 Climate Adaptation Strategy with the aim of involving people and deliver climate change messages emphasizing solutions as well as the benefits of action, and offering the community a meaningful role in the action to address the problem.

6 Conclusions

In general, the impact of SLR and subsidence appears to be underestimated and needs to be addressed in a systemic way. Their impact as well as the vulnerability of the coastal cities requires to be effectively examined and integrated in the city’s planning system in order to lessen the impacts on the local economy, society, nature, biodiversity, water resources and human health. Some municipalities are already well-equipped to involve the local community on standard planning issues, however the specific challenge of SLR calls for planners to develop innovative tools and strategies to be effective. Many coastal cities areas are just beginning to experience the impact of the rising sea level, this time lapse allows to foresee the best adaptation strategies tackling the climate change impacts not only by the approaches of coping and incremental adaptation, but addressing the systemic character of climate change through long-term solutions aiming at transformative adaptation. There is a need for more integrated management planning in order to address the rising of the sea level and subsidence.

References

- Barisky, T. and Sustainability Group, City of Vancouver (2015). A Public Engagement Toolkit for Sea Level Rise.
- City of Miami Beach (2015). Miami Beach Sea Level Resiliency.
- EEA (2016). Urban Adaptation to Climate Change in Europe 2016: Transforming Cities in a Changing Climate. Luxembourg: Publications Office, European Environment Agency.
- EEA (2016a). The European Environment — State and Outlook 2015 (SOER 2015), European Environment Agency.
- EEA (2017). Climate Change, Impacts and Vulnerability in Europe 2016: An Indicator-Based Report, European Environment Agency.
- Hallegatte, S., Green C., Nicholls R. J., and Corfee-Morlot. J. (2013). Future Flood Losses in Major Coastal Cities. *Nature Climate Change* 3 (9): 802–6. doi:10.1038/nclimate1979.
- Horton, B. P., Rahmstorf S., Engelhart S. E. and Kemp A. C. (2014). Expert Assessment of Sea-Level Rise by AD 2100 and AD 2300. *Quaternary Science Reviews* 84 (January): 1–6.
- Miami-Dade County (2016). Assessment of Available Tools to Create a More Resilient Transport System - Final Report in Support of the Sea Level Rise Task Force Comm. Resolution R-235-16.
- NOAA - National Oceanic and Atmospheric Administration (2017). Global and Regional Sea Level Rise Scenarios for the United States.
- Neumann, B., Vafeidis A. T., Zimmermann J., and Nicholls R. J. (2015). Future Coastal Population Growth and Exposure to Sea-Level Rise and Coastal Flooding - A Global Assessment. Edited by Lalit Kumar. *PLOS ONE* 10 (3): e0118571.
- Perks, J., Horrocks L., and Ricardo-AEA Ltd. (2011). Adaptation Strategies for European Cities - Report for EC Directorate of Climate Action.
- Pötz, H., Anholts T., and de Koning M. (2014). Multi-Level Safety: Water Resilient Urban and Building Design. Amersfoort: STOWA.
- Stocker, T., ed. (2014). Climate Change 2013: The Physical Science Basis: Working Group I Contribution to the Fifth Assessment Report of the Intergovernmental Panel on Climate Change. New York: Cambridge University Press.
- The City of New York, and Department of city planning (2014). Coastal Climate Resiliency - Retrofitting Buildings for Flood Risk.
- UN-Habitat (2016). Urbanization and Development: Emerging Futures. World Cities Report 2016. Nairobi, Kenya: UN-Habitat.
- Weltbank (2013). Turn down the Heat Climate Extremes, Regional Impacts, and the Case for Resilience. Washington, DC: World Bank.
- Zecca, A., and Chiari L. (2012). Lower Bounds to Future Sea-Level Rise. *Global and Planetary Change* 98–99 (December): 1–5. doi:10.1016/j.gloplacha.2012.08.00.

Nature-based stormwater strategies and urban environmental quality

P. Sabbion, M. Canepa

Department of Architecture and Design (DAD), University of Genoa, Italy

Corresponding author: Paola Sabbion, paola.sabbion@unige.it

Abstract

Healthy hydrological systems control stormwater runoff, allow for groundwater recharge, and provide water quality. On the contrary, today in urban environments impervious surfaces have increased stormwater runoff, affecting ecosystems and leading to hydrogeological instability and flooding risks. In particular, development and climate change affect water resources in terms of quantity and quality, altering the functions of many ecosystems with a negative effect also on well-being of people. Mitigation and adaptation strategies, which limit the effects of climate change and resource consumption, are crucial to achieve sustainable development in cities and improve environmental quality. The implementation of vegetated green and blue infrastructure (GBI) at city-scale is a key action to this process. It is necessary to examine this issue under three priority areas: the technical-scientific adaptation to new strategies and innovations in progress, the regulatory simplification of the territory governance, and the finding of economic resources.

1 Introduction

Many countries in the world are facing the challenge of managing their impact on the environment, especially in urban areas, trying to improve its quality and dealing with the aging of infrastructure. In any urban areas different components are involved, in particular the water system, providing water supply, sanitation, and drainage services (Mitchell, 2006). The aim is making cities more sustainable and healthy, involving economic viability, social stability, and wise use of resources while protecting and nourishing the natural environment (Leitmann 1999). In particular, water management has a central role in the sustainability of our cities.

In fact, one of the fundamental function of a healthy hydrological system is to retain water, allowing for stormwater runoff regulation and groundwater recharge. The natural water cycle entails rain permeating into the ground and gradually filtering into rivers and groundwater. Land covered with vegetation has a typical sponge effect. On the contrary, impervious urban surfaces increase stormwater runoff. Water tends to flow faster due to lower permeability, causing the quantity and rate of surface runoff to increase and sometimes hydrogeological instability and flooding risk (Shuster et al., 2005).

During the last decades, with the aim to increasing water cycle sustainability, a transition from conventional engineering-based water management to eco-system preservation and restoration has occurred. New approaches pursue the restoration of structures typical of undeveloped catchment areas, shifting from water drainage to slower flows and an increased permeability. This leads to a reduction of stormwater runoff, exploiting the integration of green and blue techniques as infiltration, vegetative uptake and evapotranspiration.

Conventional stormwater management approaches have often failed to pursue environmental preservation due to the incapacity to address the variations to the flow regime caused by conventional drainage. In many cities (i.e., New York, U.S.) during heavy rainstorms combined sewers can receive high flows that treatment plants are unable to handle. The mix of stormwater and untreated wastewater discharges directly into the waterways, causing combined sewer overflows (CSOs). Aside from this particular issue, water coming into contact with anthropic surfaces always collects toxic substances

and pollutants that have a negative impact on ecosystems and fluvial and marine coasts. This explains why the reduction of the ecological quality of water is an emerging issue worldwide. In Europe, European regulations have established that it is urgent to “ensure that the good status of surface water and groundwater is achieved and that deterioration in the status of waters is prevented” (European Parliament, 2000), similar to the provisions of Clean Water Act (CWA) in U.S.

In order to focus on the role of nature-based stormwater strategies on urban environmental quality, this paper recognises different aspects of urban water system issues and solutions. The aim of the study underlines the need to integrate different approaches in urban water system planning, considering provision and management aspects.

2 Green and blue infrastructure implementation advantages

The 2013 European Commission Communication, Green Infrastructure (GI), Enhancing Europe's Natural Capital, states that GI is strategically designed and managed to provide ecosystem services (ES) on a wide scale. Green and blue infrastructure (GBI) includes natural, semi-natural, and artificial networks of multifunctional ecological systems related to urban areas (Tzoulas *et al.*, 2007). It can help stormwater management, decreasing untreated water loads on conventional sewage systems and the impact of metropolitan areas on water bodies pollution. It features waterways, wetlands, woodlands, wildlife habitats, greenways, parks, and other natural areas, which contribute to the health and quality of life for communities and people (Benedict and McMahon, 2001; Benedict *et al.*, 2006; European Commission, 2010).

Multifunctionality is among the most interesting outcomes of GBI. Environmental co-benefits comprise biodiversity conservation and climate change adaptation; social benefits include water drainage and creation of green spaces (EEA, 2015). Nature-based solutions can provide greater sustainable, cost-effective, multi-purpose and flexible alternatives than traditional grey infrastructure (European Commission, 2015). GBI also provides economic benefits creating job and business opportunities in fields such as landscape management, recreational activities, and tourism. It can stimulate retail sales and commercial vitality as well as other economic activities in local business districts due to the value of ES (Rouse, 2013). GBI can help to preserve or increase property values, attract visitors, residents, and business to a community, reducing energy consumption, healthcare, and related costs.

Ecosystems can inspire culture, art and design and contribute to the sense of place. Supporting a network of regional parks, trails, foreshores and waterways, GBI can enhance the health benefits stemming from the access to natural areas, which have been driven by relevant economic investments. Terrestrial ecosystems provide a number of vital services to people and society, including biodiversity, food, water resources, carbon sequestration, and recreation. The future capability of ecosystems to provide these services is determined by changes in socioeconomic characteristics, land use, biodiversity, atmospheric composition, and climate (Costanza *et al.*, 1992; Metzger *et al.*, 2006). The importance of the services provided by ecosystems for human well-being seems most evident in cities, as urban centres depend on a healthy natural environment that continuously offers a range of benefits, known as ES, including drinking water, clean air, healthy food, and protection against floods (TEEB, 2011).

According to the urban ecology approach, cities should be considered as ecological systems. Green areas, in fact, play a crucial role and their interconnection is crucial despite being often regarded as separate from human activities (Benedict *et al.*, 2006; van Bueren, 2012). A water sensitive planning and design should thus include urban layout and landscaping, considering nonconventional water sources including roofs runoff, stormwater, greywater and wastewater, controlling and preventing pollution, stormwater flow and quality management. Sometimes it can use a mixtures of soft (ecological) and hard (infrastructure) technologies; and, according with Mitchell (2006), non-structural tools such as education, pricing incentives, regulations, and restriction regimes.

3 Results

Approaches and strategies for GBI implementation are emerging in different countries and at various scales: stormwater Best Management Practices (BMPs) and Low Impact Development (LID) in U.S., Sustainable Urban Drainage Systems (SuDS) in UK and water sensitive urban design (WSUD) in Australia. These concepts tend to integrate green and blue infrastructure (GBI) with urban planning and flood risk management. This strategies recognises the need to shift from traditional control solutions based on centralised storage and water distribution to new approaches, which focus on lower-risk areas, local collection and distribution, slower flows, and increased permeability. BMPs, developed mainly in the United States, include non-structural measures for development planning and structural measures focused on stormwater treatment components (for volume, speed and quality control). WSUDs, spread in Australia and England, also aims to minimise the impact of developed areas preventing flood risk, limiting water consumption and enhancing environmental protection. In the United States and Canada, LID offers design strategies to curb runoff and deliver small-scale structural practices to imitate predevelopment hydrology through infiltration, evapotranspiration, filtration and detention processes. Sustainable Drainage System guidelines, the most disseminated in Europe, cope with impervious surfaces to achieve water quality, amenity, biodiversity, prioritising flood prevention and source control.

The U.S. Environmental Protection Agency provides cities with local municipal grants, along with technical support in order to implement GBI (EPA, 2011). In Japan researchers developed models, and conducted longitudinal field studies in which they measured the regulating effect of retention, detention and infiltration on the volume and discharge of runoff. The Government of British Columbia in Canada adopted an approach to stormwater management: agree that stormwater is a resource (ADAPT), planning at four scales – regional, watershed, neighbourhood and site – a simulation model was developed and subsequently adopted by all Canadian Provinces for evaluation of planning alternatives (Carmon *et al.*, 2010). In GB the British Construction Industry Research and Information Association (CIRIA) turned from sustainable drainage to sustainable water (and wastewater) management in connection with land-use planning, taking into account social, economic and environmental aspects (Carmon *et al.*, 2010).

GBI incorporation not only enhances the capacity of these cities to supply water and prevent flooding, but also provides health benefits and a better quality of life. There are several cities, around the world, where trans-disciplinary conservation of urban ES and water management are the foundation of urban design. This approach has been adopted over 20 years ago in Portland (Oregon): here catchment-scale green infrastructure, green streets, flood management, river restoration and wastewater services are integrated to deliver improved flood management and water supply. In Malmo (Sweden), the regeneration of the Augustenborg neighbourhood was at first driven by flood risk management (Kazmierczak and Carter, 2010), and the presence of green infrastructure has also improved the liveability of the city's open spaces.

Several tools aim to include GBI in urban areas and estimate their effects. For example, in Miami (U.S.) the CITYgreen tool systematically includes GBI such as parks, urban forests and wetlands into urban planning (TEEB, 2011; Förster, 2011). The ES provided in Miami relate mainly to stormwater protection, air and water quality improvement and climate regulation (i.e., all regulation services).

GBI proves to be so effective thanks to vegetation performing a number of hydrologic functions within the natural water cycle. For this reason, vegetation has become an important component of the Water Sensitive Urban Design (WSUD) strategies in Australia and of the Best Management Practices (BMPs) and Low Impact Development (LID) in the United States. These systems and related guidelines seek to replicate the natural water cycle in urban areas. Hydrologic functions provided by trees and plants are canopy interception, stemflow, soil infiltration, evapotranspiration, hydraulic lift/redistribution, groundwater recharge, and conveyance of large storms. Water quality can similarly be improved by natural systems filtering pollutants (Benedict and McMahon, 2001). Vegetation plays an important role with regard to biofiltration, as it enhances the capacity of soils to remove pollutants through a combination of biological, chemical, and physical processes (Riser-Roberts, 1998; Pilon-

Smits, 2005). All these benefits can restore the ecological condition of urban rivers reduce overflow and flood risk, and increase water quality to enhance and protect biodiversity.

4 Policy, management and social aspects

Stormwater management objectives are included in the UE Climate Change Adaptation Strategy for Urban Settlements, which includes the development of Climate Resilience Studies, assessing the expected impacts. Tools that are embedded into neighbourhood-scale plans and sustainability initiatives to assess their performance, including the Ecocity initiative in Europe and the EcoDistricts Toolkit in the U.S., projects aimed at identifying strategies for sustainable urban development.

In addition, a worldwide programme, called C40 Cities Climate Leadership Group is implemented in more than 80 of the world's megacities. This program is focused on tackling climate change and driving urban action to reduce greenhouse gas emissions and climate risks (C40 Cities, 2016). The European Union (EU) recently highlighted the importance of water policies. EU has established a series of Policies regarding water to achieve these objectives and has devised regulating strategies also to tackle climate change effects. These include the Directive 2013/39/EU of the European Parliament and of the Council, amending the Water Framework Directive 2000/60/EC (European Parliament, 2000) and the Directive on environmental quality standards in the field of water policy (2008/105/EC). GBI is among the main strategies implemented for urban sustainability. They are crucial for their capacity to incorporate and integrate different GBI BMP features.

In fact, it is possible to distinguish two categories of BMPs: non-structural BMPs and structural BMPs. Non-structural BMPs include normative, regulatory, and educational guidelines for land-use planning to limit the conversion of rain in runoff, with subsequent impacts on the territory. These solutions are identified with Stormwater Better Site Design Practices, precisely because they are applied at a planning phase, in particular for new developments. Structural BMPs, instead, are focused on strategies and techniques for stormwater treatment at the beginning of the drainage system to intercept the rainfall on the ground. The main purposes of BMPs include: surface flow speed control; reduction of runoff volume from urbanised areas; and reduction of pollutant and contaminant sources.

Greenways and open spaces can incorporate and connect BMP features for the mitigation of environmental impacts associated with runoff (Perini and Sabbion, 2017). These practices may create a hydrologic regime more similar to pre-development conditions, where total runoff volume is reduced through infiltration and storage (consequently reducing the impact of urban impervious surfaces on rivers) (Davis *et al.*, 2012). Treatment BMPs are of particular interest since they provide connections among GBI. They can include vegetative biofilters (Filter Strip - Buffer Strip - Wet and Dry Vegetated Swales - Bioretention/Rain gardens), infiltration systems (Permeable Pavements - Infiltration Trench - Infiltration Pond - Bioretention/Rain gardens), and ponds (Detention and Retention basins - Dry Extended Detention Basin - Wet Retention Pond - Wetland Pond).

According to European provisions, the Member States, should be focusing on prevention: "Flood risk management plans should take into account the particular characteristics of the areas they cover and provide for tailored solutions according to the needs and priorities of those areas", including "the promotion of sustainable land use practices, improvement of water retention as well as the controlled flooding" (European Parliament and Council of the European Union, 2007). For this reason, EU is currently planning the future research programme Horizon2020 (2014-2020) as a way to increase Member States' efforts to map and assess ecosystems and their services. In the UK the concept that urban environments need to adapt to climate change effects, producing water sensitive cities, has led to the promotion of Blue-Green Flood Risk Management approaches and the implementation of green infrastructure to restore the natural water-cycle (Everett and Lamond, 2014).

Every Member State is required to integrate EU directives in its specific policies, developing and implementing national strategies of governance to attain the required obligations. Therefore, the normative framework of Member States can vary significantly and can have a great impact on the effectiveness and flexibility of territorial management tools (Giachetta, 2013).

Moreover, administrative bodies should never forget the role of local communities in the implementation of GBI. Bottom-up initiatives can in fact improve critical environmental conditions in

urban areas. Local participation especially in the United States is based on a deep-rooted tradition, community organisations and activist involvement. Interesting bottom-up initiatives supporting GBI implementation are based in biggest cities to counteract also social deprivation (Cohen, 2008). The result of local communities' struggles against environmental threats are often effective also against health disparities and the lack of social and political capital. In Europe, traditionally top-down oriented, planning practices are slowly but gradually including community efforts, dealing with water resource management and flood risk.

5 Conclusions and discussions

A number of studies have proved that stormwater management components such as permeable pavements, vegetated swales, rain gardens, and landscaping are very effective to reduce runoff (50-95% average) and pollutants (30-99%). Stormwater floods are often the result of episodes, perhaps singularly of small size, but overall decisive. Considering these results, nature-based stormwater treatment strategies are something that should be among the priorities of the city administrations and which can no longer be postponed.

Therefore, it is necessary to promote land management culture and intervention policy, according with wider strategies (from high scale infrastructural to targeted micro-interventions) in densely constructed area. Best Management Practices should include non-structural measures for development planning and structural measures focused on stormwater treatment components (for volume, speed and quality control).

A water sensitive city includes the concept of resilience to extreme climatic events and climate change plays a key role and represents the interaction between different branches of water science, engineering, and other domains such as urban planning and design. In this context, we consider resilience as the ability of a system to cope with or recover from flooding and droughts and also to retain original identity in some form in the face of long-term change (Rodriguez *et al.*, 2014). Water quality in cities thus is challenge for more sustainable and more liveable cities worldwide.

References

- Benedict, M. A., McMahon, E. T. and Conservation Fund. (2006). *Green infrastructure: linking landscapes and communities*. Washington, DC: Island Press.
- C40 Cities. (2016). C40 Cities. [Online]. Available at: <http://www.c40.org/> [Accessed: 7 June 2016].
- Carmon, N., Shamir, U. (2010). *Water-sensitive planning: integrating water considerations into urban and regional planning*[Online]. Available at: doi:10.1111/j.1747-6593.2009.00172.x [Accessed: 5 December 2016].
- Costanza, R., Norton, B. G. and Haskell, B. D. (1992). *Ecosystem health: new goals for environmental management*. Washington, D.C.: Island Press.
- Cohen, S. (2008). *Sustainable South Bronx: Helping the Bronx Become a Sustainable Community*. New York Observer. [Online]. Available at: <http://observer.com/2008/06/sustainable-south-bronx-helping-the-bronx-become-a-sustainable-community/> [Accessed: 2 April 2014].
- EPA. (2011). *Land Revitalization Fact Sheet Green Infrastructure*. [Online]. Available at: http://www.epa.gov/landrevitalization/download/fs_green_infrastructure.pdf.
- Everett, G. and Lamond, J. (2014). A conceptual framework for understanding behaviours and attitudes around 'Blue-Green' approaches to Flood-Risk Management. In: 18 June 2014, p.101–112. [Online]. Available at: doi:10.2495/FRIAR140091 [Accessed: 15 December 2015].

- European Commission. (2010). Green infrastructure. [Online]. Available at: <http://ec.europa.eu/environment/nature/info/pubs/docs/greeninfrastructure.pdf>.
- European Commission. (2015). Nature-Based Solutions | Environment - Research & Innovation. [Online]. Available at: <https://ec.europa.eu/research/environment/index.cfm?pg=nbs> [Accessed: 10 December 2015].
- European Parliament. (2000). Directive 2000/60/EC of the European Parliament and of the Council of 23 October 2000 establishing a framework for Community action in the field of water policy.
- European Parliament and Council of the European Union. (2007). Directive 2007/60/EC of the European Parliament and of the Council of 23 October 2007 on the assessment and management of flood risks.
- Förster, J. (2011). Multiple benefits of urban ecosystems: spatial planning in Miami, USA. In: *TEEB Manual for cities: ecosystem services in urban management*. [Online]. Available at: TEEBweb.org.
- Giachetta, A. (2013). Diffusion of Sustainable Construction Practices. A Case of International Cooperation. *Open Journal of Energy Efficiency*, 02 (01), p.46–52. [Online]. Available at: [doi:10.4236/ojee.2013.21008](https://doi.org/10.4236/ojee.2013.21008) [Accessed: 22 January 2014].
- Kazmierczak, A. and Carter, J. (2010). Adaptation to climate change using green and blue infrastructure. A database of case studies. [Online]. Available at: http://orca.cf.ac.uk/64906/1/Database_Final_no_hyperlinks.pdf [Accessed: 15 December 2015].
- Leitmann, J. (1999). *Sustaining cities: environmental planning and management in urban design*. McGraw-Hill, USA.
- Metzger, M. J., Rounsevell, M. D. A., Acosta-Michlik, L., Leemans, R. and Schröter, D. (2006). The vulnerability of ecosystem services to land use change. *Agriculture, Ecosystems & Environment*, 114 (1), p.69–85. [Online]. Available at: [doi:10.1016/j.agee.2005.11.025](https://doi.org/10.1016/j.agee.2005.11.025) [Accessed: 22 January 2014].
- Mitchell, V. Grace (2006). *Applying Integrated Urban Water Management Concepts: A Review of Australian Experience* [Online]. Available at: [doi 10.1007/s00267-004-0252-1](https://doi.org/10.1007/s00267-004-0252-1) [Accessed: 5 December 2016].
- Perini, K. and Sabbion, P. (2017). *Urban Sustainability and River Restoration: Green and Blue Infrastructure*. John Wiley & Sons.
- Rouse, D. C. (2013). *Green infrastructure: a landscape approach*. Chicago, IL: American Planning Association.
- Rodriguez, C., Ashley R., Gersonius, B., Rijke, J., Assela, P., Zevenbergen, C. (2014). Incorporation and application of resilience in the context of water-sensitive urban design: linking European and Australian perspectives. [Online]. *WIREs Water* 2014, 1:173–186. doi: 10.1002/wat2.1017.
- Shuster, W. D., Bonta, J., Thurston, H., Warnemuende, E. and Smith, D. R. (2005). Impacts of impervious surface on watershed hydrology: A review. *Urban Water Journal*, 2 (4), p.263–275. [Online]. Available at: [doi:10.1080/15730620500386529](https://doi.org/10.1080/15730620500386529).
- TEEB. (2011). *TEEB Manual for cities: ecosystem services in urban management*. In: UNEP and the European Union (ed.), *The economics of ecosystems and biodiversity. Manual for cities: Ecosystem services in urban management*.

Tzoulas, K., Korpela, K., Venn, S., Yli-Pelkonen, V., Kaźmierczak, A., Niemela, J. and James, P. (2007). Promoting ecosystem and human health in urban areas using Green Infrastructure: A literature review. *Landscape and Urban Planning*, 81 (3), p.167–178. [Online]. Available at: doi:10.1016/j.landurbplan.2007.02.001 [Accessed: 22 January 2014].

HEAT ENERGY DEMAND AND INDOOR COMFORT

An integrated methodology for the simulation of buildings and open spaces interaction to define climate adaptive strategies: the case study of the Duchesca district in Naples, Italy

Eduardo Bassolino, Francesco Scarpati

Department of Architecture, University of Naples Federico II, Italy

Eduardo Bassolino, eduardo.bassolino@unina.it

Francesco Scarpati, francescoscarpati.a@gmail.com

Abstract

The research is motivated by the current shortage of theoretical methods and technological tools to investigate the relationship between the indoor and outdoor microclimates and to anticipate climate changes and their impact on urban environments.

It has been defined a methodology that, making use of appropriate IT tools (ENVI-met, Ecotect Analysis, Grasshopper 3D), and exploiting the interoperability of their outputs, reveals the quantitative and qualitative impact of outdoor environmental conditions on indoor comfort. This goal is achieved by collecting the outputs of different simulations and environmental analyses into a single parametric virtual environment.

The methodological process supports the definition of the urban regeneration project of the Duchesca district in Naples, Italy, showing how climate-adaptive design solutions for outer urban spaces to reduce thermal comfort (PMV) respectively by 61.5% in 2015 and 57.2% in 2050s, to ensure a simultaneous improvement of indoor comfort in the analysed building with a reduction of 80% in 2015 and 74% in 2050s.

1 Introduction

The effects of the current climatic changes, and the rise in the global average temperatures impacts urban environments, resulting in phenomena of microclimatic alterations (UHI, heatwaves, etc.) which ultimately lead to thermal discomfort and health problems for the users. The low adaptability (in terms of performances) of buildings and open spaces, together with the lack of maintenance and the antiquity of the technical solutions, is making highly urbanized environments critical places to live, especially during the summer season. The tendency of temperatures to increase (RCP 8.5 Scenario, AR5 - IPCC, 2014), in case the scheduled reduction in CO₂ emission (cf. COP21, 2015 United Nations Climate Change Conference. Paris) should not be realized, will have a noticeable impact on urban life, both in open space and in indoor environments.

In this historical period, when the economic reprise is still slow, and when performance retrofit interventions are therefore hard to implement, intervening on open spaces through climate adaptive design for outdoor requalification can turn out to be an effective strategy on improving urban comfort. The enhancement of the environmental conditions in the open space generates effects of microclimatic mitigation, which bring a notable improvement on buildings' performance (namely, on indoor comfort).

As the effects of Climate Change are becoming a central issue in the world politics and the cities management, it is necessary to take them in account into the design process. Moreover, these phenomena have effects both on the outdoor and indoor environments, bringing the designers to the necessity of considering them simultaneously. "Only recently, research communities and professional organisations have started to incorporate the factor of climate change in software-based environmental simulation with a view to inform adaptation planning and design" (Peng and Elwan, 2014). Though, we still assist to a

shortage of theoretical methods and technological tools to investigate the relationship between the indoor and outdoor microclimates and to anticipate climate changes and their impact on urban environments. While it is assured that an improvement of the outer thermos-hygrometric conditions ensures an improvement of the inner ones, few researches, aimed to establish not only the qualitative but the quantitative relation between outdoor and indoor environments, have been conducted (see Peng and Elwan, 2012 and 2014).

2 Forewords and objectives

The only significant case in the previously described filed is the research “An outdoor-indoor coupled simulation framework for Climate Change–conscious Urban Neighbourhood Design”, (Peng and Elwan, 2014), in which, “Utilizing two existing software systems, ENVI-met for urban neighbourhood outdoor simulation and Ecotect for building indoor simulation” it was demonstrated “how a workflow can be implemented to play out climate change scenarios on urban neighbourhoods and the buildings located within” (Peng, Elwan 2014).

On the other hand, the workflow described in “Parametric Environmental Climate Adaptive Design: The Role of Data Design to Control Urban Regeneration Project of Borgo Antignano, Naples” (Ambrosini, Bassolino, 2015), provides an approach that, using different software environments, enables the development of open space optimization solutions for the reduction of the urban Heat Island phenomena, while maintaining that fundamental characteristic of interoperability between data, thanks to the organization of the information in a parametric work environment.

Taking in account the results of these previous studies, the following research is aimed to define a methodology that, making use of appropriate information technology tools, and taking in account the interoperability of their outputs, ensures a simultaneous monitoring between different parametric software environments and the determination of the quantitative and qualitative impact that the outdoor environmental conditions produce on the indoor comfort.

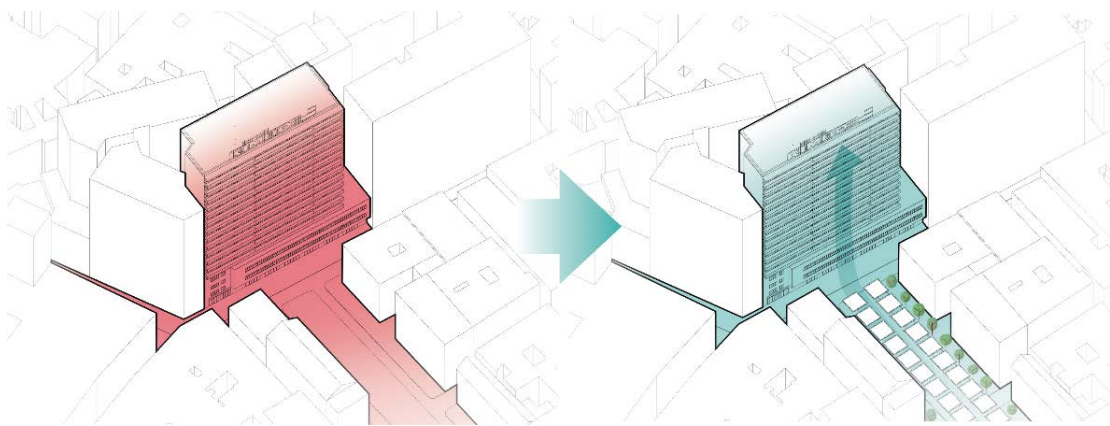


Figure 1. Interaction between outdoor and indoor environments.

3 Definition of the methodological workflow

The specificity of the software that simulate separately outdoor and indoor environments requires the simultaneous use of different tools, with the necessity of exporting and importing different files and then repeat the operation, until the definition of a final solution. In order to overcome the fragmentation of different outputs and files and to ensure the exchange between different software environments, it was decided to use the software environment Rhinoceros 3D and the graphical algorithm editor Grasshopper 3D for parametric modelling, which “provide a platform for data exchange between different software [...] and many Grasshopper’s plug-in” (Bassolino and Ambrosini, 2016).

1. On the other hand, the use of the software ENVI-met for the outdoor comfort simulations allows “to produce simulated urban micro-climate conditions specific to any locations” and “generate localized weather data specific to the building’s immediate outdoor surroundings” (Peng and Elwan, 2014), despite the usual weather files generated by weather station, which are often based on environmental condition different from the ones of the urban assets.

In this way, it is possible to directly relate the outdoor environmental comfort data, produced by ENVI-met, to the indoor comfort analyses, generate in the environment Grasshopper 3D-EnergyPlus thanks to Grasshopper’s plug-ins Ladybug and Honeybee. The possibility of working in a parametric virtual environment ensures the interoperability of the different outputs and to read the results of the analyses on the same model where the design is defined.

The application of the previous defined methodology to a regeneration project of the Duchesca district in Naples, Italy, shows the feasibility of the workflow as integration of the design process.

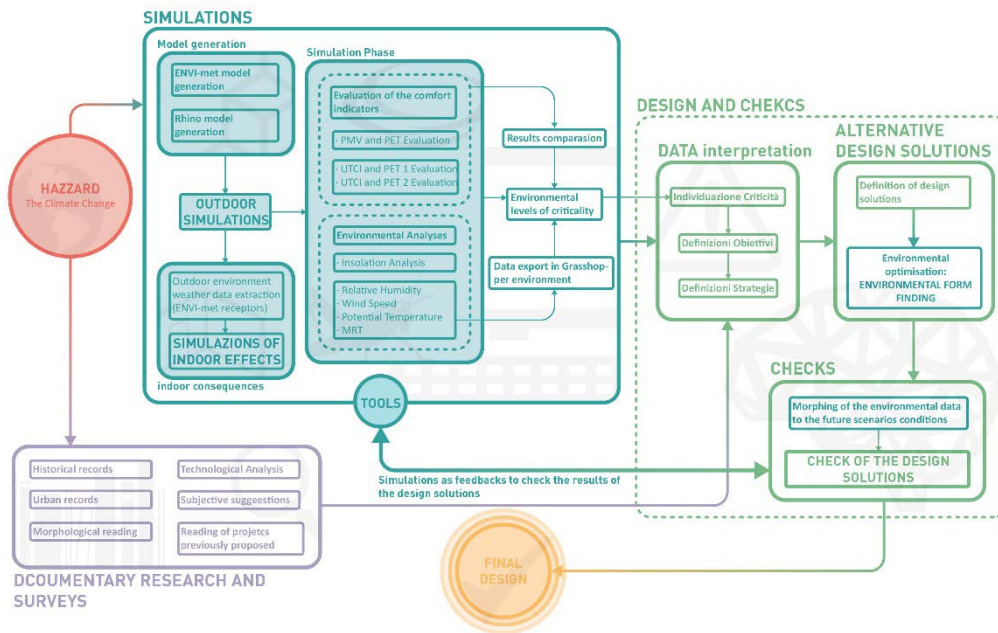


Figure 2. Synoptic flow chart - Definition of the methodological workflow applied.

4 The case study of the Duchesca district in Naples

Modelling the study area

The case study of this research process is the Duchesca district of Naples, an area of the city of Naples the historic centre and the western periphery. Here, the lack of green infrastructure and the dense overbuilding contributed to alter the local microclimate and rise the temperatures. The first step was to create a 3D model of the area, by using the official cartography of the municipality of Naples and surveys *in situ*. The model, which was generated in the Rhinoceros 3D, was used as base for any prior environmental analyses, to simultaneously read the results of outdoor and indoor analyses and to define all the design proposals.

Outdoor microclimate analyses and generation of the local weather file

The second step consisted in the outdoor microclimate simulation of the analysed area, using the holistic simulation software ENVI-met. Once modelled the area in the ENVI-met interface, it has been set up the configuration file for 2015 with: 1) wind speed = 2 m/s; 2) wind direction = 247°; 3) air temperature = 300 K (26.85 °C); 4) relative humidity at 2 m = 47.15%; 5) specific humidity at 2500 m = 2.8731 g/kg;

and, not modifying the data for wind speed and direction, for 2050s with: 1) air temperature = 302.4 K (29.25 °C); 2) relative humidity at 2m = 47.15%; 3) specific humidity at 2500m = 3.3272 g/kg, that are mean values of the 24 hours before the starting time of simulation at 6 am. To determinate the thermal comfort of a generic person, it was considered an adult man, (whose characteristics are: 35 years old, 175 cm high, 75 kg), who is walking at a speed of 0.83 m/s and has an activity of energy exchange of 116 W/m² with the environment and a corresponding clothing factor of 0.5. After that, it was possible to start the simulation, obtaining a large volume of outputs which described the locale microclimate. In particular, the Predicted Mean Vote - PMV (Fangers 1972, UNI-EN-ISO 7730: 1994) and the Mean Radiant Temperature - MRT (UNI-EN-ISO 7726: 1998) indexes showed a critical situation and high summer heat stress with simulated mean values of PMV respectively of 5,87 in 2015 and 6,40 in 2050s and MRT values of 87,9 °C for 2015 and of 88,1 °C for 2050s. By defining an algorithm in Grasshopper, the results of the simulation were import in the Rhinoceros' three-dimensional model, allowing to read the data directly on the surfaces of the model and to generate the data for the Physiologically Equivalent Temperature - PET (Mayer, Höpfe 1987; Höpfe 1999; Matzarakis et al.1999), and specifically obtaining mean values of PET respectively of 43,37 °C in 2015 and 43.90 °C in 2050s.

By placing some “atmospheric receptors” around a specific building, a tabular system, which describes the urban microclimate condition of the specific area, was generated. This data were then converted into a weather file in format .epw by the use of Ecotect's weather tool and EnergyPlus' EP Launch.

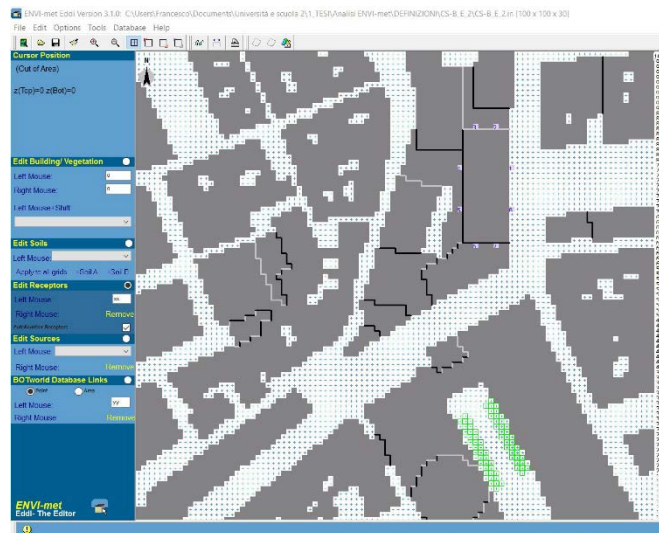


Figure 3. ENVI-met Analyses interface. Set-up of ENVI-met receptors.

Indoor microclimate analyses

The case study chosen for the indoor analyses is the known as “Palazzo Kimbo”, a concrete building of the fifty years surrounded by the analysed context. Basing on the results of some surveys, an apartment type of the chosen building was drawn and modelled in the Rhinoceros environment. The software used for the simulation is EnergyPlus, thanks to Grasshopper's plug-ins Ladybug and Honeybee, which generate a bridge between the different software environment. Once defined EnergyPlus based construction's properties, the energetic model of the indoor environment has been simulated. Instead of defining the single materials of the building's constructions, thanks to some technological surveys, it was possible to just define the single U-values of the technological parts of the building: 1) $U = 1,98 \text{ W/m}^2 \cdot \text{K}$ for the ceiling construction; 2) $U = 1,54 \text{ W/m}^2 \cdot \text{K}$ for the walls construction; 3) $U = 4,08 \text{ W/m}^2 \cdot \text{K}$ for the windows. The weather file used for these simulation is the one generated through ENVI-met data. The reading of the PMV, MRT and PET indexes once again reveals a situation of high summer stress (respectably of the PMV of 1,50 in 2015 and 2,30 in 2050s, for MRT of 30,60 °C in 2015 and 31,50 °C in 2050s and 31,1 °C in 2015 and 33,00 °C in 2050s for PET), as consequence of the constructive characteristics of the simulated environment and of the outer local microclimate.

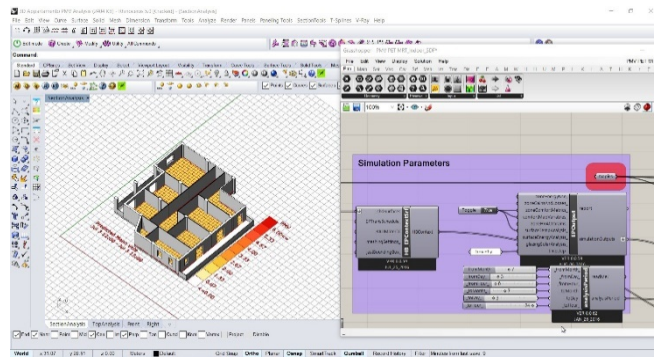


Figure 3. Indoor Simulation in Rhino-Grasshopper environment.

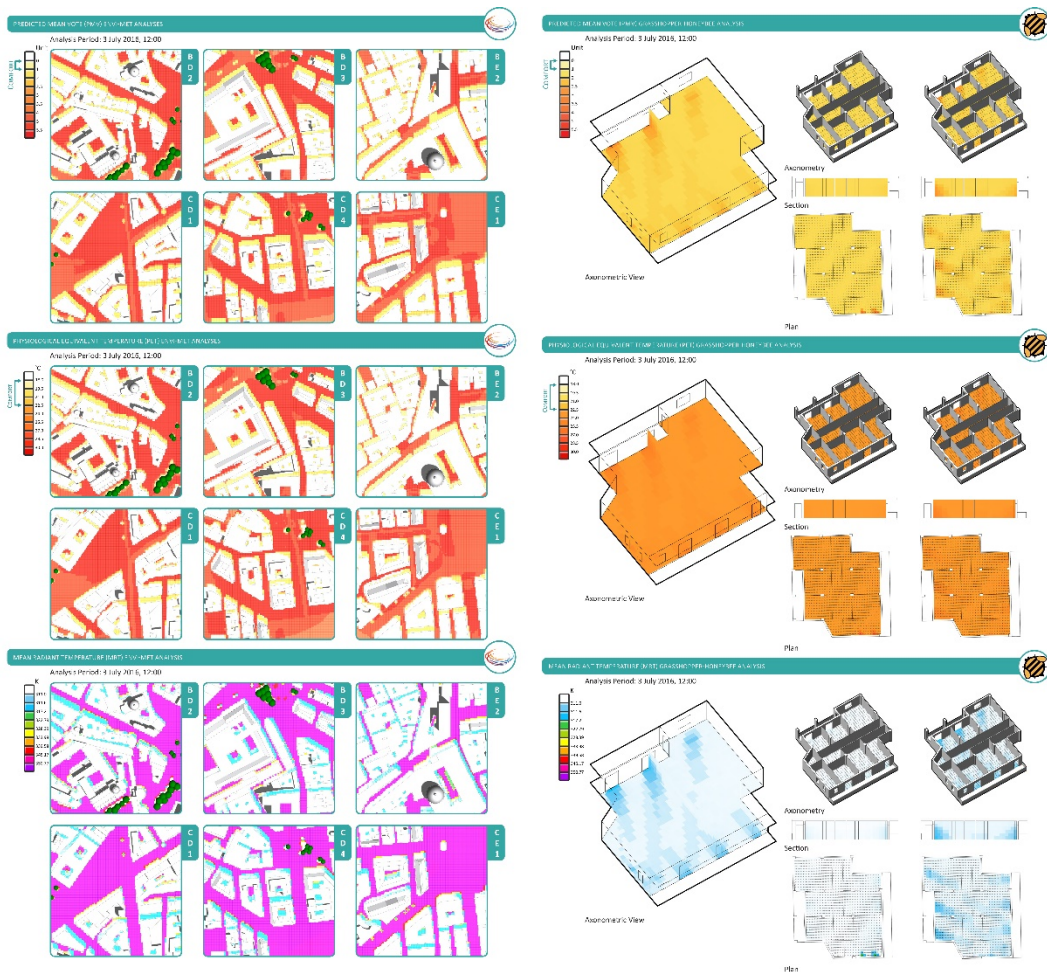


Figure 4. Outdoor and indoor environmental comfort index analysed at the starting conditions in 2015.

Iteration of the process and definition of the final solution

By iterating the previous process for any design proposal, a solution, which contributes to increase the outdoor and indoor comfort condition, could be found. For each proposal, a different weather file was generated, so that the indoor analyses was directly related to the outer improvements. In the final solution, in particular, it was noticed that the reduction of PMV index in the outdoor environment contributes to a consequential decrease of the inner comfort index, without intervening on the built construction. The same circumstance was also highlighted by the index MRT and PET. The values of the previous index

are contained in Table 1 (as regards the outer space) and in Table 1 (for what concerns the inner environment).

Table 1. Results of the outdoor environmental comfort analyses .

	Outdoor comfort index			
	Before		After	
	2015	2050s	2015	2050
PMV	5,87	6,40	2,5	2,74
MRT	87,90 °C	88,10 °C	44,90 °C	45,42 °C
PET	43,37 °C	43,90 °C	30,16 °C	39 °C

Table 2. Results of the indoor environmental comfort analyses.

	Indoor comfort index			
	Before		After	
	2015	2050s	2015	2050
PMV	1,50	2,30	0,3	0,6
MRT	30,60 °C	31,50 °C	26,90 °C	27,40 °C
PET	31,10 °C	33,00 °C	27,60 °C	28,10 °C

Thus, the possibility of working in a parametric environment and to read the results directly on the surfaces of the model guarantees an immediate and better understanding of the relation between indoor and outdoor environment and of the effect that outer conditions produce on the inner space.

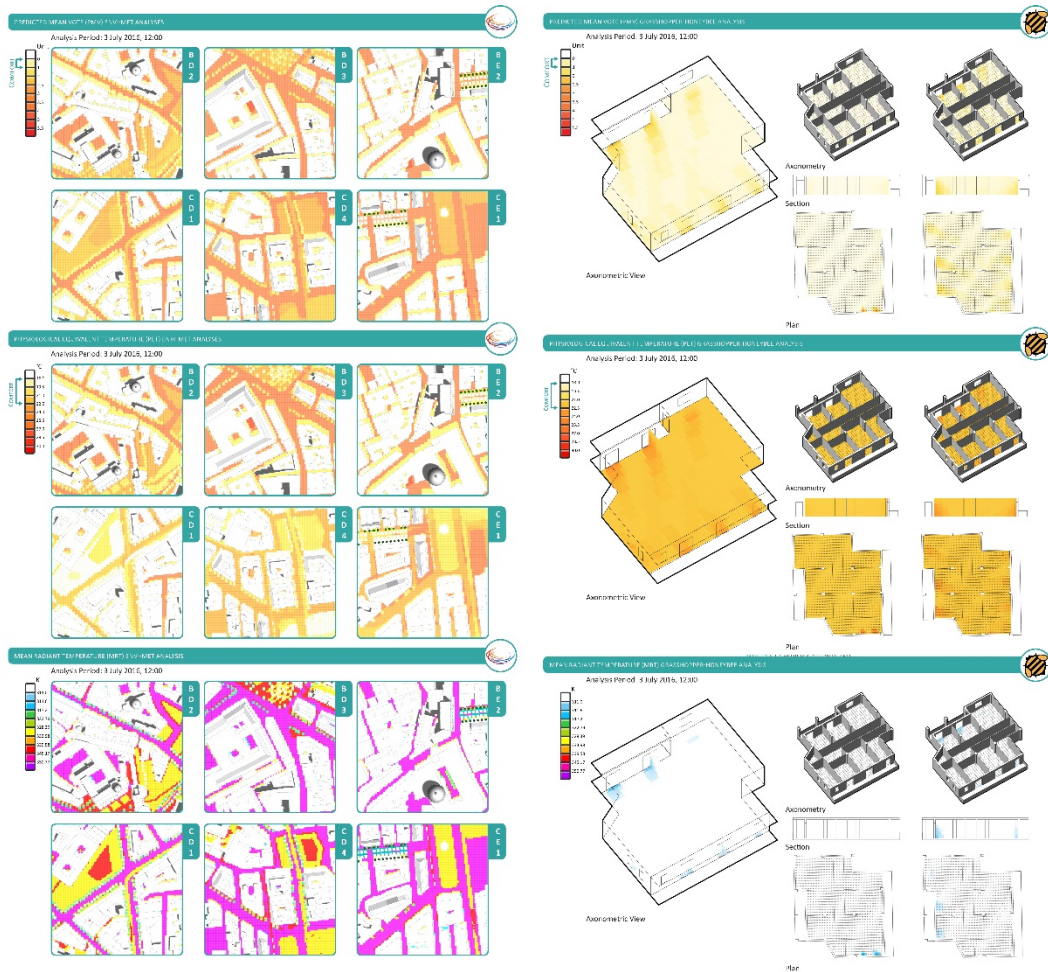


Figure 5. Outdoor and indoor environmental comfort index analysed at the final solution conditions in 2015.

5 Conclusion

The results obtained from the iterative simulation process between outdoor and indoor (both in the current scenario and in the prospective future scenario) highlighted a reduction of the PMV values of 61.5% in 2015 and of 57.2% in 2050s, of the MRT values 49.0% in 2015 and of 48.5% in 2050s and PET values 30.0% in 2015 and of 11.2% in 2050s for the outdoor environment, while a reduction of the PMV values of 80% in 2015 and 74% in 2050, of the MRT values 11.5% in 2015 and of 14.0% in 2050s and of the PET values 12.0% in 2015 and of 16.0% in 2050s were obtained for the indoor simulation.

Those results were obtained by the regeneration of the surrounding area around the analysed building with adaptive strategies aimed to reduce perceived thermal comfort and finalized to a significant improvement of outdoor comfort conditions. The permeability of soils was raised by increasing permeable pavers and green areas, which reached the 30% of the whole horizontal surfaces. Trees and rain garden systems were placed to avoid urban flooding and increase shadowed areas. Similar effects were obtained through the installation of shelters and artificial tree structures, which guaranteed control of solar radiation and wind factor. The thermal load on urban surfaces was reduced using cool pavers, with high albedo values.

The application of an iterative simulation methodology outdoor-indoor to the project for the requalification of the Duchesca district shows the validity of computational design and of data exchange across different IT tools, but most importantly it shows the real benefits of a *climate adaptive design*

approach, as well as its social and economic feasibility. The project proposal for the open space can guarantee, by itself, an actual improvement of the indoor environmental conditions to the surrounding buildings, making up for the lack of initiatives for requalification, and improve the urban comfort conditions, also in view of future climatic scenarios.



Figure 6. Synthesis of the main adaptive design strategies applied in the project.

References

- Ambrosini, L., Bassolino E. (2016). Parametric Environmental Climate Adaptive Design: The Role of Data Design to Control Urban Regeneration Project of Borgo Antignano, Naples. *Procedia - Social and Behavioral Sciences* **216**, 948–959.
- Fanger, P. O. (1982), *Thermal Comfort. Analysis and Application in Environment Engineering*. McGraw Hill Book Company, New York.
- IPCC (2014), Working Group III to the Fifth Assessment Report of the Intergovernmental Panel on Climate Change, *Climate Change 2014 - Mitigation of Climate Change*. Cambridge University Press, Cambridge and New York.
- ISO - International Organization for Standardization (1994), ISO 7730/1994 - Determination of the PMV and PPD indices and specification of the conditions for thermal comfort.
- ISO - International Organization for Standardization (1999), ISO 7726:1998 - Ergonomics of the thermal environment -- Instruments for measuring physical quantities.
- Losasso M., D'Ambrosio V. (2014). Progetto ambientale e riqualificazione dello spazio pubblico: il grande progetto per il centro storico di Napoli sito Unesco. *Technè - Journal of Technology for Architecture and Environment*, a. VI, 7, 64–74.

Peng C., Elwan A.F.A (2012), Bridging Outdoor and Indoor Environmental Simulation for Assessing and Aiding Sustainable Urban Neighbourhood Design. *ArchNet-IJAR: International Journal of Architectural Research* 6-3, pp. 72-90.

Peng, C., Elwan A.F.A. (2014). An outdoor-indoor coupled simulation framework for climate Change-conscious urban neighborhood design. *Simulation* 90, pp. 874–891.

Ratti C., Claudel M. (2014). *Architettura open source. Verso una progettazione aperta*. Einaudi, Turin.

Ratti C., Mattei M. G. (2013). *Smart city, smart citizen. Meet the media guru*. EGEA, Milano.

Tedeschi A. (2011). *Architettura parametrica: introduzione a Grasshopper*. La Pensur, Naples.

Tedeschi A. (2014). *Algorithms-aided design: parametric strategies using Grasshopper*. La Pensur, Naples.

Designing and Evaluating District Heating Networks with Simulation Based Urban Planning

I. Bratov¹, C. Bonnet², A. Chokhachian², G. Schubert¹, F. Petzold¹, T. Auer²

¹Chair for Architecture Informatics

²Chair of Building Technology and Climate Responsive Design
Faculty of Architecture, Technical University of Munich, Germany
Corresponding author: ivan.bratov@ai.ar.tum.de, cecile.bonnet@tum.de

Abstract

The integration of energy and indoor comfort aspects into the early stage of urban planning is essential to conceive energy efficient urban structures and to avoid expensive compensation measures in the later building design. This could end up with increased insulation levels, complex air conditioning systems as well as increased energy demand during the building usage or inefficient energy supply concepts. Besides indoor comfort and the energy demand for heating, cooling, ventilation and daylight, energy supply options based on district heating (or cooling), have to be considered in an early stage of design as they may constitute highly efficient alternatives with respect to building specific heating units. Incidentally, this sub-project is part of the project titled Collaborative Design Platform (CDP) which is a computer based real time tool for urban development in early stages of design decision making. Referring to a subproject intending to integrate different energy aspects into the CDP, the paper concentrates on district heating networks (DHN). The objective of this study is to evaluate the possibilities of implementing a new plug-in in the early stage of urban development in order to design and evaluate the adequacy of district heating networks.

1 Introduction

In recent decades, District Heating Networks have found large improvements both in practice and modeling. The main advantages of district heating networks are the reduction of pollutant and thermal emissions in the city area as well as increasing the safety, due to the absence of combustion systems at the final users of thermal energy. For the same reason also the transportation of fuel in the city area can be significantly reduced by the use of district heating networks. In this scenario, the district heating allows to achieve high conversion efficiencies by centralizing in few large power plants the need of thermal energy in household sector (Ancona, Bianchi, Branchini, & Melino, 2014). In order to improve the operation of district heating systems, it is necessary for the energy companies to have reliable optimization routines, both computerized and manual, implemented in their organizations. However, before a development plan for the heat-producing units can be constructed, a prediction of the heat demand first needs to be determined (Dotzauer, 2002). This fact is also necessary in the early stages of urban planning where the rough idea of street networks, accessibilities and building massing are sketched, however in that scale it is not easy to find a tool which is able to simulate and give feedback in real time to iterate several alternatives through the urban design and planning decision making processes.

It is already being proved that the simulation of the urban models including the district heating network (DHN) system is possible to be coupled with an optimization algorithm in order to illustrate the potential of such an approach for determining the optimal solution or a set of near-optimal solutions for a very complex system synthesis and design (Curti, von Spakovsky, & Favrat, 2000). Nevertheless, extending the idea of optimization and decision making methods into early stages of urban design needs more exploration. One of the recent developments that enables the possibility of iterative decision making is Collaborative Design Platform (CDP). CDP as a computer based real time simulation and visualization

tool is developed for urban planning in the early stages of design decision making which gives the opportunity as a flexible platform to include simulation and analysis add-ons with different objectives. The following section is going to discuss the concept of CDP in more depth and detail.

2 Background Collaborative Design Platform (CDP)

By the advent of computer simulation tools into architecture and urban design professions, most of the contributions in recent years devoted to modeling, drafting and managing of design solution mainly at the end of the planning process. The CDP project has started with the idea of coupling physical and digital contexts in early stages of urban design to be able to run real time analysis to get feedback on design and planning proposals (Schubert, 2014). The concept is an interactive table with a touch screen to load the urban data regarding buildings, routes and infrastructures within the boundaries of the design location. The platform enables its user to run real time simulations for physical models within an interactive and communicative interface. The framework focuses on establishing a tool with an interactive interface for collaborative design thinking in order to investigate digital methods that can be transferred to conceptual planning (Schubert, Riedel, & Petzold, 2013). This approach enables visualization of planning decisions in early phases to be discussed and shared between citizens, stakeholders and other planner in a collaborative milieu.

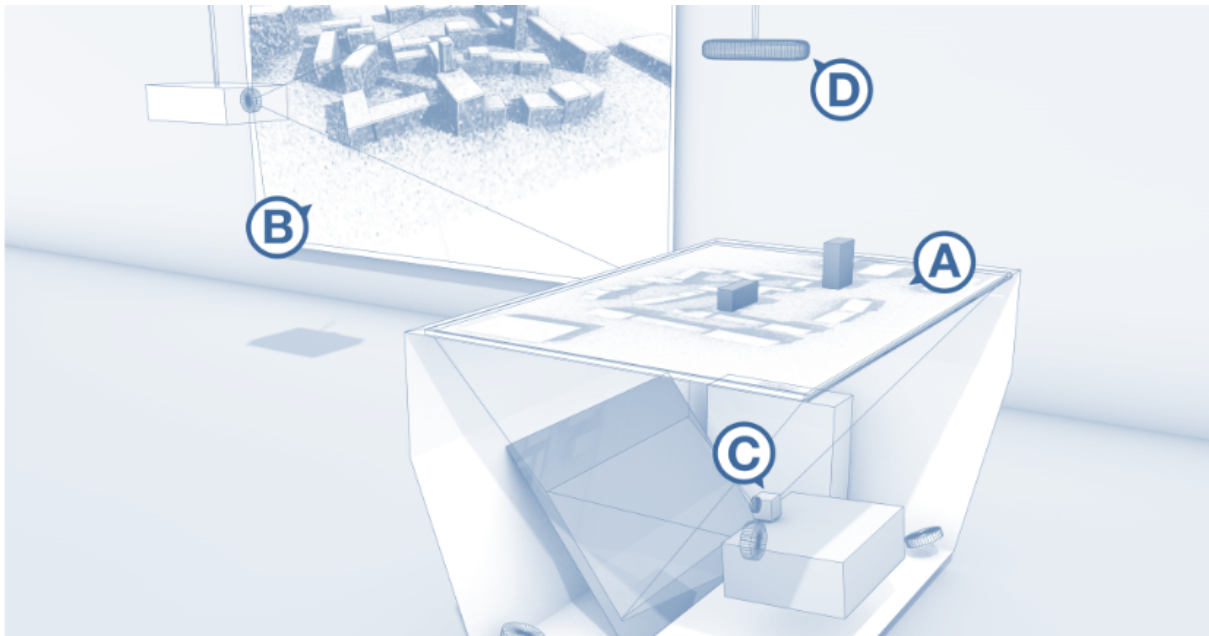


Figure 1: Hardware concept: Multi touch table in combination with Microsoft Kinect 3D camera and additional perspective display

CDP table consists of hardware and software concept of the prototype. The hardware setup (Fig. 1) is based on a custom-made, large-format multi-touch table. This is the work surface and design platform for the architect (A). The underlying plan information is derived from GIS data in City GML format, which is displayed as figure ground on the surface of the multi-touch table. A perspective view (B) of the entire scene is displayed on a separate, vertically mounted touch screen that accepts touch input. The camera (C) captures an impression of the “footprint” of the placed objects (position, size, angle, shape), anchors these in the coordinate system and makes it possible to track the movement of objects as well as fingers. An additional IR depth camera (D) mounted above the multi-touch table captures the real 3D geometry model of the objects placed on the table. Each distinct element of the footprint is registered and allocated an ID, which can then be linked directly with the digitized 3D form obtained from the IR camera. This combination makes it possible for the user to shift or turn registered objects without its 3D form to be recognized and computed in real time. Every change to the real model – whether a block is modified, shifted, removed or a new object is placed on the table’s surface has a direct real-time impact

on the digital image, as well as the calculations, the perspective view and the virtual sketch. The CDP (Fig. 2), with the concept of combining physical and digital models to be coupled with real time analysis has several challenges into diverse directions and scales. Starting from the requirements of architectural and urban planning processes following key points could be addressed:



Figure 2: CDP // Collaborative Design Platform

2.1 *Creative thinking and decision making*

Quick spread of digital tools in architecture and urban design professions has limited the potential of these tools to be embedded into the design process. Mainly, the common application of design and planning tools is restricted to end process evaluations. However sometimes it is possible that computers give new ideas to the designer by spontaneous actions, but the main guider is the architect to choose between the alternatives. We cannot expect computers as creative as human because, the human itself have made computers exist but there can be a collaborative process between human and computer. The computer enables imagination transferred to build environment.

A collaborative design process requires tools to transform the linearity of such an approach into iteration oriented and feedback based loops. In that way, the end point outcome can be improved integrating real time feedbacks and solutions. The CDP aims to bridge this gap by pushing back the mutual discussion into early stages of design through the introduction of a circular decision supported thinking process.

2.2 *Variety of applicable plug-ins*

Each design task or design approach based on the complexity of task and key features requires a certain set of tools to justify decisions. This means that the parameters and analysis to be checked in different projects could vary based on the design question that is going to be answered by any set of tools. Within the last two years, the CDP has built a large number of plug-ins for different simulation and analysis purposes. The most significant developments are: shadow and radiation analysis, 2D wind simulations, coupled mixed and augmented reality, real time sketching etc (Schubert, 2012). Within the process of development, the recent idea focuses mainly on energy performance analysis on city and neighborhood scale. In this regard, the question of designing district heating networks and evaluating their viability in early planning level is considerable. This paper includes recent achievements to implement this concept into the CDP platform.

3 Plug-in for District heating network

District heating offers a set of benefits compared to building specific heating plants concerning energy efficiency (high efficiency of the central heating plant, optimal design specific to base, medium and peak loads), possibility to use large scale renewable energy resources (waste heat, deep geothermal energy, etc.) as well as a higher degree of flexibility. However it requires a sufficient density of heat demand to ensure a cost and energy efficient operation (limiting heat losses in the grid). The higher the heat demand of the supplied buildings in relation to the grid length, the more efficiently and economically a heating network can be operated (Lund, Möller, Mathiesen, & Dyrelund, 2010).

Besides the construction standards of the buildings, depending to a high degree on their construction period, the parameters defined in the urban planning process, such as building orientation, form and shapes, distance between buildings, height of the buildings and building usage have a significant influence on the heat demand of the buildings and thus on the density of heat demand.

Within this regard, the goal of this project was to define a method and to implement it in the CDP in order to design and optimize the grid of district heating networks, evaluate the heat demand related to the length of the grid and thus give a first evaluation of its economic feasibility. This should permit to analyze the influence of the urban design and structure on the district heating supply options in the early urban planning stages. For that, the following aspects had to be integrated in the Collaborative Design Platform (CDP):

- Optimal grid generation for heating networks
- Positioning of the heat plant (manually / automatic optimization)
- Determination of the heat demand of the individual buildings in the considered area
- Calculation of the heat demand per meter grid (specific to each section) and graphical representation for first feasibility evaluation

4 Calculation of the of heat demand per building

In view of the calculation of the heat demand per meter grid, the demand of the individual buildings in the design area for heating and domestic hot water is determined in a first step. This is done by applying a simplified method based on statistical data-specific heat demand values depending, for residential buildings, on the building usage, type and construction period (Wohngebäudetypologie, 2015). For non-residential buildings the specific values are only dependent on the building use (Staatsministerium, 2011). The method thus does not consider the exact building form, but it is based on the energy reference area of the building (habitable / useful area). Industrial buildings are not considered due to their very individual requirements.

For a first rough estimation of the economic feasibility of heating networks, as intended in this project, this method is considered as sufficiently accurate. However, it requires an extensive database with detailed information about the buildings (usage, type of building, construction period, habitable / useful area, etc.). In case such an accurate data base is not or just partly available, the required information can be accessed through an on-site survey of the buildings in the study area, and implemented in the digital database (GIS).

Since the heat demand for each building is independent from outside parameters (other buildings, position, orientation, etc.), the computation can be performed in parallel. When a new building is added to the design area, or one of the dependent parameter for the heat demand is changed, it has its requirement (re-)calculated, before (re-)introducing the building to the grid. The evaluations are then directly stored in the instances of the data structure for buildings in the CDP Framework. Figure 3 shows screen shot of the CDP display with district heating network connecting buildings to the power plant.

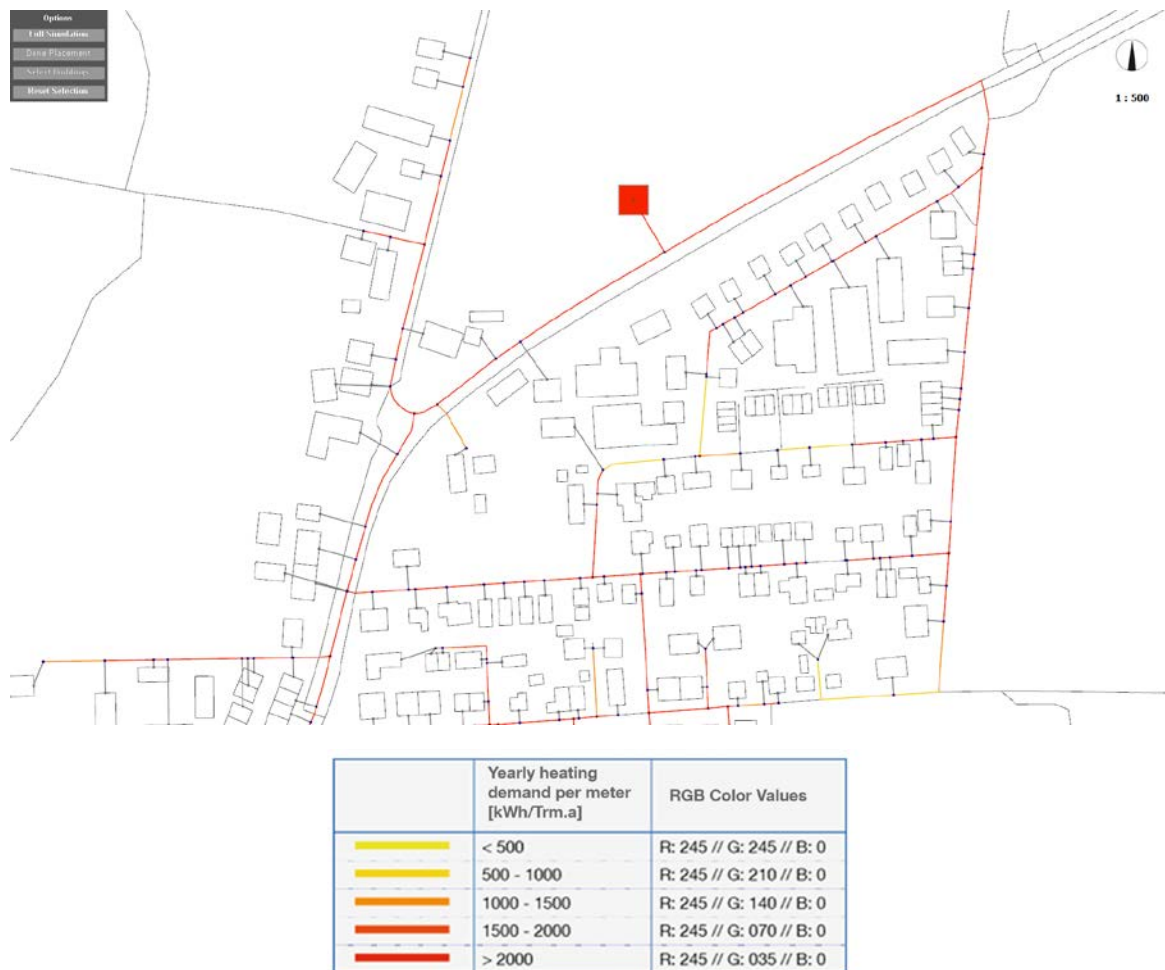


Figure 3: Evaluation of heating network

5 Network Generation and positioning of the heat plant

Due to the complexity of heating networks, a few assumptions and simplifications were made. This greatly assisted in the automation of the network creation. The following limitations were imposed:

- The network does not contain any closed circuits (star like network).
- Only preferred buildings are connected to the network.
- The network can run only under streets. Exception is the connection between buildings and the rest of the network.
- Buildings are connected with the network through the middle point of the nearest façade to the network.
- The heating plant is connected on a similar principal as other buildings.

Based on these rules, an initial undirected graph is created matching the structure of all roads. Afterwards, all buildings are simultaneously connected to the graph, as described in the rules. Taking into consideration where the heat plant is placed, the Dijkstra Algorithm for the single-source shortest path problem is applied (Dijkstra, 1959). Utilizing the generated paths from the algorithm transforms the graph to a Minimum Spanning Tree (MST) (Cormen, Leerson, Rivest, & Stein, 2001). Such a tree contains all points connected with those edges, with a minimal total distance and without cycles.

Based on this approach two different methods, depending on the positioning of the heat plant, are conceptualized and developed. The concept of optimizing DHN is based on 2 different choices, first way is to place the power plant manually by the user, second is based on finding optimum location for the power plant to

be places.

5.1 *Selective position based on user input*

The core of the method validation and evaluation of the network is based on a heat network, whose plant is placed by the user. The location, size and orientation of the heat plant is defined through a physical object that the users places on the surface of the table. Based on the definition of the plant the network is constructed and analyzed in real time (Figure 3). Based on the principles of CDP the power plant or energy source could be modified and placed in different location and at the same time real time calculations visualized on the table surface to find best possible location for the planning scenario.

5.2 *Automatic position evaluation*

On this method, the designing context is discretized using a Quadtree structure (Finkel & Bentley, 1974). For each cell of the Quadtree a heat plant is placed in the centre of it. From there the base approach is applied to generate a heat network. Each network is evaluated based on the total distance and heat distribution of the segments of the network and a color value is then associated based on the worst and best performing networks (Figure 4). Since the generation and evaluation of each Quadtree cell is independent of all other cells, each cell evaluation is run in parallel.

The algorithm starts at the first level of the Quadtree, where only one cell, that's the size of the whole design space, is created and evaluated. Each cell from the next level of the Quadtree starts only when all cells from the previous level are complete. Since each cell of a finer level is contained within a coarser one, it is possible for the heat plant in both to connect to the same segment and only the distance between the plant and the segment to be the difference between the generated networks. For this reason a list of all previously generated networks is stored during the algorithm runtime. Every time a plant is placed, the algorithm checks if there was a similar network already generated. In that case it directly uses the stored information and modifies only the distance between the plant and the rest of the network. If there is no similar network, a new one is generated and stored in the list.



Figure 4: Evaluation of several heating systems simultaneously

6 Computation of the heat demand per meter grid

The heat demand per meter grid is determined for each grid segment by asserting how much heat passes through it. This is computed by adding the heat demand of all buildings that pass through it divided by its length. It is then represented in the CDP according to a fixed colored scale (see Fig. 3). In that way, it is possible to evaluate if some parts of the study area should not be connected to the network because of too low demand density. The value of 500 kWh per year and trace meter [kWh/Trm.a], as defined by the KfW subsidy program for renewable energy “Erneuerbare Energie Premium” [KfW], is often used in Germany as a threshold for economic feasibility. For that, heat losses in the grid are not considered. Only the main trace is taken into account in the calculation, not the individual house connections.

In order to test the accuracy of the developed method, a comparison could be realized for a district in which real heat consumption values are available. To evaluate the accuracy of the developed plug-in, the designed heating network can later be compared to an existing heating network. Figure 5 summarizes the overall procedure of DHN calculation through CDP development.

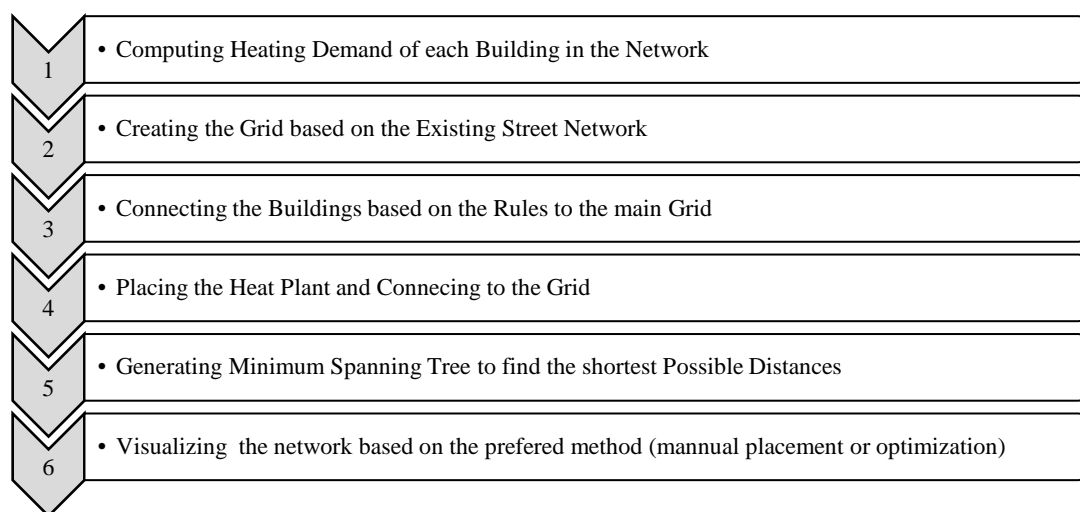


Figure 5: overall process of DHN integration with CDP

7 Summary

Over the framework of the project, integrating DHN to CDP, an interactive simulation for heating network optimization and creation was designed and implemented on top of the Collaborative Design Platform. The simulation computes based on easily extendable rules the heat demand for buildings in the area and with the computed information creates heating networks based on the position of the plant. The approach offers two options for the user in order to place the plant in the desired design context. The automatic position evaluation creates a “heat map” of all available positions and how they compare to one another. Based on this process the user has the chance to use physical boxes to place on the surface of the CDP and compare the actual networks. The implementation as a reactive simulation expands the use of the CDP and enables laymen (such as stackers, authorities, etc.) to be directly involved in the planning process, taking into account objective criteria through the decision making progression.

Acknowledgement

This research was supported and funded by ZukunftBAU research initiative within the project under the title of “Simulationsgestützte Entwurfsplanung im städtebaulichen Kontext unter Berücksichtigung energetischer und raumklimatischer Aspekte”

References

- Ancona, M. A., Bianchi, M., Branchini, L., & Melino, F. (2014). District Heating Network Design and Analysis. *Energy Procedia*, 45, 1225-1234. doi: <http://dx.doi.org/10.1016/j.egypro.2014.01.128>.
- Curti, V., von Spakovsky, M. R., & Favrat, D. (2000). An environomic approach for the modeling and optimization of a district heating network based on centralized and decentralized heat pumps, cogeneration and/or gas furnace. Part I: Methodology. *International Journal of Thermal Sciences*, 39(7), 721-730. doi: [http://dx.doi.org/10.1016/S1290-0729\(00\)00226-X](http://dx.doi.org/10.1016/S1290-0729(00)00226-X).
- Dotzauer, E. (2002). Simple model for prediction of loads in district-heating systems. *Applied Energy*, 73(3), 277-284. doi: [http://dx.doi.org/10.1016/S0306-2619\(02\)00078-8](http://dx.doi.org/10.1016/S0306-2619(02)00078-8).
- Lund, H., Möller, B., Mathiesen, B. V., & Dyrelund, A. (2010). The role of district heating in future renewable energy systems. *Energy*, 35(3), 1381-1390. doi: <http://dx.doi.org/10.1016/j.energy.2009.11.023>.
- Schubert, G. (2012). Early Design Support – Interaktive Simulationen in frühen Entwurfsphasen. Paper presented at the Forum Bauinformatik 2012, Bochum, Germany.
- Schubert, G. (2014). Interaction forms for digital design: a concept and prototype for a computer-aided design platform for urban architectural design scenarios. (Doctorate), Technical University of Munich.
- Schubert, G., Riedel, S., & Petzold, F. (2013). Seamfully Connected: Real Working Models as Tangible Interfaces for Architectural Design. In J. Zhang & C. Sun (Eds.), *Global Design and Local Materialization: 15th International Conference, CAAD Futures 2013, Shanghai, China, July 3-5, 2013. Proceedings* (pp. 210-221). Berlin, Heidelberg: Springer Berlin Heidelberg.
- Staatsministerium, B. (2011). Leitfaden Energienutzungsplan, Bayerisches Staatsministerium für Umwelt und Gesundheit. Bayerisches Staatsministerium für Wirtschaft, Infrastruktur, Verkehr und Technologie, Oberste Baubehörde im Bayerischen Staatsministerium des Innern (Hrsg.): Lehrstuhl für Bauklimatik und Haustechnik, Technische Universität München.
- Wohngebäudetypologie, D. (2015). Deutsche Wohngebäudetypologie Beispielhafte Maßnahmen zur Verbesserung der Energieeffizienz von typischen Wohngebäuden. Darmstadt: Institut Wohnen und Umwelt GmbH, erarbeitet im Rahmen der EU-Projekte TABULA und EPISCOPE.

Urban climate influence on building energy use

K. R. Gunawardena and T. Kershaw

Department of Architecture and Civil Engineering, University of Bath,
Claverton Down, Bath, BA2 7AY, UK.

Corresponding author: T. Kershaw, t.j.kershaw@bath.ac.uk

Abstract

Building energy demand in cities is expected to be affected as a warming climate, increasing frequency and severity of extreme heat events, and the urban heat island effect (UHI) cumulatively exacerbate heat related risks. To mitigate such climate loading and reduce energy bills, the way that buildings are constructed have changed over recent decades. This paper examines not only how the UHI affects space-conditioning loads within urban office buildings, but also how the trend of replacing traditional heavyweight stone facades with lightweight highly glazed and insulated ones affects both the magnitude and timing of the UHI and resulting building energy use. The paper addresses this through a simulation study of a typical street canyon based on the Moorgate area of London. Results show that including the UHI within a dynamic thermal simulation has an adverse effect on annual space-conditioning, with a 4 % increase in demand for buildings with stone facades, while those with a glazed construction show a 10 % increase. The study therefore demonstrates that the trend in urban centres to construct highly glazed buildings with lightweight insulated facades increases space-conditioning loads and consequently adversely affects the UHI, thereby creating a vicious cycle of additional urban heating that exacerbates the impacts of climate change. The study in turn stresses the significance of accounting for UHI loads in estimating urban energy use, for which a combined simulation approach has been presented as a practical pathway.

1 Introduction

Projections of climate change and increasing frequency and severity of extreme heat events are likely to have an adverse influence on the global trend towards urbanisation (UN 2014). In addition to such global and synoptic scale climate modifications, the meso-to-microscale urban setting is challenged by the long-established warming induced by the heat island effect (UHI) (Howard 1833, Oke 1987). Collectively, such global-to-microscale climatic conditions exert significant influence on the sustainable operation of urban settlements. Understanding the interactions between the built-environment and its dynamic climatic context is therefore necessary for the sustainable planning of urban growth.

$$\text{Net radiation} + \text{Anthropogenic heat} = \text{Convection} + \text{Evaporation} + \text{Heat storage} \quad (1)$$

Essential to this understanding is the ‘urban energy balance’ Eq. (1), which represents the partitioning of incoming and outgoing energy flows of the urban surface system (Oke 1982). The typically warmer climate experienced in such urban areas is explained by the net positive thermal balance that leads to the formation of UHIs. This net positive thermal balance arises from changes to their surface properties such as increased surface roughness, reduced albedo, reduced green and blue space for evaporation, and increased heat generated from human activities (anthropogenic heat). The resulting UHI effect can be considered as an added environmental thermal load that affects how energy is used within buildings (Grimmond et al. 2010). This energy use is also a contributing heat source of the UHI. Higher building energy usage could therefore contribute to the storage of greater thermal energy in the urban system and thereby help generate and intensify UHIs (Oke 1987). This suggests that if high-energy solutions are used to ventilate and cool buildings, a vicious cycle of warming may result, creating an ever worsening and unhealthy urban environment. This is made more complicated by the regeneration of inner-city areas following a trend of replacing traditional modestly glazed heavyweight façades with lightweight highly

glazed and insulated ones. The purpose of this study is to identify this influence and its degree of significance to building energy loads through the comparison of ‘dense and opaque’, and ‘light and transparent’ dominant construction build-ups. The method for addressing this considers simulations of an idealised central canyon, based on the morphology of the Moorgate area of London (Figure 1b).

1.1 Applied model: the Urban Weather Generator

To overcome the many challenges of accounting for the complexities of the interconnected urban climate, this study uses a modified version (5.1.0 beta, Norford et al. 2017) of the multiscale coupled framework termed the ‘Urban Weather Generator’ (UWG) (Norford et al. 2015). The UWG presented schematically in Figure 1a, is based on Monin-Obukhov similarity theory and is composed of four coupled sub-models that include a Rural Station Model (RSM), Vertical Diffusion Model (VDM), Urban Boundary Layer Model (UBLM), and an Urban Canopy and Building Energy Model (UC-BEM) based on the Masson (2000) Town Energy Balance scheme and a building energy model developed by Bueno et al. (2012). These sub-models exchange data to calculate modified temperature and humidity values and compile a modified weather file in the EnergyPlus (.epw) format for use by dynamic building thermal modelling software. A summary of the basic data exchanges involved is presented in Figure 1a, while detailed descriptions are offered in Bueno et al. (2013), (2014). The UWG has been verified against field data from Basel, Toulouse, and Singapore (Bueno et al. 2013, 2014, Nakano et al. 2015). The verifications from Basel and Toulouse demonstrated that urban climate estimation requires both canopy and boundary layer effects in order to account for the aggregated influence of the UHI over the entire city; with more than half the influence observed in urban canyons attributed to the mesoscale effect. The resolution of such boundary layer influences require mesoscale processes to be reconciled with the aid of higher-scale atmospheric simulations coupled within a framework as employed by the UWG (Bueno et al. 2013).

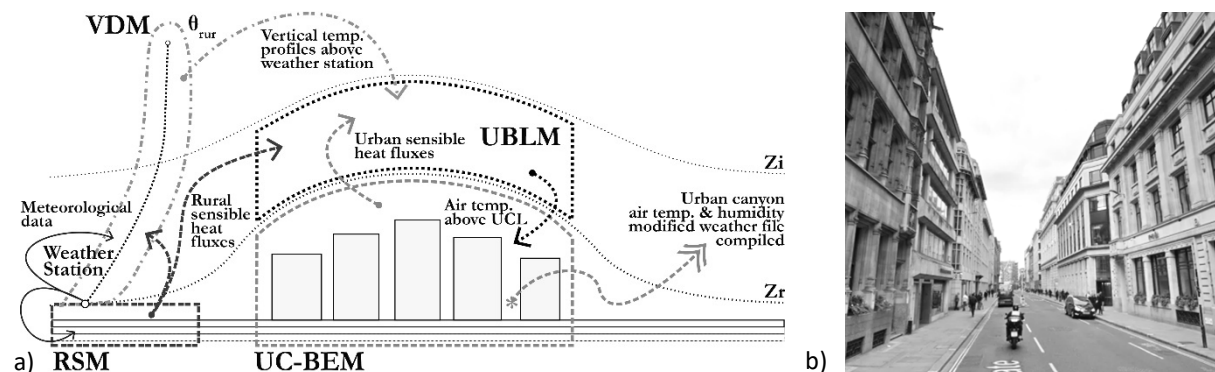


Figure 3. Domain of the UWG modules and data exchanges in an ideal city, based on Bueno et al. (2013) (a); Typical street canyon view of Moorgate, London, from ©Google Street-view, 2017 (b).

2 Method

The morphology of the Moorgate area in London is idealised in this study by averaging parameters to produce an urban roughness profile with a characteristic radius of 500 m. The characteristics of this urban roughness (detailed in Appendix: Table 2), together with a rural weather file (in .epw format) are input into the UWG (5.1.0 beta) to generate weather profiles that account for the UHI influence on air temperature and humidity values for the canyon scenarios considered (see Table 1). The rural weather data used for this study is the Design Summer Year (DSY) for the Reading area (60 km due west of the Moorgate site), which was generated using the UKCP09 Weather Generator, the full methodology of which is described in Eames et al. (2011).

The generated UWG profiles for the canyon scenarios were then applied to a thermal model of the Moorgate street canyon and surrounding buildings, created in the dynamic simulation modelling package IES-VE (2015) to estimate space-conditioning loads for the respective scenarios.

Table 1. Simulation scenarios.

Scenario	Weather file used	Construction
Base Stone	Design Summer Year (DSY) for Reading (unmodified).	
Stone: 0.30	The above modified using the UWG, i.e. with the dominant construction of Stone facades and resulting UHI influence included.	
Base Glazed	Design Summer Year (DSY) for Reading (unmodified).	Using glazed facades with default GR: 0.30, detailed in Appendix: Table 2 (hypothetical scenario).
Glazed: 0.30	The above modified using the UWG, i.e. with the dominant construction of Glazed facades and resulting UHI influence included.	Additional hypothetical variations using the following GRs: Glazed A: 0.15; Glazed B: 0.30; Glazed C: 0.50 and Glazed D: 0.90.

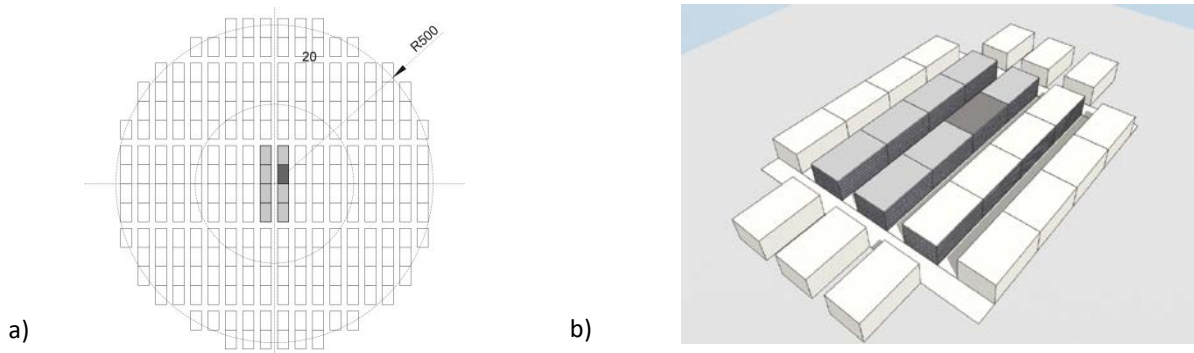


Figure 4. Idealised 500 m radial urban configuration based on Moorgate morphology used for UWG climate file generation (a); focused area of the street canyon considered for IES-VE energy simulations (b).

3 Results

The following considers firstly, the features of the urban weather files generated by the UWG with the influence of the UHI included, and secondly, their cooling and heating load implications for the highlighted building in Figure 2a, b that belongs to the central Moorgate street canyon.

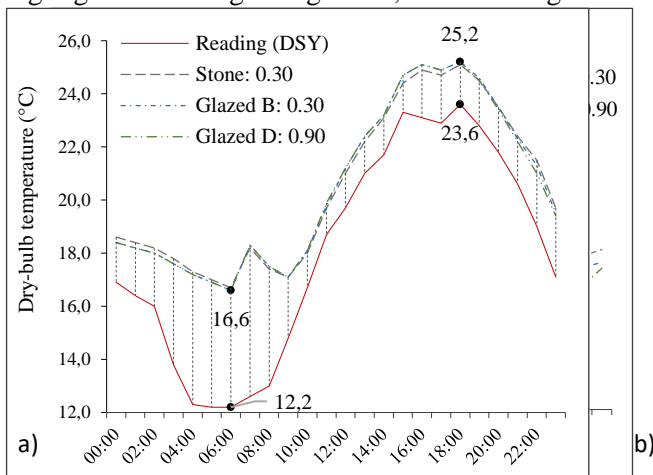


Figure 5. Summer solstice (21-Jun) dry-bulb temperature profiles (a); and UHI ΔT or intensity profiles (K) (b); for Stone, Glazed B, and Glazed D scenarios relative to the Base Reading (DSY) profile.

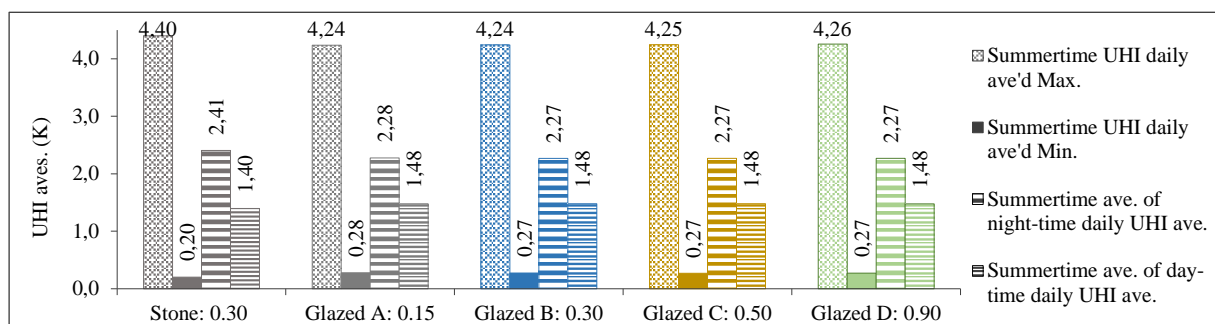


Figure 6. Summertime (May-Sep) UHI features for scenarios simulated (K).

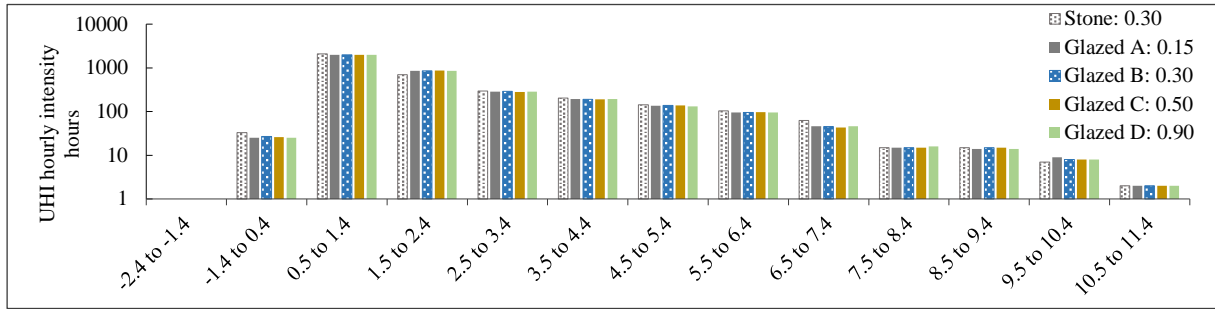


Figure 7. Summertime (May-Sep) UHI intensity (K) frequencies, Log10 (hours).

3.1 Canyon microclimate profiles

The summertime UHI average daily maximums for these scenarios range from 4.24 to 4.40 K, while the average daily minimums range from 0.20 to 0.27 K (Figure 4). Although the latter average daily minimums are positive values, hourly UHI intensity or ΔT data identified cool islands (negative ΔT) in all scenarios with intensities ranging from <0 to -2 K that represented $\sim 1.7 - 2.5$ % of the (3,672) hours simulated. These hourly UHI ΔT values also identified peaks ranging from >6.4 to ≤ 12.4 K that represented 2 - 3 % of the total hours simulated (Figure 5). Notably, the Stone scenario showed the highest hours reaching peak and minimum values (max ~ 3 %, min ~ 2.5 %) relative to Glazed scenarios. When hours of the day are separated into daytime (from 6 AM to 6 PM) and night-time (the residual) UHI intensity values, the daily daytime averages ranged from 1.39 to 1.48 K, and night-time averages ranged from 2.27 to 2.41 K. The night-time averages therefore were higher than daytime values. While this is true for averages, the summer solstice (21-June) illustrates an example where the hourly UHI ΔT maximum for the day was reached in the morning at around 7 AM, almost two hours after sunrise (around 4:50 AM) (Figure 3b). This summer solstice UHI profile also showed that the night-time averages were higher for the Stone scenario relative to Glazed scenarios, while the converse was true during the midday to evening period of the day.

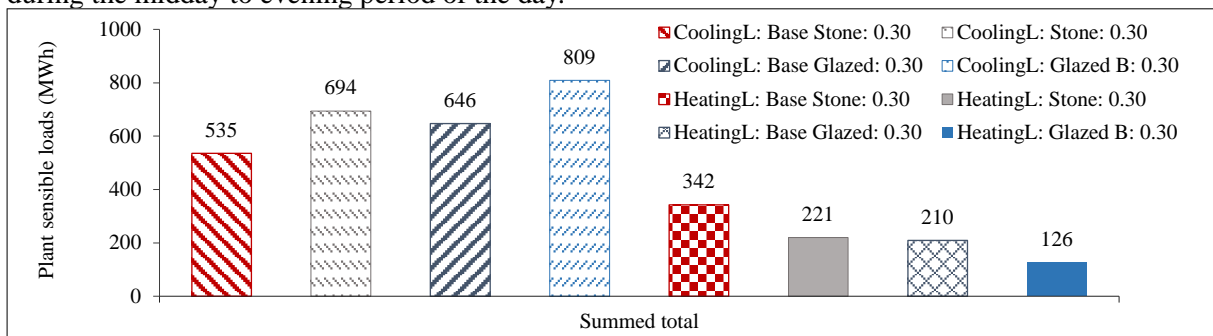


Figure 8. Cooling and heating plant sensible loads for Base and including UHI influence for both Stone and Glazed facade simulations (all with GR: 0.30).

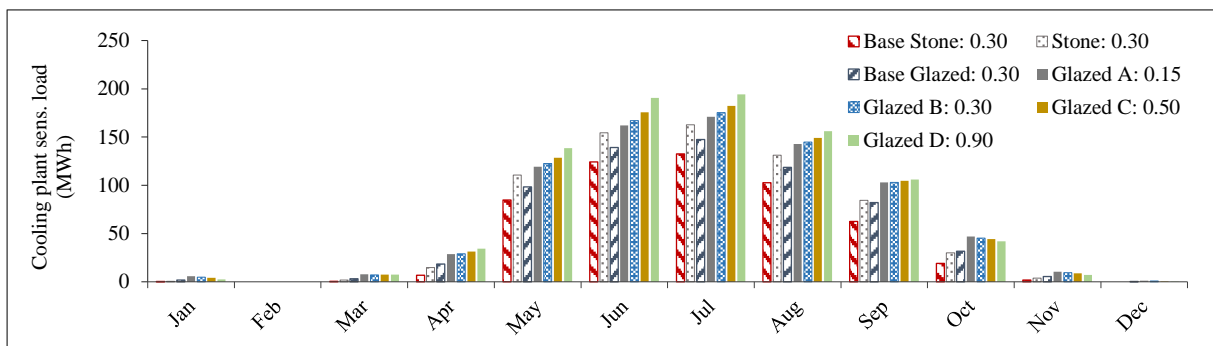


Figure 9. Cooling plant sensible load monthly totals (MWh).

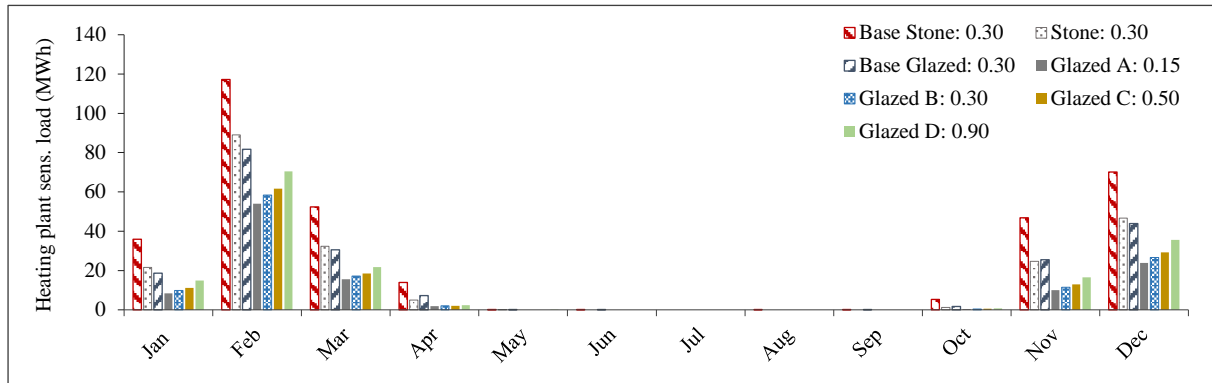


Figure 10. Heating plant sensible load monthly totals (MWh).

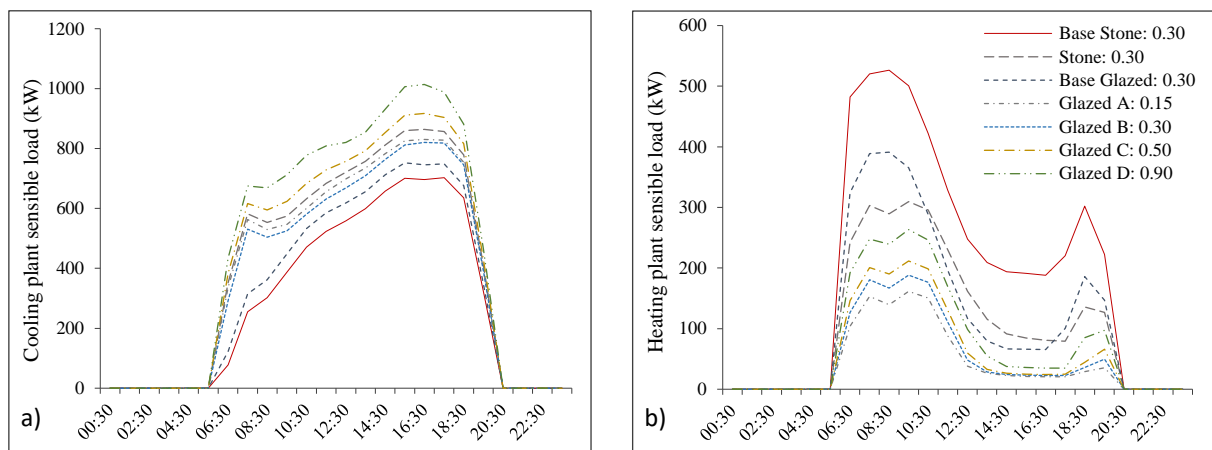


Figure 11. Summer solstice (21-Jun) cooling load (a); winter solstice (21-Dec) heating load (b); (kW).

3.2 Space-conditioning loads

Including UHI influence on heating and cooling load values (Figure 6 to Figure 9) demonstrated significant differences between the Stone and Glazed scenarios. For the Stone scenario relative to its Base Stone simulation, including the UHI influence resulted in a 30 % increase in summertime cooling demand, while winter heating demand was reduced by 36 %. Overall, this meant that the influence of the UHI had an adverse effect on the space-conditioning demand of around 37 MWh, or a 4 % increased demand for the office building (Figure 6). When the Base Glazed scenario was compared against the Glazed scenario B simulation that included the UHI influence (both with GR: 0.30), this resulted in a 26 % increase in cooling demand and a 41 % decrease in heating demand. Overall, this meant that the influence of the UHI had an adverse effect on the space-conditioning demand of around 82 MWh or a 10 % increased demand for the office building (Figure 6).

When Glazed scenarios A to D were considered (Figure 7 and Figure 9a), cooling demands showed considerable increase relative to the Base Glazed simulation, with scenario D showing the greatest (36 %), and scenario A with the lowest (24 %) increase. In contrast when heating loads were considered, scenarios A through to D showed reduced demands with scenario A showing the greatest (46 %), and scenario D with the lowest (22 %) decrease (Figure 8 and Figure 9b). The effect of GR increase

addressed by the relative comparison to Glazed A scenario with the lowest GR: 0.15, showed net space-conditioning demand increase respectively to D scenario with GR: 0.90 (B=40, C=106, D=227 %, increases relative to A). The effect of transforming the heavyweight facades to lightweight glazing addressed by the comparison between the Stone scenario against Glazed B scenario (both with GR: 0.30 and UHI influence included), showed the net effect on annual space-conditioning load demand increased by around 21 MWh or a 2.3 % increase for the office building (relative heating load reduced by 43 %, although cooling load increased by 17%, see Figure 6).

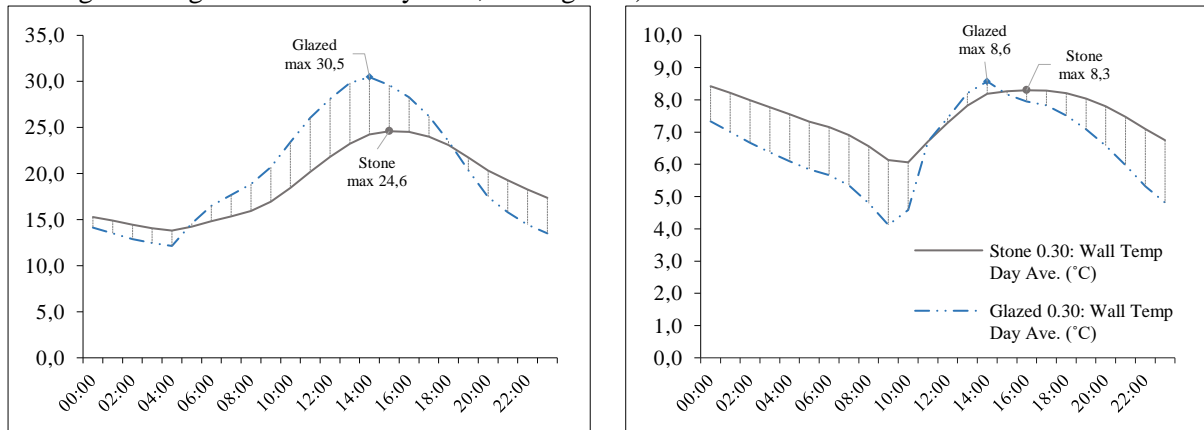


Figure 12. Summer solstice (21-Jun) (a); winter solstice (21-Dec) (b); building wall surface temperatures ($^{\circ}\text{C}$).

4 Discussion

Historical observations of the London UHI reveals a diverse representation. The earliest observations of Howard (1833) noted that London was 0.6 K warmer in July, while in November was 1.2 K warmer than the country. Howard (1833) also observed that at night it was 2.05 K warmer, and during the day 0.19 K cooler relative to the country. Examining temperature data for the period from 1931-60, Chandler (1965) found the annual mean to be 1.4 K warmer for central London, and noted 0.9 K warmer daytime maximum temperatures, with summertime monthly mean value of 1.6 K, and 1.2 K for winter. More recently, Watkins et al. (2002) presented measured data from 1999 to show a summertime (Jun-Aug) excess of ~ 2.8 K, and a peak value of 8 K. Data from 1999 also demonstrated a maximum summertime daytime UHI of 8.9 K, while a maximum nocturnal UHI of 8.6 K was found during clear-sky periods when the wind velocity was below 5 ms^{-1} (Kolokotroni and Giridharan 2008). In winter their data showed that the maximum UHI was 9 K both day and night with similar wind velocities (Giridharan and Kolokotroni 2009). In a recent study of west London urban parks, Doick et al. (2014) observed summertime nocturnal UHI peaks of 10 K on certain nights.

In this study the summertime average UHI for the street canyon ranged between 1.84 to 1.86 K for the scenarios simulated. Considering the above historic values and the results presented earlier, the UHIs simulated by the UWG could be said to fall within a plausible range. The lower UHI averages for the daytime relative to the night-time simulated across the scenarios is consistent with most UHI studies (Oke 1987, Wilby 2003). However, Howard's (1833) finding of 0.19 K cooler daytime (i.e. cool island) London temperatures relative to the country was not predicted by any of the simulations of this study. In general, the occurrence of cool island conditions were noticeably less than expected at this canyon and were limited to hourly occurrences as noted in the results section. This may be attributed in this study to the 20 m street width being wide enough to minimise the canyon shading effect, and the notably higher anthropogenic heat output used for the Moorgate area (based on data from the Iamarino et al. (2012) simulation study) contributing to relatively higher daytime canyon temperatures. This latter significance of anthropogenic heat output is demonstrated by the summer solstice UHI profile (Figure 3a, b). With this profile, although the night-time UHI had accumulated heat to present reasonably higher canyon temperatures around dawn (~ 4 -5 AM), the onset of the office building activity profile provides a boost of anthropogenic heat to elevate (spike) temperatures to reach an even higher UHI ΔT maximum at a delayed peak time after 7 AM.

When the summertime average UHI for the canyon and its breakdown into daytime and night-time averages were considered, the Stone scenario presented higher values relative to Glazed scenarios. When hourly resolution data was reviewed, the Stone scenario showed the highest proportion of hours reaching UHI ΔT maximum values. This suggests that urban fabrics with dominant heavyweight stone constructions such as at Moorgate could generate a warmer heat island effect to be experienced in the street canyon particularly at night, relative to ones dominated by lightweight glazed constructions. The Stone scenario also showed the highest proportion of hours reaching UHI ΔT minimum values, predominantly during the day. This indicates that even though this material profile has the potential to generate a warmer canyon temperature profile in the night-time, during the daytime it also has the potential to contribute greater to the experience of cool island conditions. This observation may be attributed to the buffering properties offered by the thermal mass of heavyweight materials such as stone. The materiality of urban form influences the surface energy balance by affecting both net radiation and heat storage. The radiative properties of materials are considered as emissivity and albedo, while storage properties are affected by heat capacity and thermal conductivity. The radiative property of albedo (α) or solar reflectance is defined as the percentage of solar energy reflected by a surface, and is a significant determinant of material surface temperatures (Oke 1987, Taha 1997, Jacobson 2005). Since 43 % of solar energy is in the visible wavelengths (400-700 nm), material colour is strongly correlated with albedo, with lighter coloured surfaces having higher values ($\alpha \sim 0.7$) than darker surfaces ($\alpha \sim 0.2$) (Taha et al. 1988). In this study the stone is assumed to be Portland (typical for the Moorgate area), which is of a lighter colour and a relatively high mean albedo of 0.6. This in turn contributes to lower radiation absorption by the facade material that helps to reduce its surface temperature. As Figure 10a, b for summer and winter solstice surface temperature profiles for external walls demonstrate, during the midday period the temperature is lower for Stone surfaces compared to Glazed. Furthermore the difference is more pronounced during the summer when solar radiation contribution is at its greatest. This surface temperature difference between heavyweight and lightweight constructions can affect the urban microclimate both directly and indirectly. The direct effect is experienced in the form of its influence on reducing canyon ambient temperatures as relatively cooler surfaces would have relatively lower sensible flux. The indirect effect works in conjunction with material heat storage properties to modify building energy use and its feedback to the microclimate.

Higher degrees of radiation reflection from high albedo materials mean that less energy is available for transfer into their depth. From the residual energy that is absorbed, a material's ability to store heat (capacity), which at times is referred to as thermal mass, and thermal diffusivity, the ease by which heat penetrates into a material (function of thermal conductivity and volumetric heat capacity), determines its thermal inertia, a measure of the responsiveness of a material to temperature variations. Heavyweight materials such as stone have relatively higher diffusivity, heat capacity, and thermal inertia, which means that their temperature fluctuations through the diurnal cycle are minimised (Gartland 2008). Thus, when radiation energy is received by such surfaces, the non-reflected energy is mostly absorbed and stored and when the climate above is relatively cooler, is re-radiated (as longwave) or purged back to the climate. This lag is evident when examining both surface temperature profiles (Figure 10), which show a lower daily variability range (amplitude) and delay in peak (phase shift) for Stone surfaces relative to Glazed surfaces. From the building's perspective, the material of the envelop absorbing more heat and storing it means that less thermal energy is making its way into the internal environments. This in turn helps to reduce their cooling loads and resulting heat rejection feedback to the climate, which is particularly evident in the daytime. This storage benefit of the heavyweight stone facade however can have a negative effect in the winter, as a significant proportion of the initial energy expenditure may be used to heat the facade rather than the internal environment. Lightweight glazed constructions on the other hand demonstrate faster response to microclimate thermal changes, which explains the reduced demand in winter heating load (Figure 8). Including the higher thermal load from the UHI therefore transfers readily into the internal spaces of the building to present a significant 'winter warming effect' (40 % reduction with the same GR: 0.30). However, increasing the areas of glazed fabric area (GR) predictably increases fabric heat loss, which in turn reduces the winter warming effect experienced. In the summer, it is clear that the higher cooling demand in such scenarios is generated by the increased solar gain that results with increased glazed facade areas.

Materiality of urban built form can influence both the properties of the UHI as well as its impact on the building performance of this built form. The properties of the dominant material profile in an urban setting is identified in previous research to modify the intensity and timing of when the UHI peak is likely to be observed (Oke 1987). Cities made of predominantly lower diffusivity materials are therefore suggested to reach their UHI peak soon after sunset, while those made with higher diffusivity materials such as stone are unlikely to reach theirs until sunrise (Gartland 2008). This study demonstrates this to be true for the Stone scenario with the peak evident towards sunrise. However, the Glazed scenarios do not demonstrate the phase shift to confirm the suggested observation for lightweight constructions (Figure 3a, b). Conversely, the thermal efficiencies of the building envelope have a significant influence on the degree of benefit or detriment to their space-conditioning loads presented by the UHI load. In this study, the space-conditioning loads demonstrated that a Stone construction could be said to accommodate the additional thermal load from the UHI relatively better over the course of the year than a lightweight Glazed construction of the same GR.

5 Summary

In an urban development, the material constructions used and their properties of emissivity and albedo, together with heat capacity and thermal conductivity, determine how solar energy is reflected, emitted, and absorbed by surfaces. The properties of the dominant material within this urban setting may affect the intensity and the timing of when the UHI peak is likely to be observed, and how the UHI load itself is transferred into internal environments, thereby affecting their space-conditioning performance. However, the selection of materials for constructing urban developments is influenced by many other factors in addition to their thermal properties. Buildability and assembly issues, economics, supply, regulatory guidance, cultural and historic context, and aesthetics can all influence the materiality of a development or even the character of entire cities subject to which influence gains primacy. It is worth noting that materiality is an aspect of existing built-environments that can be reasonably altered to offer heat mitigation, perhaps to a greater degree of practicability than the alteration of existing morphology. The study has shown that the trend in urban centres to construct highly glazed buildings with lightweight insulated facades increases space-conditioning loads and adversely affects the UHI, thereby creating a vicious cycle of additional urban heating that exacerbates the impacts of climate change. The study in turn stresses the significance of accounting for UHI loads in estimating urban energy use, for which a combined simulation approach of using an urban climate model and a building energy model has been presented as a feasible pathway to assess the impact of different urban constructions.

Appendix

Table 2. Key parameters used for simulations

	Parameter description	Moorgate based parameters
Block	Canyon and context block dimensions	L: 60 m × D: 35 m × H: 24.5 m
	Average floor height and storeys	3.5 m × Seven storeys
	Assumed building use and area in radius	Medium office; 3,410,400 m ²
	Wall material and thickness	Portland stone / gypsum plaster Thickness: 0.3 / 0.025 m; U-value: 2.33
	Roof material and thickness (flat roof)	Gravel / expanded polystyrene / concrete / ceiling tiles Thickness: 0.075 / 0.1 / 0.3 / 0.05 m; U-value: 0.24
	Glazing	GR: 0.3; U-value: 1.93 W m ⁻² K ⁻¹
	Initial temperature of construction	20 °C
	Gains: lighting/equipment/occupancy	12 W m ² / 25 W m ² / 6 m ² person ⁻¹ Based on medium office schedules

	Parameter description	Moorgate based parameters
	Infiltration and ventilation	0.5 ach and 0.002 m ³ s ⁻¹ m ⁻² respectively
	Cooling system and heating efficiency	Air and 0.80 respectively
	Daytime and night-time set points	Based on medium office schedule
	Heat rejected to canyon	50 %
Simplified Construction	Wall material and thickness	Anti-sun glass cladding / expanded polystyrene / gypsum plasterboard
<i>Glazed</i>		Thickness: 0.010 / 0.1 / 0.025 m; U-value: 0.31
Roads	Material and Thickness	Asphalt / 0.5 m
Urban & rural road	Vegetation coverage ratio	0.005 and 0.8 respectively
	Average building height	24.5 m
	Horizontal building density ratio	0.598
	Vertical to horizontal urban area ratio	0.99
	Non-building sensible & latent heat rejection	22.68 W m ⁻² and 2.268 W m ⁻² respectively
	Characteristic neighbourhood radius	500 m
	Day and night-time UBL heights	1000 m and 80 m respectively
	Tree coverage ratio	0.001
	Tree and grass latent fractions	0.7 and 0.5 respectively
	Vegetation albedo	0.25
	Vegetation contribution start-end	4-10 (months)
	Latitude, longitude for Reading	51.446, - 0.957
	Distance from Moorgate site	~60 km due west

References

- Bueno, B., Norford, L., Hidalgo, J. and Pigeon, G. (2013). The urban weather generator, *Journal of Building Performance Simulation*, 6(4), 269-281.
- Bueno, B., Norford, L., Pigeon, G. and Britter, R. (2012). A resistance-capacitance network model for the analysis of the interactions between the energy performance of buildings and the urban climate, *Building and Environment*, 54, 116-125.
- Bueno, B., Roth, M., Norford, L. and Li, R. (2014). Computationally efficient prediction of canopy level urban air temperature at the neighbourhood scale', *Urban Climate*, 9, 35-53.
- Chandler, T. J. (1965). *The Climate of London*, London: Hutchinson & Co Ltd.
- Doick, K. J., Peace, A. and Hutchings, T. R. (2014). The role of one large greenspace in mitigating London's nocturnal urban heat island, *Sci Total Environ*, 493, 662-71.
- Eames, M., Kershaw, T. and Coley, D. (2011). On the creation of future probabilistic design weather years from UKCP09, *Building Services Engineering Research & Technology*, 32(2), 127-142.
- Gartland, L. (2008). *Heat Islands: Understanding and Mitigating Heat in Urban Areas*, Oxford: Routledge.
- Giridharan, R. and Kolokotroni, M. (2009). Urban heat island characteristics in London during winter, *Solar Energy*, 83(9), 1668-1682.
- Grimmond, C., Roth, M., Oke, T. R., Au, Y., Best, M., Betts, R., Carmichael, G., Cleugh, H., Dabberdt, W. and Emmanuel, R. (2010). Climate and more sustainable cities: climate information for improved planning and management of cities (producers/capabilities perspective), *Procedia Environmental Sciences*, 1, 247-274.
- Howard, L. (1833) *The climate of London : deduced from meteorological observations made in the metropolis and at various places around it*, London: Harvey and Darton, J. and A. Arch, Longman, Hatchard, S. Highley [and] R. Hunter.

- Iamarino, M., Beevers, S. and Grimmond, C. S. B. (2012). High-resolution (space, time) anthropogenic heat emissions: London 1970-2025, *International Journal of Climatology*, 32(11), 1754-1767.
- IES-VE (2015) IES-Virtual Environment 2015, V 2015.1.0.0, Glasgow: Integrated Environmental Solutions Ltd.
- Jacobson, M. Z. (2005). Fundamentals of atmospheric modeling, Cambridge: Cambridge University Press.
- Kolokotroni, M. and Giridharan, R. (2008). Urban heat island intensity in London: An investigation of the impact of physical characteristics on changes in outdoor air temperature during summer, *Solar Energy*, 82(11), 986-998.
- Masson, V. (2000). A physically-based scheme for the urban energy budget in atmospheric models, *Boundary-Layer Meteorology*, 94(3), 357-397.
- Nakano, A., Bueno, B., Norford, L. and Reinhart, C. F. (2015). Urban Weather Generator - A novel workflow for integrating urban heat island effect within urban design process, in *Building Simulation 2015*, Hyderabad, India, International Building Performance Simulation Association.
- Norford, L., Reinhart, C., Nakano, A., Bueno, B., Sullivan, J., Street, M., Zhang, L. and Lopez-Pineda, B. T. (2015). Urban Weather Generator, V 4.1.0, Cambridge, Massachusetts: Building Technology Program, Massachusetts Institute of Technology.
- Norford, L., Reinhart, C., Nakano, A., Bueno, B., Sullivan, J., Street, M., Zhang, L., Lopez-Pineda, B. T., Yang, J. and Gunawardena, K. (2017). Urban Weather Generator, V 5.1.0 beta, Bath: University of Bath.
- Oke, T. R. (1982). The Energetic Basis of the Urban Heat-Island, *Quarterly Journal of the Royal Meteorological Society*, 108(455), 1-24.
- Oke, T. R. (1987). Boundary Layer Climates, 2 ed., New York: Routledge.
- Taha, H. (1997). Urban climates and heat islands: Albedo, evapotranspiration, and anthropogenic heat, *Energy and Buildings*, 25(2), 99-103.
- Taha, H., Akbari, H., Rosenfeld, A. and Huang, J. (1988). Residential Cooling Loads and the Urban Heat-Island - the Effects of Albedo, *Building and Environment*, 23(4), 271-283.
- UN (2014) World Urbanization Prospects: Highlights, 2014 Revision, New York: United Nations.
- Watkins, R., Palmer, J., Littlefair, P. and Kolokotroni, M. (2002). The London Heat Island: results from summertime monitoring, *Building Serv. Eng. Res. Technol.*, 23(2), 97-106.
- Wilby, R. L. (2003). Past and projected trends in London's urban heat island, *Weather*, 58.

Influence of exterior convective heat transfer coefficient models on the energy demand of buildings with varying geometry

S. Iousef¹, H. Montazeri^{2,3}, B. Blocken^{2,3}, P.J.V. van Wesemael¹

¹ Architectural Urban Design and Engineering, Department of the Built Environment, Eindhoven University of Technology, Eindhoven, The Netherlands

² Building Physics Section, Department of Civil Engineering, KU Leuven, Leuven, Belgium

³ Building Physics and Services, Department of the Built Environment, Eindhoven University of Technology, Eindhoven, The Netherlands

Corresponding author: S. Iousef, s.iousef@tue.nl

Abstract

A detailed review of the literature shows that existing exterior convective heat transfer coefficient (CHTC) models implemented in Building Energy Simulation tools consider building geometry either incompletely or not at all. This paper therefore investigates the impact of existing exterior CHTC models on the calculated energy demand of buildings with varying building geometry. Seven CHTC models are compared. The results show that the use of different CHTC models can significantly affect the calculated building energy demand. This is especially the case for the cooling demand. This impact is more pronounced for buildings with H_b (windward height) $\geq W_b$ (windward width), where absolute deviations in cooling demand reach 42%. For buildings with $H_b \leq W_b$, the impact becomes less pronounced (up to 25%). For buildings with $H_b = W_b$, the influence of CHTC models is defined by its individual impact on buildings with $H_b \geq W_b$ and $H_b \leq W_b$.

1 Introduction

Building Energy Simulation (BES) tools are widely used for predicting the energy use of buildings. Calculation of the convective heat exchange in BES at building facades is based on the so-called exterior convective heat transfer coefficient (CHTC) models (Mirsadeghi et al., 2013). CHTC models are normally derived from experimental methods either in reduced or full-scale tests. The reduced-scale experiments are usually performed for flat plates for which relatively low Reynolds numbers and few wind directions are considered (Montazeri et al., 2015). The full-scale experiments are performed using heated plates that are placed on the building facades. In this case, CHTC is calculated based on a limited measurement points across the facades and is mainly a function of wind speed and wind direction. Consequently, the aforementioned CHTC models are applicable for specific building configurations and geometries (Defraeye et al., 2011). To the best of our knowledge, research on the influence of exterior CHTC models on the energy performance of buildings with different geometry has not yet been performed. Therefore in this paper, the impact of existing exterior CHTC models on the calculated outcomes of the energy demand of buildings with varying building geometry is investigated. Simulations are performed using the BES tool EnergyPlus and the evaluations are based on annual energy consumptions of buildings with different geometry. To gain insight into the impact of CHTC models, the results are compared with the new generalized CHTC model developed by Montazeri and Blocken (2017). The aforementioned CHTC model is based on high-resolution 3D steady RANS CFD simulations of convective heat transfer at the facades of 87 buildings and contains reference wind speed at 10 m height (U_{10}), the width (W) and the height (H) of the windward building facade as parameters.

2 New generalized CHTC model

New generalized models for surface-averaged forced CHTC at building facades and roofs have been developed that contain the reference wind speed, the width and the height of the windward building facade as parameters (Montazeri *et al.*, (2015), Montazeri and Blocken (2017)). Since the focus of the present study is on the windward facade, reference is made only to the CHTC model for the windward facade.

3D steady RANS CFD simulations of forced convective heat transfer at the facades of 87 isolated buildings are performed on a high-resolution grid. The realizable $k-\epsilon$ turbulence model (Shih *et al.*, 1995) is used in combination with the single equation Wolfshtein model (Wolfshtein, 1969).

Figure 1 shows the surface-averaged ratio $\text{CHTC}/(U_{10}^{0.84})$ in relation to H and W for the windward facade. The new generalized CHTC model, that describes the plane in Figure 1, is a trivariate polynomial and is a function of the reference wind speed at 10 m height (U_{10}), windward facade width (W) and building height (H). Reference wind speed is selected to be at 10 m height to be in line with standard arrangement for weather station anemometers (Defraeye *et al.* 2011). In order to define the accuracy of the CHTC model, in and out-of-sample evaluations are performed. The coefficient of performance R^2 for the in-sample accuracy evaluation of the polynomial is 0.9977. Moreover, the application of the CHTC model on the windward facade for out-of-sample combinations of U_{10} , H and W shows that maximum and average deviations of 6.1% and 3.5% are found and the respective coefficient of performance R^2 is 0.9925.

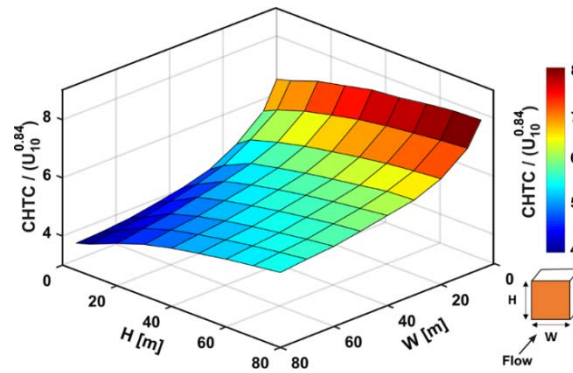


Figure 1. Profile of surface-averaged $\text{CHTC}/(U_{10}^{0.84})$ on the windward facade for buildings with different building dimensions H and W (depth is 20 m for all cases) (modified from Montazeri and Blocken (2017)).

Table 1. CHTC model as a function of U_{10} , W and H on the windward facade.

$$\text{CHTC} = U_{10}^{0.84} (a_0 + a_1 W + a_2 W^2 + a_3 W^3 + a_4 W^4 + a_5 H + a_6 H^2 + a_7 H^3 + a_8 H^4 + a_9 WH + a_{10} WH^2 + a_{11} WH^3 + a_{12} W^2 H + a_{13} W^2 H^2 + a_{14} W^2 H^3 + a_{15} W^3 H + a_{16} W^3 H^2 + a_{17} W^3 H^3)$$

$a_0 = 7.559$	$a_1 = -2.277E-1$	$a_2 = 6.037E-3$	$a_3 = -7.801E-5$
$a_4 = 3.810E-7$	$a_5 = 4.485E-2$	$a_6 = -8.190E-4$	$a_7 = 1.080E-5$
$a_8 = -6.020E-8$	$a_9 = 1.047E-3$	$a_{10} = -2.430E-5$	$a_{11} = 1.793E-7$
$a_{12} = -3.591E-6$	$a_{13} = 1.385E-7$	$a_{14} = -1.353E-9$	$a_{15} = -9.369E-8$
$a_{16} = 1.757E-9$	$a_{17} = -9.134E-12$		
$R^2 = 0.9977$			

3 BES simulations

In order to perform the dynamic building energy simulations, the BES tool EnergyPlus is used. Three groups of residential buildings are considered: buildings (1) with H_b (building height) $\geq W_b$ (building width); (2) with $H_b \leq W_b$; (3) with $H_b = W_b$ (square windward facade). For the first building group, H_b

varies from 10 m to 80 m and $W_b = 10$ m. For the building group with $H_b \leq W_b$, W_b varies from 10 m to 80 m and $H_b = 10$ m. For buildings with $H_b = W_b$, H_b and W_b vary simultaneously from 10 m to 80 m. All buildings (in total 22) consist of multiple apartments. Each apartment has one zone, no interior partitions and 12 m² of windows only on the windward facade (south exposure).

Different CHTC models for the windward facade are investigated while for the leeward facade and roof CHTC models are fixed i.e. ClearRoof and EmmelVertical, respectively. Seven CHTC models are considered for windward facade: TARPWindward, MoWiTTWindward, Nusselt-Jurges, McAdams, Mitchell, EmmelVertical and Montazeri & Blocken (reference model). A detailed description of these CHTC models can be found in the Engineering reference of EnergyPlus (U.S. Department of Energy, 2016) and in the paper by Montazeri and Blocken (2017). The evaluation is based on the annual space cooling and heating demand.

4 Results

It is observed that the use of higher insulation values results in a much weaker impact of the surface-averaged CHTC on heating and cooling demand. This is because, with the increase of the insulation values of the building envelope, the contribution of the convective resistance of the exterior of the building envelope becomes small compared to the overall wall thermal resistance (Zhang *et al.*, 2013). Furthermore, the influence of variations in surface-averaged CHTC is less pronounced on the heating demand compared to the cooling demand. During summer, cooling is significantly influenced by the convective removal of solar gains from the exterior opaque surfaces, while during winter time, the solar gains are rather small and therefore contribute at a minor level to the total heating energy demand (Mirsadeghi *et al.*, 2013).

Figure 2 shows the annual space cooling demand for building with varying geometry for different CHTC models. For buildings with $H_b \geq W_b$, the average absolute deviations of the TARPWindward and Mitchell with the reference model, in annual space cooling demand, are 37% and 29% respectively. For these CHTC models, the deviations in annual space cooling demand increase as the building height increases and reach a maximum value of 42% and 33% at $H = 80$ m, respectively. In contrast to the previous building group, the impact of CHTC models on the prediction of the energy demand of buildings with varying width is less pronounced. For this group of buildings ($H_b \leq W_b$), the use of the TARPWindward and Mitchell model leads to average absolute deviations of 16% and 12%, with the reference model, in annual space cooling demand, respectively. Maximum deviations are found to be 25% and 20% respectively. Finally, for buildings with $H_b = W_b$ (square windward facade) for a given building height, the deviations are lower than the ones observed for the buildings with only the height being increased. This behaviour is attributed to the simultaneous and individual impact of the CHTC models on the simulated energy demand of buildings as the width increases. For the TARPWindward and Mitchell model, the average absolute deviations with the reference model for the annual space cooling demand are 26% and 19%, respectively.

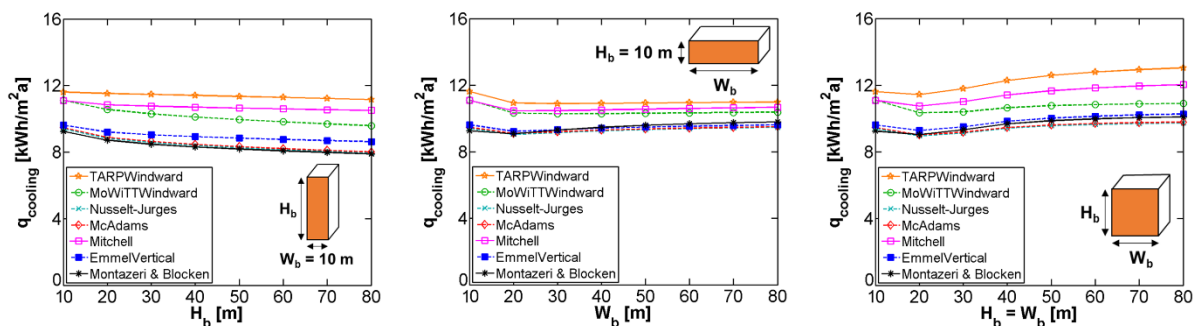


Figure 2. Annual space cooling demand obtained by different CHTC models (as implemented in EnergyPlus) for buildings with (a) $H_b \geq W_b$, (b) with $H_b \leq W_b$; (c) and $H_b = W_b$ (square windward facade).

5 Conclusions and future work

BES simulations are performed to investigate the impact of exterior CHTC models on the energy performance of buildings with different geometry. The following conclusions are made:

- Selection of appropriate CHTC model has a high impact on the calculated annual space cooling demand for buildings where $H_b \geq W_b$. In this case, deviations up to 42% are observed for annual space cooling.
- The impact of CHTC models on the estimation of the energy demand for buildings with $H_b \leq W_b$ is less pronounced.
- By increasing the building height and width simultaneously ($H_b = W_b$), the observed deviations for the annual energy demand are defined by the individual impact of the CHTC model on buildings where height and width are treated separately.

The focus in this study is on the windward facade. Future studies should focus on the impact of exterior CHTC models for leeward facades and roofs on the predicted energy demand. Moreover, further studies should account more complex urban configurations where the shading effects of neighbouring buildings are of significant importance for the building energy consumption.

Acknowledgements

The research is financially supported by the PhD Impulse Program of Eindhoven University of Technology in collaboration with the construction company Heijmans B.V., the Netherlands. Hamid Montazeri is currently a postdoctoral fellow of the Research Foundation - Flanders (FWO) and is grateful for its financial support (project FWO 12M5316N). The authors also gratefully acknowledge the partnership with ANSYS CFD.

References

- Defraeye, T., Blocken, B., and Carmeliet, J. (2011). Convective heat transfer coefficients for exterior building surfaces: Existing correlations and CFD modelling. *Energy Conversion and Management* 52, 512–522.
- Mirsadeghi, M., Cóstola, D., Blocken, B., and Hensen, J.L.M. (2013). Review of external convective heat transfer coefficient models in building energy simulation programs: Implementation and uncertainty. *Applied Thermal Engineering* 56, 134–151.
- Montazeri, H., Blocken, B., Derome, D., Carmeliet, J., and Hensen, J.L.M. (2015). CFD analysis of forced convective heat transfer coefficients at windward building facades: Influence of building geometry. *Journal of Wind Engineering and Industrial Aerodynamics* 146, 102–116.
- Montazeri, H., and Blocken, B. (2017). New generalized expressions for forced convective heat transfer coefficients at building facades and roofs. *Building and Environment* 119, 102–116.
- Shih, T-H., Liou, W.W., Shabbir, A., Yang, Z., and Zhu, J. (1995). A new k- ϵ eddy viscosity model for high Reynolds number turbulent flows. *Computers & Fluids* 24, 227–238.
- U.S. Department of Energy (2016). EnergyPlus engineering reference. Available at <http://www.energyplus.net/> [Accessed May 5, 2016].
- Wolfshtein, M. (1969). The velocity and temperature distribution in one-dimensional flow with turbulence augmentation and pressure gradient. *International Journal of Heat and Mass Transfer* 12, 301–318.

Zhang, R., Lam, K.P., Yao, S-c., and Zhang, Y. (2013). Coupled EnergyPlus and computational fluid dynamics simulation for natural ventilation. *Building and Environment* 68, 100–113.

On the effect of passive building technologies and orientation on the energy demand of an isolated lightweight house

R. Vasaturo¹, I. Kalkman¹, T. van Hooff^{1,2}, B. Blocken^{1,2}, P. van Wesemael³

¹Department of the Built Environment, Eindhoven University of Technology, the Netherlands

²Building Physics Section, Department of Civil Engineering, KU Leuven, Belgium

³Architectural Urban Design and Engineering, Eindhoven University of Technology, the Netherlands

Corresponding author: R. Vasaturo, r.vasaturo@tue.nl

Abstract

The rise of the average global temperature owing to climate change will lead to substantial variations in heating and cooling demands of buildings. The application of climate change adaptation measures is often considered and investigated in literature to reduce the energy demand for heating and cooling. Less attention is paid to the role of building orientation in the future climate. The present work investigates the impact of passive adaptation measures and orientation on the energy demand of an isolated lightweight house using building energy simulations (BES), considering two climate scenarios. Combined application of solar shading and a higher thermal resistance of the building envelope results in total savings in heating and cooling demand up to 11.0% and 14.7% for current and future climate scenarios, respectively. The role of building orientation is expected to change due to the climate change. Total energy savings up to 4.4% and 2.9% can be achieved when proper orientation is adopted for the case with no measures applied.

1 Introduction

The Royal Netherlands Meteorological Institute (KNMI) predicts that by 2085 the yearly average temperature in the Netherlands will increase up to +3.7 °C according to the worst case scenario (KNMI, 2015), with consequences on heating and cooling demands of buildings. Previous work focused on the effectiveness of several passive climate change adaptation measures in decreasing heating and cooling demands, considering different types of buildings and/or climate scenarios (e.g. van Hooff et al., 2016). Another factor to take into account is the building orientation, since it can affect the solar heat gain through the windows and therefore the energy demand (Pacheco et al., 2012).

In order to address the research gap found in literature, the present work investigates the combined impact of several passive adaptation measures and building orientation on heating and cooling energy demands of an isolated lightweight house, for both current and future climate scenarios.

2 Geometry and simulation

The building analyzed in the present work is based on the one-person lightweight house Heijmans ONE (Heijmans B.V., 2016). A peculiarity of this building is the extensive presence of glazing on a single facade and only a single window on the back facade, whereas no windows are present on the sides (Fig. 1). Consequently, the solar heat gain through the front facade is potentially higher than the other facades, and heating and cooling demands could therefore be highly influenced by the building orientation. The building walls and roof are modeled using two layers of particleboard, with polyurethane (PU) foam between them, resulting in a value of thermal resistance $R_C = 5.0 \text{ m}^2\text{K/W}$. The transparent parts of the envelope (windows and glass doors) are modeled using a U-value (thermal transmittance) of $1.2 \text{ W/m}^2\text{K}$ and a solar heat gain coefficient equal to 0.4 (i.e. glazing with low transmittance of solar radiation). The prescribed values for ventilation and infiltration rate are $0.9 \text{ dm}^3/\text{sm}^2$ and 0.2 air changes per hour (ACH), while set points for heating and cooling are established according to the most recent Dutch national

guidelines (see van Hooff *et al.*, 2016). The building energy simulations are performed using the software EnergyPlus. Two climate scenarios are considered in the present work: current and future climate. The latter considers the climate for the year 2050. In both cases the location of Beek, in the Netherlands, is chosen. The annual weather data for the current climate are obtained from the International Weather for Energy Calculations (IWEC) database by the American Society of Heating, Refrigerating and Air-Conditioning Engineers (ASHRAE). The CCWorldWeatherGen (2013) tool is employed to generate the annual weather file for the future climate through a morphing procedure, starting from the weather file for current climate.

The adaptation measures considered are white roofs and walls (WR + WW) and white roof (WR), i.e. the albedo of the exterior surfaces is increased from $\alpha = 0.3$ to $\alpha = 0.7$, exterior solar shading (SS), green roofs (GR) with leaf area index equal to 5, increased thermal resistance (TR), from $R_C = 5.0 \text{ m}^2\text{K/W}$ to $R_C = 6.5 \text{ m}^2\text{K/W}$, daily natural ventilation (NV) through openable windows (Fig. 1), and a combination of exterior solar shading and increased thermal resistance (SS + TR). An overview of these measures is presented in the work of van Hooff *et al.* (2016). The case where no measures are applied is considered as base case (BC).

The results of the simulations are presented in terms of annual heating, cooling and total (heating and cooling) energy demand for the building considered, expressed in kWh per m^2 of floor area. The simulations are performed for eight building orientations (N, NE, E, SE, S, SW, W, NW).

3 Results

3.1 Energy demand for current and future climate

The results for heating, cooling and total (heating + cooling) demands are presented in Table 1 for the two climate scenarios considered. The results are averaged values over the eight different orientations. In 2050, due to the higher temperatures during the entire year compared to the current climate, a decrease of the heating demand of 22.5% is predicted. For the same reason, the expected cooling demand in 2050 is more than doubled (+114.7%) compared to the one obtained for the current climate. The resulting heating/cooling energy demand ratios are respectively 12.4 and 4.5 for current and future climate. As a result, considering the summation of heating and cooling demands, a reduction of 12.3% of the total demand is found for the future climate (Tab. 1).

Table 2. Energy demands for the two climate scenarios averaged over eight orientations. Values in kWh/m².

climate scenario	heating demand	cooling demand	total demand
current	109.6	8.8	118.4
future (2050)	84.9	18.9	103.8

3.2 Effects of the passive adaptation measures on the energy demand

The results are reported in terms of variation with respect to the average heating, cooling and total demands over the eight orientations considered (BC values in Table 2). It can be concluded that none of the measures considered is capable of significantly decreasing the heating demand with the exception of the case where TR is considered ($R_C = 6.5 \text{ m}^2\text{K/W}$), for which a reduction of about 7% is achieved compared to the BC. The application of WR + WW leads to an increase of 3% for the heating demand due to the lower heat gain through the building walls during the winter, caused by a higher reflection of the solar radiation, whereas all the other measures do not significantly affect the heating demand.

When cooling demand is considered, remarkable differences are found compared to the BC when WR + WW, SS and NV are applied. Applying WR + WW reduces the cooling demand by 23% (current climate) and 17% (future climate), while SS effectively reduces it by 58% and 47%; finally, the natural ventilation decreases the cooling demands by 23% and 14%. On the other hand, WW (7% and 5%), GR (7% and 5%), TR (3% and 2%) are less effective compared to the other measures.

In terms of total energy demand, the use of TR is the most effective single measure in the current climate (-7.1% compared to the BC). Nevertheless, in the future climate the adoption of SS leads to higher

energy savings (-8.1%) due to the higher weight of the cooling demand with respect to the current climate. In addition, the application of SS + TR is proposed as a best case, since both heating and cooling demands are minimized. This brings 11.0% savings for the current climate and 14.7% for the future climate scenario compared to the respective base cases.

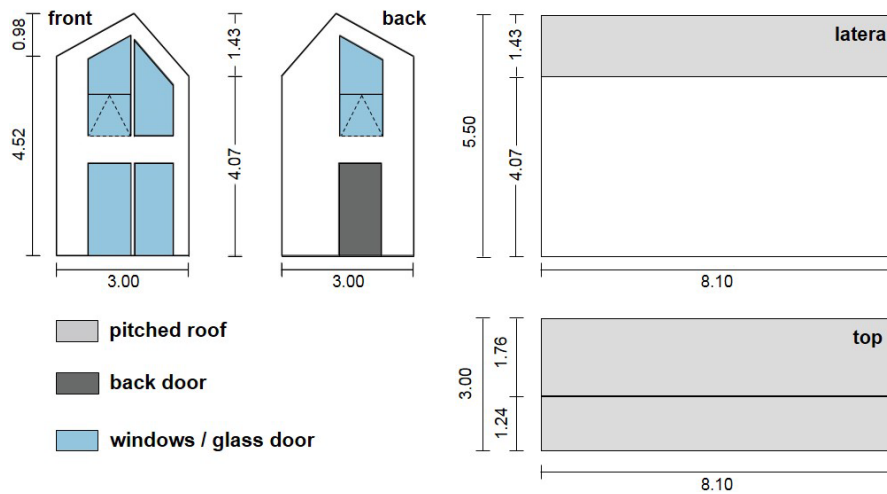


Figure 1. Building geometry. Dimensions in m. Dashed triangles indicate openable windows.

Table 2. Energy demands for the two climate scenarios, averaged over eight orientations, considering different passive adaptation measures. Differences are reported with respect to the base cases.

	current climate			future climate (2050)		
	heating [kWh/m ²]	cooling [kWh/m ²]	total [kWh/m ²]	heating [kWh/m ²]	cooling [kWh/m ²]	total [kWh/m ²]
BC	109.6	8.8	118.4	84.9	18.9	103.8
Measure	Δ [%]	Δ [%]	Δ [%]	Δ [%]	Δ [%]	Δ [%]
WR + WW	+3.1	-22.7	+1.2	+2.9	-16.9	-0.7
WR	+0.6	-6.8	+0.1	+0.6	-4.8	-0.4
SS	+0.5	-58.0	-3.8	+0.6	-47.1	-8.1
GR	-0.5	-6.8	-1.0	-0.5	-5.3	-1.3
TR	-7.4	-3.4	-7.1	-7.5	-2.1	-6.6
NV	-0.2	-22.7	-1.9	+0.5	-14.3	-2.2
SS + TR	-6.9	-61.4	-11.0	-6.8	-50.3	-14.7

3.3 Effects of the orientation on the energy demand

The orientation of the building is referred to the front facade; e.g. the building is oriented towards east when the front facade faces east. The results are reported as a difference with respect to the average over the eight orientations considered (BC values in Table 2) and in terms of total energy demand (Fig. 2). In the current climate scenario the change in orientation leads to variations of the heating demand from -5.2% (S) to +3.2% (NW); similarly, for the future climate scenario variations between -5.3% (S) and +3.2% (NW) compared to the base case are predicted. In terms of cooling demands, savings up to 30.8% (current climate) and 24.1% (future climate) can be obtained when the building faces N; on the other hand, an increase of 22.3% and 17.4% is found when the building faces SW for the current and future climate, respectively. The results can be explained by the fact that when the building is oriented towards S, SE and SW, the solar heat gain is much higher compared to N, NE and NW. In addition, for the current climate, the changing heating/cooling demand ratio influences the role of the orientation. For instance, considering the orientations N and NE, for which the cooling demand is minimized, it is possible to observe a slight decrease of the total energy demand (Fig. 2) compared to the average for the future climate scenario (-1.9% and -0.2%), differently from the current climate for which a small increase is predicted (+0.6% and +1.4%). Similarly, the orientations SE and SW result in a decrease for the current

climate compared to the average (-1.3%), while for the future climate an increase is present for these orientations (+0.1% and +0.7%, respectively), because of the lower ratio heating/cooling demand. Nevertheless, in both scenarios the highest energy savings are obtained when the building faces S (-4.4% and -2.9% for current and future climate, respectively), whereas the highest total energy demand is obtained when the building faces NW (+1.8%, current climate) and W (+2.4%, future climate).

4 Conclusions

In this work the results of building energy simulations of an isolated lightweight house are presented. The most important conclusions are:

- The heating/cooling demand ratios for current and future climate scenarios are respectively 12.4 and 4.5 for the BC (heating demand dominates).
- In the future climate the predicted total energy demand is 12.4% lower than in the current climate.
- Considering single adaptation measures, the application of TR brings the highest reduction of total energy demand in the current climate (-7.1%), whereas SS is more effective in the future climate (-8.1%) due to the lower heating/cooling demand ratio. A combination of SS + TR leads to the highest total energy savings, which are 11.0% and 14.7% for the current and future climate, respectively.
- Orientation affects the energy demand of the building; i.e. the total demand varies between -4.4% and +1.8% for the current climate and between -2.9% and +2.4% for the future climate. The highest total energy savings are obtained when the building faces S for both climate scenarios considered.

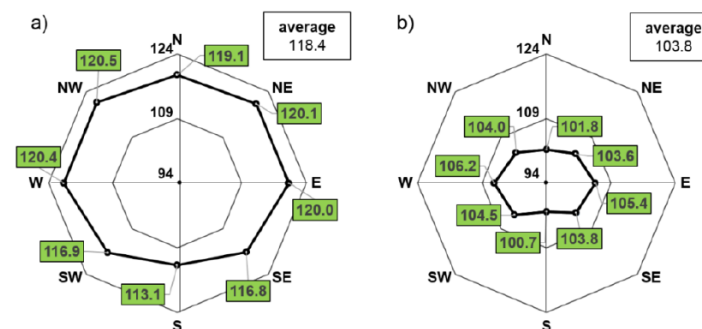


Figure 2. Annual total energy demand for a) current and b) future climate for the base case. Values in kWh/m². Average values are 118.4 kWh/m² and 103.8 kWh/m² for a) and b), respectively.

Acknowledgements

This research was financially supported by the PhD Impulse Program of the Eindhoven University of Technology, in collaboration with the construction company Heijmans B.V., the Netherlands.

Twan van Hooff is currently a postdoctoral fellow of the Research Foundation Flanders (FWO) and acknowledges its financial support (project FWO 12R9715N).

References

CCWorldWeatherGen (2013). Climate change world weather file generator manual, version 1.8. Sustainable energy group, University of Southampton.

Heijmans B.V. (2016). Heijmans ONE. Prijsoverzicht en Technische Beschrijving.

KNMI (2015). *KNMI'14* climate scenarios for the Netherlands. A guide for professionals in climate adaptation. De Bilt, The Netherlands.

Pacheco, R., Ordóñez, J., and Martinez, G. (2012). Energy efficient design of building: A review. *Renewable & Sustainable Energy Reviews* 16, 3559-3573.

Van Hooff, T., Blocken, B., Timmermans, H.J.P. and Hensen, J.L.M. (2016). Analysis of the predicted effect of passive climate adaptation measures on energy demand for cooling and heating in a residential building. *Energy* 94, 811-820.

The Gavoglio area: a military area in the earth of Genoa to be rediscovered and regenerated

C. Vite, C. Lepratti, R. Morbiducci

Department of Architecture and Design (dAD), Polytechnic School, University of Genoa, Italy

Corresponding author: C. Vite, clara.vite@arch.unige.it

Abstract

The authors present the first results of a project carried out thanks to the work and synergy of different stakeholders: the university, the municipality of Genoa and the citizens of the studied district. The aim is to rediscover an abandoned area in the earth of Genoa and to give it back to the neighbourhood in order to improve the quality of the life in a dense building stocks area of the city.

In the paper is presented the area, its history and growth, the first analysis of the district and the military buildings, from the environmental and typological point of view. The results of the first analysis could be suggest some ideas for the future renovation strategies.

1 Introduction

Genoa is an Italian city founded in the 4th century BC as an important roman port. The Medieval period was the first great period of the city and then after the Second World War, Genoa experienced great urban development, assuming the role of industrial and port centre within the industrial triangle of Genoa, Milan, and Turin. The rapid population growth and economic development have resulted in the need to provide housing. These new buildings were built by filling all the space behind the historical part of the city. In this rapid growth, some industrial areas that were previously located in peripheral areas have been incorporated and become an integral part of the new urban fabric (Amato 1992).

Among all the areas later dismantled from the 80's onwards, there is the Gavoglio areas behind the main Genoa railway station in a densely populated residential district. The regeneration of this area is part of the whole process of city renewal (Tillman Lyle 1996). There are already two European projects on the area: a Horizon 2020 project about the demonstration of innovative nature based solutions in cities and an Urbact III project named "2nd Chance Waking up the sleeping giants" that has the purpose of revitalizing those places that are now abandoned and disused. These two projects and the centrality of the area led to the decision to renovate the military area. The idea is to transform it into an urban technological park and to reuse the existing buildings with new functions.

2 The military area named "Gavoglio"

The military area named "Gavoglio" is a large building complex (Fig. 1c) that extends over 50,000 square meters immediately behind the railway station of Genoa. (Fig. 1a e 1b) Only people living in the nearby neighbourhoods like Lagaccio, Oregina and San Teodoro, have a visual contact with its large pavilions, while the barracks do not exist for the rest of the city. Many studies on the "Lagaccio" district, where the buildings studied are, have highlighted the multicultural and multi-ethnic character of the area. A characteristic that has been maintained in recent years, and which, unlike other areas of the city, has involved less common problems of heterogeneous ethnic groups.

The neighbourhood has been developed since the second half of the 19th century assuming from the very beginning the character of a popular neighbourhood inhabited mainly by workers. The Lagaccio district has extended up the steep slopes of the hills, slowly filling the gap between the historical roadways. This growth was particularly pronounced in the post-war period. In this period, large

residential buildings filled any useful area of the valley, transforming the area from a rural area into a residential urban area (Fig. 2a and 2b). The result of this rapid action is the presence of very dense building stocks with narrow road and poor services.

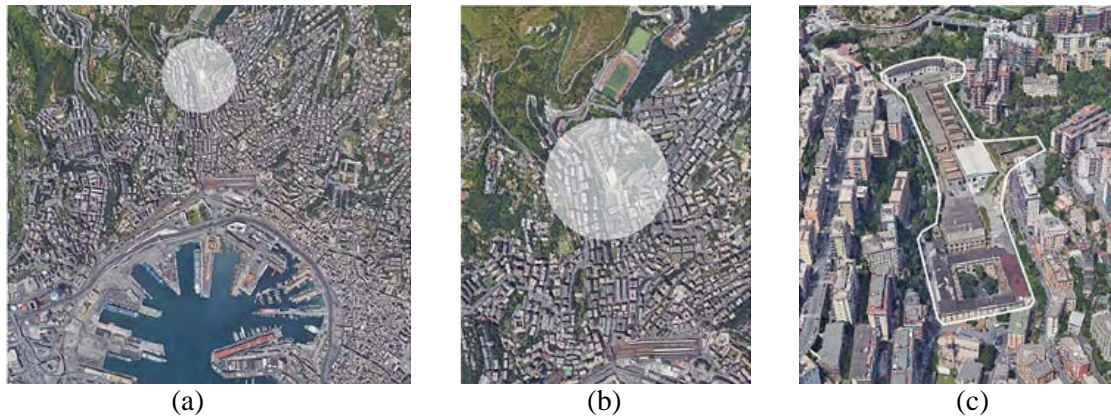


Figure 13. Localization of “Lagaccio” district in Genoa (a), identification of the military buildings (b) and delimitation of the studied area (source: Google Maps).



Figure 14. Historic view of the “Gavoglio” area before (a) and after (b) the urbanization process.

In 1652, in order to use the existing lake of this area to generate power an armoury was built here. In the later years, the decommissioning of this building, the abandonment of the sites and the many drowning in the lake, brought the bad reputation of the district. Only in the first half of the nineteenth century, it was built the military areas, as we know it today as a factory for the production of powders. The main building and some secondary depots were built to replace the seventeenth century factory. In the following years, other buildings were built to integrate the old powders still existing.

Since the 1980s, when the military use of most of the buildings was definitively ceased, numerous requests were made by citizens to convert it to urban use. Initially they asked only to improve road links but then they also asked to revitalize green spaces and services.

The Gavoglio area consists of several buildings with different destinations assigned during the time. In particular, there are spaces for housing use, production activities, service spaces and storage.

The presented study focuses on two main buildings:

- the main body that it is articulated on four building elements welded together and made at different times and it is structured around a central courtyard named “Piazza Italia” (Fig. 3a);
- the shed named “Proiettificio” was also built in various phases, from 1850s to the time before World War II. It represents a valuable example of industrial archaeology (Fig. 3b).



Figure 15. View of the main building (a) and the shed named “proiettificio” (b).

3 Actual state analysis

The present study analyse the military area in order to verify the best strategies for the future renovation scenarios. The entire area and each buildings have been analysed. In particular the two main ones that are subjected to architectural restriction and they will therefore be an integral part of any future project. In the next two paragraphs, climate data of the district is presented and the results of the analysis of the typological aspects of the buildings (DeKay and Brown 2014).

3.1 Environmental Detail

The first step of the analysis of the actual state is developed at environmental level. The aim is to study and understand the context in which the buildings are located. The environmental factors can affect internal living well-being, resulting in positive or negative conditions to its natural determinations.

As mentioned above, the Gavoglio are located at the bottom of a valley in a highly urbanized area not far from the sea (Fig. 1). The area presents the peculiarities of the Mediterranean climate, which consist of a period of summer dryness and rainy winters with mild temperatures.

Data on the climate characteristics were collected, in particular are analysed: temperatures and rainfall (Fig. 4), wind speed and directions (Fig. 5), relative humidity and irradiation. All the data are available free on the website of ARPAL and ISPRA and they are collected from the available weather station located in the port area near the case study site.

In particular, with regard to temperatures, the graph (Fig. 5) shows that the coldest month is February with a minimum temperature of 3.3°C while July is the hottest with a maximum temperature of 26.4°C. The rainy month is October with 179.53 mm of rain, while the driest one is July with 27.51 mm. Analysing the historical record of the monthly average rainfall since 1980, a peak of 609 mm can be observed in October 2014; the month in which Genoa has been flooded. These phenomena must be taken into account to manage flood phenomena. In particular, the Gavoglio area has a specific vulnerability due to the system of streams, which convey in one.

The Fig. 4 shows that in the winter months the wind prevailing direction is North (about 4.54 m/s) so in the renovation project of this area it is necessary to provide protection from the winter wind from the north. In the summer months, the prevailing direction is that of the South-East (about 2.81m/s) so at the design level it is possible to think about solutions that can convey the summer winds inside the buildings to provide natural cooling.

Moreover, to understand the climatic features of the area, it is important to have information on the relationship between sun and project area. A first analysis can be done by studying the sun paths with regard to Height and Azimuth (Fig. 6). The graphs show the Sun's trajectories over a day, one per month, for several days of the year.

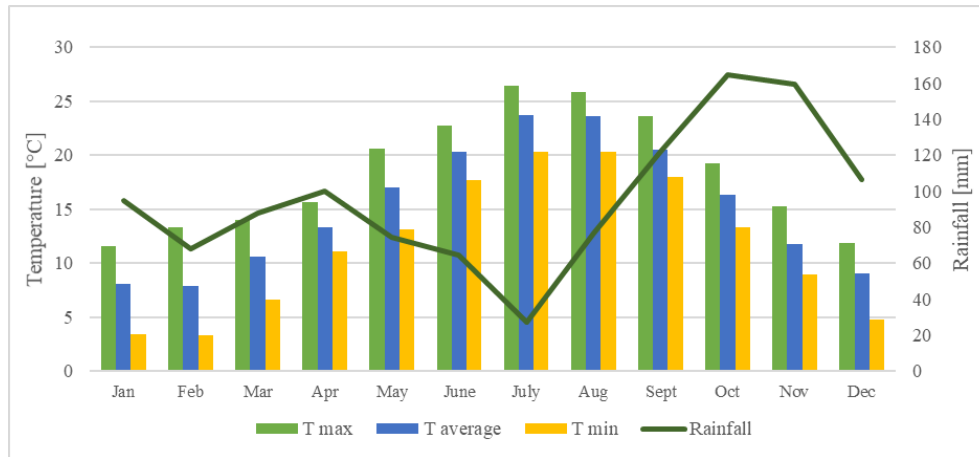


Figure 16. Graph with temperature and rainfall in the Gavoglio area.

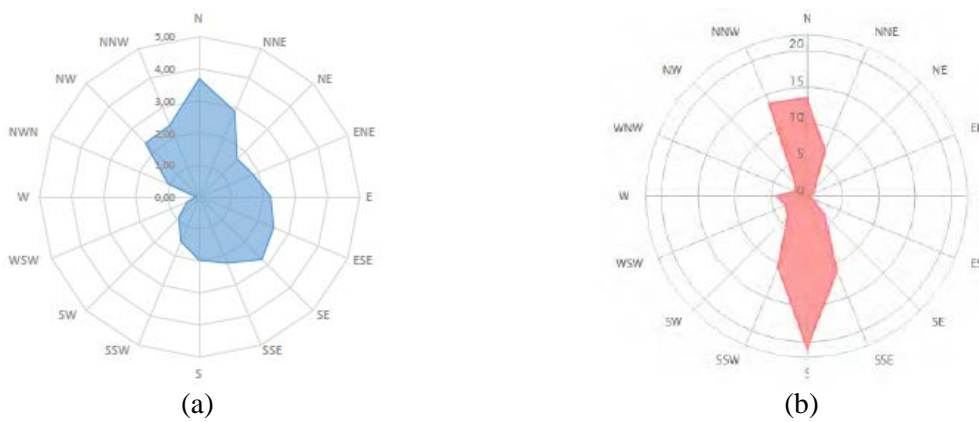


Figure 17. Annual average wind speed [m/s] (a) and wind directions distribution [%] (b).

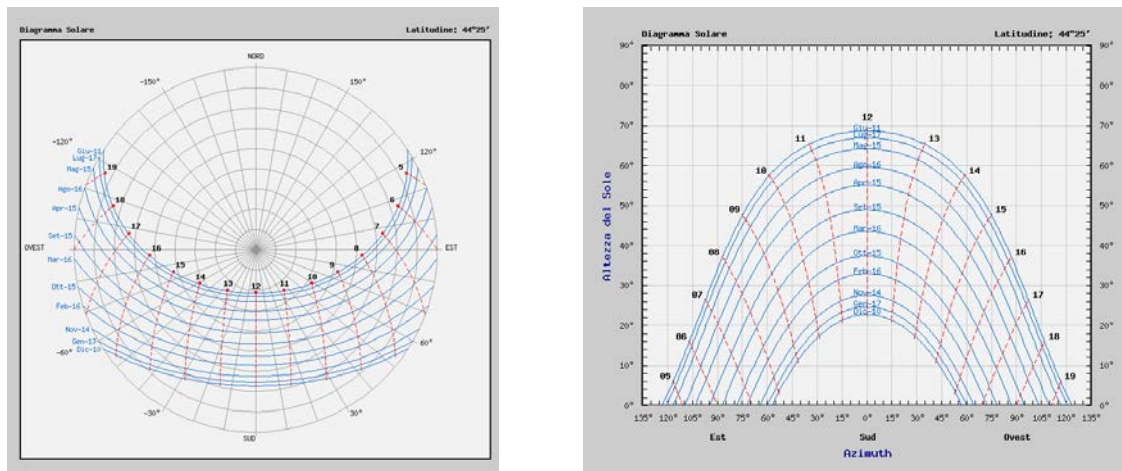


Figure 18. Sun path polar chart.

3.2 Typological Detail

The analysis of the relation between the external environment and the building located in a specific place is the main objective of the typological level. In particular, the analysis is about two main aspect: the buildings orientation related to the sun, the wind, and the shape of the buildings.

In this paper, the results obtained from simulations on solar irradiation and wind are reported.

The Figure 7a and 7b show the results obtained by solar simulation with the plugin Insight for Autodesk Revit. The study of the solar irradiation on the buildings are analyses in order to identify the energy

contribution for each seasons. These values are therefore useful during the project phase to identify the choices that help to get the best contribution during the winter and reduce radiation during the summer. The colour scale in the picture represents the amount of annual solar energy on the buildings: from 0 kWh/m² in dark blue up to a maximum of 1613 kWh/m² in red.

It is clear that the roofs are red because they are the parts most affected by the sun's rays so they have the maximum value. The northern walls are in light blue or yellow because are less affected.

The study of the irradiation has therefore allowed organizing the new functions of the constructed, distributing them in such a way as to guarantee the most appropriate level of lighting that different activities require. The poor solar radiation conditions make design choices necessary to make the most of the low contribution guaranteed on the prospectuses; the use of classic shutters as darkening elements provides greater freedom to those who will benefit from the building, allowing adjusting the percentage of light for the environments.

The wind simulation with Autodesk Flow Deign, using the data reported in the section 3.1, shows that the valley is crossed by winds both in winter and in summer (Fig. 8). In particular, where the winds are canalized between the buildings there are some critical situations, like in the central area of the main building.

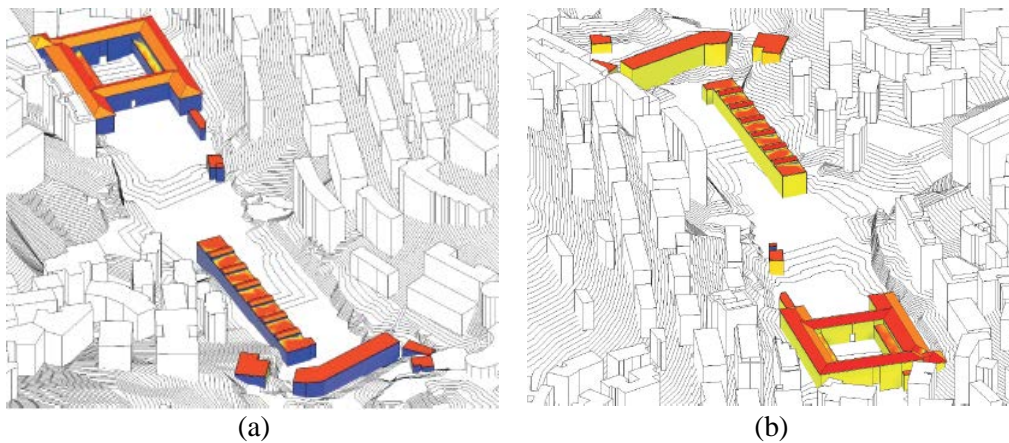


Figure 19. North view (a) and South view (b) of the solar radiation analysis.

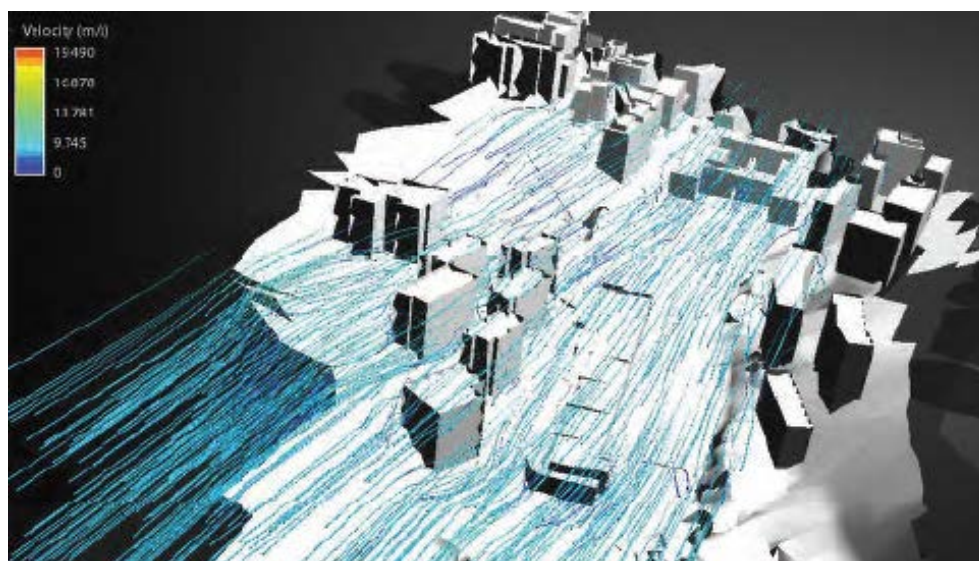


Figure 20. North view of the wind simulation.

4 Future transformation scenarios

The municipality has already developed two different scenarios to realize some actions chosen among those with more strength emerged during the discussion with associations and the population.

In general, it is planned to realize a very large area of green spaces equipped for leisure, play and sports, after demolition of most unbound industrial buildings. The total surface area for these functions is approximately 16,600 m² in scenario 1 or 10,300 m² in scenario 2, depending on the amount of demolition. Both proposed scenarios provide for a considerable amount of demolition, with the aim of improving the quality of the spaces for public use and the permeability of the soils. The Scenario 1 foresees a decrease of approximately 9000 m² of covered area while in scenario 2 the decrease would be around 4500 m².

The analyses carried out and presented in the previous paragraph on the actual state of the area are a good starting point for the development of future scenarios. In particular, they help to understand the whole area and its climatic conditions, the connections between the studied district and the surrounding area of the city, the relationship between buildings and climate. For example, they have been useful to understand that the strong winds hovering the area and the future demolitions require special attention to avoid situations of discomfort. In addition, solar analysis suggests the better location for particular functions that require direct natural light or where PV plants can be installed to optimize the renewable energies use and which parts of the area do not receive enough irradiation and therefore it is not advisable to place your outdoor activities.

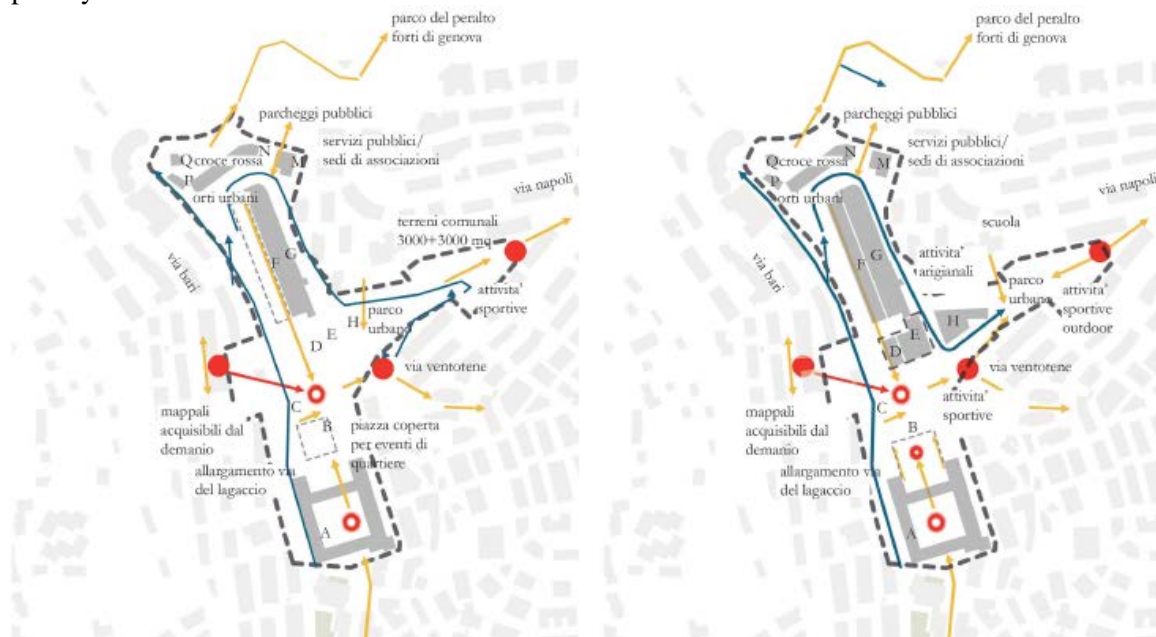


Figure 21. The two future scenarios chosen by the municipality of Genoa.

Acknowledgments

The authors want to thank the Municipality of Genoa for the collaboration and the opportunity to develop this research and all the students who have collaborated and contributed.

References

- Amato, A. (1992). *L'ulivo Sul Tetto, 1892-1992: Cent'anni Di Edilizia Genovese Fra Storia E Ricordo*. Genova: Cassa Edile Genovese.
- DeKay, Mark, and G. Z. Brown (2014). *Sun, Wind and Light: Architectural Design Strategies*. 3 edition. Wiley.
- Tillman Lyle, John (1996). *Regenerative Design for Sustainable Development*. Wiley.

Urban-CEQ international conference focuses on the evaluation of environmental quality of urban areas, considering a wide range of environmental problems, such as thermal comfort and air quality, and their effects on citizen life conditions and health. The event aims to be a meeting between specialists of fluid dynamics, designers and managers of urban areas in order to identify areas of frontier research, the sharing of useful targets for the improvement of urban environmental quality.

More than two thirds of European citizens live in cities, where many environmental problems are concentrated, such as lack of thermal comfort and poor air quality, which seems to be also responsible for life-threatening conditions. It is more and more necessary that the urban regeneration strategies are linked to objectives of environmental quality improvement.

ISBN: 978-88-97752-91-2

